EFFECT OF GEM-DIFLUORINATION ON THE CONFORMATION OF SELECTED HYDROCARBON SYSTEMS

Maciej Skibiński

A Thesis Submitted for the Degree of PhD
at the
University of St Andrews

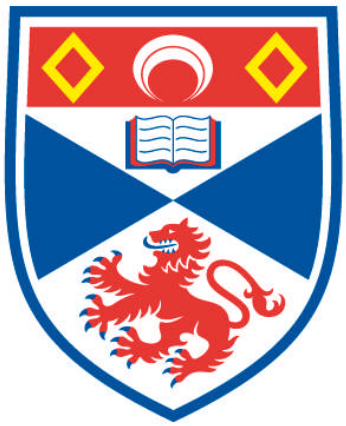

2014

Effect of *gem*-Difluorination on the Conformation of Selected Hydrocarbon Systems

Maciej Skibiński

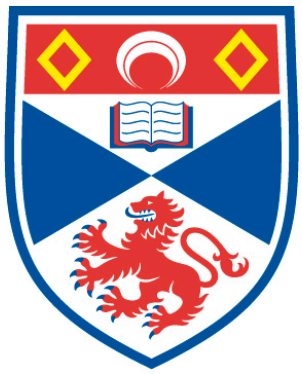

University of St Andrews

A Thesis Presented for the Degree of Doctor of Philosophy at the University of St Andrews

February 3rd 2014

CANDIDATE'S DECLARATIONS

I, Maciej Skibiński, hereby certify that this thesis, which is approximately 30.000 words in length, has been written by me, that it is the record of work carried out by me and that it has not been submitted in any previous application for a higher degree.

I was admitted as a research student in March 2010 and as a candidate for the degree of Doctor of Philosophy in May 2011; the higher study for which this is a record was carried out in the University of St Andrews between 2010 and 2013.

Date.....signature of candidate.....

SUPERVISOR'S DECLARATIONS

I hereby certify that the candidate has fulfilled the conditions of the Resolution and Regulations appropriate for the degree of Doctor of Philosophy in the University of St Andrews and that the candidate is qualified to submit this thesis in application for that degree.

Date.....signature of supervisor.....

PERMISSION FOR ELECTRONIC PUBLICATION

In submitting this thesis to the University of St Andrews I understand that I am giving permission for it to be made available for use in accordance with the regulations of the University Library for the time being in force, subject to any copyright vested in the work not being affected thereby. I also understand that the title and the abstract will be published, and that a copy of the work may be made and supplied to any *bona fide* library or research worker, that my thesis will be electronically accessible for personal or research use unless exempt by award of an embargo as requested below, and that the library has the right to migrate my thesis into new electronic forms as required to ensure continued access to the thesis. I have obtained any third-party copyright permissions that may be required in order to allow such access and migration, or have requested the appropriate embargo below. The following is an agreed request by candidate and supervisor regarding the electronic publication of this thesis:

Access to printed copy and electronic publication of thesis through the University of St Andrews.

Date.....signature of candidate.....

Date.....signature of supervisor.....

ACKNOWLEDGEMENTS

Firstly, I would like to thank Prof. David O'Hagan for giving me the opportunity to study for a PhD in his research group, for all his support and encouragement.

In addition I would like to thank the DOH research group, especially Dr Małgorzata Marańska, Dr Nawaf Al Maharik, Dr Jason Chan, Dr Alastair Durie, Dr Neil Keddie, Rodrigo Cormanich and Stephen Thompson for their scientific advice and general help in the laboratory.

I would also like to thank Prof. Steven Nolan, Dr César Urbina-Blanco and the rest of the SPN research group for fruitful collaborative work.

I would like to extend very special thanks to Prof. Alexandra Slawin for priceless encouragement and X-ray analysis.

I am also grateful for invaluable help and support of the DP and EK group members, especially Tamara Kosikova and Stefan Borsley.

I am also thankful to all the academic and technical staff of the Chemistry Department: Dr Alan Aitken, Dr Catherine Botting, Dr Tomas Lebl, Dr Iain Smellie, Caroline Horsburgh, Peter Pogorzelec, Melanja Smith and Sylvia Williamson.

Finally, I would like to thank my parents, family and friends for their support.

TABLE OF CONTENTS

TABLE OF ABBREVIATIONS

Ac	acetyl
BuLi	butyllithium
b.p.	boiling point
bs	broad singlet
CI	chemical ionisation
CSD	Cambridge Structural Database
d	doublet
ddd	doublet of doublets of doublets
ddt	doublet of doublets of triplets
DAST	diethylaminosulfur trifluoride
DBH	5,5-dimethyl-1,3-dibromohydantoin
DCE	1,2-dichloroethane
DCM	dichloromethane
Deoxofluor	bis(2-methoxyethyl)amonosulfur trifluoride
DFE	1,2-difluoroethane
DFT	density functional theory
DME	1,2-dimethoxyethane
DMF	*N,N*-dimethylformamide
DSC	differential scanning calorimetry
EI	electron impact ionisation
ES	electrospray ionisation
Et	ethyl
eq	equivalent
Fluolead	4-(*t*-butyl)-2,6-dimethyl-phenylsulphurtrifluoride
GC	gas chromatography
gem	geminal
HRMS	high resolution mass spectrometry
IR	infrared spectroscopy
J	coupling constant

k	rate constant
LRMS	low resolution mass spectrometry
m	multiplet
Me	methyl
MOST	morpholinosulfurtrifluoride
m.p.	melting point
MS	mass spectrometry
n	normal
NBO	natural bond orbital
NIS	*N*-iodosuccinimide
NMR	nuclear magnetic resonance
ppm	parts per milion
PTFE	polytetrafluoroethylene
RT	room temperature
RCM	ring-closing metathesis
s	singlet
t	triplet
t	tertiary
T_d	tetrahedral
TFA	trifluoroacetic acid
TFAA	frifluoroacetic anhydride
THF	tetrahydrofuran
TLC	thin layer chromatography
TREAT-HF	triethylamine trihydrofluoride
Ts	tosyl
UV	ultraviolet
VDW	van der Waals radius
w/v	% weight per volume
w/w	% weight per weight
XtalFluor-E	(diethylamino)difluorosulfonium tetrafluoroborate
XtalFluor-M	morpholinodifluorosulfinium tetrafluoroborate

ABSTRACT

Owing to its unique electronic properties, the CF_2 group has the potential to affect the conformation and polarity of molecules. The Introduction provides an overview of the conformational effects induced by the incorporation of fluorine into hydrocarbons, *e.g. gauche* effect, 1,3-C,F bond repulsion and angle deviation in organofluorine compounds. A summary of synthetic strategies for the introduction of the *gem*-difluoride motif into organic molecules is also presented.

In order to explore the conformational impact of the CF_2 group in alicyclic hydrocarbon systems, cyclododecane was employed as the molecular framework. In 1,1,4,4- and 1,1,7,7- tetrafluorocyclododecanes, two CF_2 groups replaced CH_2 units within the square [3333] cyclododecane ring where the spacing enables the CF_2 groups to occupy adjacent or opposite corner locations. In the case of 1,1,6,6-tetrafluorocyclododecane, one of the CF_2 groups was forced to the edge position, which changes the ring conformation dramatically. Strategic incorporation of two CF_2 groups is shown to either stabilise or significantly alter the conformation of the cyclododecane framework, a revealing conformational preference of the CF_2 group to locate at the corner rather than the edge position of hydrocarbon rings. The study extends to larger cycloalkanes, rectangular [3434] cyclotetradecanes and square [4444] cyclohexadecanes. The target cycloalkanes bearing two CF_2 units were assembled through a novel synthetic route, employing ring-closing metathesis (RCM) as the key step. X-Ray structure analyses revealed that the CF_2 groups occupy exclusively corner locations of these rings too. The spacing between the CF_2 moieties dictates the overall ring conformations and offers a useful tool for controlling molecular arrangement.

An accelerating role of the CF_2 group, relative to the CH_2 group, on the ring-closing metathesis of C5-substituted 1,8-nonadienes has also been studied. Remarkably, the CF_2 group exhibited a similar reaction rate to that observed for nonadienes bearing 1,3-dioxolane or dimethylmalonate groups. This effect was rationalised by the thermodynamic stability of the cycloheptene products, rather than a Thorpe-Ingold effect.

1

Introduction

1.1 The influence of fluorine on the conformation of hydrocarbons

Fluorine, the smallest element in the halogen group, is recognised for its high electron affinity. This is dictated by the limited shielding of the positively charged fluorine nucleus by only two electrons of the inner-shell. Additionally, a fluorine atom requires only one electron to reach the configuration of the noble gas neon.

Incorporation of fluorine into hydrocarbons can influence their physical and chemical properties as a result of the significant difference in electronegativity between the carbon and fluorine atoms. The presence of a strong and highly polarised C-F bond alters hydrogen acidity, the thermal and oxidative stability, lipophilicity and the dipole moment of organic compounds and can be a design tool in the development of new performance materials.[1–5] Also, the

conformation of hydrocarbons can be influenced by the introduction of fluorine atoms.

1.1.1 The *gauche* effect

The *gauche* effect is a well known conformational bias induced by the incorporation of a fluorine atom into a hydrocarbon. It was first described by Wiberg from Density Functional Theory (DFT) calculations. He reported that 1,2-difluoroethane **1** (DFE) displays a preference for a *gauche* over an *anti* conformation. The calculated value was reported to be 0.79 kcal mol^{-1}.[6] In contrast, the analogous 1,2-dichloroethane **2** (DCE) favours the *anti* over the *gauche* conformer by 1.44 kcal mol^{-1} (Figure 1.1).

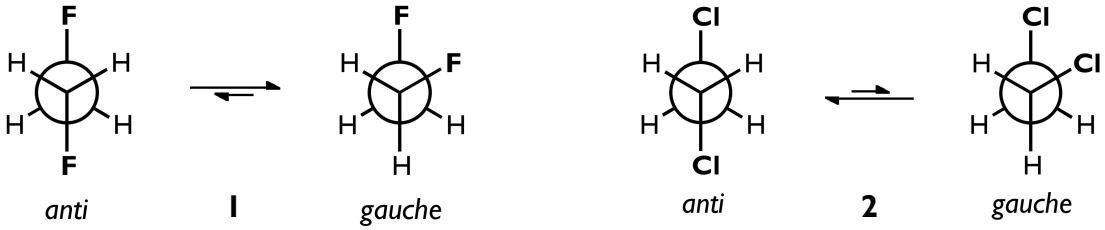

Figure 1.1 DFT [B3LYP/6-311+G] derived energy difference (ΔG_{298K}) between the *anti* and *gauche* conformers of 1,2-difluoroethane **1** and 1,2-dichloroethane **2** as determined by Wiberg.[6]

Further DFT analysis of this gauche effect conducted by Goodman and co-workers revealed that the *gauche* geometry facilitates an overlap between the electron rich σ_{CH} bonding orbital and the electron deficient σ^*_{CF} antibonding orbital. This results in a hyperconjugative $\sigma_{CH} \rightarrow \sigma^*_{CF}$ stabilisation (Figure 1.2).[7]

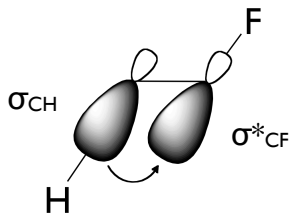

Figure 1.2 Graphical representation of hyperconjugative interaction between σ_{CH} and σ^*_{CF} orbitals.

1.1.2 1,3-C-F bond repulsion

Compounds with fluorine atoms positioned 1,3- to each other along a hydrocarbon chain, display repulsion between the polarised fluorine atoms $^{\delta-}$F. This is induced by the high polarisation of the C-F bonds. Such intramolecular dipolar repulsion has been investigated in 1,3-difluoropropane **3** employing a combination of experimental and theory studies.[8] Relative energies calculated for the four conformers of 1,3-difluoropropane **3a-3d** are presented in Figure 1.3.

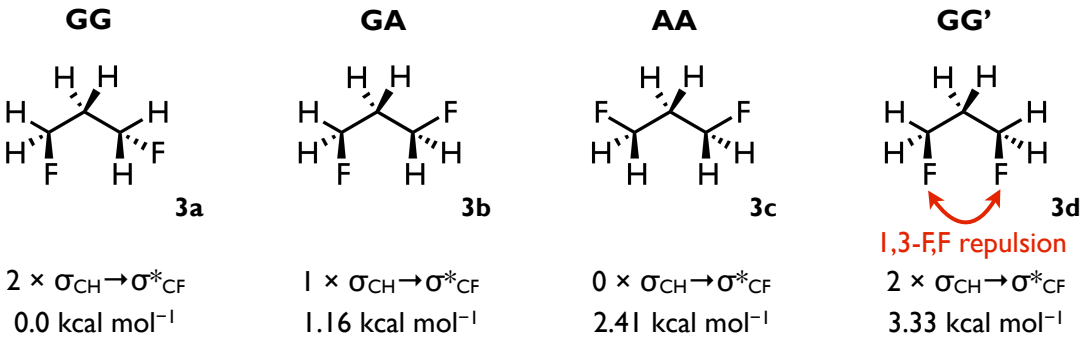

Figure 1.3 The relative energies of the conformers of 1,3-difluoropropane **3** derived from theory calculations at MP2/6-31+G** level. Hyperconjugative $\sigma_{CH}\rightarrow\sigma^*_{CF}$ interactions account for the high stability of the conformer GG (**3a**). However, the 1,3-F,F dipolar repulsion determines the conformational energy preference between the two *gauche-gauche* conformers GG (**3a**) and GG' (**3d**).[2,8] Figure adapted from Ref. 2.

The lowest energy conformer GG (**3a**) has two stabilising $\sigma_{CH} \rightarrow \sigma^*_{CF}$ interactions whereas the AG conformer (**3b**) has only one, thus accounting for the 1.16 kcal mol^{-1} increase in energy. The hyperconjugative $\sigma_{CH} \rightarrow \sigma^*_{CF}$ stabilisation is absent in the conformer AA (**3c**), resulting in a higher energy of 2.41 kcal mol^{-1} relative to **3a**. Conformer GG' (**3d**) was found to be energetically less favoured than conformer GG (**3a**) (ΔE = 3.33 kcal mol^{-1}), despite the same number of stabilising hyperconjugative $\sigma_{CH} \rightarrow \sigma^*_{CF}$ interactions. It was rationalised by Wu and co-workers that the destabilisation observed in **3d** arises from the 1,3-F,F dipolar repulsion between the two parallel C-F bonds.

A combination of the *gauche* effect together with 1,3-dipolar repulsion has a significant impact on the conformation of multivicinal fluorinated hydrocarbon chains. It was found by O'Hagan *et al.*, employing single crystal X-ray analysis, that compounds **4** and **5**, containing the all-*syn* multivicinal fluorine motif, have their C-F bonds arranged in a helical, rather than the typical *anti* zig-zag fashion (Figure 1.4).

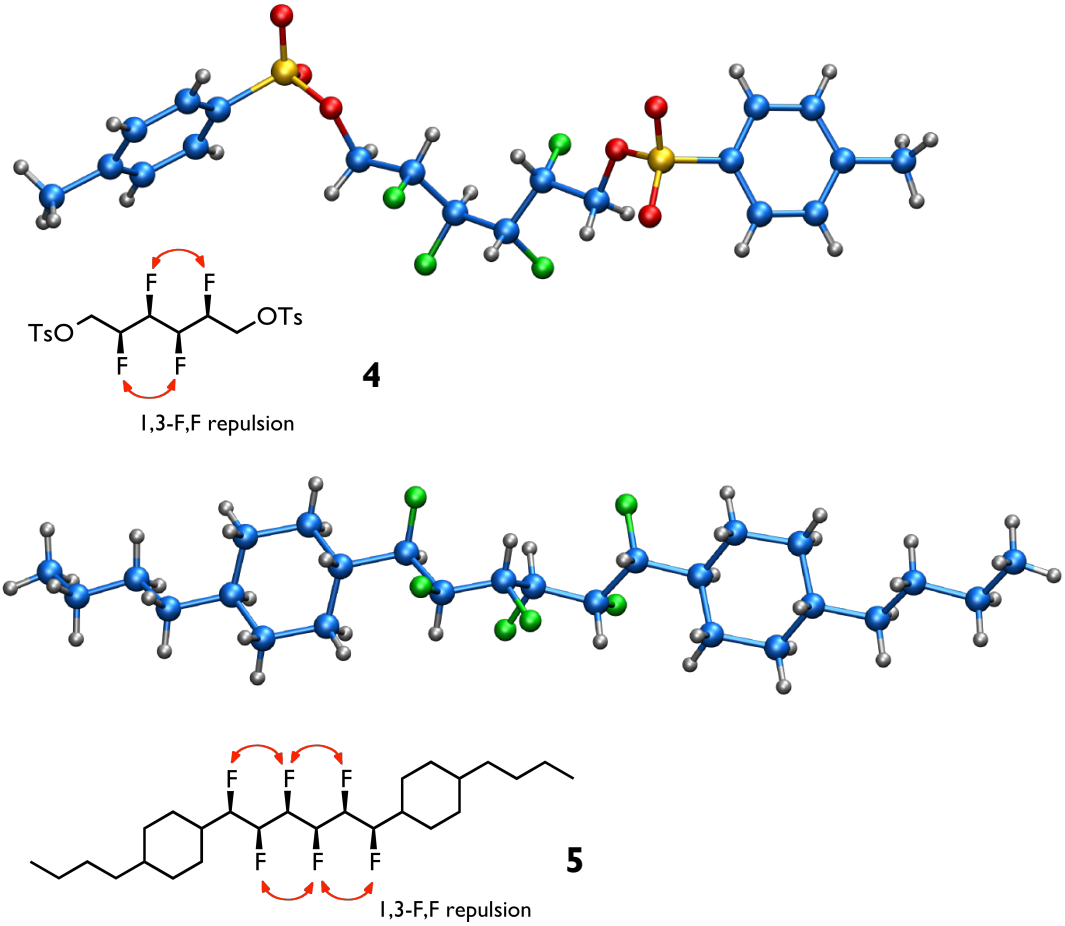

Figure 1.4 X-ray crystal structures of **4** and **5**. The helical conformation of the all-*syn* multivicinal fluorinated hydrocarbons accommodates the stabilising hyperconjugative $\sigma_{CH} \rightarrow \sigma^*_{CF}$ interactions and allows to avoid 1,3-F,F repulsion. [2,9,10]

This helical arrangement preserves the stabilising hyperconjugative $\sigma_{CH} \rightarrow \sigma^*_{CF}$ interactions, whilst allowing the molecules to avoid repulsive intramolecular 1,3-F,F interactions.[9]

1.1.3 Bond angle deviations in fluorinated hydrocarbons

Mack and co-workers found, from a combination of theoretical calculations and electron spectroscopy studies, that the introduction of fluorine at C2 in propane leads to a deviation of the C-C-C bond angle.[11] Figure 1.5 shows a

progressive C-C-C angle widening from 112.0º in propane **6**, and 114.6º in 2-fluoropropane **7**, through to 115.3º in 2,2-difluoropropane **8**.

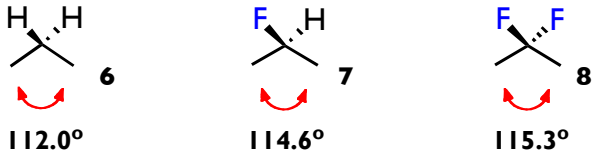

Figure 1.5 Effect of fluorination on C-C-C bond angles in propane **6** as determined by Mack.[11]

Similar trends for the F-C-F and H-C-H angle deviation have been observed by Donald in the fluoromethane series (Figure 1.6).[12] The F-C-H bond angle in fluoromethane **10** is narrower (108.7º) than tetrahedral. This results in a widening of the corresponding H-C-H bond angle (110.2º). Difluoromethane **11** has the widest H-C-H bond angle (113.4º) and the narrowest F-C-F bond angle (108.4º) in the series.

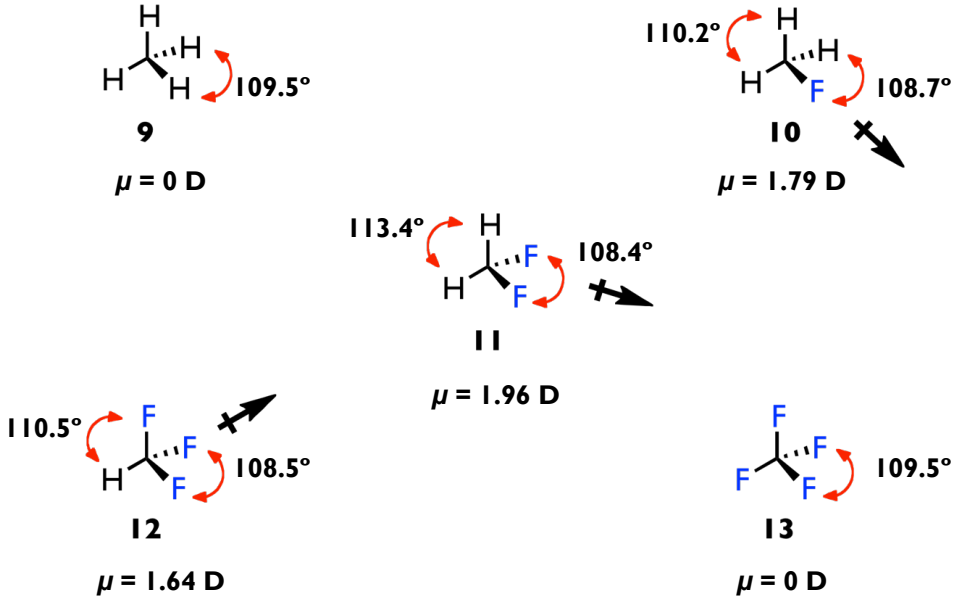

Figure 1.6 Bond angles and molecular dipoles of methane **9** and fluoromethanes **10-13**.[12]

The presence of fluorine also generates a molecular dipole in CH_3F, CH_2F_2, and CHF_3. This dipole is largest (μ = 1.96 D) for the CF_2 species (Figure 1.6).

The observed distortion in the geometry around the *gem*-difluorinated carbon atom arises from the large difference in electronegativity between the carbon and fluorine atoms. The valence electron density of the carbon atom is shifted towards the more electronegative fluorine atom (Figure 1.7).

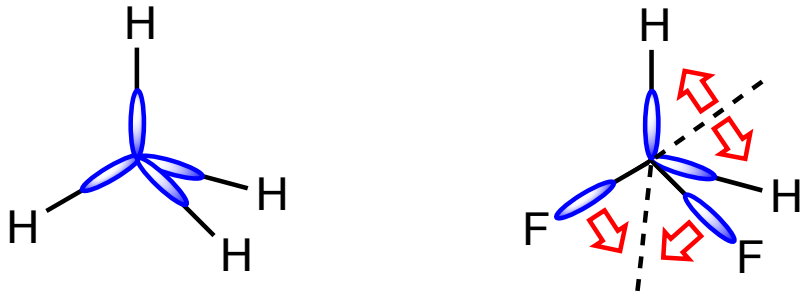

Figure 1.7 Graphical representation of the electron density shift in methane **9** and difluoromethane **11**.

This density shift leads to a relaxation of the repulsion between the C-F bonds, and, as a consequence, the F-C-F bond angle becomes narrower than tetrahedral.

Similarly, results of theoretical calculations carried out by Wiberg revealed that fluorine withdraws electron density much more readily than the less electronegative chlorine, thus leading to a more significant increase in the positive charge on the carbon atom.[13] Conversely, the electron-donating SiH_3 group induces negative polarisation at the carbon atom (Figure 1.8).

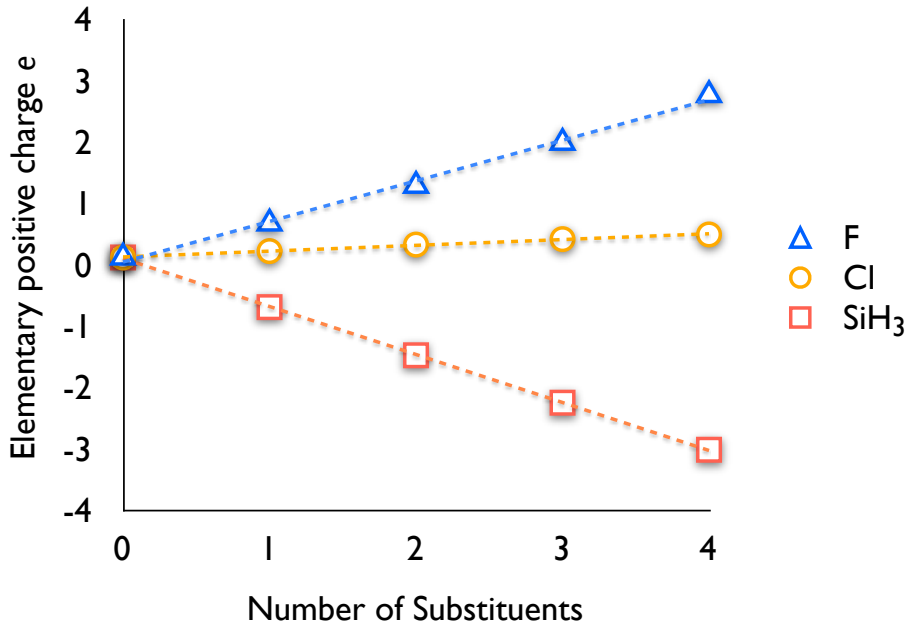

Figure 1.8 Relationship between the charge at the central carbon and the number of substituents in methane **9**.[13]

The change in the electronic character of the substituent causes a redistribution of electron density around the carbon atom and leads to a deviation in sp^3 hybridisation. According to Bent's rule, "*atomic p character concentrates in orbitals directed toward electronegative substituents*" as p electrons are less tightly held by the carbon nucleus.[14] Thus, fluorine atom attracts electrons more readily from sp^3 orbitals than from sp^2, as the sp^3 hybrid orbitals have larger p character.[2] For example, the isodesmic interconversion of methane **9** and vinyl fluoride **14** with fluoromethane **10** and ethylene **15** indicates that fluorine atom displays a preference for the sp^3 hybridised carbon atoms (Scheme 1.1).

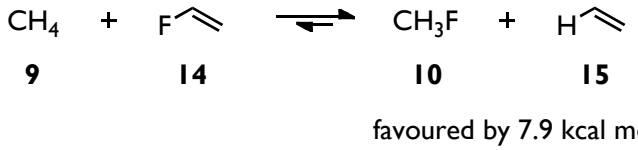

Scheme 1.1 Isodesmic interconversion of methane **9** and vinyl fluoride **14** with fluoromethane **10** and ethylene **15** illustrates the preference of the fluorine atom to bond to sp^3 rather than sp^2 hybridised carbon.[2,15]

Also, 1,1-difluoro-1,5-hexadiene **16** undergoes a Cope rearrangement, which favours the more thermodynamically stable, sp^3-CF_2 product **17** (Scheme 1.2).[2,16]

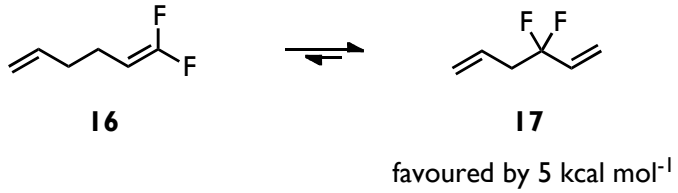

Scheme 1.2 Cope rearrangement of 1,1-difluoro-1,5-hexadiene **16**.[2,16]

1.1.4 Steric and electronic influence of the difluoromethylene CF_2 group in long aliphatic chains

In order to explore the influence of the fluorine substitution on the conformation of long aliphatic hydrocarbons, a series of fluorine-substituted fatty acids **18b-c** and tristearins **19b-c** were prepared by O'Hagan *et al.* in 1995 (Scheme 1.3).

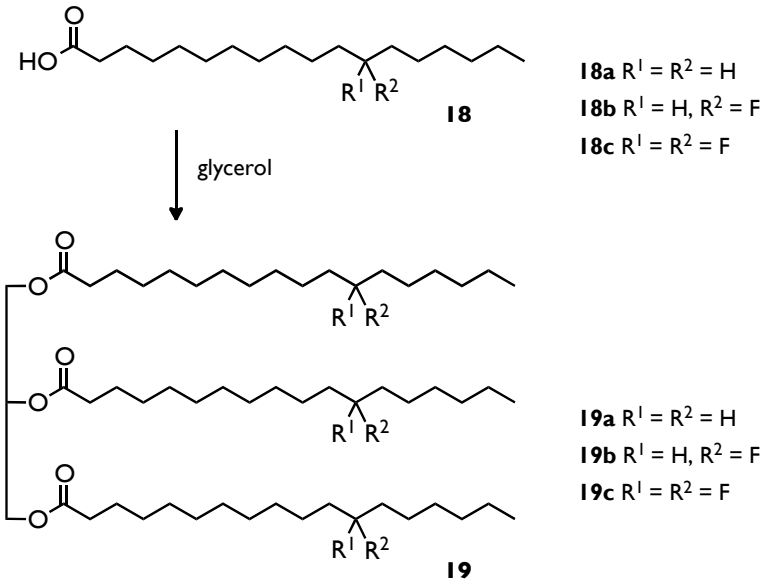

Scheme 1.3 Preparation of selectively tristearins **19a-c** by condensation of stearic acids **18a-c** and glycerol.[17] Figure adapted from Ref. 17.

Tristearin **19a** displays a polymorphic nature in the solid state. Differential scanning calorimetry (DSC) evaluation of **19b-c** showed that these fluorinated tristearins undergo a phase transition below their melting points too. The 12-fluoro-tristearin **19b** was found to maintain a similar melting point (m.p. = 73 ºC) and a polymorphism profile to that of tristearin **19a** (m.p. = 72 ºC). However, the tristearin analogue bearing difluoromethylene groups (**19c)** was found to have a lower phase transition point as well as a lower overall melting point (m.p. = 58 ºC). These observations suggest that the CF_2 group increases the disorder in the hydrocarbon chain relative to the –CHF **19b** and $–CH_2$ **19a** analogues.

In order to probe the influence of the fluorine substitution on the conformational mobility of the hydrocarbon chain, Langmuir isotherms of the free stearic acids **18a-c** were measured. The carboxylic acids were deposited

on a water subphase and subsequently compressed to evaluate their ability to form monolayers. The floating monolayers were then expanded and subsequently recompressed in order to assess their stability. It was observed that both stearic acid **18a** and 12-fluorostearic acid **18b** form stable monolayers. However, the initially formed monolayer of 12,12-difluorostearic acid **18c** was found to be unstable, and instead reorganised into a bilayer (Figure 1.9).

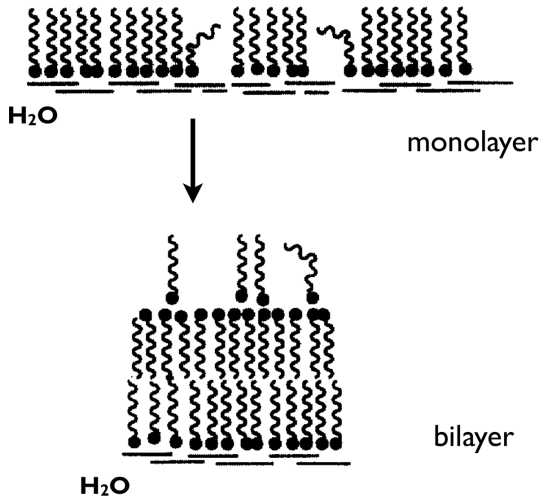

Figure 1.9 Schematic representation of monolayer and bilayer of the stearic acids **18a-c** on a water subphase.[18] Figure adapted from Ref. 18.

It was suggested that incorporation of the CF_2 group relaxes the unfavourable 1,4-H,H interactions in the hydrocarbon chain as a consequence of the wider CH_2-CF_2-CH_2 angle (Scheme 1.4).

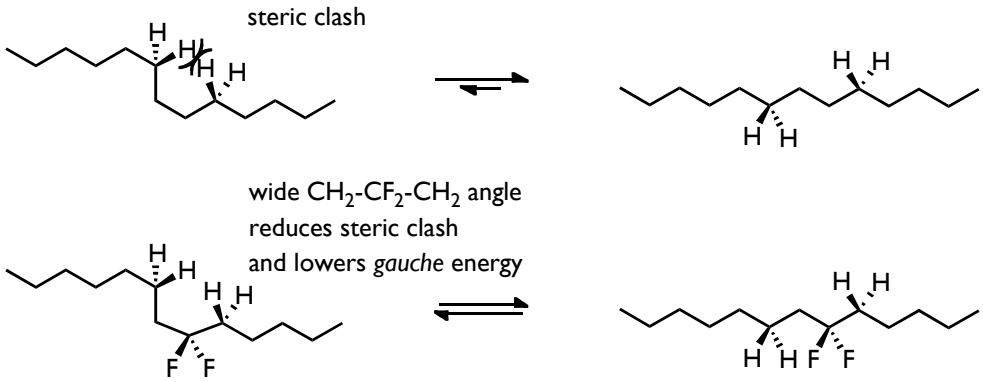

Scheme 1.4 Deformation of the hydrocarbon chain induced by incorporation of the CF_2 group.[19] Scheme adapted from Ref. 19.

A wider CH_2-CF_2-CH_2 angle leads to an increase in the population of *gauche* conformers affording a higher degree of conformational flexibility in the CF_2-substituted hydrocarbon chains. The increased flexibility of the hydrocarbon chain results in less efficient packing of the molecules in the film and, as a consequence, increased disorder of the monolayer.

In a more recent study, Wang *et al.* reported a synthesis of palmitic acids **20b-d** bearing regiospecifically incorporated CF_2 groups (Figure 1.10).[20]

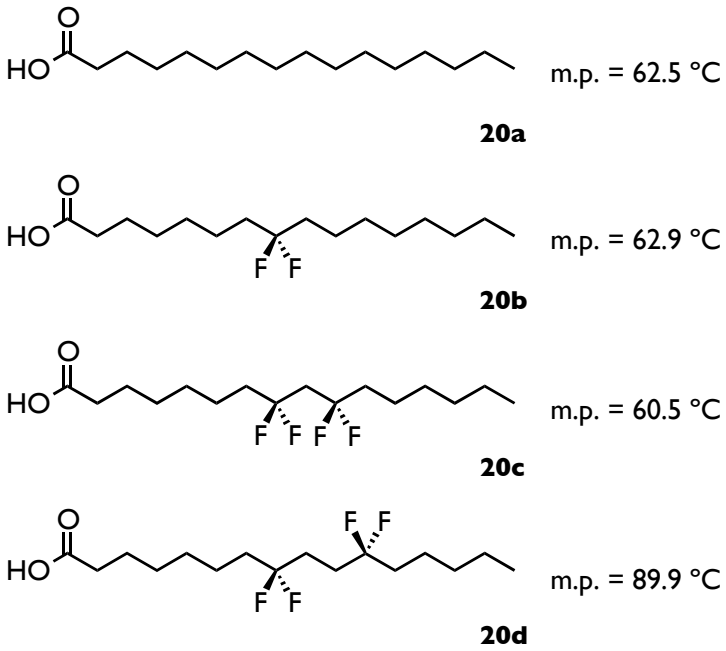

Figure 1.10 Palmitic acids **20a-20c** display similar m.p. whereas the m.p. of **20d** is significantly higher.[20]

DSC analysis revealed that 8,8-difluorohexadecanoic acid **20b** maintains a similar melting point (m.p. = 62.9 ºC) to that of palmitic acid **20a** (m.p. = 62.5 ºC). Substitution with a single CF_2 group at C-8 in hexadecanoic acid had therefore a negligible influence on the melting point. Similarly, tetrafluorodecanoic acid **20c** bearing two CF_2 groups located 1,3 relative to each other did not exhibit a major change in the melting point (m.p. = 60.5 ºC). However, a broad melting peak recorded for **20c** suggests a higher disorder in the solid state of this compound. 8,8,11,11-Tetrafluorohexadecanoic acid **20d** was found to display a significantly higher and sharp melting point (m.p. = 89.9 ºC) indicating a more organised molecular packing.

Two of the hexadecanoic acids, **20b** and **20d**, were crystalline solids and their solid state structures were solved using single crystal X-ray analysis. However,

consistent with the DSC analysis, **20c** was found to be significantly more amorphous in nature and a suitable crystal could not be obtained. Figure 1.11 shows the resultant structures and *anti* zig-zag chain conformation exhibited by **20b** and **20d**.

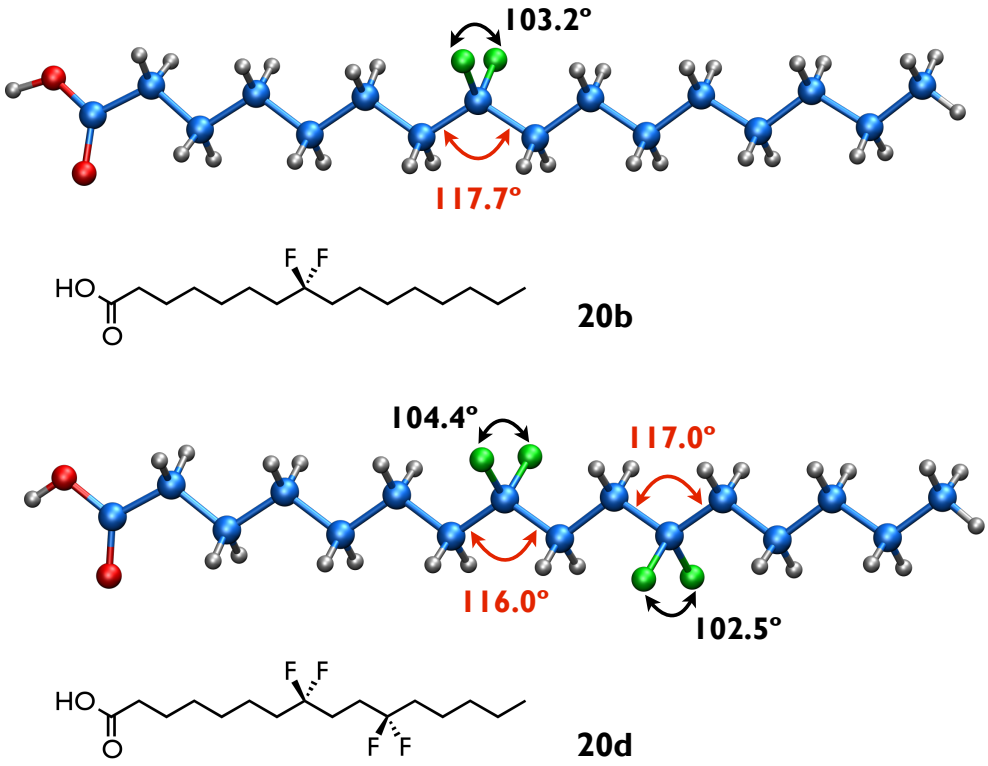

Figure 1.11 The X-ray crystal structures of a) 8,8-difluorohehadecanoic acid **20b** b) 8,8,11,11-tetrafluorohexadecanoic acid **20d**, as determined by Wang and co-workers.[20]

In each case the CH_2-CF_2-CH_2 angles were found to be wider than the CH_2-CH_2-CH_2 angles of the aliphatic chain. The CH_2-CF_2-CH_2 angle increased to 117.7º in **20b**, and to 116.0º (at C8) and 117.0º (at C11) in **20d**. Concomitantly, narrowing of the F-C-F bond angle was observed for both hexadecanoic acids **20b** (103.2º) and **20d** (104.4º at C8 and 102.5º at C11). Following this observation it is clear that *gem*-difluorination induces a deviation in the CH_2-CF_2-CH_2 and F-C-F bond angles. This is consistent with

the trends observed for the previously discussed geometries of methane **11** and propane **8** carrying two *geminal* fluorine atoms.

It was rationalised that the *anti* parallel orientation of the fluorine atoms in the 1,4-di-CF_2 motif offers an intramolecular dipole-dipole relaxation and provides stability and a higher molecular order in the solid state (Scheme 1.5).

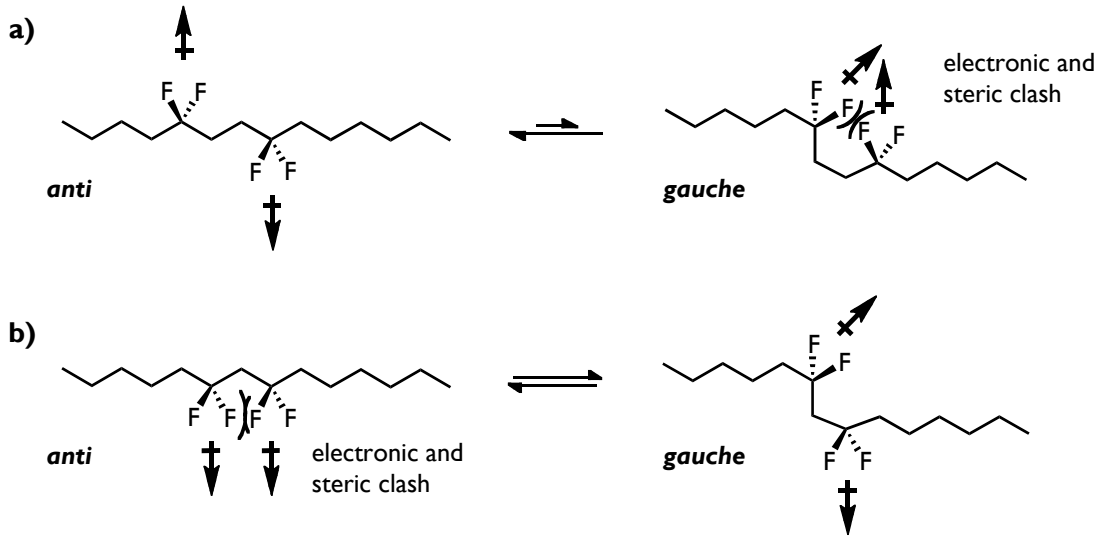

Scheme 1.5 Conformational interconversion of a) 1,4-di-CF_2 motif b) 1,3-di-CF_2 motif, as proposed by O'Hagan.[20]

The preferred conformation of **20c** could not be determined; however, the non-crystalline nature of the palmitic acid **20c** together with a low melting point relative to **20d** suggests a higher degree of disorder in the aliphatic chain. Maintaining the *anti* zig-zag conformation in **20c** would result in the two difluoromethylene groups pointing parallel to each other. Such a spatial orientation of the polarised fluorine atoms $^{\delta-}$F is unfavourable both due to dipolar repulsion and intramolecular 1,3-repulsion. The steric and electronic interaction can therefore account for the observed increased disorder of **20c**, bearing the 1,3-di-CF_2 motif.

1.2 Introduction of the *gem*-difluoride motif into organic molecules

Since organofluorine compounds find application as agrochemicals, pharmaceuticals and functional materials, methods of introducing fluorine into organic frameworks has become an important field of organic chemistry research. Nowadays, there is a range of reported methods for incorporating *gem*-difluoride groups.

1.2.1 *gem*-Difluorination with sulfur tetrafluoride

Carbonyl compounds can be converted into the corresponding *gem*-difluoromethylene derivatives by direct fluorination with sulfur tetrafluoride (SF_4) in the presence of anhydrous HF.[21] The mechanism for this reaction (Scheme 1.6), proposed by W. Dmowski[22] involves:

- generation of SF_3^+ as a strong electrophile, and then attack by the carbonyl oxygen;
- intramolecular transfer of fluoride to the highly electrophilic carbonyl group, followed by release of sulfonyl fluoride;
- neutralisation of the *α*-fluoro carbenium ion by addition of fluoride from $(FHF)^-$.

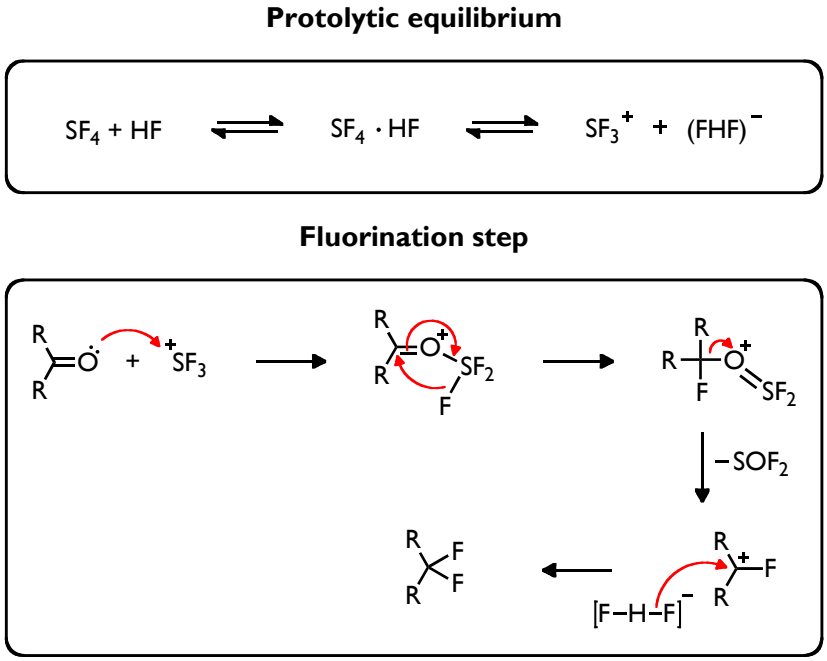

Scheme 1.6 Proposed mechanism of *gem*-difluorination of ketones with SF_4.[22]

SF_4 is also known to convert hydroxy and carboxylate groups into mono- and trifluoro-methyl groups respectively (Scheme 1.7).[22]

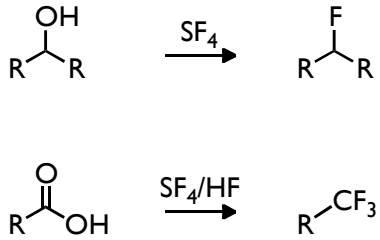

Scheme 1.7 Fluorination of alcohols and carboxylic acids with SF_4.[22]

Although SF_4 is a very versatile fluorinating agent, handling it is not very convenient. Sulfur tetrafluoride is a highly toxic and corrosive gas (b.p. = −38 ºC), and therefore all reactions must be carried out in autoclaves under elevated pressure, with careful consideration of safety measures to avoid HF exposure.[23]

1.2.2 *gem*-Difluorination with aminofluorosulfuranes

The necessity of developing safer and more easy to handle fluorinating agents, led to the introduction of diethylaminosulfur trifluoride (DAST) **22**, a liquid alternative to SF_4. DAST **22** is synthesised by treating diethylaminotrimethylsilane **22** with SF_4 (Scheme 1.8).[24]

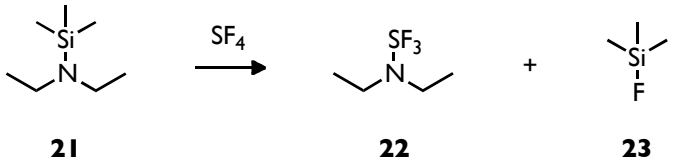

21 **22** **23**

Scheme 1.8 The synthesis of DAST **22**.[24]

DAST **22** (b.p. = 46-47 ºC)[24] is much easier to handle, although the increased steric demand decreases its reactivity in comparison to SF_4. The mechanism of fluorination is also different (Scheme 1.9).[25]

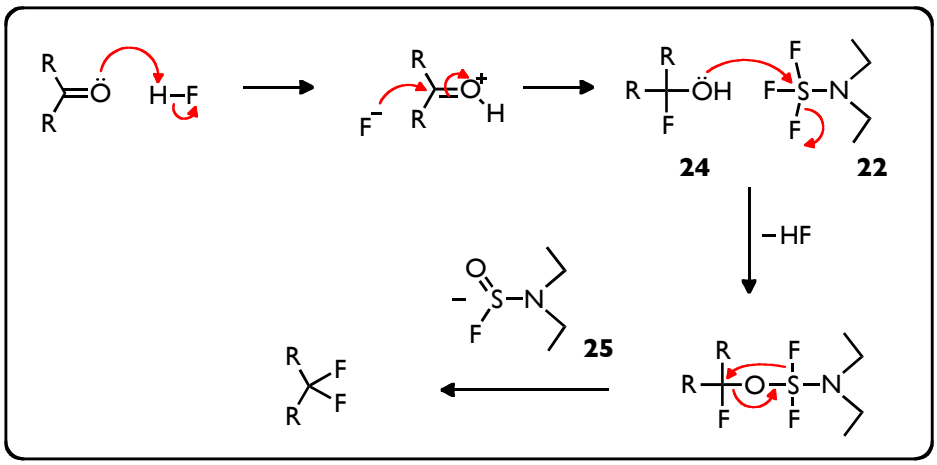

Scheme 1.9 Mechanism of *gem*-difluorination of carbonyl compounds with DAST **22**.[25]

The initial step involves the generation of HF from the reagent and requires traces of water. An *α*-fluoro alcohol **24** is then formed by HF addition onto the

carbonyl group. The oxygen of the newly formed hydroxyl group displaces the fluorine on the sulfur and this leads to elimination of HF. An intramolecular transfer of fluorine follows, from sulfur to carbon, eliminating *N,N*-diethylfluorosulfinamide **25**.

Due to the weak sulfur-nitrogen bond, DAST **22** undergoes a highly exothermic decomposition above 60 ºC, becoming potentially explosive at higher temperatures.[1,26]

DAST **22** has been successfully employed in deoxofluorination reactions of a range of organic substrates including alcohols, ketones, aldehydes and carboxylic acids (**26-29**) (Scheme 1.10).[27]

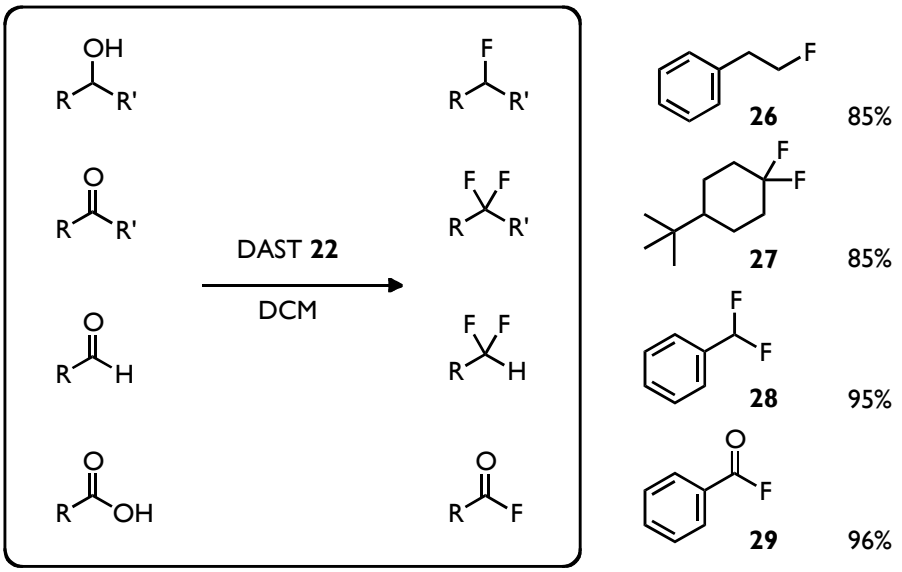

Scheme 1.10 Fluorination of various functional groups with DAST **22**.[27]

Other, more thermally stable SF_4 derivatives, such as bis(2-methoxyethyl)aminosulfur trifluoride – Deoxofluor[27] **30**,

morpholinosulfurtrifluoride – MOST[28] **31**, and 4-(*t*-butyl)-2,6-dimethyl-phenylsulphurtrifluoride - Fluolead[29,30] **32** have been developed (Figure 1.12).

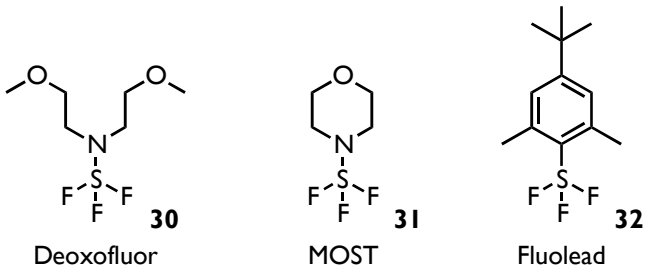

Figure 1.12 Alternative fluorinating agents to DAST **22**.

Although the decomposition temperature of Deoxofluor **30** is similar to that reported for DAST **22**, the rate of a thermal run-away reaction is significantly lower and it occurs without subsequent explosion.[1] Both MOST **31** and Fluolead **32** are thermally more stable than DAST **22** and Deoxofluor **30**. Lack of a sulfur-nitrogen bond in Fluolead **32** significantly increases its stability and it can be readily used at temperatures up to 150 ºC.

1.2.3 Dialkylaminodifluorosulfinium salts

Recently, XtalFluor-E **33** and XtalFluor-M **34**, crystalline dialkylaminodifluorosulfinium salts have been introduced as versatile fluorinating agents (Figure 1.13).[26,31]

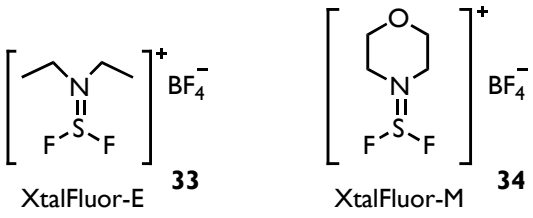

Figure 1.13 Dialkylaminodifluorosulfinium salts XtalFluor-E (**33**) and XtalFluor-M (**34**).

These reagents are synthesised directly from DAST **22** or MOST **31** with boron trifluoride, as presented in Scheme 1.11.

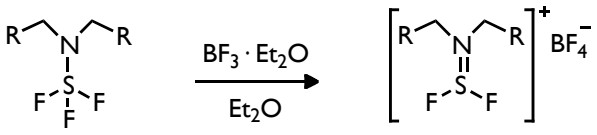

Scheme 1.11 Preparation of dialkylaminodifluorosulfinium tetrafluoroborate salts from aminofluorosulfuranes and $BF_3{\cdot}Et_2O$.[31]

Unlike the previously described aminofluorosulfuranes **22, 30** and **31**, these salts do not generate free HF upon hydrolysis, and therefore HF promoters, such as triethylamine trihydrofluoride (TREAT-HF) are required for efficient transformation. So far, they have displayed high activity in fluorination reactions of a range of organic compounds, such as alcohols, ketones, aldehydes and carboxylic acids (**27**,**35-37**) (Scheme 1.12).

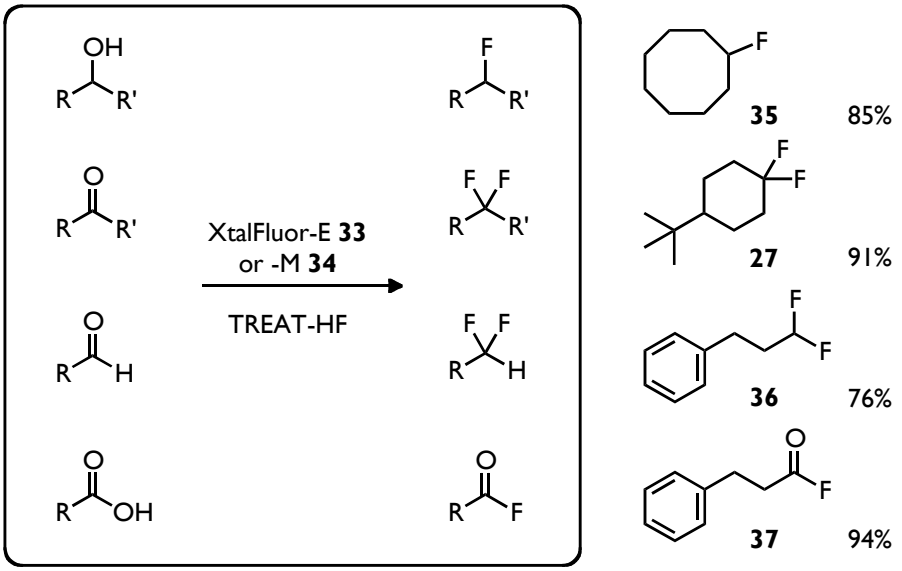

Scheme 1.12 Fluorination of various functional groups with XtalFluor-E (**33**) or -M (**34**) in the presence of TREAT-HF.[26,31]

The enhanced thermal stability of dialkylaminodifluorosulfinium salts **33-34** enables their use at much higher temperatures, in comparison with the corresponding aminofluorosulfuranes **22** and **31**. It often shortens the reaction time and enables fluorination of more resistant substrates. XtalFluor-E (**33**) and XtalFluor-M (**34**) are relatively new reagents and their scope and value remains to be fully determined.

1.2.4 Oxidative fluorodesulfurisation

Sondej and Katzenellenbogen have described an oxidative fluorodesulfurisation method for *gem*-difluorination.[32] Ketones are readily converted into their corresponding dithioacetal derivatives upon reaction with ethanedithiol in the presence of a Lewis acid. The resulting thioacetals undergo reactions with soft electrophilic oxidants, in the presence of a ~70% w/w solution of anhydrous hydrogen fluoride-pyridine (HF-pyridine)[33] (Scheme 1.13).

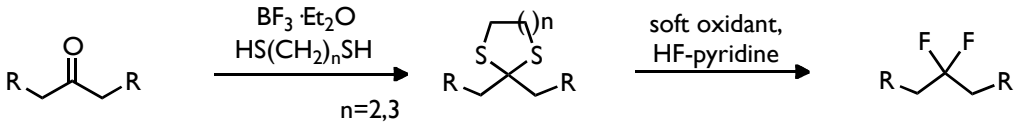

Scheme 1.13 *gem*-Difluorination of carbonyl compounds through dithioacetalisation and subsequent oxidative fluorodesulfurisation.

The most commonly employed reagents for this transformation include 5,5-dimethyl-1,3-dibromohydantoin (DBH) **38** or *N*-iodosuccinimide (NIS) **40** (Figure 1.14).[32]

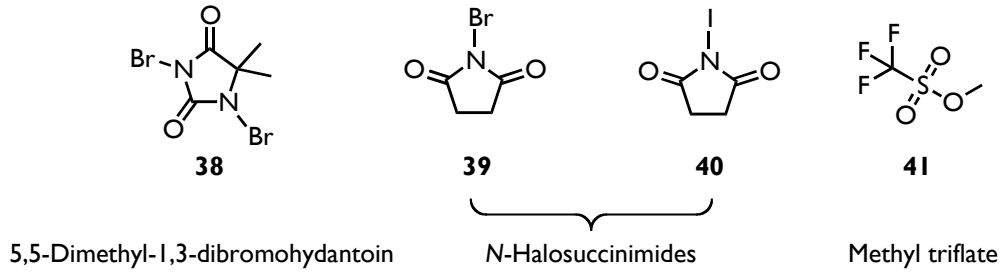

Figure 1.14 Soft electrophilic reagents employed in oxidative fluorodesulfurisation reactions.

The initial step of the oxidative fluorodesulfurisation involves attack of the dithioacetal sulfur atom on the electrophilic halide X^+, affording a halosulfonium intermediate **42** (Scheme 1.14). This intermediate **42** undergoes ring-opening to give a sulfur-stabilised carbocation **43,** which is subsequently captured by fluoride ion. The second sulfur atom reacts then with X^+ to give the halosulfonium intermediate **44**. The second fluorine atom is indroduced through a S_N2 reaction affording the final *gem*-difluoro product.[34]

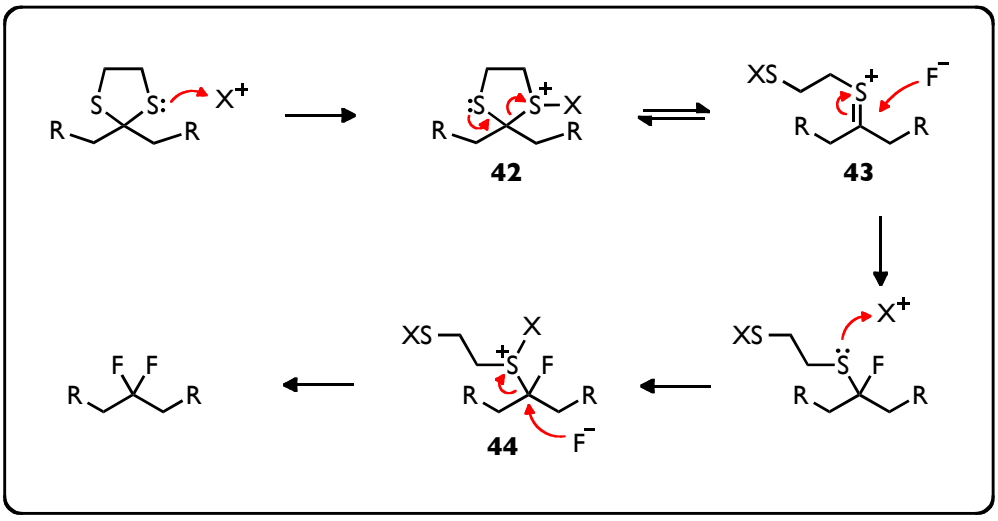

Scheme 1.14 Proposed mechanism of oxidative fluorodesulfurisation of dithiolanes.[34]

Various dithioacetals **45-47** have been successfully converted to their corresponding *gem*-difluorides **48-50** employing oxidative fluorodesulfurisation (Scheme 1.15).

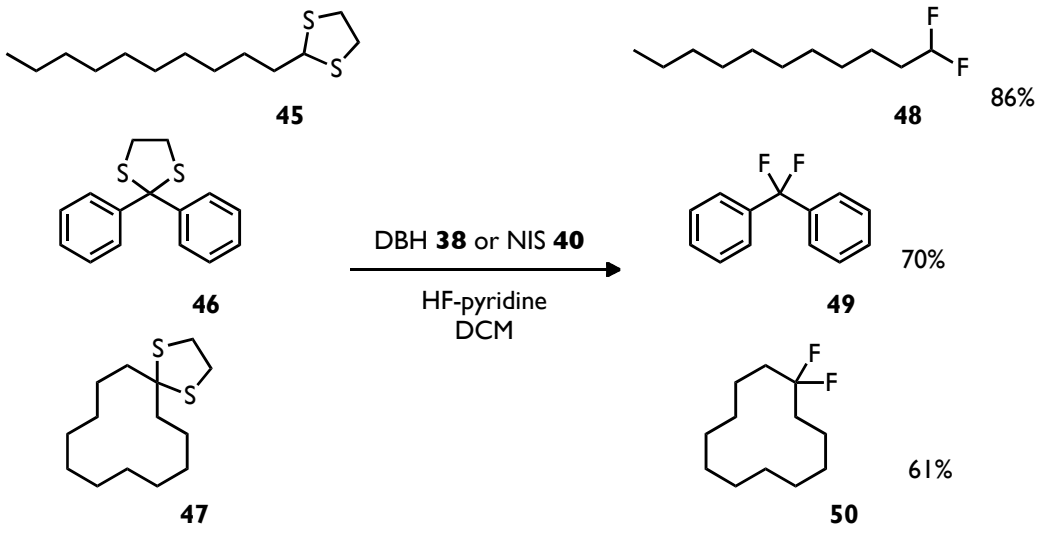

Scheme 1.15 Examples of *gem*-difluorination of 1,3-dithioacetals **45-47** employing HF-pyridine and DBH **38** or NIS **40**.[32]

Hydrogen fluoride pyridine solution is very corrosive, thus oxidative fluorodesulfurisation reactions need to be carried out in PTFE vessels. In 1995, Fujisawa and co-workers proposed a modified protocol for oxidative fluorodesulfurisation avoiding the use of HF-pyridine.[34] A variety of *gem*-difluorides (**50, 54, 55**) can be readily accessed from their corresponding 1,3-dithiolanes (**47, 51, 52**) on treatment with *N,N*-diethyl-1,1,2,3,3,3-hexafluoropropylamine **53**, water and a thiophilic oxidant *e.g.* DBH **38** or NIS **40** (Scheme 1.16). Reagent **53**, also known as Ishikawa's reagent, was originally prepared as a deoxofluorination reagent and was widely employed for the fluorination of alcohols and carboxylic acids, affording alkyl and acyl fluorides.[35]

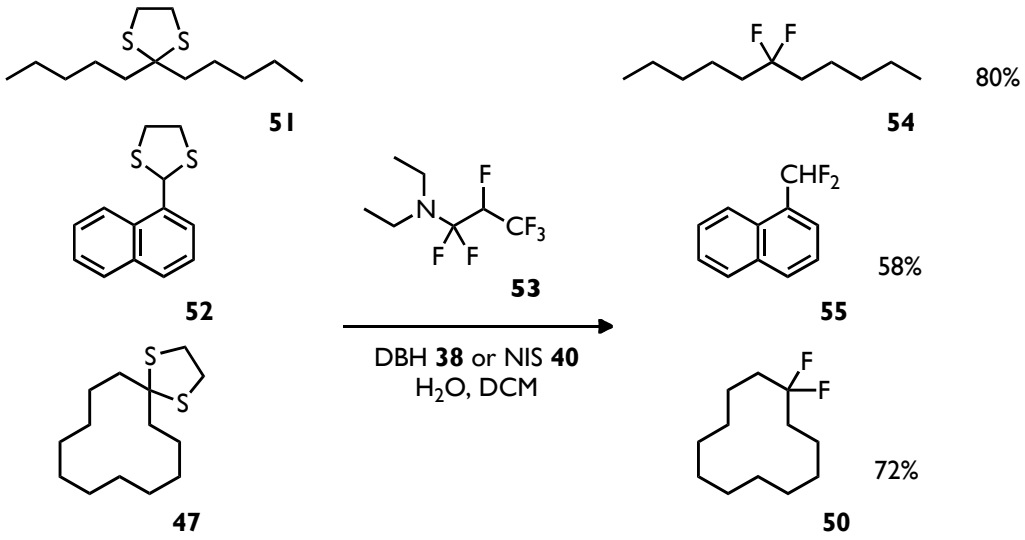

Scheme 1.16 Oxidative fluorodesulfurisation of 1,3-dithiolanes using Ishikawa's reagent **53**.[34]

The reaction mechanism of this modified method proceeds similarly to the mechanism of oxidative fluorodesulfurisation presented in Scheme 1.14. However, in this case, hydrogen fluoride is generated from *N,N*-diethyl-1,1,2,3,3,3-hexafluoropropylamine **53** and water (Scheme 1.17).[35]

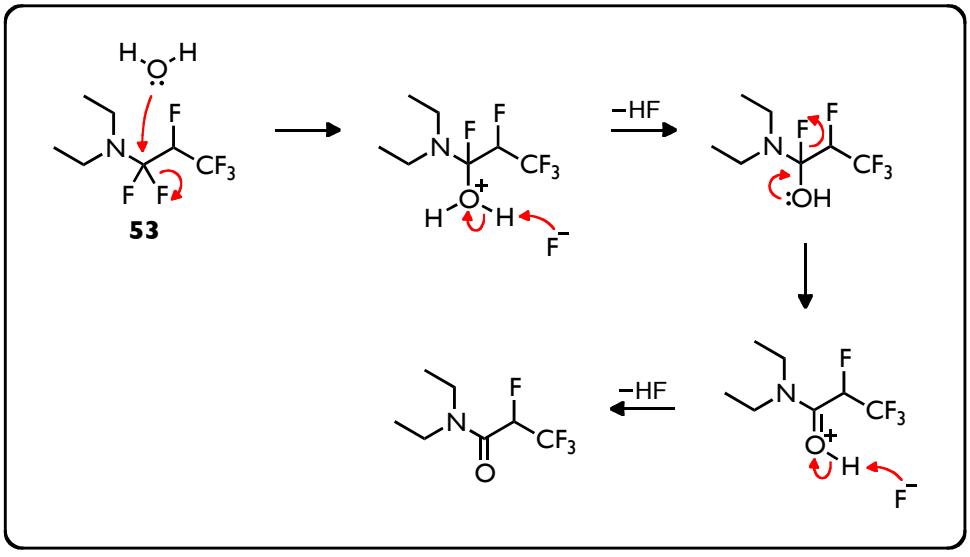

Scheme 1.17 Generation of HF from *N,N*-diethyl-1,1,2,3,3,3-hexafluoropropylamine **53** and water based on a reaction mechanism of the reagent **53** with alcohols.[35]

1.2.5 *gem*-Difluorination of carbonyl compounds using BrF_3

In 1994, Rozen's group reported a novel method for incorporating the *gem*-difluorine motif into hydrocarbon molecules using commercially available bromine trifluoride (BrF_3).[36] Bromine trifluoride, an interhalogen compound, contains a non-solvated, highly reactive fluoride, along with a highly electrophilic bromonium species.

Rozen's methodology involves transformation of the parent ketones to their corresponding hydrazones, oximes or azines (Scheme 1.18). Subsequent *gem*-difluorination occurs readily upon reaction with BrF_3. This reaction requires air and moisture free conditions, using halogenated solvents, such as $CHCl_3$, $CFCl_3$, CCl_4, since BrF_3 reacts violently with oxygenated solvents and water.[36,37]

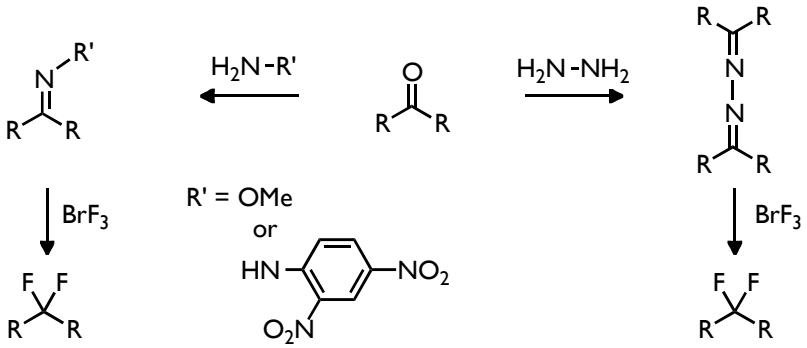

Scheme 1.18 Transformation of ketones to the corresponding hydrazones, oximes or azines followed by subsequent *gem*-difluorination using BrF_3 as proposed by Rozen.[36]

A variety of *gem*-difluorides including **59**, **60** and **61** have been accessed from their corresponding hydrazones **56**, **57** and **58**, employing BrF_3 (Scheme 1.19).[36] The main limitation of this method is the reactivity of the electrophilic bromine with aromatic substrates.

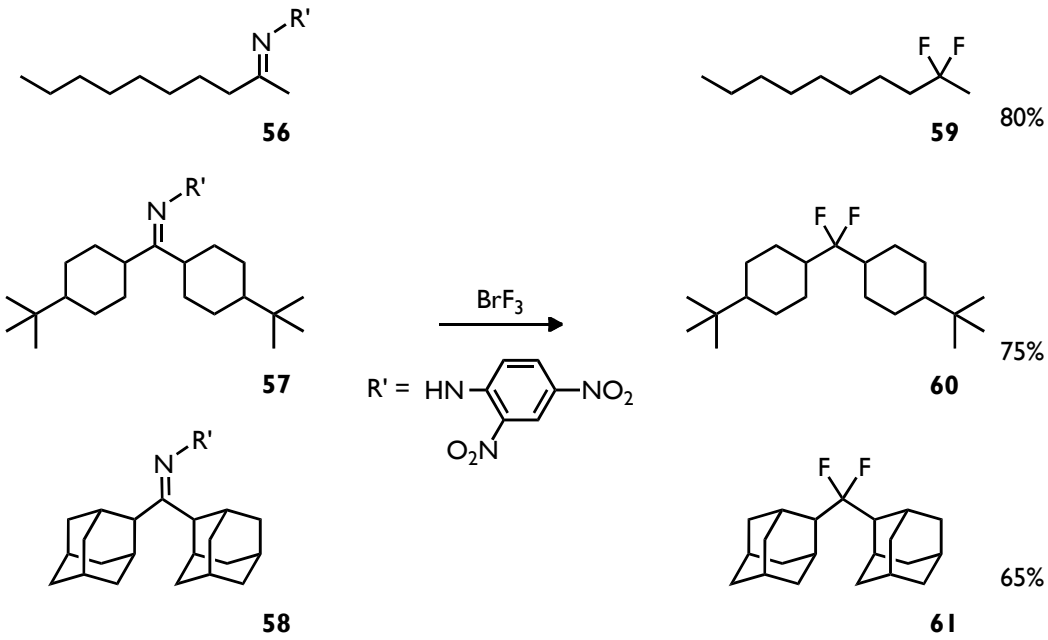

Scheme 1.19 *gem*-Difluorination of hydrazones **56-58** using BrF_3.[36]

In a more recent study Rozen employed BrF_3 in the *gem*-difluorination of 1,3-dithianes.[38] However, the scope of this research was limited to transformations involving only 2-alkyl-1,3-dithianes (Scheme 1.20).

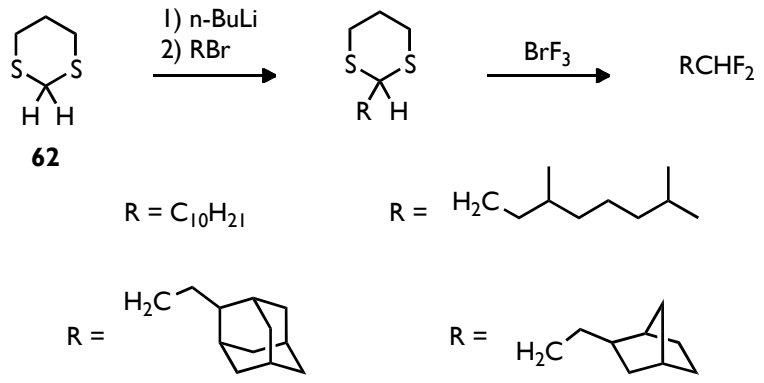

Scheme 1.20 Formation of 2-alkyl-dithianes from 1,3-dithiane **62** followed by *gem*-difluorination using BrF_3 as proposed by Rozen.[38]

Although no mechanistic studies have been carried out, the authors comment that the sulfur or nitrogen atoms coordinate to the electron deficient,

hypervalent bromine, followed by a subsequent nucleophilic addition of fluoride to the electrophilic carbon.[37]

1.2.6 *gem*-Difluorination of carbonyl compounds *via* *gem*-bistrifluoacetates

In 2010, Tojo and coworkers presented a novel, two-step *gem*-difluorination method.[39] In this protocol, ketones react with trifluoroacetic anhydride (TFAA), affording *gem*-bistrifluoroacetates. These compounds can be easily converted to their corresponding *gem*-difluorides using HF-pyridine in the presence of trifluoroacetic acid (TFA) (Scheme 1.21).

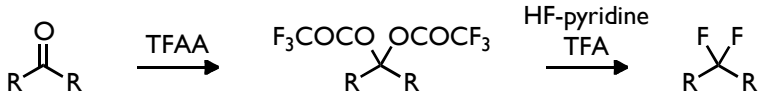

Scheme 1.21 Transformation of ketones to the corresponding *gem*-bistrifluoroacetates followed by *gem*-difluorination using HF-pyridine and TFA.

Addition of a catalytic amount of TFA initiates the reaction by protonating the carbonyl group of the bistrifluoroacetate (Scheme 1.22). The trifluoroacetoxy group is then replaced with fluoride *via* nucleophilic substitution. The second fluorine atom is installed in the same manner through protonation of the carbonyl group and subsequent substitution with the fluoride.[39]

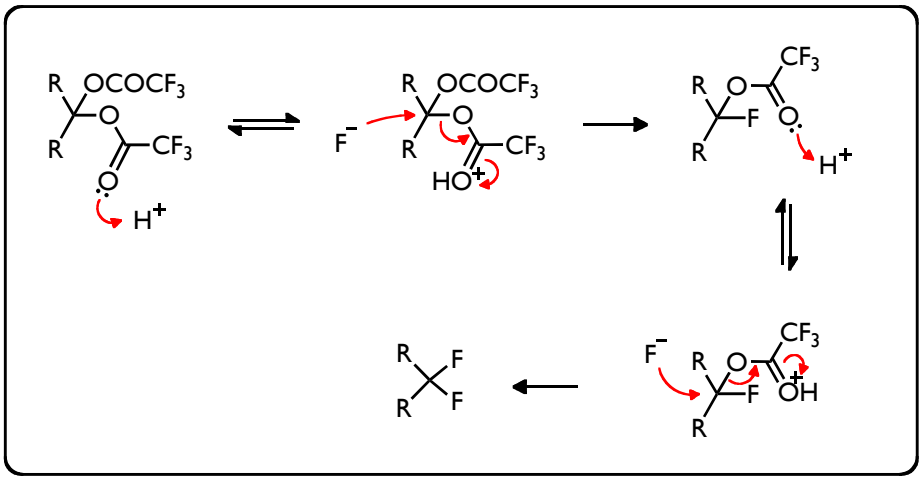

Scheme 1.22 Putative mechanism for the formation of *gem*-difluorides from the *gem*-bistrifluoroacetate precursors.[39]

A variety of ketones, such as cycloheptanone **63**, heptan-5-one **64** or acetophenone **65** were efficiently converted to their corresponding *gem*-difluorides **66-68** employing Tojo's methodology (Scheme 1.23).[39,40]

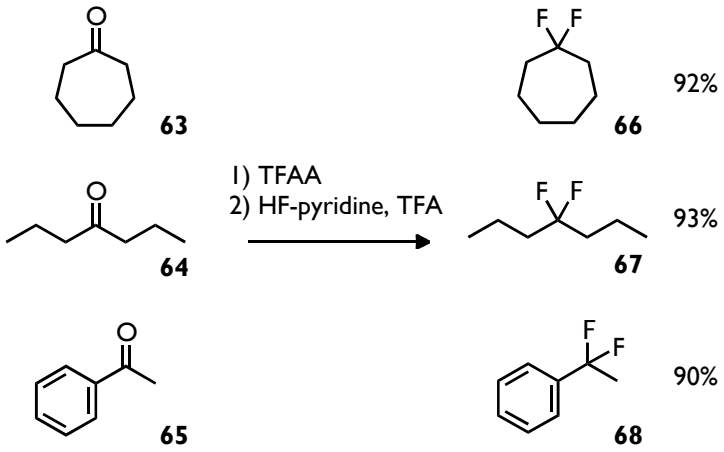

Scheme 1.23 Examples of *gem*-difluorination using Tojo's methodology.[40]

1.3 Aims and objectives

The examples presented in the introduction show that incorporation of fluorine into hydrocarbons can alter their physical properties.

The aim of the research presented in this thesis is to further investigate the influence of the difluoromethylene motif as a group that could be used as a design feature to influence the conformation of alicyclic and open-chain hydrocarbon systems.

1.4 References

1. P. Kirsch, *Modern Fluoroorganic Chemistry: Reactivity, Applications*, Wiley-VCH, Weinheim, 2004.

2. D. O'Hagan, *Chem. Soc. Rev.*, 2008, **37**, 308–319.

3. K. Müller, C. Faeh, F. Diederich, *Science*, 2007, **317**, 1881–1886.

4. K. L. Kirk, *Org. Process Res. Dev.*, 2008, **12**, 305–321.

5. S. Purser, P. R. Moore, S. Swallow, V. Gouverneur, *Chem. Soc. Rev.*, 2008, **37**, 320–330.

6. K. B. Wiberg, T. A. Keitht, M. J. Frischt, M. Murcko, *J. Phys. Chem.*, 1995, **99**, 9072–9079.

7. L. Goodman, H. Gu, V. Pophristic, *J. Phys. Chem. A*, 2005, **109**, 1223–1229.

8. D. Wu, A. Tian, H. Sun, *J. Phys. Chem. A*, 1998, **102**, 9901–9905.

9. L. Hunter, A. M. Z. Slawin, P. Kirsch, D. O'Hagan, *Angew. Chem. Int. Ed.*, 2007, **46**, 7887–7890.

10. L. Hunter, P. Kirsch, A. M. Z. Slawin, D. O'Hagan, *Angew. Chem. Int. Ed.*, 2009, **48**, 5457–5460.

11. H.-G. Mack, M. Dakkouri, H. Oberhammer, *J. Phys. Chem.*, 1991, **95**, 3136–3138.

12. K. J. Donald, M. C. Böhm, H. J. Lindner, *J. Mol. Struct.*, 2004, **710**, 1-11.

13. K. B. Wiberg, P. R. Rablen, *J. Am. Chem. Soc.*, 1993, **115**, 614–625.

14. H. A. Bent, *Chem. Rev.*, 1960, **61**, 275–311.

15. S. N. Pieniaze, K. N. Houk, *Angew. Chem. Int. Ed.*, 2006, **45**, 1442–1445.

16. W. R. Dolbier, A. C. Alty, O. Phanstiel, *J. Am. Chem. Soc.*, 1987, **109**, 3046–3050.

17. L. Dasaradhi, D. O'Hagan, M. C. Petty, C. Pearson, *J. Chem. Soc. Perkin Trans. 2*, 1995, 221–225.

18. D. O'Hagan, I. Kumadaki, M. Petty, H. Takaya, C. Pearson, *J. Fluorine Chem.*, 1998, **90**, 133–138.

19. Y. Wang, M. Skibiński, A. M. Z. Slawin, D. O'Hagan, *Pure Appl. Chem.*, 2012, **84**, 1587–1595.

20. Y. Wang, R. Callejo, A. M. Z. Slawin, D. O'Hagan, *Beilstein J. Org. Chem.*, 2013, **111**.

21. D. R. Strobach, G. A. Boswell, *J. Org. Chem.*, 1971, **36**, 818–820.

22. W. Dmowski, *J. Fluorine Chem.*, 1986, **32**, 255–282.

23. T. Nickson, *J. Fluorine Chem.*, 1991, **55**, 169–172.

24. W. J. Middleton, *J. Org. Chem.*, 1975, **40**, 574–578.

25. M. Hudlicky, *Org. React.*, 1987, **35**, 513–637.

26. A. L'Heureux, F. Beaulieu, C. Bennett, D. R. Bill, S. Clayton, F. Laflamme, M. Mirmehrabi, S. Tadayon, D. Tovell, M. Couturier, *J. Org. Chem.*, 2010, **75**, 3401–3411.

27. G. S. Lal, G. P. Pez, R. J. Pesaresi, F. M. Prozonic, *J. Org. Chem.*, 1999, **64**, 7048–7054.

28. L. N. Markovskij, V. E. Pashinnik, A. V. Kirsanov, *Synthesis*, 1973, 787-789.

29. T. Umemoto, R. P. Singh, 2008, 1–34.

30. T. Umemoto, R. P. Singh, Y. Xu, N. Saito, *J. Am. Chem. Soc.*, 2010, **132**, 18199–18205.

31. F. Beaulieu, L.-P. Beauregard, G. Courchesne, M. Couturier, F. LaFlamme, A. L'Heureux, *Org. Lett.*, 2009, **11**, 5050–5053.

32. S. C. Sondej, J. A. Katzenellenbogen, *J. Org. Chem.*, 1986, **51**, 3508–3513.

33. C. G. Bergstrom, R. T. Nicholson, R. M. Dodson, *J. Org. Chem.*, 1963, **28**, 2633–2640.

34. M. Shimizu, T. Maeda, T. Fujisawa, *J. Fluorine Chem.*, 1995, **71**, 9–12.

35. A. Takaoka, H. Iwakiri, N. Ishikawa, *Bull. Chem. Soc. Jpn.*, 1979, **52**, 3377–3380.

36. S. Rozen, E. Mishani, A. Bar-Haim, *J. Org. Chem.*, 1994, **59**, 2918.

37. S. Rozen, *Acc. Chem. Res.*, 2005, **38**, 803–12.

38. R. Sasson, A. Hagooly, S. Rozen, *Org. Lett.*, 2003, **5**, 769–771.

39. M. Tojo, S. Fukuoka, H. Tsukube, *J. Fluorine Chem.*, 2010, **131**, 29–35.

40. S. Fukuoka, M. Tojo, *Jpn. Kokai Tokkyo Koho*, 1989, JP 1–199922.

2

Synthesis and structure of CF_2-cyclododecanes

2.1 Introduction

2.1.1 Cyclododecane – conformation and disorder

In 1960 the Scottish crystallographer Jack Dunitz published the X-ray study of cyclododecane **69**,[1] showing that the twelve-membered ring had a square-like structure. Each edge was built of four nearly planar *anti* zig-zag methylene units (Figure 2.1). Cyclododecane **69** is the smallest cycloalkane, which can be crystallised at room temperature, however, at that time, Dunitz was not able to precisely determine the arrangement of the hydrogen atoms within the crystal structure because of the high level of crystal disorder. The corner CH_2-CH_2-CH_2 bond angles (116-117º) were found to be wider than the typical tetrahedral angle (109.5º). Such distortion suggests a certain degree of angle strain in the cyclododecane ring.

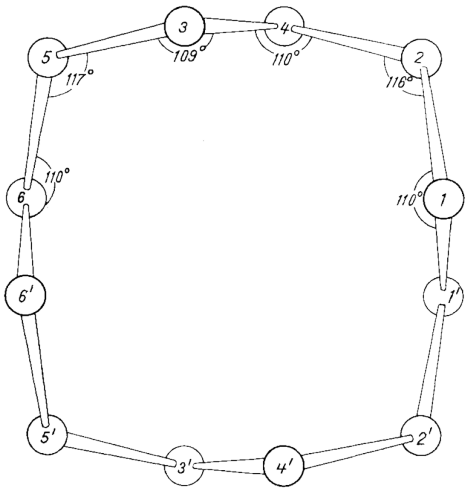

Figure 2.1 X-ray crystal structure of cyclododecane **69** as determined by Dunitz.[1]

The strain energy of cyclododecane **69** is relatively low in comparison with other cycloalkanes where it has the smallest strain energy of the medium size rings (n = 7-12) (Table 2.1).[2]

$(CH_2)_n$	***Strain energy (kcal mol^{-1})***	$(CH_2)_n$	***Strain energy (kcal mol^{-1})***
3	27.5	10	12.4
4	26.3	11	11.3
5	6.2	12	4.1
6	0.1	13	5.2
7	6.2	14	1.9
8	9.7	15	1.9
9	12.6	16	2.0

Table 2.1 Strain energy of (3-16)-membered cycloalkanes.[2]

2.1.2 Strain in alicyclic systems

The concept of ring strain was first proposed by Adolf von Baeyer in 1885. He correctly assumed that three and four membered hydrocarbon rings are of high energy because of the deviation of bond angles from tetrahedral,[3] and summarized his angle strain theory; "*The four valences of the carbon atom act in the directions that connect the center of a sphere with the corners of a tetrahedron and that form an angle of 109°28' with each other. The direction of the attraction can experience a deviation, that will, however, cause an increase in strain correlating with the degree of this deviation.*"[4]

Adolf von Baeyer applied his analysis to six and higher membered rings, which he considered to be planar, with deformations of valency angles. At that time, von Baeyer did not appreciate that these rings would be nonplanar, nevertheless strain is present in medium rings (C_7-C_{12}), although it is not caused solely by deviation of bond angles. The total strain of cyclic hydrocarbons can be viewed to consist of three components:

- angle strain (von Baeyer's strain) – which arises from non-standard bond angles.
- torsional strain (Pitzer strain) – which arises from deviation from preferred torsion angles: "*medium rings cannot adopt exclusively staggered, energetically favorable, partial conformations without leading to unacceptably short distances between hydrogen atoms belonging to transannular methylene groups*"[5]

- transannular strain (van der Waals strain) – which arises from repulsive interactions between non-bonded atoms, when their distances are below the sum of their van der Waals radii (VDW) (Table 2.2)

Atom	*VDW* (Å)	*Atom*	*VDW* (Å)	*Atom*	*VDW* (Å)
C	1.77	**O**	1.50	**Cl**	1.82
H	1.20	**S**	1.89	**Br**	1.86
N	1.66	**F**	1.46	**I**	2.04

Table 2.2 Van der Waals radii of selected atoms.[6]

Experimental strain values are generally determined from the difference between the heat of combustion of the cycloalkane and the corresponding strain free *n*-alkane with the same number of carbons, *e.g.* cyclopropane and propane. As strain energy depends on the mutual arrangement of atoms and bonds in space, it is essential to determine the molecular structure in order to expose the source of ring strain.

2.1.3 Conformational analysis of medium and large cycloalkanes

In 1973, an energy minimisation study presented by Johannes Dale, gave a good indication about the possible conformations of a number of medium and large cycloalkanes including cyclododecane **69**.[7] The calculations only considered the changes in the dihedral angles at the C-C bonds, while the

deformation of the valence angles and changes in bond lengths were ignored. Formation of a cyclic hydrocarbon from a linear *anti* zig-zag chain requires a certain number of *gauche* arrangements in the structure. As these are higher in energy, the preferred conformers tend to have the fewest possible number of *gauche* bonds. Dale's study revealed that the most favourable conformers of even-membered rings tend to adopt quadrangular shapes, typically a square or rectangle. Less regular conformations were also found to be permitted but were higher in energy. Quadrangular conformations have four corner carbon atoms, *gauche*-linked with their 'neighbouring' methylene groups. These bridging units are organised as linear *anti* zig-zag chains. Figure 2.2 shows the four possible combinations of numbers of even or odd bonds that can result in a quadrangular conformation of the even-memberd cycloalkanes.

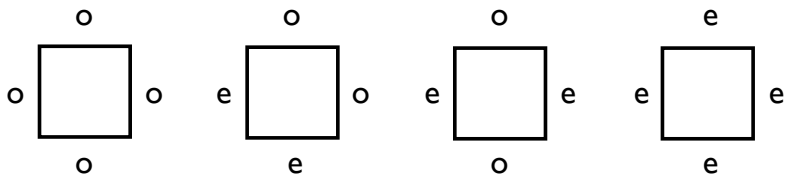

Figure 2.2 Allowed combinations of ring sides with even (e) or odd (o) number of bonds in even-membered cycloalkanes.[7]

For the odd-membered rings, three- or five-corner conformations were found to be preferred. These are limited to only two triangular and four pentangular conformations (Figure 2.3.).

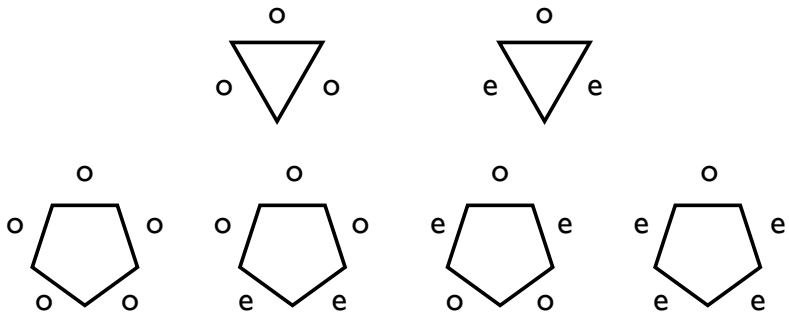

Figure 2.3 Allowed combinations of odd-membered ring sides with even (e) or odd (o) number of bonds.[7]

Each number (o or e) equals the sum of bonds between two corners of the ring. Dale introduced a simple notation system, which became a useful tool in describing different conformers of cycloalkanes. The so-called Dale's notation represents a set of numbers for one conformer, placed in a square bracket, starting with the lowest. Each of the three lowest conformers of cyclododecane **69** is characterised by a different numerical representation, anticipating deviation in the arrangement of the carbon skeleton (Figure 2.4).

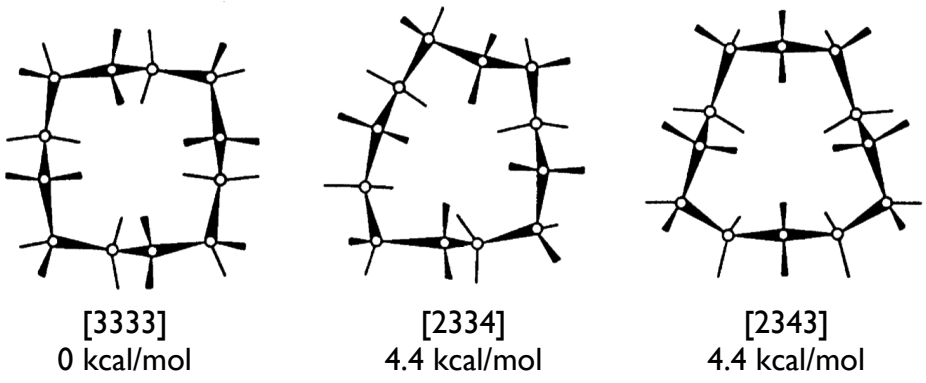

Figure 2.4 The energy differences between conformations of cyclododecane **69** as determined by Dale.[7]

The preferred square conformer in Figure 2.4 is identical to the X-ray crystal structure proposed by Dunitz.[1] There are three bonds between each of the

four corners, hence the [3333] notation. The next lowest conformers, [2334] and [2343], deviate from the square conformation, as a result of rearranged corner positions. Both were found to be over 4 kcal/mol higher in energy[7] presumably due to unfavourable steric interactions, originating from angular, torsional and intra-annular distortions.

Based on X-ray and computational studies, Dunitz proposed an 'averaged' model of cyclododecane **69**, describing the arrangement of the hydrogen atoms in space.[5] In the square [3333] structure (Figure 2.5), eight 'intra-annular' hydrogen atoms are pointing towards the centre of the molecule and eight 'extra-annular' are pointing outside the ring.

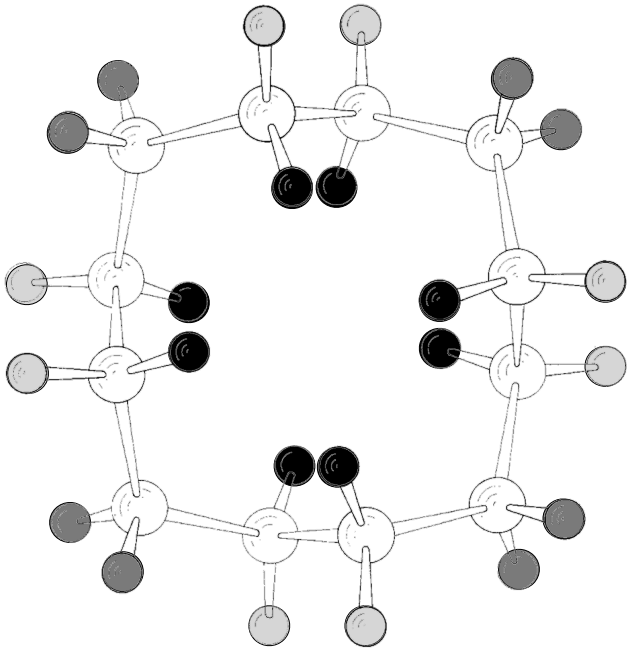

Figure 2.5. Cyclododecane **69** – 'averaged' molecular model with intra-annular (●), extra-annular (●) and corner (●) hydrogens, as determined by Dunitz.[5]

The shortest nonbonded 1,4-H,H distances between the intra-annular hydrogen atoms lie in van der Waals proximities (2.0 - 2.1 Å). As this range

falls below the sum of the van der Waals radii (H,H 2.40 Å) there is substantial strain due to repulsive transannular interactions. The limited space in the centre of the ring makes substitution of the hydrogens very difficult and substitution would cause a significant deformation of the carbon skeleton.

Building on the previously calculated conformational minima of medium and large cycloalkanes, Dale extended the investigation to the conformations of *gem*-dimethyl substituted alicyclic derivatives.[8] He predicted that substitution with a single *gem*-dimethyl motif is restricted to the corner position in all of the rings examined in the study ($C_{9\text{-}16}$). In the case of *gem*-dimethyl disubstitution, the $(CH_3)_2$ groups must adopt the corner positions of the ring, if the conformation is to remain unperturbed. As shown in Figure 2.6, 1- (**A**), 1,4- (**B**) And 1,7- (**C**) *gem*-dimethyl substitution of cyclododecane **69** does not result in perturbation of the ring conformation.

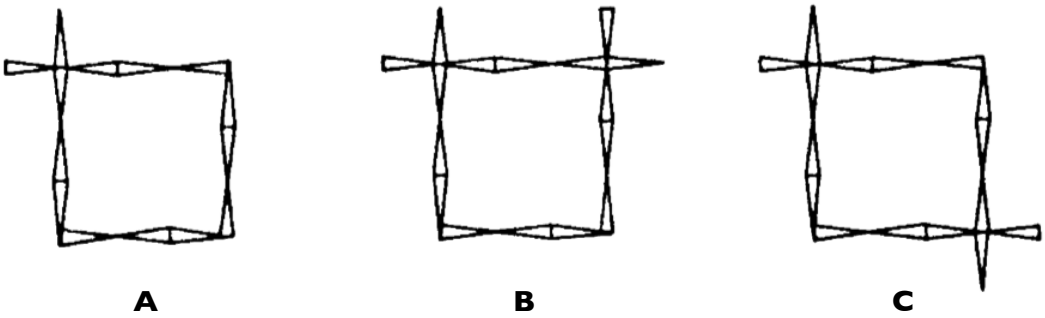

Figure 2.6 The lowest energy conformations of 1,1-dimethylcyclododecane (**A**), 1,1,4,4-tetramethylcyclododecane (**B**) and 1,1,7,7-tetramethylcyclododecane (**C**), as determined by Dale.[8]

On the other hand, if the relative positions of the two *gem*-dimethyl groups do not correspond to corner atoms, the ring conformation is distorted in such way as to enable the *gem*-dimethyl substituents to avoid edge positions. The

corners in 1,1,5,5- and 1,1,6,6- tetramethylcyclododecanes are rearranged, in order to accommodate both of these bulky *gem*-dimethyl groups, as shown in Figure 2.7.

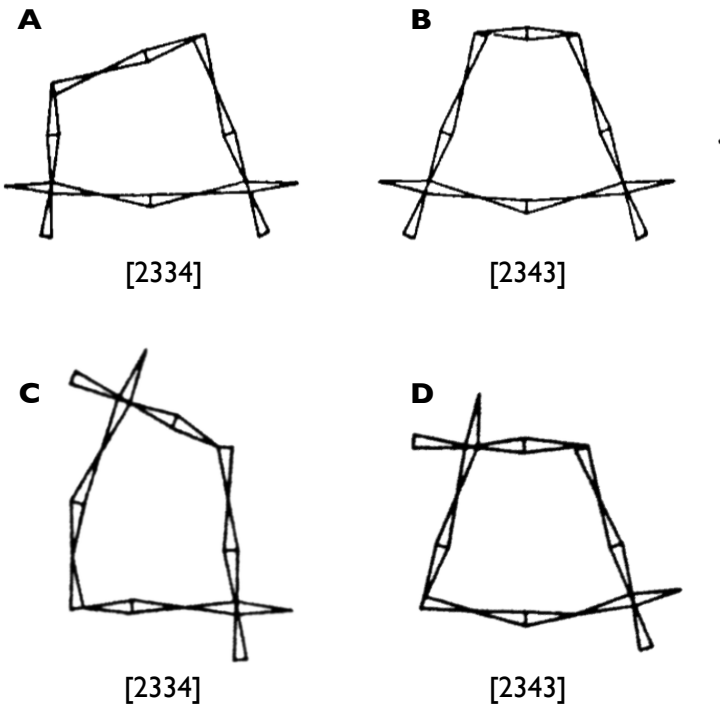

Figure 2.7 The two lowest energy conformations of 1,1,5,5-tetramethylcyclododecane (**A**, **B**) and 1,1,6,6-tetramethylcyclododecane (**C, D**), as determined by Dale.[8]

2.2 Aims of the project

Building on the modelling studies and X-ray analysis of cyclododecane **69**,[1,5,7,8] it was decided to use cyclododecane as a framework to explore the nature of the *gem*-difluoro group on the conformation of alicyclic hydrocarbons.

As a preliminary to this study, an analysis of X-ray data within the Cambridge Structural Database (CSD) was conducted in order to investigate the

geometry of the $R^1CH_2CF_2CH_2R^2$ motifs. For all 36 motifs in this category, the CH_2-CF_2-CH_2 ***Θ*** bond angles are an average of ~117.7º, significantly wider than tetrahedral (Figure 2.8).

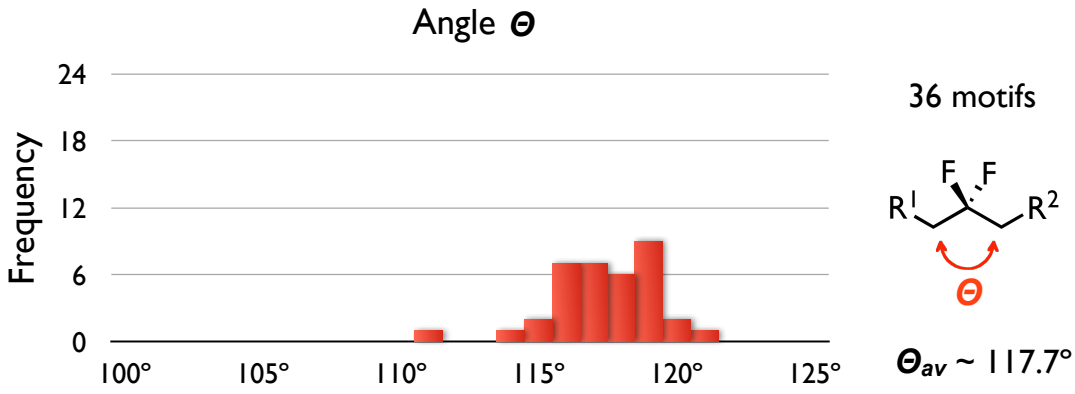

Figure 2.8 Histogram reporting the range of CH_2-CF_2-CH_2 ***Θ*** angles angles from 36 $R^1CH_2CF_2CH_2R^2$ motifs within the Cambridge Structural Database (CSD).

By contrast, the F-C-F ***Φ*** bond angles are narrower, with a range between 103º and 106º, significantly narrower than tetrahedral (Figure 2.9).

Figure 2.9 Histogram reporting the range of F-C-F ***Φ*** angles angles from 36 $R^1CH_2CF_2CH_2R^2$ motifs within the Cambridge Structural Database (CSD).

Based on the CSD search results it was envisaged that angle strain in cyclododecane **69** could be accommodated if the CF_2 group was installed in the corner of the cyclododecane ring. Additionally, incorporation of a *gem*-CF_2

motif into a cyclododecane ring would increase the degree of molecular order by limiting the number of possible conformations.

1,1-Difluorocyclododecane **50** had been previously prepared in the group by treatment of cyclododecanone **70** with SF_4 in the presence of HF (Scheme 2.1).

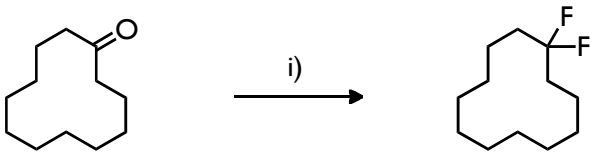

70 **50**

Scheme 2.1. *gem*-Difluorination of cyclododecanone **X** i) SF_4, HF, DCM.

Attempts to determine the X-ray crystal structure of this low-melting gel-like solid (m.p. = 44 ºC) proved difficult. Despite the presence of a single CF_2 motif, the molecule displayed a high degree of conformational disorder in the solid state. Despite many attempts a satisfactory structure could not be solved, however the disordered crystal structure did indicate that the most probable location of the CF_2 group was at the corner positions (Figure 2.10).

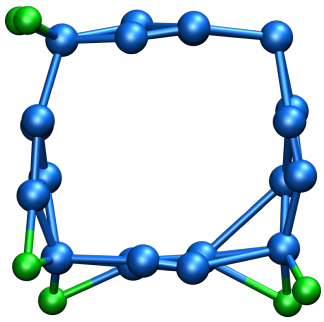

50

Figure 2.10 X-ray crystal structure of CF_2-cyclododecane **50** shows disorder. However fluorine density is present at the corners. (A. M. Z. Slawin)

Computational modelling also indicates the corner position as energetically more favoured for the CF_2 group. As part of this work, Prof. P. Kirsch of Merck (Darmstadt, Germany) carried out theory calculations to assess the relative energies of a corner *versus* an edge CF_2 in cyclododecane (Figure 2.11). The corner structure was calculated as being more stable by 2.86 kcal/mol.

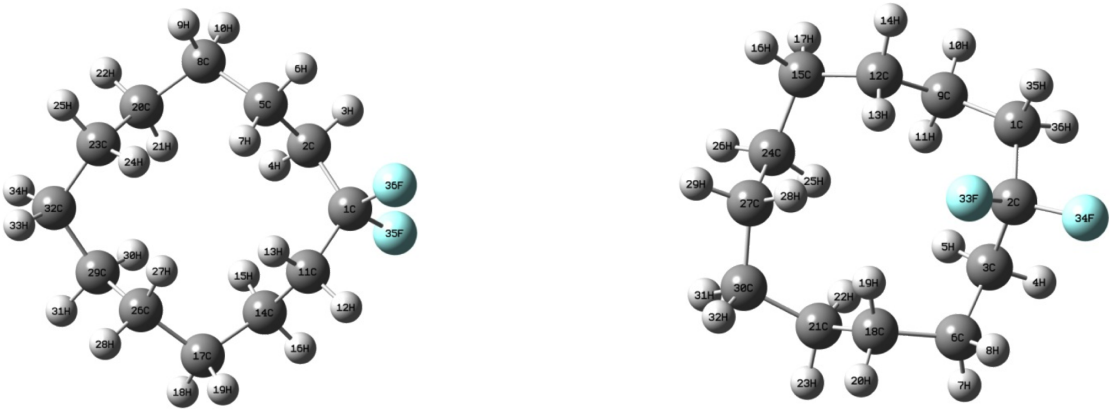

Figure 2.11 Gaussian modeling (MP2/6-311 + G(2d,p)//B3LYP/6-311 + G(2d,p) + ZPE) of 1,1-difluorocyclododecane **50**. (Peer Kirsch, Merck, Darmstadt)

It was anticipated that incorporation of a second CF_2 group at the corner position may offer structural stability to cyclododecane **69** by further limiting the number of possible conformations. Thus the 1,4- and 1,7-CF_2 compounds (**74** and **75**) became synthetic targets (Scheme 2.2a and 2.2b) in this project. Since the van der Waals radius of the fluorine atom is slightly larger than that of the hydrogen atom (1.46 Å *versus* 1.20 Å)[6], disubstitution in positions other than the corner may result in distortion of the conformation. In order to further explore the potential of the difluoromethylene motif to influence the conformation of cyclododecane **69**, 1,1,6,6-tetrafluorocyclododecane **76** was selected as a third synthetic target (Scheme 2.2c). In this case if a [3333] structure is maintained, then a CF_2 group is forced to an edge position.

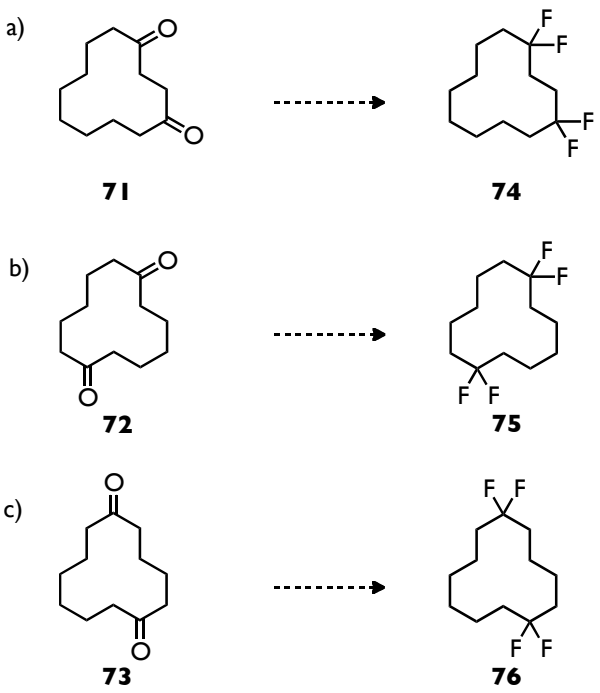

Scheme 2.2 Target CF_2-cyclododecanes: 1,1,4,4-tetrafluorocyclododecane **74**, 1,1,7,7-tetrafluorocyclododecane **75** and 1,1,6,6-tetrafluorocyclododecane **76**.

2.3 Results and discussion

2.3.1 Attempts to prepare 1,1-difluorocyclododecane

The difficulty of manipulating SF_4 from a health and safety perspective, forced the use of an alternative method for the introduction of the *gem*-difluoro groups. A number of strategies were examined in order to establish conditions for converting mono- and di-ketones to their corresponding *gem*-difluorides.

Syntheses of 1,1-difluorocyclododecane **50** were attempted using commercially available cyclododecanone **70** and a variety of fluorinating agents including DAST **22**, Deoxofluor **30**, MOST **31** and Fluolead **32** (Scheme 2.3). Reactions were monitored by ^{19}F NMR spectroscopy, and were

carried out in both THF and DCM, however, there was no sign of conversion of the ketone to the desired product or any partially fluorinated side products.

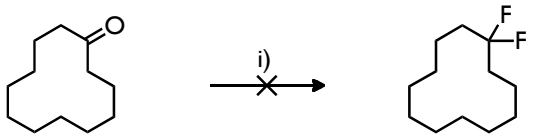

70 **50**

Scheme 2.3 Deoxofluorination of cyclododecanone **70**. Reagents and conditions: i) DAST **22** or Deoxofluor **30** or MOST **31** or Fluolead **32**, DCM or THF

It was anticipated that increasing the concentration of fluoride by combining a deoxofluorinating agent and a source of HF may provide forcing reaction conditions. A number of reactions were carried out starting with cyclododecanone **70**, a fluorinating agent and either HF-pyridine or triethylamine trihydrofluoride (TREAT-HF). Again, there was no sign of any organo-fluorination product.

Deoxofluorination at higher temperatures using the more thermally stable fluorinating agents, such as Fluolead **32** and XtalFluor-E **33** did not show any sign of a conversion to the desired product (Scheme 2.4).

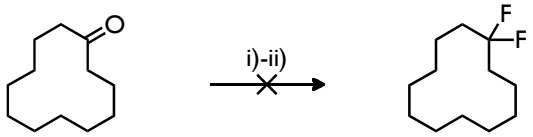

70 **50**

Scheme 2.4 Deoxofluorination of cyclododecanone **70** at higher temperatures. Reagents and conditions: i) XtalFluor-E **33**, TREAT-HF, DCE, 90 ºC, ii) Fluolead **32**, DME, 120 ºC, sealed PTFE vessel.

Oxidative fluorodesulfurisation[9] has been shown to generate *gem*-difluorination product from dithiolanes. Therefore this approach was

explored. In the event the conversion of cyclododecanone **70** to the corresponding 1,3-dithiolane **47** worked well generating the product in 85% yield (Scheme 2.5).

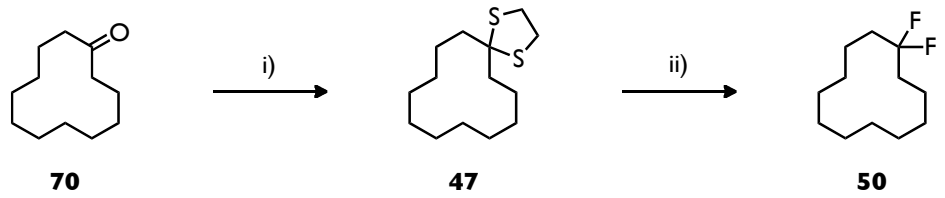

Scheme 2.5 Two-step route to 1,1-difluorocyclododecane **50**. Reagents and conditions: i) 1,2-ethanedithiol, BF_3·AcOH, RT, 85%; ii) NIS **40**, HF-pyridine, DCM, −78 ºC to RT, 32%.

This material was a colourless crystalline solid (m.p. 81-83 ºC), which allowed for X-ray structure analysis to be carried out. Two crystallographically independent structures were found in the unit cell (Figure 2.12) and both confirmed the expected [3333] ring conformation.

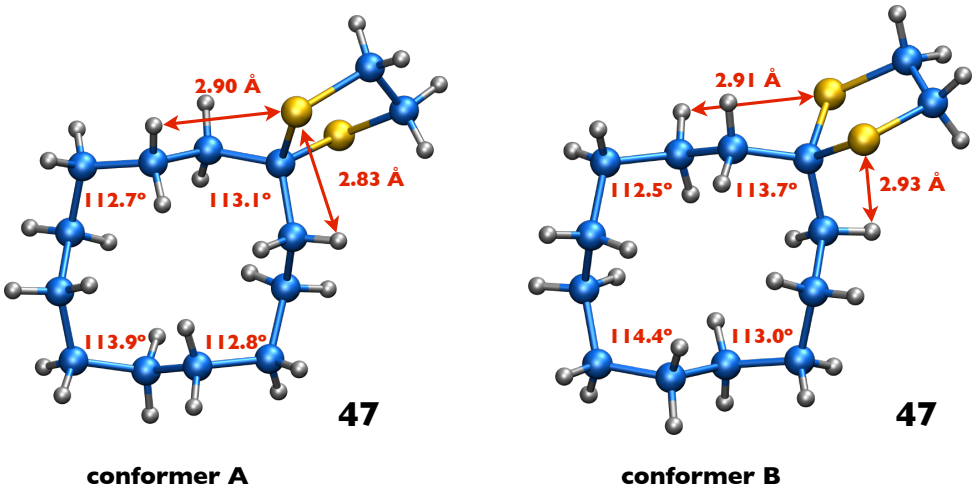

Figure 2.12 X-ray crystal structure of 1,4-dithiaspiro[4.12]hexadecane **47** highlighting corner CH_2-C($S_2C_2H_4$)-CH_2 and CH_2-CH_2-CH_2 angles, together with short 1,2- and 1,3-H,S transannular contacts. (with A. M. Z Slawin)

Both of the resultant conformers had the dithioacetal ring located at a corner position. The corner C-C-C angles (112.5 – 114.4º) were found to be narrower

in comparison to those determined by Dunitz for cyclododecane **69** (116.0º, 117.0º).[1] Further examination of the crystal structure revealed that the 1,2- and 1,3-H,S transannular contacts (*e.g.* 2.83, 2.90 Å), were shorter than the sum of the van der Waals radii of sulfur and hydrogen atoms (3.09 Å),[6] indicating a steric tension of the dithiolane motif on neighbouring methylene groups.

Subsequent fluorination using *N*-iodosuccinimide **40** and HF-pyridine gave 1,1-difluorocyclododecane **50** in 32% yield (Scheme 2.5). Once this alternative *gem*-difluorination method had been established, the 1,3-dithiolane derivatives of cyclododecane-1,4-dione **71**, cyclododecane-1,7-dione **72** and cyclododecane-1,6-dione **73** became synthetic targets.

2.3.2 Synthesis and conformational analysis of 1,1,4,4-tetrafluorocyclododecane

2.3.2.1 Cyclododecane-1,4-dione

The synthesis of cyclododecane-1,4-dione **71** was carried out following a protocol described in the literature (Scheme 2.6).[10] This involved a Norrish Type II photolysis of commercially available cyclododecanone **70**, using a medium pressure mercury lamp. The resulting [8.2.0]-bicyclic alcohol **77** was oxidised by Jones oxidation[11] to give diketone **71**. The yield over the two steps was 21%.

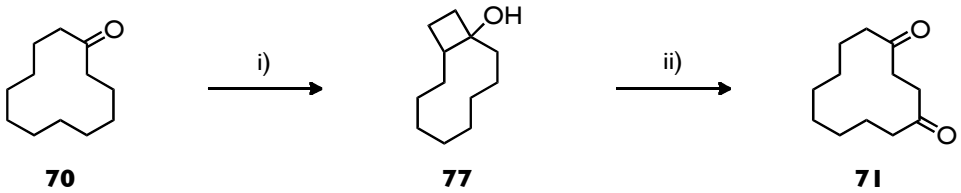

Scheme 2.6 Two-step synthesis of cyclododecane-1,4-dione **71**. Reagents and conditions: i) hv, cyclohexane, RT; ii) CrO_3, H_2SO_4, H_2O, acetone, 21% (over two steps).

An X-ray crystal structure of the resultant 1,4-diketone **71** was determined (Figure 2.13), revealing that the carbon skeleton is of the square type [3333], similar to that of cyclododecane as described by Dunitz[1].

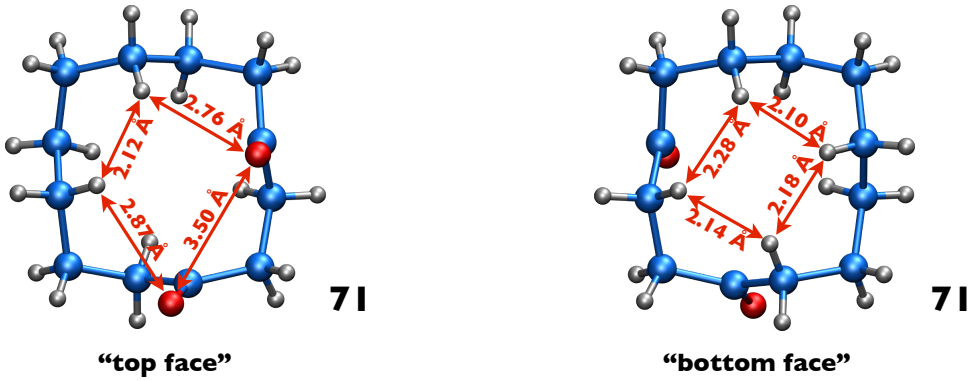

Figure 2.13 X-ray crystal structure of cyclododecane-1,4-dione **71**. (with A. M. Z Slawin)

It is clear that the carbonyl groups avoid the corner positions. Instead they are situated on the edges and forced by the *anti* zig-zag carbon skeleton to sit on the same face of the ring. Such an orientation has been reported previously.[12] This arrangement reduces repulsive 1,4-H,H interactions between intra-annular hydrogen atoms, across the ring, as two of the methylene units are replaced by the planar carbonyl groups.

2.3.2.2 1,4,9,12-Tetrathiadispiro[4.2.4.8]icosane

In the next step of the synthetic route cyclododecane-1,4-dione **71** was converted to the corresponding bis-dithiolane derivative **78** through

dithioacetalisation. This involved a reaction with 1,2-ethanedithiol in the presence of BF_3 (Scheme 2.7).

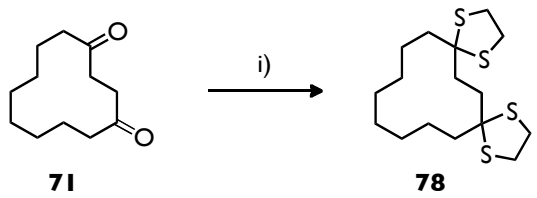

Scheme 2.7 Conversion of cyclododecane-1,4-dione **71** to corresponding dithiolane **78**. Reagents and conditions: i) 1,2-ethanedithiol, BF_3·AcOH, RT, 92%

The resulting dithiolane **78** was obtained in a 92% yield. This material was a white crystalline solid, again allowing for X-ray crystal structure analysis. As observed for the previously investigated 1,4-dithiaspiro[4.12]hexadecane **47**, two crystallographically independent structures were found in the unit cell (Figure 2.14).

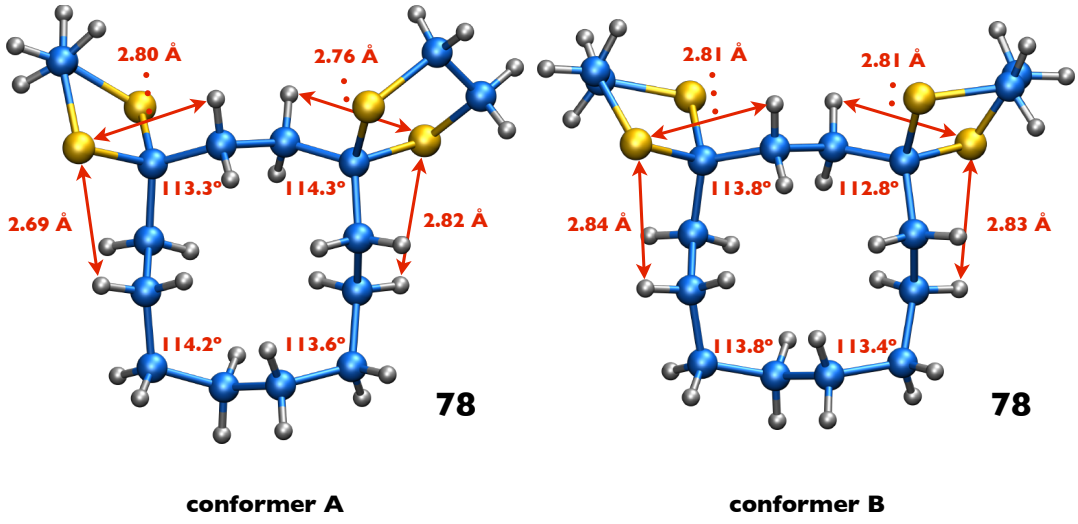

Figure 2.14 X-ray crystal structure of 1,4,9,12-tetrathiadispiro[4.2.4.8]icosane **78** highlighting corner CH_2-C($S_2C_2H_4$)-CH_2 and CH_2-CH_2-CH_2 angles, as well as short 1,2- and 1,3-H,S transannular contacts. (with A. M. Z Slawin)

Again, both conformers had the bulky dithioacetal rings located at corner positions of the square [3333] ring. Further investigation of the resulting

structures revealed short 1,2-H,S (*e.g.* 2.76 Å), 1,3-H,S (*e.g.* 2.69 Å) and 1,4-H,H (2.09-2.32 Å) contacts, indicating unfavourable transannular interactions. Additionally, all corner C-C-C angles were found to be wider than tetrahedral (112.8-114.2º), perhaps illustrating presence of angular strain in the ring.

2.3.2.3 1,1,4,4-Tetrafluorocyclododecane

1,4,9,12-Tetrathiadispiro[4.2.4.8]icosane **78** was subsequently subjected to oxidative fluorodesulfurisation with *N*-iodosuccinimide **40** and HF-pyridine (Scheme 2.8).

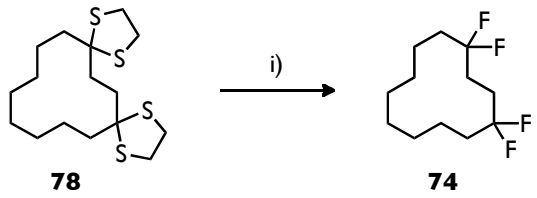

78 **74**

Scheme 2.8 *gem*-Difluorination of 1,4,9,12-tetrathiadispiro[4.2.4.8]icosane **78**. Reagents and conditions: i) NIS **40**, HF-pyridine, DCM, −78 ºC to RT, 28%.

Initially the reaction did not proceed well, resulting in only a 3% yield. This may be due to HF elimination from the product as a result of the vigorous and exothermic purification process, which involved filtration through a pad of basic alumina. Instead, solid sodium bicarbonate was used to neutralise the remaining HF during workup. Additionally, it was found important to conduct the reaction under strictly non-aqueous conditions to avoid hydrolysis of the dithiolane substrate to the parent ketone. Thus the *N*-iodosuccinimide **40** and dithiane **78** were dried under high vacuum over P_2O_5 prior to use. With these modifications the yield was improved to 28% and the product was isolated as

a clear crystalline solid (m.p. = 80 ºC), which was amenable to X-ray structure analysis. In contrast to the disordered structure of 1,1-difluorocyclododecane **50**, introduction of the second CF_2 motif afforded a much higher molecular order in **74**. As anticipated, the difluoromethylene groups tend to locate at the corners rather than at the edges of the square [3333] ring (Figure 2.15). Moreover, the CH_2-CF_2-CH_2 bond angles in **74** are much wider (119.8º, 116.6º) and the F-C-F bond angles (104.4º, 104.8º) narrower than tetrahedral, consistent with the CSD survey described in Figures 2.8 and 2.9. This angle widening leads to an increase in the 1,4-H,H transannular distances on the CF_2-substituted corners of the ring (*e.g.* 2.24 Å *versus* 2.12 Å on unsubstituted side) reducing 1,4 steric strain in **74** (Figure 2.15b).

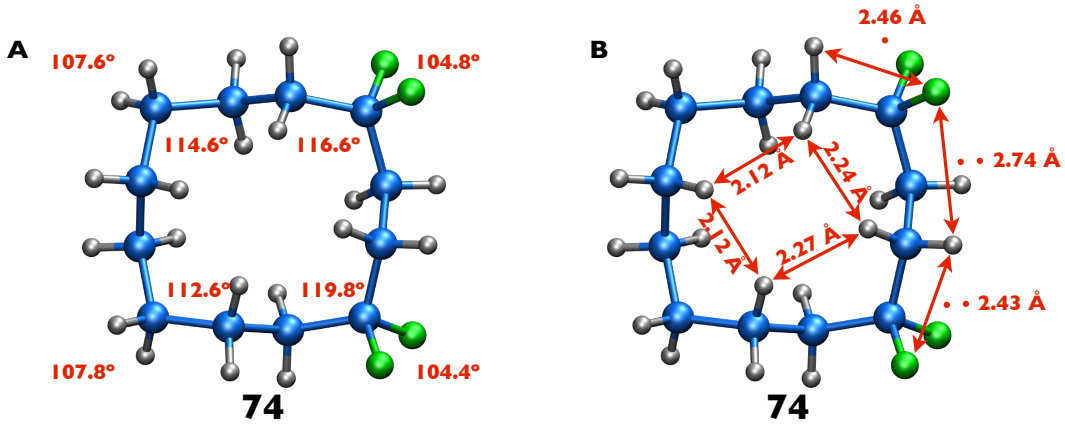

Figure 2.15 X-ray crystal structure of 1,1,4,4-tetrafluorocyclododecane **74** highlighting: the corner C-C-C, H-C-H and F-C-F bond angles (**A**), b) the 1,2-H,F, 1,3-H,F and 1,4-H,H transannular contacts (**B**). (with A. M. Z. Slawin)

In addition, the 1,2-H,F transannular contacts (*e.g.* 2.43, 2.46 Å), were found to be significantly shorter than the sum of the van der Waals radii of fluorine and hydrogen (2.66 Å)[6] and indicate a significant steric impact of the CF_2 group on the neighbouring methylene groups. Short 1,3-H,F contacts were not observed in the solid state of 1,1,4,4-tetrafluorocyclododecane **74**.

Investigation of $^{19}F\{^{1}H\}$ NMR spectra of 1,1,4,4-tetrafluorocyclododecane **74** at variable temperatures revealed that the singlet observed at room temperature splits into an AB-system at 192 K (Figure 2.16). This indicates that at low temperatures, interconversion is slowed down sufficiently that the geminal fluorine atoms are magnetically nonequivalent on the NMR time scale.

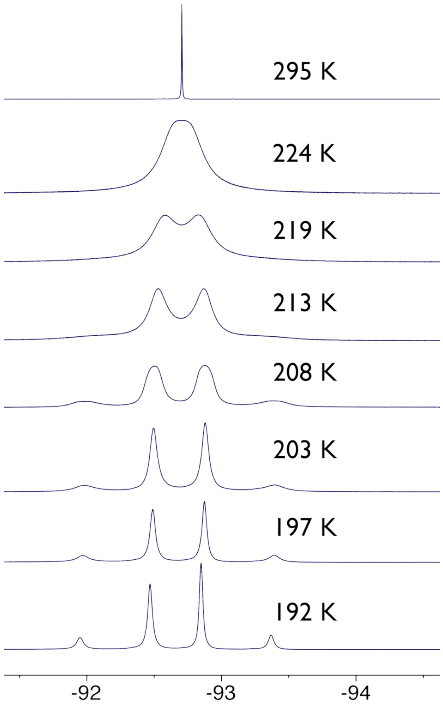

Figure 2.16 Partial plot of proton decoupled ^{19}F spectrum of 1,1,4,4-tetrafluorocyclododecane **74** at 192 K shows AB system. (T. Lebl)

To gain further insight into the dynamic properties of the twelve-membered ring **74**, a lineshape analysis of the proton decoupled ^{19}F NMR spectra, recorded across the temperature range of 192-219 K, was conducted by Dr Tomas Lebl at the University of St Andrews. The experimental data was fitted to the Eyring equation, providing activation parameters of

the ring interconversion process ($\Delta G^{\ddagger}_{298K}$ = 9.58 kcal mol^{-1}, $\Delta H^{\ddagger}$ = 9.20 kcal mol^{-1} and $\Delta S^{\ddagger}$ = -1.27×10^{-3} cal K^{-1} mol^{-1}). Subsequently derived $\Delta G^{\ddagger}_{163K}$ = 9.42 kcal mol^{-1} allowed direct comparison with the previously reported free energy barrier of cyclododecane **69** ($\Delta G^{\ddagger}_{163}$ = 7.30 kcal mol^{-1})[13]. It appears that introduction of two CF_2 groups in the neighbouring corners of cyclododecane enhanced conformational stability of the ring by ~2.12 kcal mol^{-1}.

2.3.3 Synthesis and conformational analysis of 1,1,7,7-tetrafluorocyclododecane

2.3.3.1 Cyclododecane-1,7-dione

The synthesis of cyclododecane-1,7-dione **72** was carried out according to a reported procedure.[14] Commercially available *cis,trans,trans*-cyclododeca-1,5,9-triene **79** underwent cyclisation on the surface of a sodium/alumina catalyst. Partial hydrogenation of the resultant conjugated diene **80**, to a bicyclic dodecene **81**, occurred after introducing hydrogen. This was followed by ozonolysis to give the target cyclododecane-1,7-dione **72** (Scheme 2.9). The yield after three steps of **72** was however very low (4%). This was substantially due to the purification process, which required the separation of a large number of side-products.

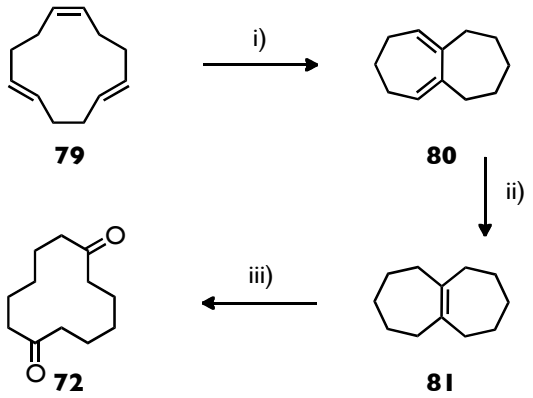

Scheme 2.9 Three-step synthesis of cyclododecane-1,7-dione **72**. Reagents and conditions: i) Na/Al_2O_3, heptane, reflux ii) H_2, Na/Al_2O_3, heptane, reflux iii) O_3, AcOH, H_2O, heptane, 0 ºC, 4% (over three steps).

Nevertheless, the diketone **72** could be isolated as a crystalline solid. The X-ray crystal structure was determined, and this was consistent with the proposed conformation by Alvik, Borgen and Dale (Figure 2.17A).[12] It was again a square type carbon skeleton with the carbonyl groups avoiding corner positions. The *anti* zig-zag carbon skeleton forces the carbonyl groups to point almost parallel to each other and from the same face of the ring. These edge locations of the carbonyl take the place of two intra-annular hydrogen atoms releasing transannular strain across the ring (Figure 2.17C). Additionally, distances between two pairs of intra-annular hydrogen atoms, on the "bottom face" of the ring, were slightly increased (2.24/2.27 Å *versus* 2.08/2.10 Å on unsubstituted side) as a result of wider CH_2-CO-CH_2 angles (Figure 2.17D).

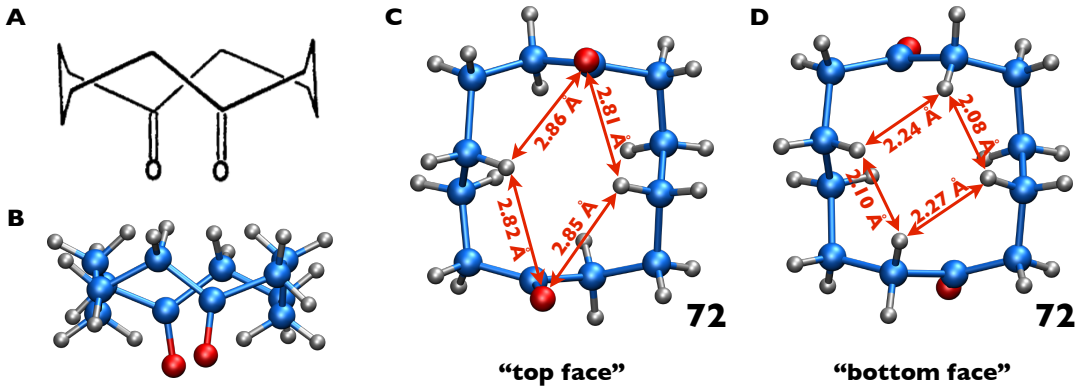

Figure 2.17 Proposed conformation (**A**)[12] and X-ray crystal structure of cyclododecane-1,7-dione **72** (**B-D**) highlighting the 1,4-H,H and 1,4-H,O transannular contacts. (with A. M. Z. Slawin)

2.3.3.2 1,4,12,15-tetrathiadispiro[4.5.4.5]icosane

Cyclododecane-1,7-dione **72** was subsequently converted to the corresponding bis-dithiolane derivative **82**. This was a relatively straightforward reaction and occurred in 54% yield (Scheme 2.10).

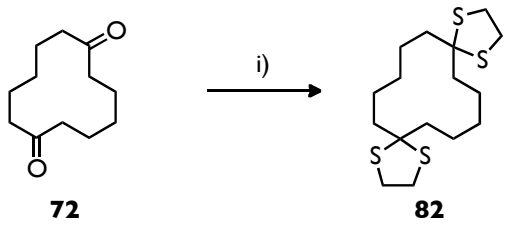

Scheme 2.10 Conversion of cyclododecane-1,7-dione **72** to corresponding dithiolane **82**. Reagents and conditions: i) 1,2-ethanedithiol, BF_3·AcOH, RT, 54%.

The crystalline product was submitted for X-ray crystal structure analysis. The resulting structure presented in Figure 2.18 revealed that the bulky dithiolane groups located at the corners of the square ring, similar to that found for analogues **47** and **78**.

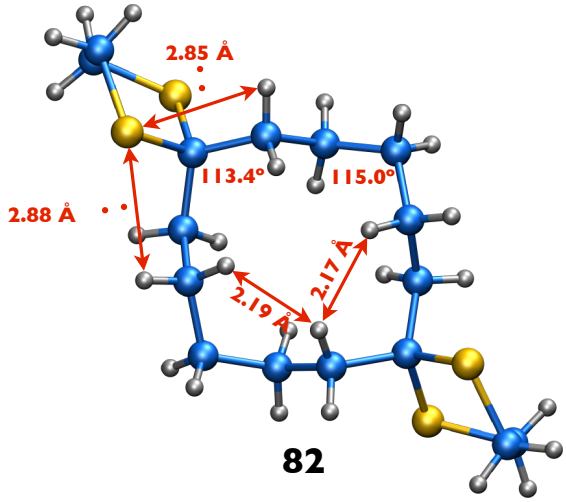

Figure 2.18 X-ray crystal structure of 1,4,12,15-tetrathiadispiro[4.5.4.5]icosane **82** highlighting corner CH_2-C($S_2C_2H_4$)-CH_2 and CH_2-CH_2-CH_2 angles, as well as short 1,2-H,S, 1,3-H,S and 1,4-H,H transannular contacts.

The CH_2-C($S_2C_2H_4$)-CH_2 angles in the dithiane-substituted corners were found to be narrower by ~1.6º when compared with the corresponding unsubstituted CH_2-CH_2-CH_2 angles. This slight compression is most likely caused by unfavorable 1,2- and 1,3-H,S transannular interactions, which arise through the short contacts between these atom pairs (*e.g.* 2.85, 2.88 Å).

2.3.3.3 1,1,7,7-Tetrafluorocyclododecane

gem-Difluorination with *N*-iodosuccinimide **40** and HF-pyridine (Scheme 2.11) afforded the desired 1,1,7,7-tetrafluorocyclododecane **75** in a good yield (57%).

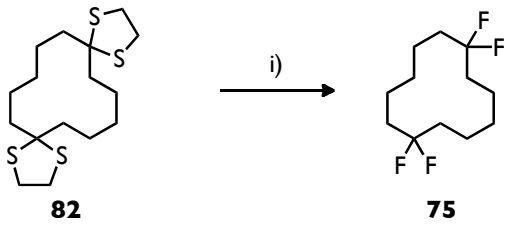

Scheme 2.11 *gem*-Difluorination of 1,4,12,15-tetrathiadispiro[4.5.4.5]icosane **82**. Reagents and conditions: i) NIS **40**, HF-pyridine, DCM, −78 ºC to RT, 57%.

Substitution in the opposite corners of the ring, with two CF_2 units, resulted in a much higher melting point (m.p. = 137 ºC). The crystalline solid was subjected to X-ray crystal structure analysis, and the resulting structure for **75** is shown in Figure 2.19.

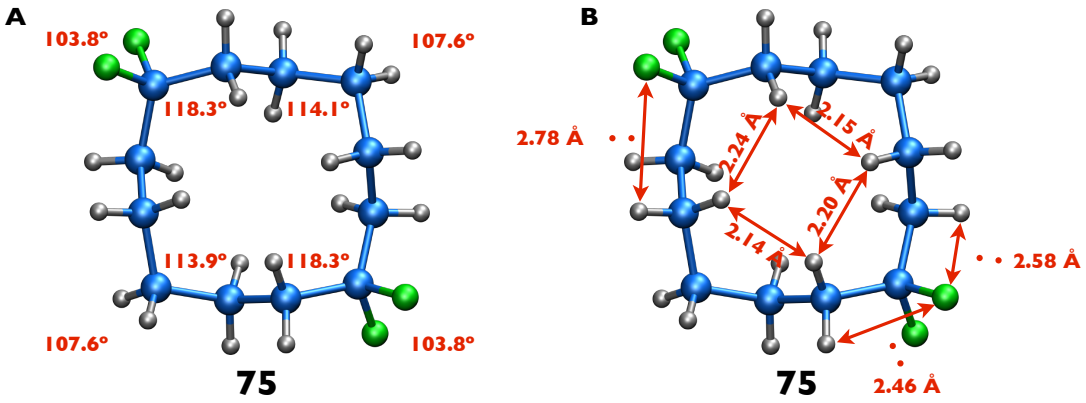

Figure 2.19 X-ray crystal structure of 1,1,7,7-tetrafluorocyclododecane **75** highlighting: the corner C-C-C, H-C-H and F-C-F bond angles (**A**), the 1,2-H,F, 1,3-H,F and 1,4-H,H transannular contacts (**B**). (with A. M. Z. Slawin)

Again, the carbon ring adopted a square type structure [3333] and the CF_2 groups were accommodated in corner positions. Both of the CH_2-CF_2-CH_2 angles were found to be much wider (118.3º) while F-C-F angles respectively narrower (103.8º), than tetrahederal. As observed previously for 1,1,4,4-tetrafluorocyclododecane **74**, the wider corner angles, across the CF_2-substituted corners of the ring, resulted in partial relaxation of unfavourable 1,4-H,H contacts (2.24/2.20 Å *versus* 2.15/2.14 Å on unsubstituted side of the ring). The 1,2-H,F transannular contacts (*e.g.* 2.46, 2.58 Å), were again shorter than the sum of the van der Waals radii of fluorine and hydrogen atoms (2.66 Å) confirming a noticeable steric influence of the CF_2 motif on the neighbouring methylene groups. Gaussian modelling, carried

out by Peer Kirsch, confirmed that the edge/edge arrangement of two difluoromethylene substituents would result in lower conformational stability (~5.91 kcal mol^{-1}), presumably due to resulting 1,4-H,H and 1,7-F,F intra-annular interactions (Figure 2.20). This suggest an energy cost of ~3.00 kcal mol^{-1}, when placing a CF_2 in an edge over a corner.

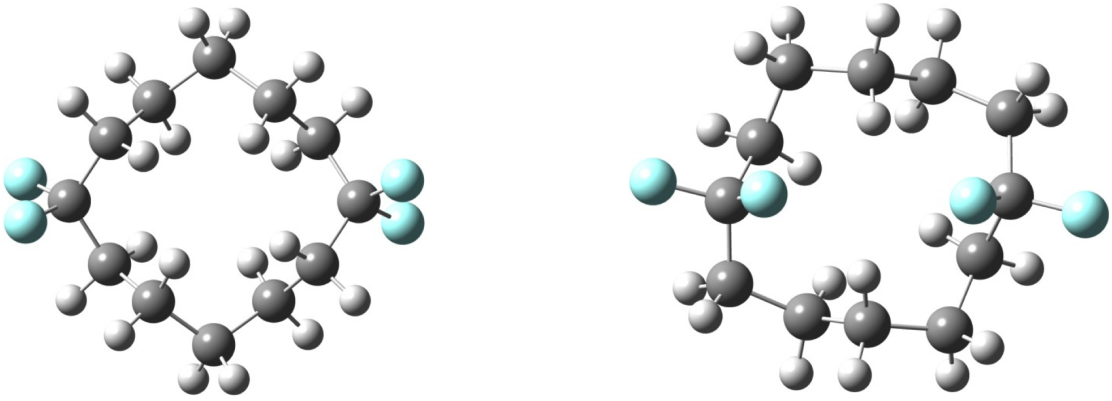

Figure 2.20 Gaussian modeling (MP2/6-311 + G(2d,p)//B3LYP/6-311 + G(2d,p) + ZPE) of 1,1,7,7-tetrafluorocyclododecane **75**. (Peer Kirsch, Merck, Darmstadt)

Low temperature $^{19}F\{^1H\}$ NMR spectroscopic analysis of 1,1,7,7-tetrafluorocyclododecane **75** did not resolve the spin system, even at 190 K. However, ^1H NMR spectra recorded across the temperature range of 203-293 K and 2D ^1H-^{13}C HSQC spectrum at 203 K revealed decoalescence of the proton resonance for the edge methylene group (Figure 2.21). The coalescence point was found to occur at 233 K and enabled evaluation of the free energy barrier ($\Delta G^{\ddagger}_{233K}$ = 10.61 kcal mol^{-1}). As the coupling patterns in the ^1H NMR spectra were too complex to allow complete lineshape analysis, the temperature dependence of the $\Delta G^{\ddagger}$ remained unknown.

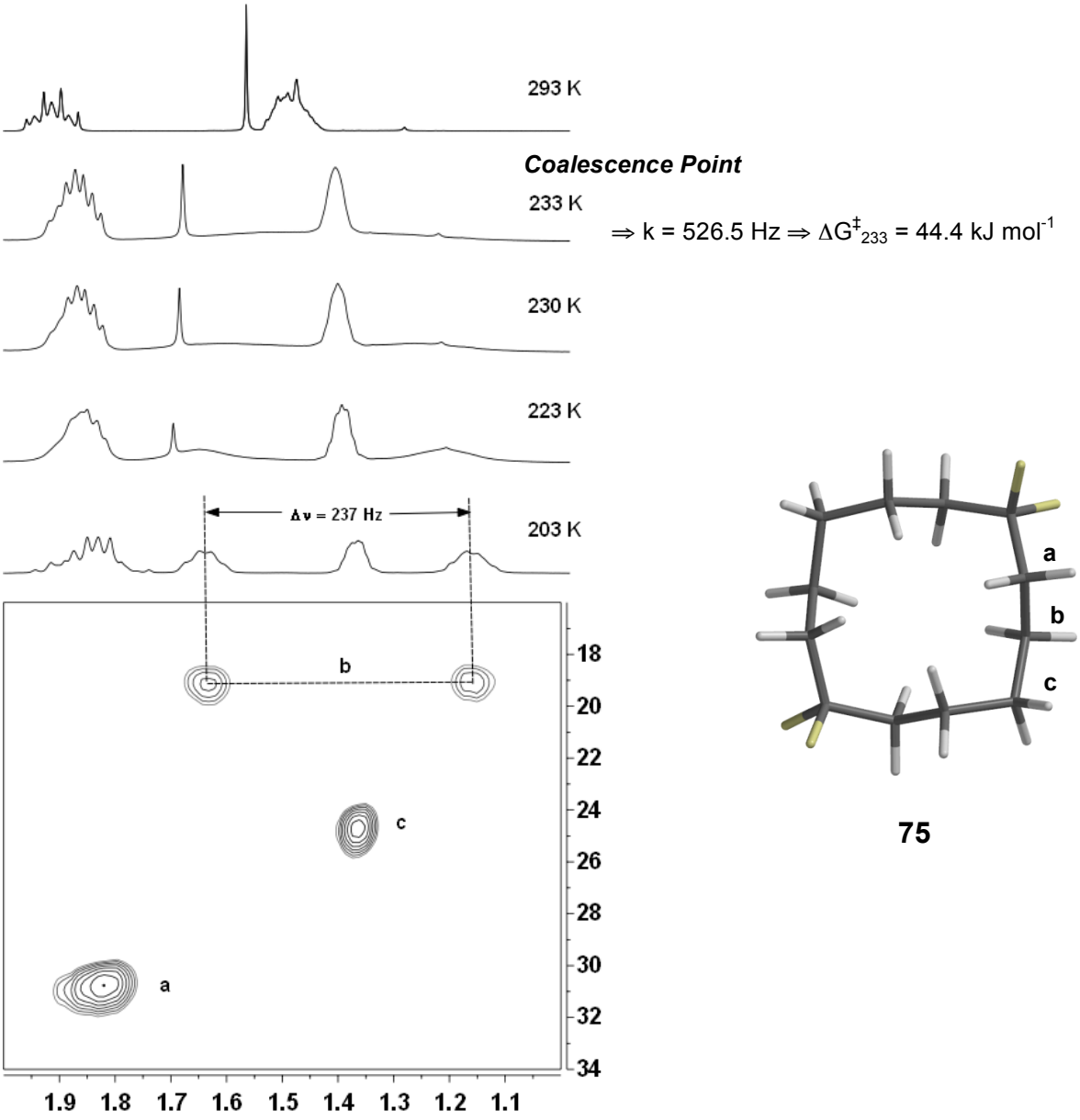

Figure 2.21 Partial plot of low temperature ^{1}H NMR spectra together with partial plot of 2D ^{1}H-^{13}C HSQC spectrum at 203 K show decoalescence of the proton resonance for the edge methylene group (**b**) in 1,1,7,7-tetrafluorocyclododecane **75**.[15] (T. Lebl)

Nonetheless, the calculated free energy barrier was found to be higher by 1.12 kcal mol^{-1} than $\Delta G^{\ddagger}$ of 1,1,4,4- analogue **74** at 233 K (9.49 kcal mol^{-1}). This increased conformational stability of the 1,1,7,7-tetrafluorocyclododecane relative to **74** can be rationalised by its higher symmetry and zero overall dipole moment.

2.3.4 Synthesis and conformational analysis of 1,1,6,6-tetrafluorocyclododecane

Synthesis of 1,4,11,14-tetrathiadispiro[4.4.4.6]icosane **87**, a precursor for the 1,1,6,6-tetrafluorocyclododecane **76**, was carried out in the group by Dr Yi Wang following the route presented in Scheme 2.12.[15]

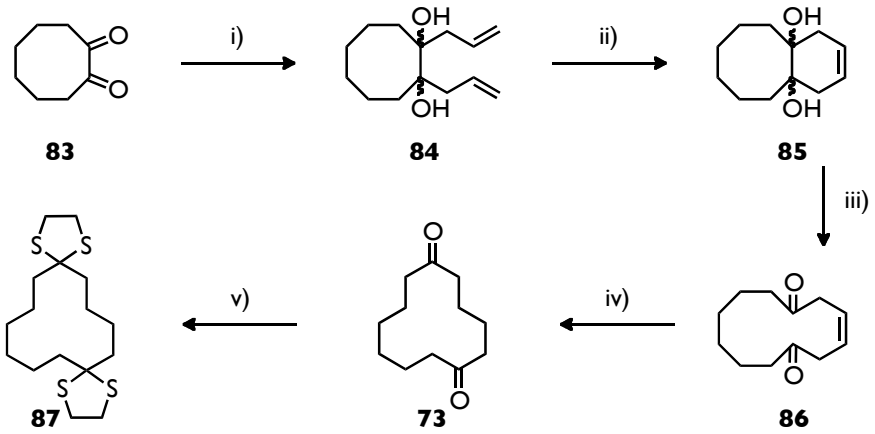

Scheme 2.12 Synthetic route to 1,4,11,14-tetrathiadispiro[4.4.4.6]icosane **87**. Reagents and conditions: i) allylmagnesium bromide, Et_2O, −20 ºC to RT, 57% ii) Grubbs 1st gen. cat. (5 mol%), DCM, RT, 77% iii) $Pb(OAc)_4$, DCM, RT, 81% iv) H_2, Pd/C, DCM, RT, 90% v) 1,2-ethanedithiol, $BF_3 \cdot Et_2O$, RT, 96%.[15] (by Dr Yi Wang)

2.3.4.1 Cyclododecane-1,6-dione

Diallylation of cyclooctane-1,2-dione **83** using allylmagnesium bromide afforded 1,2-diallylcyclooctane-1,2-diol **84** in 57% yield. The resulting olefin was subjected to ring-closing metathesis employing Grubbs 1st generation ruthenium catalyst. The reaction proved to be straightforward and gave the **85** in 77% yield. Subsequent oxidative-cleavage with $Pb(OAc)_4$ resulted in a good conversion to the unsaturated diketone **86** (81%). This reaction was followed by catalytic hydrogenation in the presence of palladium on carbon (Scheme 2.12). The resultant cyclododecane 1,6-dione **73** was isolated as a

white crystalline solid and subjected to X-ray crystal structure analysis. As observed previously for 1,4- and 1,7-cyclododecanediones **71** and **72**, the carbonyl groups were found to locate on the edge of the square [3333] carbon skeleton (Figure 2.22).

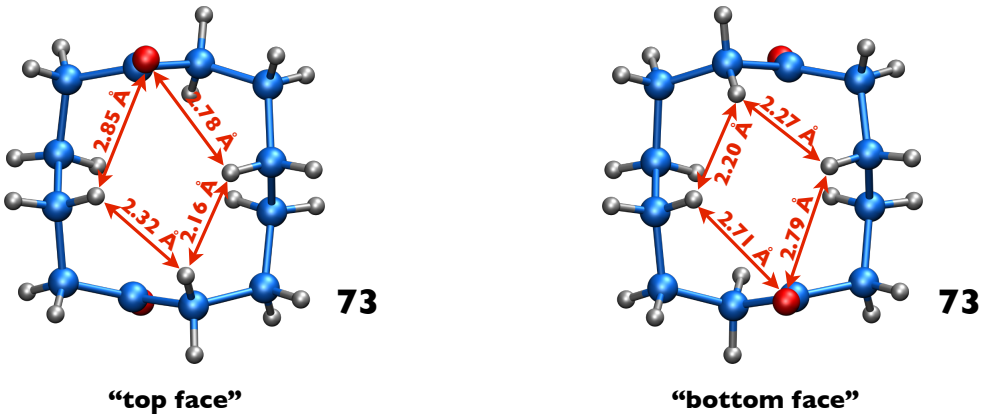

Figure 2.22 X-ray crystal structure of cyclododecane-1,6-dione **73** highlighting the 1,4-H,H and 1,4-H,O transannular contacts. (with A. M. Z Slawin)

Additionally, both of the 1,6-spaced oxygen atoms were pointing in opposite directions as a consequence of the *anti* zig-zag nature of the ring. This arrangement limited repulsive 1,4-H,H intra-annular interactions on both sides of the ring, as two of the methylene units, each with a transannular hydrogen pointing into the ring, were replaced by the flat carbonyl groups.

2.3.4.2 1,4,11,14-Tetrathiadispiro[4.4.4.6]icosane

Consecutive dithioacetalisation of the dione **73**, using 1,2-ethanedithiol in the presence of boron trifluoride, afforded 1,4,11,14-tetrathiadispiro[4.4.4.6]icosane **87** in 96% yield. The material was a white crystalline solid amenable to X-ray structure analysis. An X-ray crystal structure of the resultant 1,6-bisdithiolane **87** was determined (Figure 2.23), revealing a very obvious change in the ring conformation. The carbon

skeleton was not anymore of the square [3333] type, instead, the ring adopted a pseudo-rectangular [2334] conformation, consistent with the minimum energy structure of 1,1,6,6-tetramethylcyclododecane, calculated by Dale (Figure 2.7C)[8].

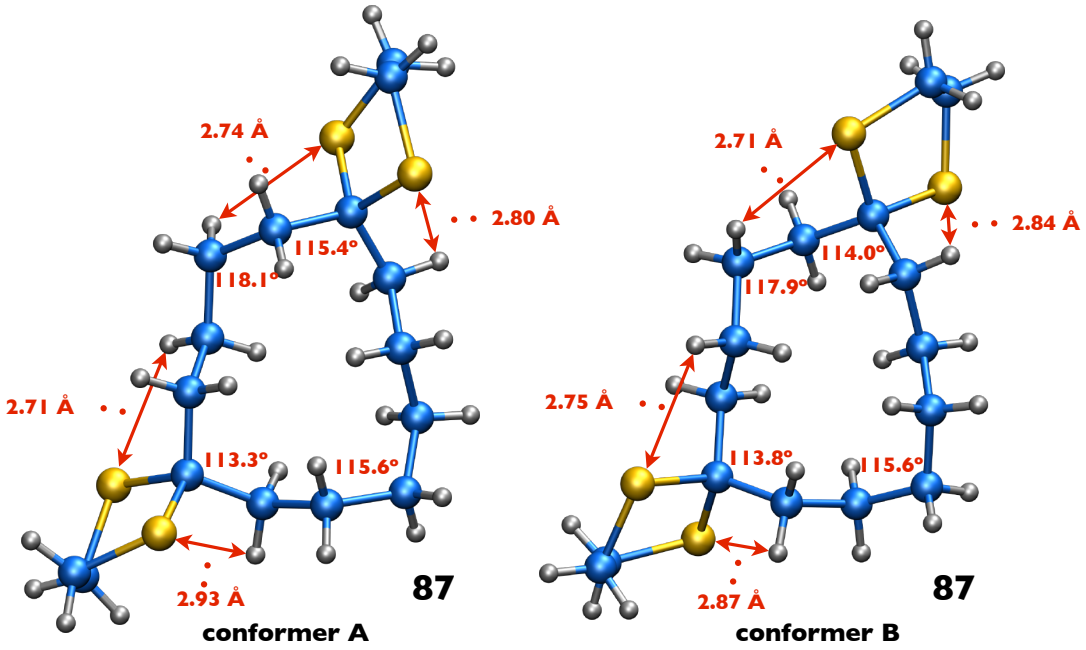

Figure 2.23 X-ray crystal structure of 1,4,11,14-tetrathiadispiro[4.4.4.6]icosane **87** highlighting corner CH_2-C($S_2C_2H_4$)-CH_2 and CH_2-CH_2-CH_2 angles, as well as short 1,2-H,S, 1,3-H,S transannular contacts.

The corner positions have rearranged to accommodate the sterically demanding dithiolane groups. Further examination of the X-ray crystal structure revealed, that the corner CH_2-C($S_2C_2H_4$)-CH_2 angles were again narrower than unsubstituted corner CH_2-CH_2-CH_2 angles. Additionally, 1,2- and 1,3-H,S transannular interactions (*e.g.* 2.84, 2.71 Å) were found to be significantly shorter than the sum of the van der Waals radii of these atom pairs (3.09 Å), indicating large steric impact of the dithiolane substituents. The ring interior remained cluttered with the 1,4-H,H intra-annular contacts varying between 2.09 and 2.32 Å, suggesting significant transannular interactions.

2.3.4.3 1,1,6,6-Tetrafluorocyclododecane

The target 1,1,6,6-tetrafluorocyclododecane **76** was accessed in a good yield (58%) through *gem*-difluorination of the bisdithiolane precursor **87**, provided by Dr Yi Wang, with *N*-iodosuccinimide **40** and HF-pyridine (Scheme 2.13).

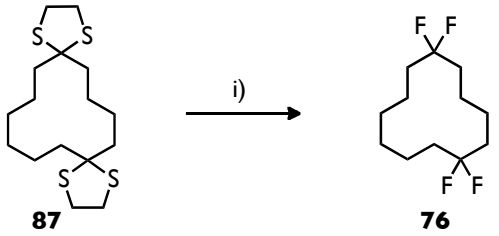

87 **76**

Scheme 2.13 *gem*-Difluorination of 1,4,11,14-tetrathiadispiro[4.4.4.6]icosane **87**. Reagents and conditions: i) NIS **40**, HF-pyridine, DCM, –78 ºC to RT, 58%.

The resulting tetrafluorocyclododecane **76** was much more amorphous in nature and had the lowest melting point (m.p. = 31 ºC) in comparison with previously described 1,4- and 1,7-CF_2 analogues **74** and **75**. A small crystal was obtained after many recrystallisation attempts and subjected to X-ray crystal structure analysis. Two similar conformers were found in the crystal lattice, both representing a distorted, pseudo-rectangular [2334] carbon skeleton, similar to that observed previously for the dithiolane precursor **87** (Figure 2.24).

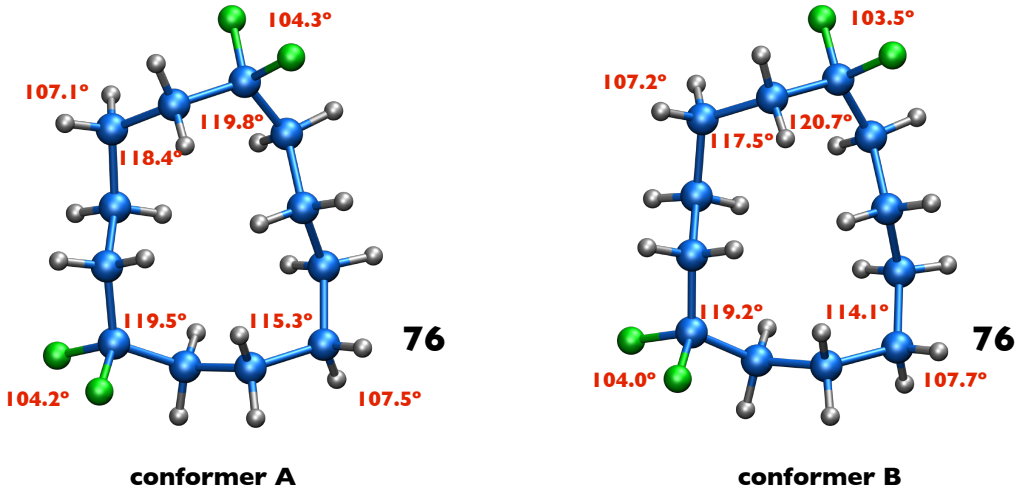

Figure 2.24 X-ray crystal structure of 1,1,6,6-tetrafluorocyclododecane **76** highlighting: the corner CH_2-CR_2-CH_2, H-C-H and F-C-F bond angles. (with A. M. Z. Slawin)

The CF_2 motifs were found to organise the ring conformation in such a way that allows both substituents to maintain a corner location. As a result of this arrangement, fluorine atoms avoid the sterically hindered intra-annular positions of the ring, and as a consequence abstain from unfavourable 1,4-HF interactions. The average width of the corner CH_2-CF_2-CH_2 angle (119.8º) was found to be larger in **76** than in previously synthesised tetrafluorocyclododecanes **74** (118.2º) and **75** (118.3º). Apart from 1,2-H,F interactions observed in both analogues (**74** and **75**), short 1,3-H,F contacts (*e.g.* 2.60 Å) were additionally found in the distorted ring of **76** (Figure 2.25). Moreover, all of the intra-annular 1,4-H,H distances were shorter than the sum of the van der Walls radii of two hydrogen atoms (2.40 Å)[6]. These structural features of 1,1,6,6-tetrafluorocyclododecane **76** suggest significant ring strain.

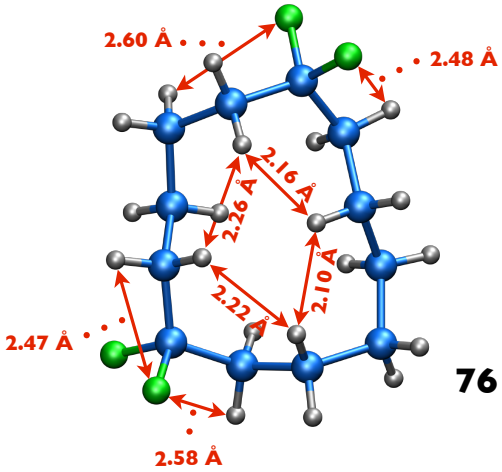

Figure 2.25 X-ray crystal structure of 1,1,6,6-tetrafluorocyclododecane **76** highlighting the 1,2-H,F, 1,3-H,F and 1,4-H,H transannular contacts. (with A. M. Z. Slawin)

A low temperature (CD_2Cl_2, 189 K) $^{19}F\{^1H\}$ and $^1H\{^{19}F\}$ NMR analysis was conducted by Dr Tomas Lebl in order to assess the conformational stability of of 1,1,6,6-tetrafluorocyclododecane **76**. Both experiments did not achieve resolution of the spin system, hence the ring interconversion barrier ($\Delta G^{\ddagger}$) could not be evaluated.

2.4 Conclusions

In summary, cyclododecane **69** has been employed as a molecular framework in order to explore the steric and electronic influence of the difluoromethylene (CF_2) group. Three tetrafluorocyclododecanes (**74**, **75** and **76**) with differentially spaced CF_2 units, have been accessed by various synthetic routes. The target cyclododecanes, together with their ketone and dithiolane intermediates, were isolated as crystalline solids and subjected to X-ray crystal structure analysis.

Carbonyl groups were found to occupy only edge positions of the ring. Such an arrangement was reported before and thought to enable relaxation of repulsive 1,4-H,H interactions by replacing transannular hydrogen atoms with a perpendicular oxygen. As disubstitution in 1,4- 1,7- and 1,6-positions allows both carbonyl groups to remain at the edge location, the square [3333] conformation of the ring is maintained (Figure 2.26).

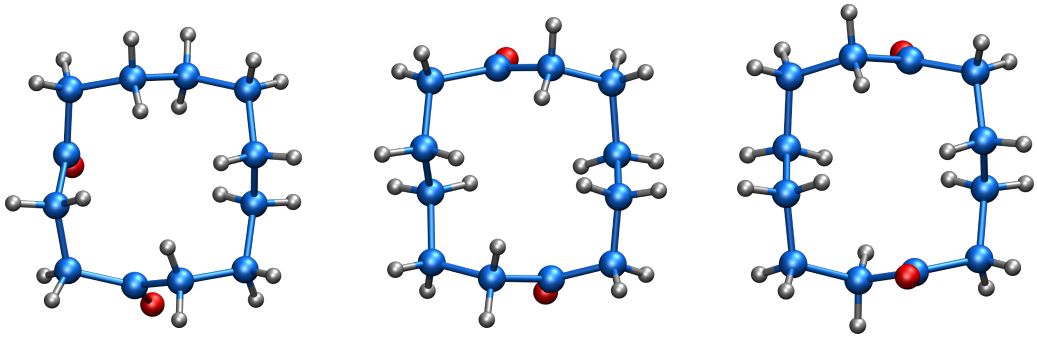

Figure 2.26 X-ray crystal structures of 1,4- (**71**), 1,7- (**72**) and 1,6- (**73**) cyclododecanediones. (with A. M. Z. Slawin)

Analysis of the X-ray structures of the dithiolane derivatives (**78, 82** and **87**) showed that these bulky substituents were accommodated exclusively at the corner positions of the carbon skeleton (Figure 2.27). This observation was found consistent with Dale's theory study on the conformations of the *gem*-dimethyl substituted cyclododecanes.[8]

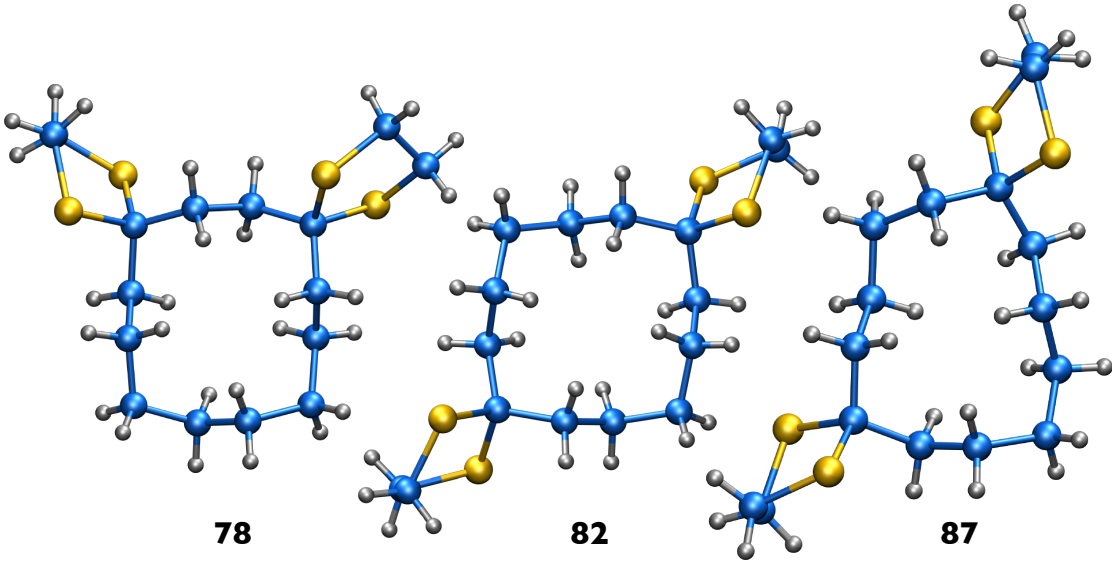

Figure 2.27 X-ray crystal structures of bisdithiolanes **78**, **82** and **87**. (with A. M. Z. Slawin)

In contrast to wide CH_2-CF_2-CH_2 angles, the CH_2-$C(S_2C_2H_4)$-CH_2 angles were similar or slightly narrower than the corresponding unsubstituted corner CH_2-CH_2-CH_2 angles. As the electronegativity of sulfur and carbon atoms is almost identical, this slight angle narrowing can be explained by the steric influence of the large sulfur atoms on the surrounding methylene groups, displayed by short 1,2- and 1,3-H,S transannular contacts.

The solid state conformations of tetrafluorocyclododecanes (**74**-**76**) were almost identical to those of their dithiolane precursors (**78**, **82**, **87**), as illustrated in Figure 2.28.

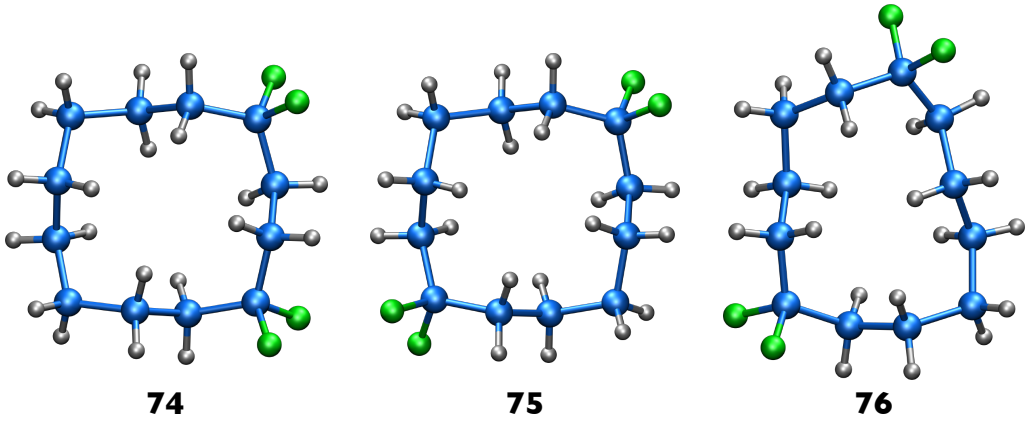

Figure 2.28 X-ray crystal structures of 1,1,4,4- (**74**), 1,1,7,7- (**75**) and 1,1,6,6- (**76**) tetrafluorocyclododecanes. (with A. M. Z. Slawin)

Experimental and theoretical studies of CF_2-cyclododecanes revealed an exclusive preference for the CF_2 moieties to occupy corner locations of the twelve-membered ring. It is likely that such substitution accommodates angular strain, manifested by wide corner CH_2-CH_2-CH_2 angles found in cyclododecane **69**, as comparable angle deviation is observed naturally for the $CH_2CF_2CH_2$ unit. Additionally, this angle widening led to relaxation of unfavourable intra-annular 1,4-H,H interactions in the congested interior of cyclododecane. Incorporation of a second CF_2 motif greatly increased the degree of molecular order of 1,4- and 1,7- tetrafluorocyclododecanes (**74** and **75**), as both exhibited much higher melting points and more organised crystal structures when compared to 1,1-difluorocyclododecane **50**. Furthermore, the free energy barrier ($\Delta G^{\ddagger}$) of **74** and **75** was evaluated as 9.49 and 10.61 kcal mol^{-1}, respectively. These are significantly higher than $\Delta G^{\ddagger}$ of unsubstituted cyclododecane **69** ($\Delta G^{\ddagger}_{163}$ = 7.30 kcal mol^{-1})[13], suggesting a stabilising effect of the CF_2 in **74** and **75**. An attempt to force one of the CF_2 groups to an edge position, by changing the relative spacing between these

two substituents, failed and resulted in significant distortion of the ring, leading to pseudo-rectangular [2334] conformation in **76**. Such strategic incorporation of two difluoromethylene groups offers a useful tool to control the conformation and introduce polarity into alicyclic hydrocarbon systems.

2.5 References

1. J. D. Dunitz, H. M. M. Shearer, *Helv. Chim. Acta*, 1960, **43**, 18–35.

2. E. V. Anslyn, D. A. Dougherty, *Modern Physical Organic Chemistry*, University Science Books, Sausalito, 2006.

3. K. B. Wiberg, *Angew. Chem. Int. Ed.*, 1986, **25**, 312–322.

4. A. De Meijere, *Angew. Chem. Int. Ed.*, 2005, **44**, 7836–7840.

5. J. D. Dunitz, J. A. Ibers, *Perspectives in Structural Chemistry Vol. II*, John Wiley and Sons, New York, 1968.

6. S. Alvarez, *Dalton Trans.*, 2013, **42**, 8617–8636.

7. J. Dale, *Acta Chem. Scand.*, 1973, **27**, 1115–1129.

8. J. Dale, *Acta Chem. Scand.*, 1973, **27**, 1149–1158.

9. S. C. Sondej, J. A. Katzenellenbogen, *J. Org. Chem.*, 1986, **51**, 3508–3513.

10. R. Helder, H. Wynberg, *Tetrahedron*, 1975, **31**, 2551–2557.

11. M. Heilbron, E. R. H. Jones, *J. Chem. Soc.*, 1946, 39–45.

12. T. Alvik, G. Borgen, J. Dale, *Acta Chem. Scand.*, 1972, **26**, 1805–1816.

13. F. A. L. Anet, T. N. Rawdah, *J. Am. Chem. Soc.*, 1978, **100**, 7166–7171.

14. T. Alvik, J. Dale, *Acta Chem. Scand.*, 1971, **25**, 1153–1154.

15. M. Skibiński, Y. Wang, A. M. Z. Slawin, T. Lebl, P. Kirsch, D. O'Hagan, *Angew. Chem. Int. Ed.*, 2011, **50**, 10581–10584.

3

Synthesis and structure of CF_2- cyclotetradecanes and cyclohexadecanes

3.1 Introduction

The strong preference of the CF_2 group to locate in the corners of a square-type cyclododecane ring has been previously described in Chapter 2. The next goal was to investigate how strategic incorporation of two CF_2 motifs would influence the conformation of larger, less strained, even-membered cycloalkanes: cyclotetradecane **88** and cyclohexadecane **89**.

3.1.1 Conformation of cyclotetradecane

Following Dale's theory study introduced in Chapter 2, the three lowest-energy conformations of cyclotetradecane **88**, were characterised by

four corners, linked by differently spaced, *anti* zig-zag methylene units (Figure 3.1).[1]

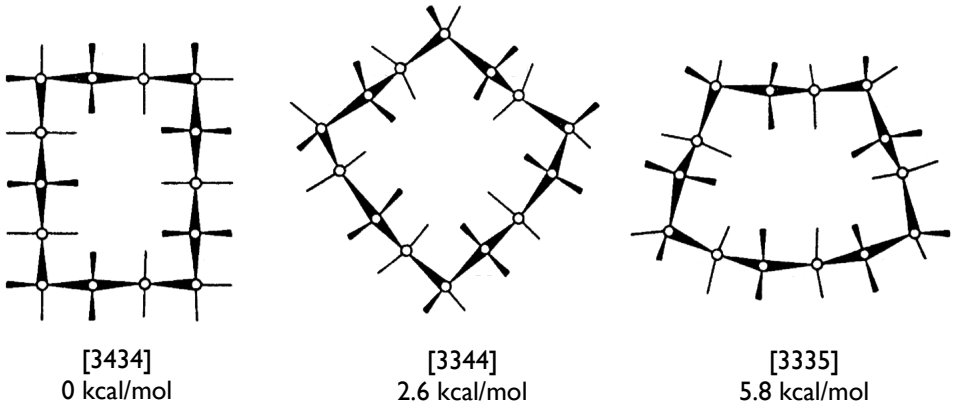

Figure 3.1 The energy differences between the conformations of cyclotetradecane **88** as determined by Dale.[1] Figure adapted from Ref. 1.

The ideal conformation of cyclotetradecane **88** was found to adopt a rectangular [3434] shape, and it was 2.6 kcal mol^{-1} lower in energy than the second most-favoured pseudo-rhomboidal [3344] structure. The energy of the third, trapezoid-like [3335] conformer was 5.8 kcal mol^{-1} higher than of the ideal [3434] structure.[1] In 1976, Groth confirmed the rectangular [3434] structure of cyclotetradecane **88** by X-ray crystallography (Figure 3.2).[2]

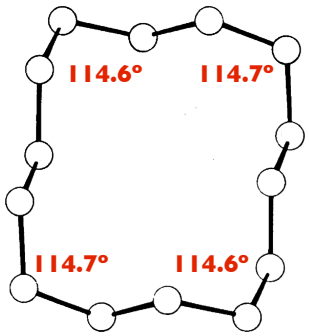

Figure 3.2 The X-ray crystal structure of cyclotetradecane **88** as determined by Groth.[2] Figure adapted from Ref. 2.

The corner CH_2-CH_2-CH_2 angles were found to be slightly narrower (114.6º, 114.7º) in comparison to those previously reported for cyclododecane **69** (116.0º, 117.0º).[3] This could be explained by a lower overall strain of the larger cycloalkane.

3.1.2 Conformation of cyclohexadecane

In contrast to the rectangular [3434] structure of cyclotetradecane **88,** Dale's study showed that the lowest energy conformer of cyclohexadecane **89** assumes a characteristic square-type [4444] conformation.[1] The four corner atoms are linked by four *anti* zig-zag chains, each comprised of three methylene units (Figure 3.3).

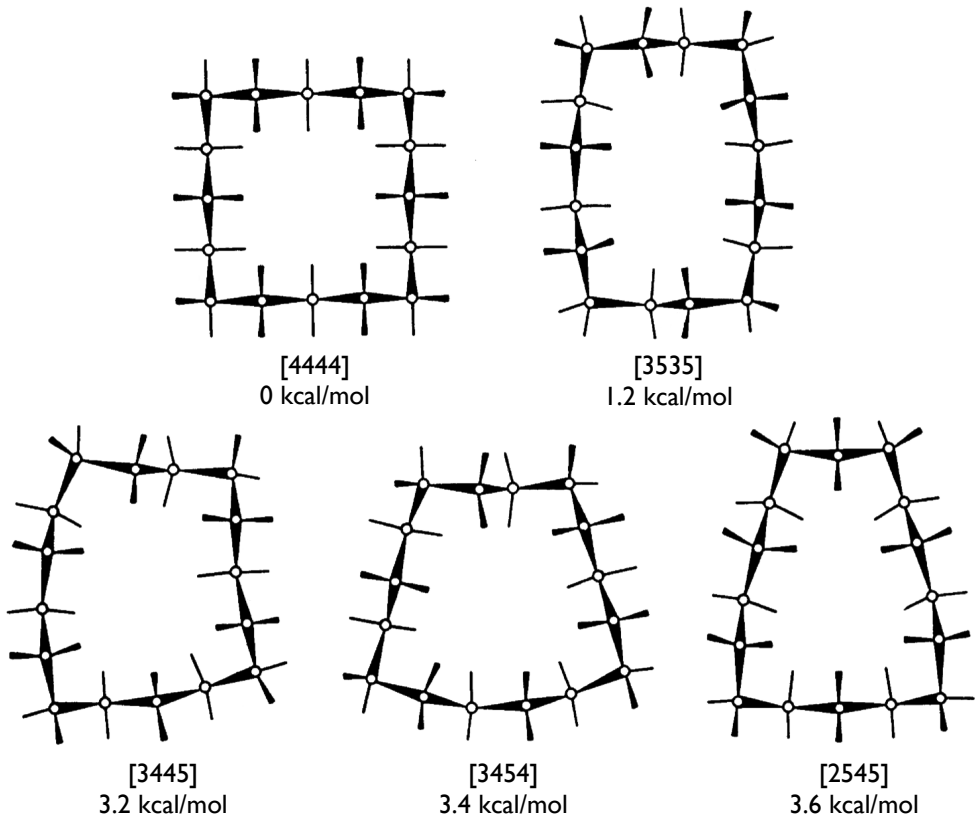

Figure 3.3 The energy differences between the conformations of cyclohexadecane **89** as determined by Dale.[1] Figure adapted from Ref. 1.

The second most-favoured rectangular [3535] carbon skeleton was found to be energetically less favoured by 1.2 kcal mol^{-1}. The three remaining quadrangular conformers ([3445], [3454] and [2545]) were found to be over 3 kcal mol^{-1} higher in energy than the ideal square [4444] structure.[1] The energy difference between the calculated conformers of cyclohexadecane **89** is slightly lower than between conformers of cyclotetradecane **88**. This shows that the larger ring system in **89** is more flexible than **88** and could potentially undergo conformational changes more readily.

Cyclohexadecane **89** is a solid at RT (m.p. = 62-63 ºC),[4] however, attempts to resolve the structure by X-ray crystallography proved difficult due to the high degree of disorder in the crystal phase.[5] Based on his computational studies, Dale predicted that introduction of two *gem*-dimethyl groups in the opposite corners of the [4444] ring could stabilise the structure by limiting the number of possible conformers.[6] Groth solved the structure 1,1,9,9-tetramethyl-cyclohexadecane **90**,[7] thus confirming the square [4444] conformation of the C_{16} ring, as calculated by Dale.[1] Two independent conformers were found in the unit cell, revealing that the *gem*-dimethyl groups occupy exclusively corner positions (Figure 3.4). The angle compression resulting from substitution with a bulky *gem*-dimethyl group became obvious when the substituted and unsubstituted corner CH_2-CR_2-CH_2 angles of the conformer A of 1,1,9,9-tetramethylcyclohexadecane **90** were compared (average corner angles: 115.7º for CH_2-$C(CH_3)_2$-CH_2 *vs.* 111.6º for CH_2-CH_2-CH_2. Such a tendency is displayed only for one of the substituted corners in conformer B of the 1,1,9,9-

tetramethylcyclododecane. This may be a result of the dynamic nature of the large alicyclic systems.

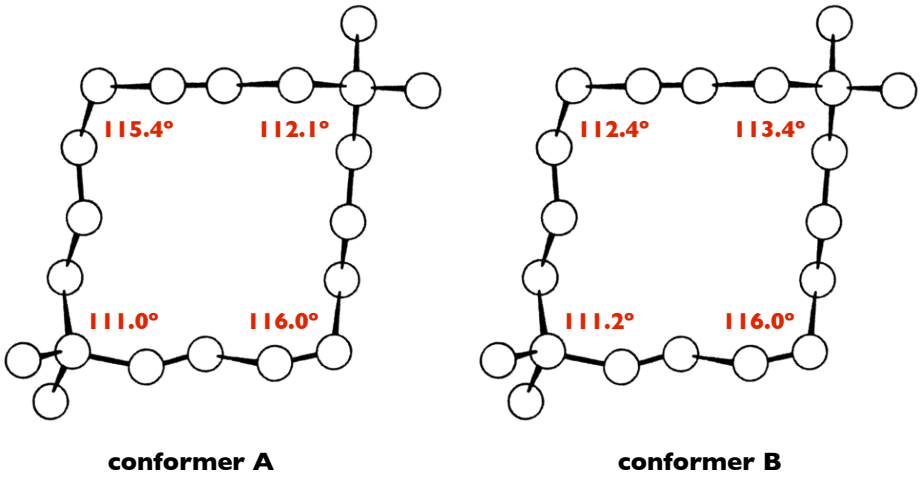

Figure 3.4 The X-ray crystal structure of 1,1,9,9-tetramethylcyclohexadecane **90** as determined by Groth.[7] Figure adapted from Ref. 7.

3.2 Aims of the project

As presented in Chapter 2, introduction of two CF_2 motifs in corner positions resulted in increased stability and order of the cyclododecane rings. Following this observation, it was decided to incorporate *gem*-difluoro groups in the neighbouring corners of cyclotetra- and cyclohexa-decanes. 1,1,4,4-Tetrafluorocyclotetradecane **91** and 1,1,5,5-tetrafluorocyclohexadecane **92** were selected as synthetic targets to induce corners for the ideal conformations of cyclotetradecane **88** [3434] and cyclohexadecane **89** [4444] as determined by Dale (Figure 3.5).[1]

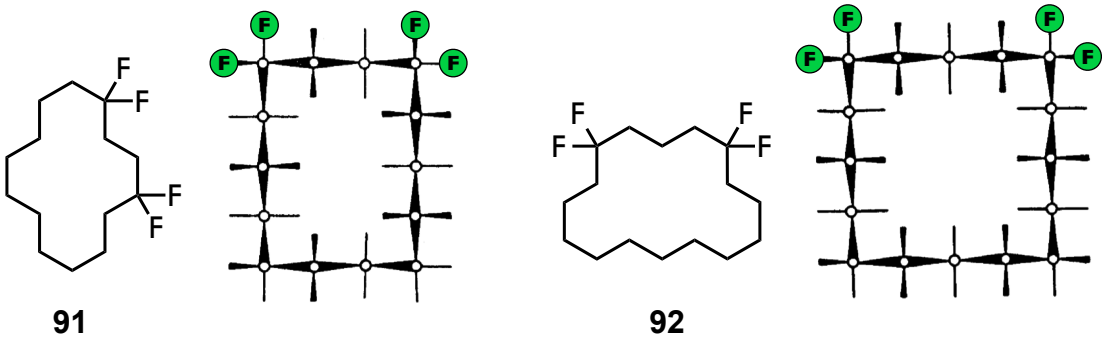

91 **92**

Figure 3.5 *gem*-Difluorination in 1,4- positions for cyclotetradecane **88** and 1,5- positions for cyclohexadecane **89** should result in corner substitution in order to maintain the ideal ring conformations determined by Dale.[1] Idealised structures.

To further explore the potential of the difluoromethylene group to modify and direct the conformation of these large ring systems, 1,1,6,6-tetrafluorocyclotetradecane **93** and 1,1,6,6-tetrafluorocyclohexadecane **94** became synthetic targets (Figure 3.6).

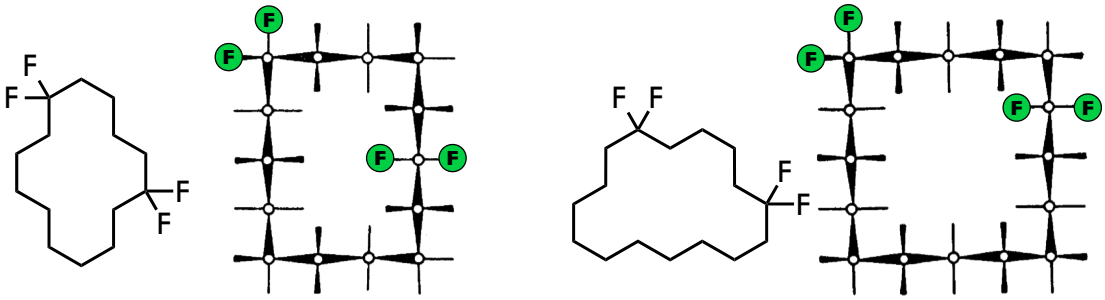

93 **94**

Figure 3.6 *gem*-Difluorination in the 1,6- positions for cyclotetradecane **88** and cyclohexadecane **89** is expected to have one CF_2 at a corner and to force the second of the CF_2 groups to an edge position.[1]

A novel route was designed, which allows the proposed strategic incorporation of the CF_2 group in the alicyclic systems (Scheme 3.1). The first step of the route involved preparation of the appropriately spaced bisdithiane linkers **95** from 1,3-dithiane **62** and the corresponding dibromoalkanes, followed by incorporation of the alkyl 'arms' with terminal olefin groups to afford the diolefins **97**. Subsequent ring closing metathesis (RCM)[8–10]

employing **M_{20}**, a recent and highly active 2nd generation ruthenium catalyst,[11,12] followed by hydrogenation and oxidative fluorodesulfurisation,[13] was expected to provide access to the target CF_2-cycloalkanes **101**.

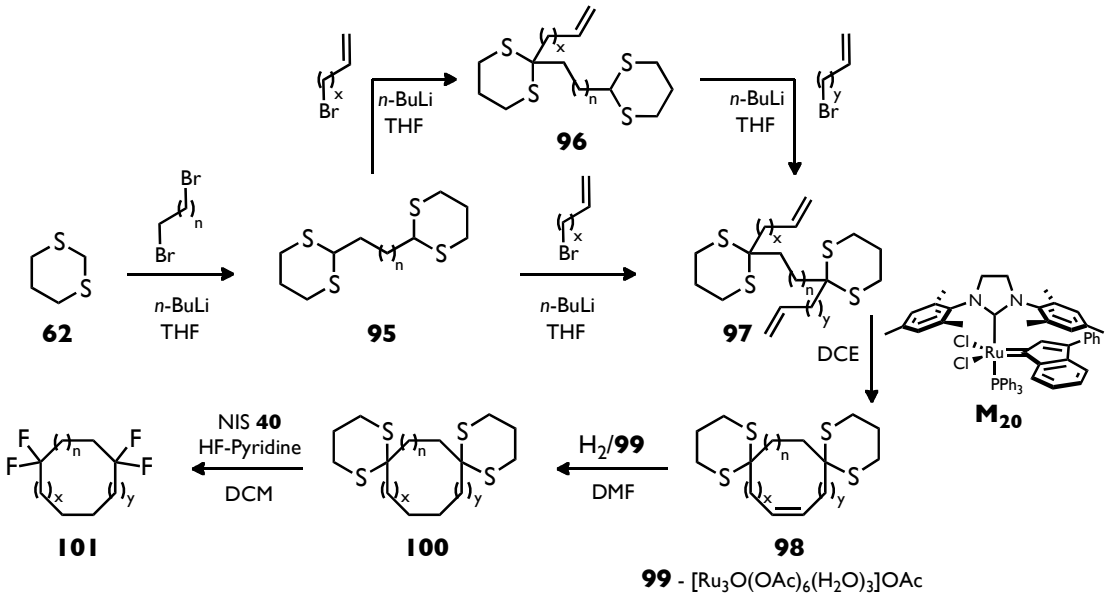

Scheme 3.1 General strategy to cycloalkanes containing two CF_2 groups.

3.2.1 Synthesis and conformational analysis of 1,1,4,4-tetrafluorocyclotetradecane

In the first step of the synthetic route to cyclotetradecane **91**, Corey-Seebach methodology was employed to access the RCM precursor **103** (Scheme 3.2).[14,15] Commercially available 2,2'-ethylenebis(1,3-dithiane) **102** was metallated using *n*-BuLi. The starting material was found to be poorly soluble in Et_2O, and therefore THF was used as the reaction solvent instead. In order to avoid potential side-reactions of the organolithium base with the solvent, the temperature was maintained below 0 ºC. Subsequent alkylation was carried out using 6-bromohex-1-ene. The lithiation/alkylation sequence was repeated twice to improve conversion towards the dialkylated product. Diolefin

103 was isolated in a good yield (73%), as a colourless viscous oil. It was then subjected to RCM cyclisation.

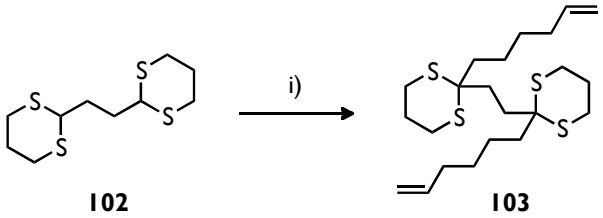

Scheme 3.2 Dialkylation of 2,2'-ethylenebis(1,3-dithiane) **102**. Reagents and conditions: i) *n*-BuLi, THF, 6-bromohex-1-ene, –25 to 0 ºC, 73%.

The ring-closing metathesis reaction was carried out at slightly elevated temperature (40 ºC), with 1.5 mol% of $\mathbf{M_{20}}$ as the catalyst (Scheme 3.3). In order to promote cyclisation over oligomerisation the reaction was conducted at relatively high dilution (0.04 M).[16] DCE, a higher boiling solvent with a low evaporation rate, was used instead of DCM to maintain the concentration of the reaction mixture. In the event the reaction proceeded with a good conversion (71%).

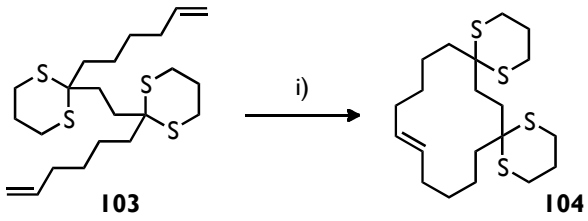

Scheme 3.3 Ring-closing metathesis of 2,2'-ethylenebis(2-(hex-5-enyl)-1,3-dithiane) **103**, Reagents and conditions: i) M_{20} (1.5 mol%), DCE, 40 ºC, 71%.

The cyclic product **104** was isolated as a colourless crystalline solid (m.p. = 135-136 ºC), and its X-ray crystal structure was determined (Figure 3.7). The structure revealed that the two sterically demanding dithiane groups adopt a chair conformation and were found as expected to occupy the

corner positions of a rectangular carbon skeleton [3434]. The *E*-stereoisomer was exclusively observed, indicating low overall ring strain in the 1,5,10,14-tetrathiadispiro[5.2.5.10]tetracos-19-ene **104**.

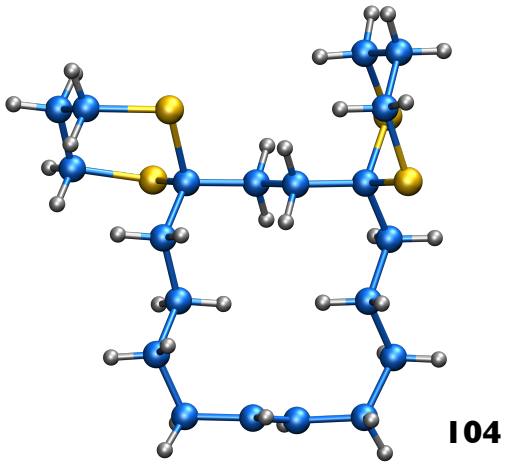

Figure 3.7 The X-ray crystal structure of 1,5,10,14-tetrathiadispiro[5.2.5.10]tetracos-19-ene **104**. (with A. M. Z. Slawin)

Hydrogenation of **104** was attempted using both palladium on charcoal and Crabtree as catalysts, however, neither set of conditions was successful. This might be explained by the tendency of sulfur to poison metal catalysts. Ricci *et al.* reported a ruthenium cluster complex, $[Ru_3O(OAc)_6(H_2O)_3]OAc$ **99**, which showed catalytic activity towards the hydrogenation of unsaturated sulfides.[17] This catalyst was found optimal for the hydrogenation of 1,5,10,14-tetrathiadispiro[5.2.5.10]tetracos-19-ene (**104**) (Scheme 3.4).

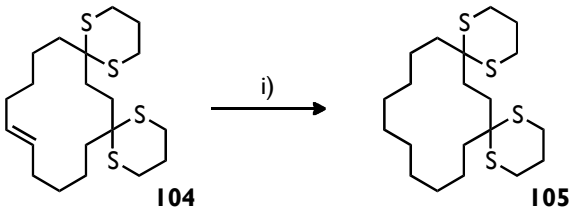

Scheme 3.4 The hydrogenation of 1,5,10,14-tetrathiadispiro[5.2.5.10]tetracos-19-ene **104**. Reagents and conditions: i) H_2 (10 bar), ruthenium catalyst **99** (15 mol%), DMF, 80 ºC, 60%.

The reaction was conducted over 48 hours in a sealed vessel, charged with 10 bar of H_2. The product (**105**) was isolated in good yield (70%) as a white crystalline solid (m.p. = 149-150 ºC), enabling the X-ray structure to be determined. As previously observed for the unsaturated analogue **104**, the dithiane motifs of **105** adopted a chair conformation and were located at the corners of the rectangular [3434] carbon ring (Figure 3.8).

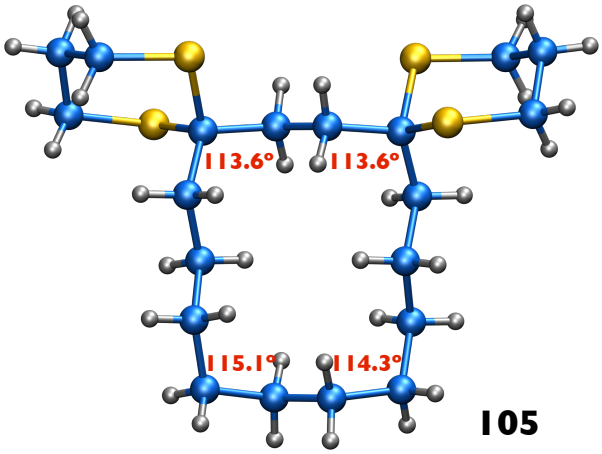

Figure 3.8 The X-ray crystal structure of 1,5,10,14-tetrathiadispiro[5.2.5.10]tetracosane **105**. (with A. M. Z. Slawin)

The CH_2-C($S_2C_3H_6$)-CH_2 angles in the dithiane-substituted corners were narrower by 0.7 to 1.5º than the corresponding unsubstituted corner CH_2-CH_2-CH_2 angles. This compression is most likely caused by unfavorable 1,2- and 1,3-H,S transannular interactions, which arise through the short contacts between these atom pairs, as observed in the solid state. (Figure 3.9).

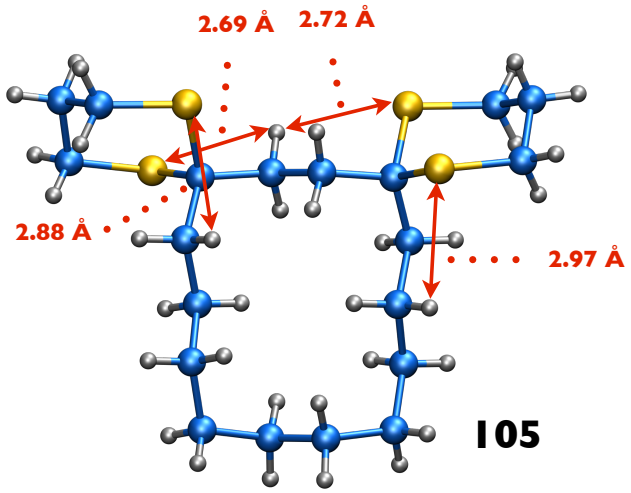

Figure 3.9 Representation of 1,2- and 1,3-H,S transannular interactions within the X-ray crystal structure of 1,5,10,14-tetrathiadispiro[5.2.5.10]tetracosane **105**.

1,1,4,4-Tetrafluorocyclotetradecane **91** was prepared using the oxidative fluorodesulfurisation protocol, previously employed in the synthesis of the CF_2-cyclododecanes (Chapter 2). The reaction was carried out in a polytetrafluoroethylene (PTFE) flask, using NIS **40** and HF-pyridine. This afforded **91** as a crystalline product (m.p. = 74 ºC) in good yield (68%) (Scheme 3.5).

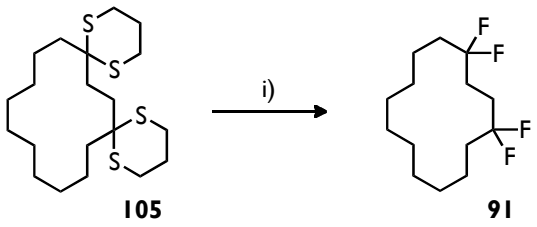

Scheme 3.5 *gem*-Difluorination of 1,5,10,14-tetrathiadispiro[5.2.5.10]tetracosane **105**. Reagents and conditions: i) NIS **40**, HF-pyridine, DCM, –78 ºC to RT, 68%.

As previously observed, X-ray crystal analysis revealed a rectangular [3434] structure, with the CF_2 motifs located at corner positions. Additionally, incorporation of the *gem*-difluorine groups resulted in a significant 4 to 5º CH_2-CF_2-CH_2 angle widening, when compared to the corresponding corner

CH_2-CH_2-CH_2 angles of cyclotetradecane.[2] At the same time, the F-C-F bond angles were narrower than tetrahedral, with values of 104.4º and 105.0º (Figure 3.10).

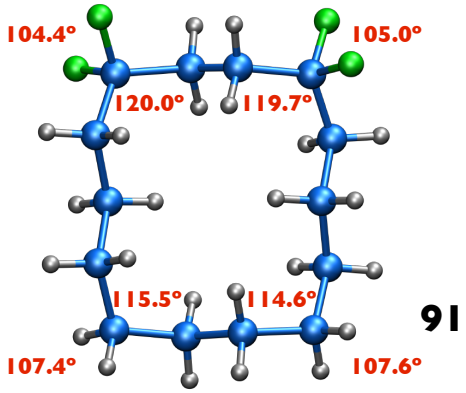

Figure 3.10 The X-ray crystal structure of 1,1,4,4-tetrafluorocyclotetradecane **91**. (with A. M. Z. Slawin)

1,2-H,F (*e.g.* 2.49, 2.52 Å) and 1,4-H,H (*e.g.* 2.16, 2.18 Å) transannular contacts were observed (above and below the face of the ring) in the solid state and they were found to be shorter than the sum of the van der Waals radii[18] of these atom pairs (H,F 2.66 Å, H,H 2.40 Å) (Figure 3.11). However, steric hindrance caused by short 1,3-H,S contacts in the dithiane precursor **105**, was found to be less significant in the corresponding 1,3-H,F interactions, confirming the lower steric impact of the CF_2 group. The above observations are in agreement with results previously obtained for CF_2-cyclododecanes (Chapter 2).

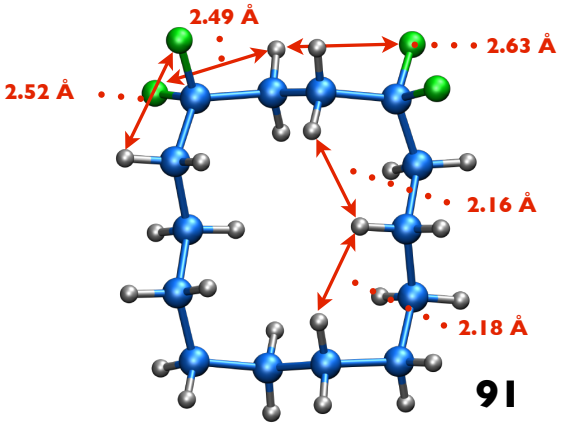

Figure 3.11 Representation of 1,2- and 1,3-H,F and 1,4-H,H transannular interactions within the X-ray crystal structure of 1,1,4,4-tetrafluorocyclotetradecane **91**.

$^{19}F\{^{1}H\}$ NMR spectroscopic analysis of 1,1,4,4-tetrafluorocyclotetradecane **91** was conducted at progressively lower temperatures to explore dynamic properties of the ring in solution. The experiment enabled partial resolution of the spin system (Figure 3.12), with a tendency towards an AB system, (previously recorded for 1,1,4,4-tetrafluorocyclododecane **74**) when the ring interconversion was slowed sufficiently.

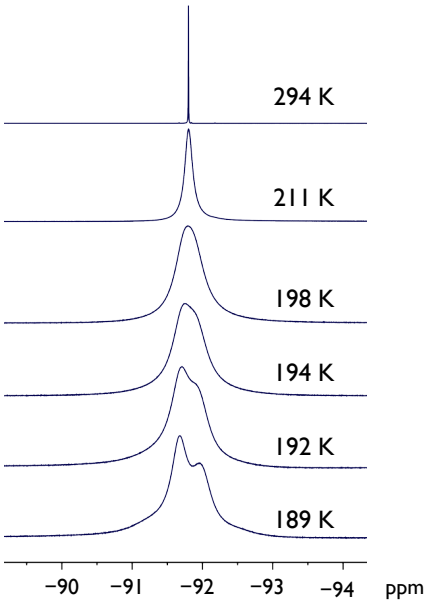

Figure 3.12 Partial plot of proton decoupled ^{19}F spectrum of 1,1,4,4-tetrafluorocyclotetradecane **91** at progressively lower temperatures. (with T. Lebl)

In conclusion, this low temperature experiment suggests that the geminal fluorine atoms are magnetically non-equivalent in the low temperature conformation.

3.2.2 Synthesis and conformational analysis of 1,1,6,6-tetrafluorocyclotetradecane

The route to the mismatched (corner/edge) 1,1,6,6-tetrafluoro-cyclotetradecane **93** started with the synthesis of the bisdithiane linker **106**, derived from 1,3-dithiane **62** by selective metallation with *n*-BuLi. The subsequent coupling of the lithiated intermediate to 1,4-dibromobutane afforded the 2,2'-butylenebis(1,3-dithiane) **106** in a good yield (65%) (Scheme 3.6).

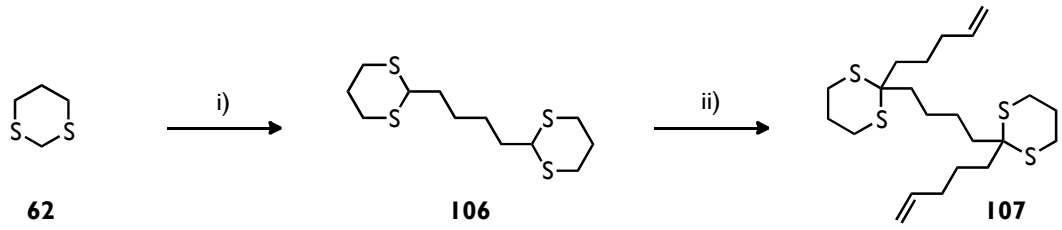

Scheme 3.6 Two-step synthesis of 2,2'-butylenebis(2-(pent-4-enyl)-1,3-dithiane) **107** *via* 2,2'-butylenebis(1,3-dithiane) **106**, Reagents and conditions: i) *n*-BuLi, THF, 1,4-dibromobutane, –30 to –5 ºC, 60%; ii) *n*-BuLi, THF, 5-bromopent-1-ene, –30 to 0 ºC, 75%.

In the next step, the dithiane spacer **106** was disubstituted through sequential lithiation and alkylation, using *n*-BuLi and 5-bromopent-1-ene (Scheme 3.6). The resulting diene **107** was isolated in 75% as a viscous oil. Ring-closing

metathesis of **107** using $\mathbf{M_{20}}$ as a catalyst proved difficult. It afforded cyclic olefin **108,** but in only 31% yield (Scheme 3.7).

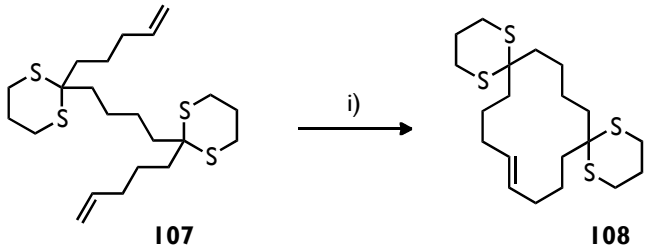

Scheme 3.7 Ring-closing metathesis of the 2,2'-butylenebis(2-(pent-4-enyl)-1,3-dithiane) **107**. Reagents and conditions: i) $\mathbf{M_{20}}$ (1 mol%), DCE, RT, 31%.

Competing oligomerisation gave the major product (cyclic olefin:oligomers ratio of 1:2 by ^{1}H NMR spectroscopy), even though the reaction was carried out at a low concentration (0.02 M). Attempts to increase the yield by employing even higher dilution conditions (0.01 M) resulted in longer reaction times with no improvement in conversion. This is most likely a result of an unfavourable conformational preorganisation of substrate **107**, arising from the combination of a large spacer and relatively short 'arms'. Moreover, the resulting 1,6-cornered product **108** is not a favoured conformer for these 14-membered rings. X-Ray crystal structure analysis of the resultant 1,5,12,16-tetrathiadispiro[5.4.5.8]tetracos-20-ene **108** revealed a distorted pseudo-trapezoid [5333] structure (Figure 3.13). As observed previously for **76** (Chapter 2) the corner positions have rearranged to accommodate the sterically demanding dithiane groups. The *E*-stereoisomer of **108** was observed exclusively, indicating that the increased ring strain does not affect the *E*/*Z* selectivity of the RCM reaction.

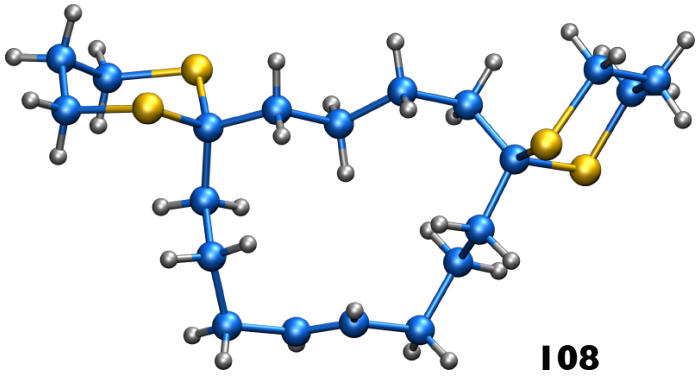

Figure 3.13 The X-ray crystal structure of 1,5,12,16-tetrathiadispiro[5.4.5.8]tetracos-20-ene **108**. (with A.M.Z. Slawin)

Hydrogenation of 1,5,12,16-tetrathiadispiro[5.4.5.8]tetracos-20-ene **108** using ruthenium catalyst **99** afforded the saturated product **109** in a good yield (70%) (Scheme 3.8).

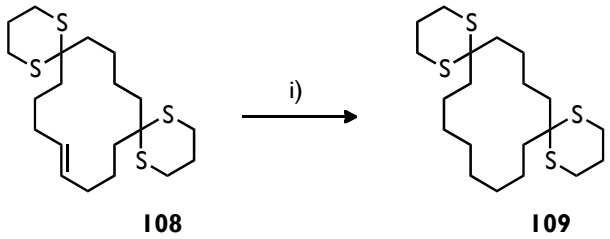

Scheme 3.8 The hydrogenation of 1,5,12,16-tetrathiadispiro[5.4.5.8]tetracos-20-ene **108**. Reagents and conditions: i) H_2 (10 bar), ruthenium catalyst **99** (30 mol%), DMF, 80 ºC, 70%.

This material was also obtained as a white crystalline solid (m.p. = 152-153 ºC), and analysed by X-ray crystallography (Figure 3.14). As observed for the unsaturated analogue **108**, dithiane substituents were found to occupy the 1,6-positions in the ring, resulting in a rearranged pseudo-trapezoidal [5333] conformation. As for **105**, slight CH_2-$C(S_2C_3H_6)$-CH_2 angle compression was observed in the dithiane-

substituted corners, most likely as a result of steric repulsion between 1,2- and 1,3-H,S atom pairs.

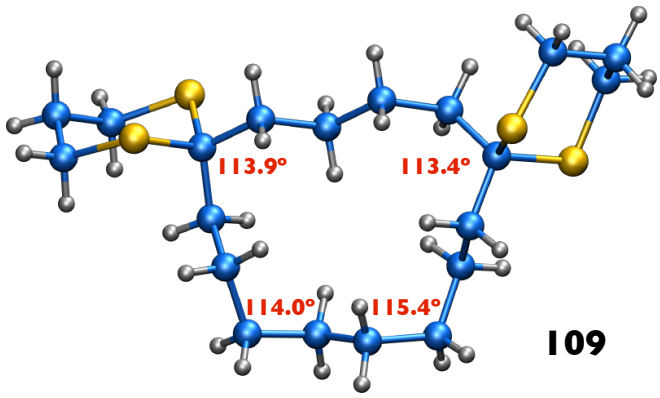

Figure 3.14 X-ray crystal structure of 1,5,12,16-tetrathiadispiro[5.4.5.8]tetracosane **109**. (with A. M. Z. Slawin)

In the next step *gem*-difluorination with *N*-iodosuccinimide **40** and HF-pyridine afforded 1,1,6,6-tetrafluorocyclotetradecane **93** in a reasonable yield (53%) (Scheme 3.9).

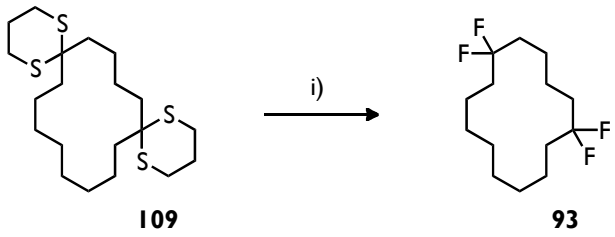

Scheme 3.9 *gem*-Difluorination of 1,5,12,16-tetrathiadispiro[5.4.5.8]tetracosane **109**. Reagents and conditions: i) NIS **40**, HF-pyridine, DCM, –78 ºC to RT, 53%.

The white crystalline product **93** (m.p. = 50 ºC) was submitted for X-ray crystal structure analysis and two crystallographically independent structures were found (Figure 3.15). Both conformers of **93** displayed a characteristic pseudo-trapezoidal [5333] carbon skeleton, similar to those of the dithiane precursors **108** and **109**. The CF_2 motifs were located at corner positions, now

rearranged to 1,6-positions of the C_{14} ring, as opposed to the 1,4-positions in **91**.

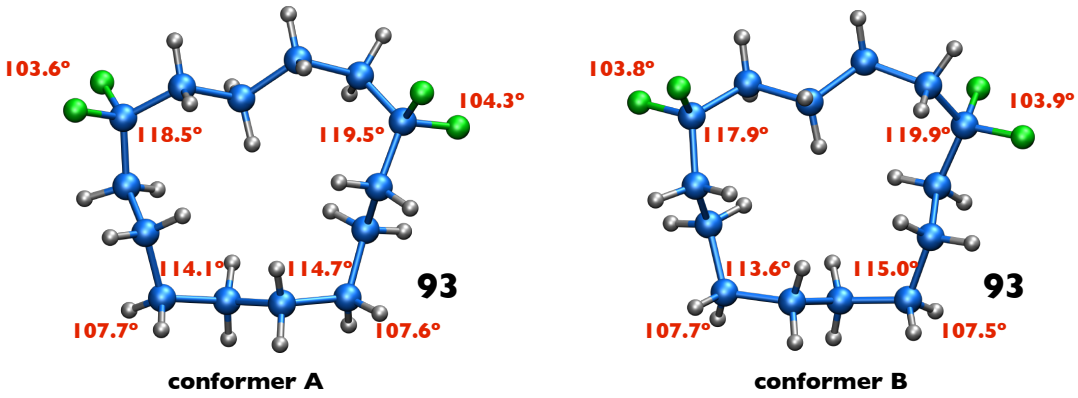

Figure 3.15 Two crystallographically independent X-ray crystal structures of 1,1,6,6-tetrafluorocyclotetradecane **93**. (with A. M. Z. Slawin)

Noticeable CH_2-CF_2-CH_2 angle widening and F-C-F angle narrowing is observed for both conformers of **93** displaying a clear distortion of the valence angles for the $CH_2CF_2CH_2$ unit. The change in conformation, from rectangular [3434] to pseudo-trapezoid [5333], resulted in shorter 1,3-H,F contacts (2.56 Å *versus* 2.63 Å in **91**), indicating a higher torsional strain (Figure 3.16A). It should also be noted that the lower symmetry of **93** disturbs the crystal packing, thus significantly decreasing its melting point, in comparison to the 1,4-CF_2 analogue **91** (50 ºC *versus* 74 ºC).

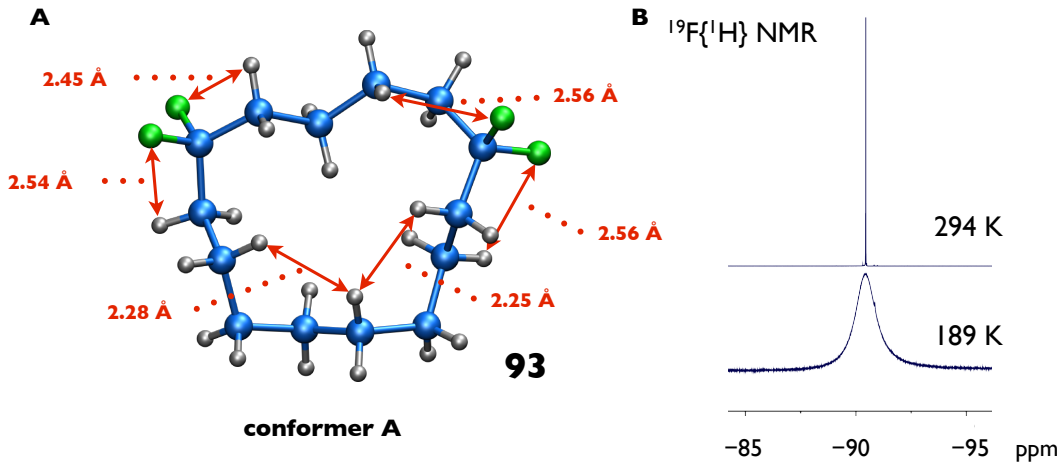

Figure 3.16 Representation of 1,2- and 1,3-H,F together with 1,4-H,H transannular interactions within the X-ray crystal structure of 1,1,6,6-tetrafluorocyclotetradecane **93** (conformer A) (**A**). Similar values were observed for conformer B (data not shown); Partial plot of proton decoupled ^{19}F spectra of 1,1,6,6-tetrafluorocyclotetradecane **93** at 294 and 189 K (**B**) (with T. Lebl).

A low temperature (CD_2Cl_2, 189 K) $^{19}F\{^1H\}$ NMR spectroscopic analysis of 1,1,6,6-tetrafluorocyclotetradecane **93** was carried out, but it was not possible to resolve the fluorine atoms into an AB system. Instead, a much broader peak was recorded at the lowest achievable temperature, indicating that the ring interconversion has not been slowed down sufficiently to generate magnetically non-equivalent *geminal* fluorine atoms at 189 K (Figure 3.16B).

3.2.3 Synthesis and conformational analysis of 1,1,5,5-tetrafluorocyclohexadecane

The lowest energy conformer of cyclohexadecane **89** adopts a square [4444] conformation with corners located at the 1,5 positions. 1,1,5,5-Tetrafluoro-cyclohexadecane **92** was designed to accommodate the CF_2 groups in the corners of cyclohexadecane **89**. 2,2'-Propylenebis(1,3-dithiane) **110**, an

appropriately spaced dithiane linker was assembled from 1,3-dithiane **62** and 1,3-dibromopropane, as summarised in Scheme 3.10.

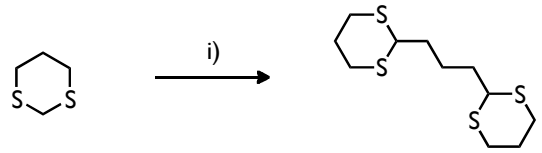

Scheme 3.10 The synthesis of 2,2'-propylenebis(1,3-dithiane) **110**. Reagents and conditions: i) *n*-BuLi, THF, 1,3-dibromopropane, −30 to −5 ºC, 62%.

For the next stage, a two-step selective disubstitution was carried out to access the unsymmetrical diene **111** (Scheme 3.11). Selective alkylation of 2,2'-propylenebis(1,3-dithiane) **110** using *n*-BuLi and 6-bromohex-1-ene resulted in **111** in a yield of 82%. Subsequent alkylation of intermediate **111** using *n*-BuLi and 7-bromohept-1-ene, afforded 1-(2-(hept-6-enyl)-1,3-dithian-2-yl)-3-(2-hex-5-enyl)-1,3-dithian-2-yl)propane **112** in 78% yield.

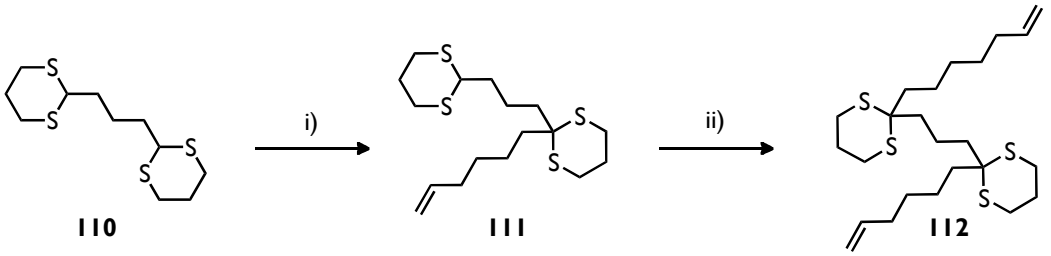

Scheme 3.11 Two-step selective alkylation of 2,2'-propylenebis(1,3-dithiane) **110**. Reagents and conditions: i) *n*-BuLi, THF, 6-bromohex-1-ene, −35 to −15 ºC, 82%; ii) *n*-BuLi, THF, 7-bromohept-1-ene, −10 to 0 ºC, 78%.

M_{20} was employed as a catalyst in the ring-closing metathesis of the diene**112** (Scheme 3.12). In order to increase the reaction output, the catalyst was added in two portions (2 × 1 mol%). The reaction was run for 24 hours and furnished 1,5,11,15-tetrathiadispiro[5.3.5.11]hexacos-21-ene **113** in good (69%) yield. The product was isolated as a viscous oil and could not be

crystallised. Subsequent hydrogenation afforded **114** in 56% yield (Scheme 3.12).

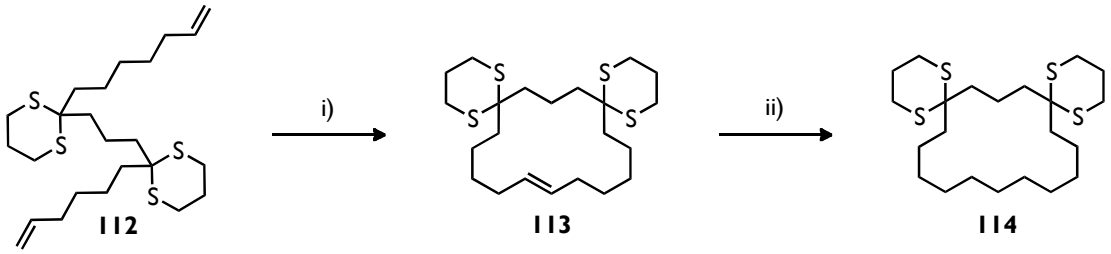

Scheme 3.12 Two-step synthesis of 1,5,11,15-tetrathiadispiro[5.3.5.11]hexacosane **114**. Reagents and conditions: i) $\mathbf{M_{20}}$ (2 × 1 mol%), DCE, RT, 69%; ii) H_2 (10 bar), ruthenium catalyst **99** (7.6 mol%), DMF, 80 ºC, 56%.

The saturated cyclic product **114** was isolated as a white crystalline solid (m.p. = 126-128 ºC) and was successfully analysed by X-ray crystallography. A square-shaped [4444] carbon ring was revealed, with the dithiane motifs sitting at corner positions (Figure 3.17). As previously observed for **105** and **109**, the angles in the dithiane-substituted corners were slightly narrower (113.7º) than the corresponding CH_2-CH_2-CH_2 corner angles (114.5º). This is again most likely due to angle compression caused by the bulky dithiane substituents, as a result of unfavorable 1,2- and 1,3-H,S transannular interactions (Figure 3.17).

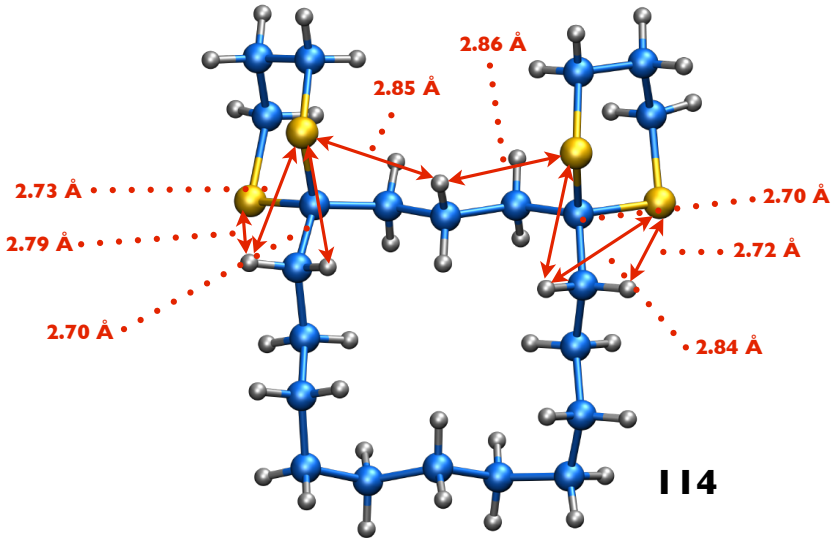

Figure 3.17 Representation of 1,2- and 1,3-H,S transannular interactions within the X-ray crystal structure of 1,5,11,15-tetrathiadispiro[5.3.5.11]hexacosane **114**.

The desired 1,1,5,5-tetrafluorocyclohexadexane **92** was obtained in a moderate yield (43%) through *gem*-difluorination with *N*-iodosuccinimide **40** and HF-pyridine (Scheme 3.13). This material was again a white crystalline solid (62.5 ºC), permitting X-ray crystal structure analysis.

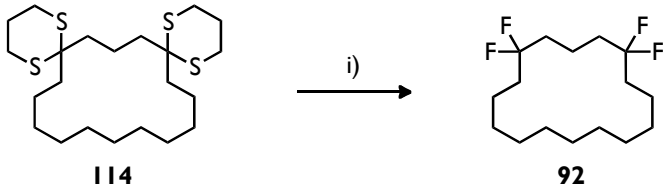

Scheme 3.13 *gem*-Difluorination of 1,5,11,15-tetrathiadispiro[5.3.5.11]hexacosane **114**. Reagents and conditions: i) NIS **40**, HF-pyridine, DCM, –78 ºC to RT, 43%.

The carbon ring was observed to adopt a square-shaped [4444] structure, with the two CF_2 motifs located at corner positions (Figure 3.18). As anticipated, the CH_2-CF_2-CH_2 bond angles are significantly wider (118.2º) and the F-C-F bond angles narrower (104.4º), than tetrahedral.

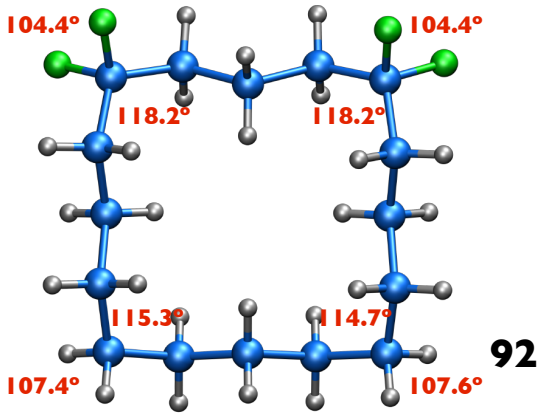

Figure 3.18 X-ray crystal structure of 1,1,5,5-tetrafluorocyclohexadecane **92**. (with A. M. Z. Slawin)

Comparison of **92** to the previously described CF_2-cyclododecanes (**74-76**) and CF_2-cyclotetradecanes (**91**, **93**) revealed that the larger ring size of **92** resulted in increased 1,4-H,H transannular distances. These were lengthened (2.40/2.42 Å *versus* 2.29/2.32 Å) as a result of wider CH_2-CF_2-CH_2 angles. The 1,2-H,F transannular contacts (*e.g.* 2.48, 2.53 Å), were found to be noticeably shorter than the sum of the van der Waals radii[18] of fluorine and hydrogen atoms (2.66 Å), suggesting a pronounced steric impact of the CF_2 group (Figure 3.19A). Short 1,3-H,F contacts were not observed in the solid state of 1,1,5,5-tetrafluorocyclohexadecane **92**, implying that the overall steric impact of the CF_2 motifs is much less significant than that of the bulky the dithiane groups.

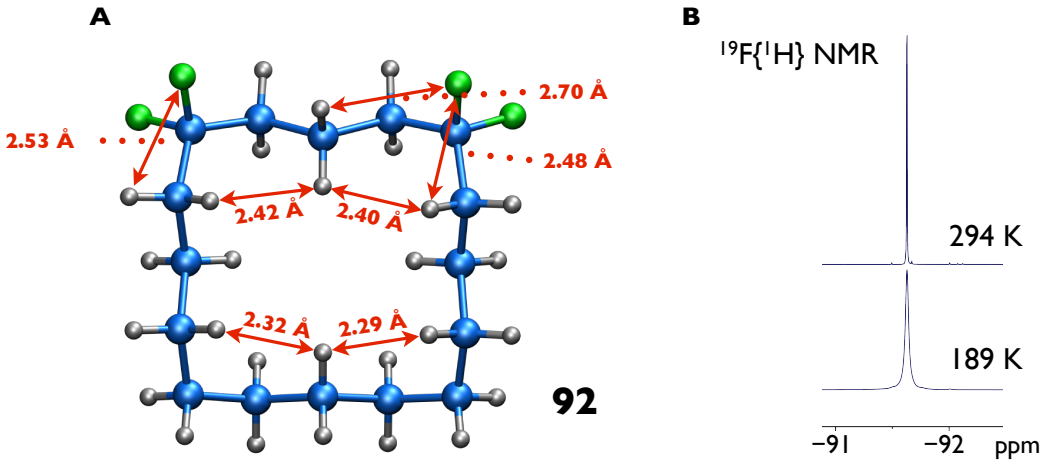

Figure 3.19 Representation of 1,2- and 1,3-H,F together with 1,4-H,H transannular contacts within the X-ray crystal structure of 1,1,5,5-tetrafluorocyclohexadecane **92** (**A**); Partial plot of proton decoupled ^{19}F spectra of 1,1,5,5-tetrafluorocyclohexadecane **92** at 294 and 189 K (**B**) (with T. Lebl).

A low temperature (CD_2Cl_2, 189 K) $^{19}F\{^{1}H\}$ NMR spectroscopic analysis of 1,1,5,5-tetrafluorocyclohexadecane **92** did not result in the resolution of the spin system. Instead, a much sharper peak was recorded when compared to the data obtained for the two tetrafluorocyclotetradecanes, **91** and **93** (Figure 3.19B). This observation suggests a faster ring interconversion in the larger C_{16} ring system.

3.2.4 Synthesis and conformational analysis of 1,1,6,6-tetrafluorocyclohexadecane

1,1,6,6-Tetrafluorocyclohexadecane **94** was synthesised in an attempt to modify the square [4444] conformation of cyclohexadecane ring, through increasing the spacing between the two CF_2 groups. The previously synthesised 2,2'butylenebis(1,3-dithiane) **106** was used as the starting linker. The alkene-terminated 'arms' were attached by sequential lithiation/alkylation

of **106**, using *n*-BuLi and 6-bromohex-1-ene (Scheme 3.14). Diene **115** was isolated as a viscous oil in 62% yield.

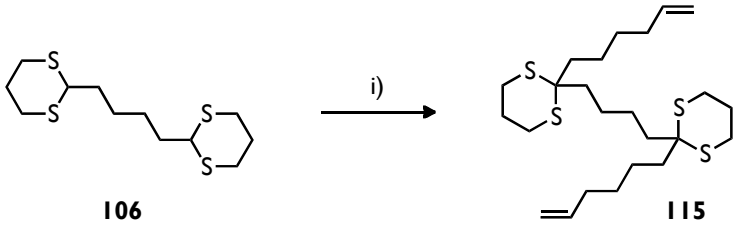

Scheme 3.14 Dialkylation of 2,2'-butylenebis(1,3-dithiane) **106**. Reagents and conditions: i) *n*-BuLi, THF, 6-bromohex-1-ene, –30 to 0 ºC, 62%.

Ring-closing metathesis of **115** was carried out at low concentration (0.02 M), in order to avoid oligomerisation of the starting diene **115** (Scheme 3.15). Two aliquots of $\mathbf{M_{20}}$ (2 × 1mol%) were used to increase the reaction conversion. 1,5,12,16-Tetrathiadispiro[5.4.5.10]hexacos-21-ene **116** was isolated as a white crystalline solid (m.p. = 154-156 ºC) in good yield (68%).

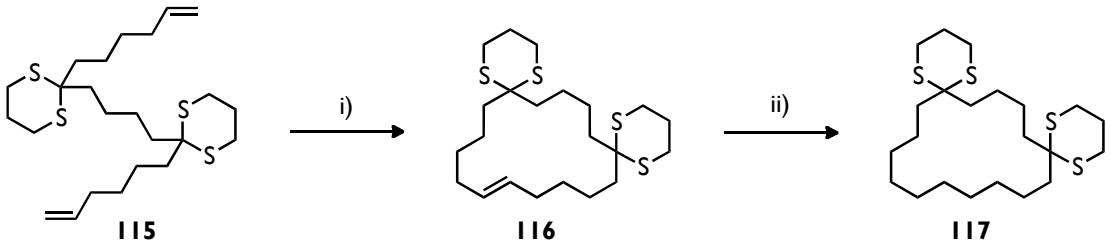

Scheme 3.15 Two-step synthesis of 1,5,12,16-tetrathiadispiro[5.4.5.10]hexacosane **117**. Reagents and conditions: i) $\mathbf{M_{20}}$ (2 mol%), DCE, RT, 68%; ii) H_2 (10 bar), ruthenium catalyst **99** (7.6 mol%), DMF, 80 ºC, 77%.

An X-ray crystal structure of the macrocycle **116** was determined, revealing a trapezoid-type [5434] carbon skeleton (Figure 3.20). As previously determined, the corner positions have rearranged to accommodate the sterically demanding dithiane groups. Again, only the *E*-stereoisomer of the product was observed.

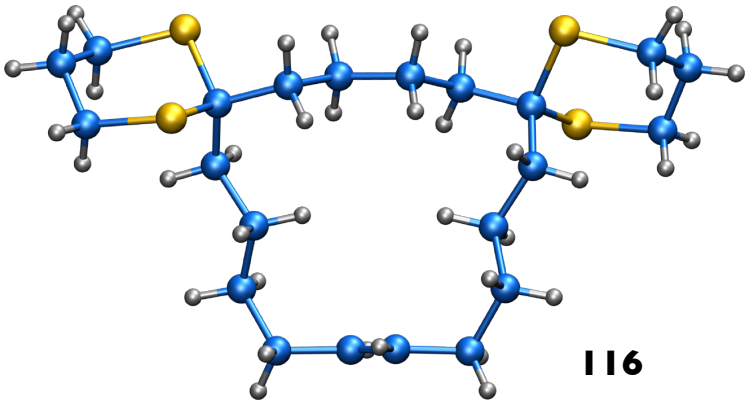

Figure 3.20 X-ray crystal structure of 1,5,12,16-tetrathiadispiro[5.4.5.10]hexacos-21-ene **116**. (with A. M. Z. Slawin)

Subsequent hydrogenation of **116**, using **99** as a catalyst, proved to be straightforward and afforded 1,5,12,16-tetrathiadispiro[5.4.5.10]hexacosane **117** in 77% yield (Scheme 3.15). The product was isolated as a white crystalline solid (m.p. = 136-137 ºC), enabling X-ray structural analysis. This again revealed a trapezoid-type [5434] carbon skeleton, similar to that of the unsaturated analogue **116** (Figure 3.21).

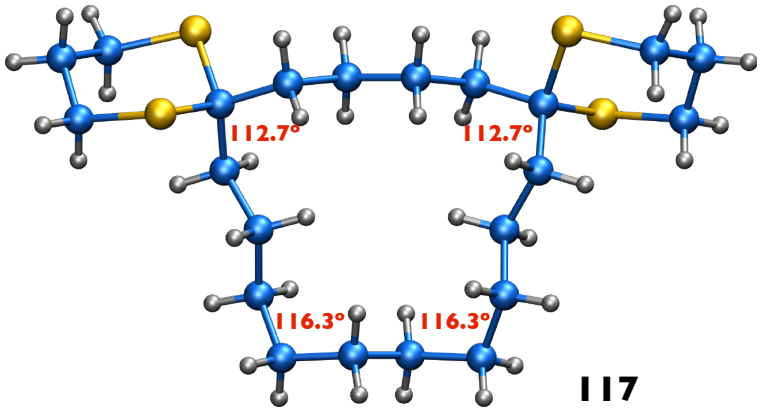

Figure 3.21 X-ray crystal structure of 1,5,12,16-tetrathiadispiro[5.4.5.10]hexacosane **117** highlighting the corner C-C-C angles. (with A.M.Z. Slawin)

Further examination of the X-ray structure of **117** showed close 1,2- and 1,3-H,S transannular contacts (*e.g.* 2.74, 2.91 Å), with distances significantly

shorter than the sum of the van der Waals radii[18] of the hydrogen and sulfur atoms (3.09 Å) (Figure 3.22). A resulting angle compression in **117** became apparent, when the difference between CH_2-CR_2-CH_2 angles of the substituted and unsubstituted corners were compared (112.7º *versus* 116.3º) (Figure 3.21).

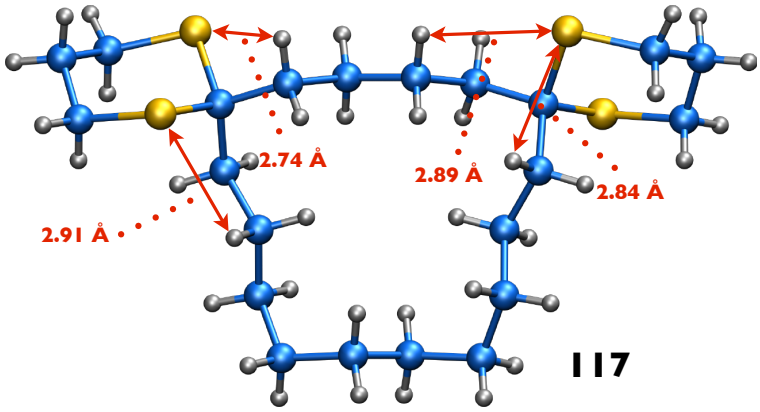

Figure 3.22 Representation of 1,2- and 1,3-H,S transannular interactions within the X-ray crystal structure of 1,5,12,16-tetrathiadispiro[5.4.5.10]hexacosane **117**.

The final step in the synthetic route involved *gem*-difluorination of **117**, using *N*-iodosuccinimide **40** and HF-pyridine. The target compound, 1,1,6,6-tetrafluorocyclohexadecane **94**, was furnished in 65% yield (Scheme 3.16).

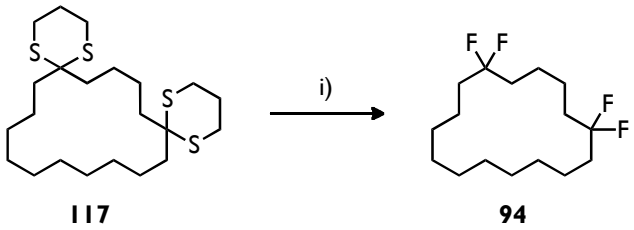

Scheme 3.16 *gem*-Difluorination of 1,5,12,16-tetrathiadispiro[5.4.5.10]hexacosane **117**. Reagents and conditions: i) NIS **40**, HF-pyridine, DCM, –78 ºC to RT, 65%.

The crystalline product **94** (m.p. = 39.5 ºC) was submitted for X-ray crystal structure analysis. A trapezoid [5434] structure was found for **94**, similar to

that for the dithiane precursors **116** and **117** (Figure 3.23). The CF_2 motifs were found to occupy corner positions of the C_{16} ring. The corners have rearranged from the 1,5-positions in **92** to the 1,6-positions in **94**. As previously observed for CF_2-cyclododecanes (**74-76**) and CF_2-cyclotetradecanes (**91-93**), the CH_2-CF_2-CH_2 angles were found to be much wider and F-C-F angles narrower than tetrahedral (Figure 3.23).

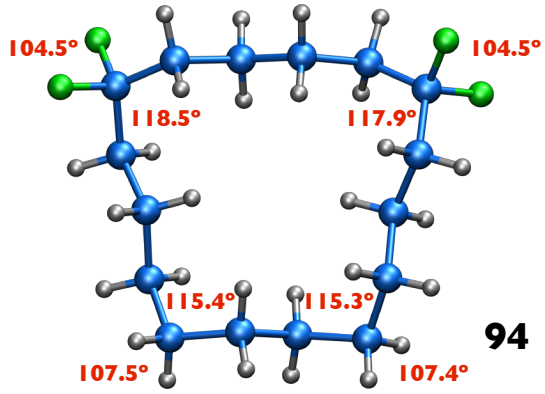

Figure 3.23 X-ray crystal structure of 1,1,6,6-tetrafluorocyclohexadecane **94**. (with A. M. Z. Slawin)

Distortion of the conformation on the CF_2-substituted side of the ring resulted in shorter 1,4-H,H transannular distances than those observed in 1,1,5,5-tetrafluorocyclohexadecane **92** (2.20/2.25 Å *versus* 2.42/2.40 Å) (Figure 3.24A). The 1,4-H,H distances on the unsubstituted side of the ring remained unchanged (2.31/2.29 Å *versus* 2.32/2.29 Å in **92**). Furthermore, the 1,2-H,F transannular contacts (*e.g.* 2.48, 2.53 Å) were significantly shorter than the sum of the van der Waals radii[18] of the fluorine and hydrogen atoms (2.66 Å), confirming the steric impact of the CF_2 group. In contrast to the relatively short 1,3-H,S contacts observed in the dithiane precursor **117**, 1,3-H,F interactions were not observed in the solid state of 1,1,6,6-tetrafluorocyclohexadecane **94**.

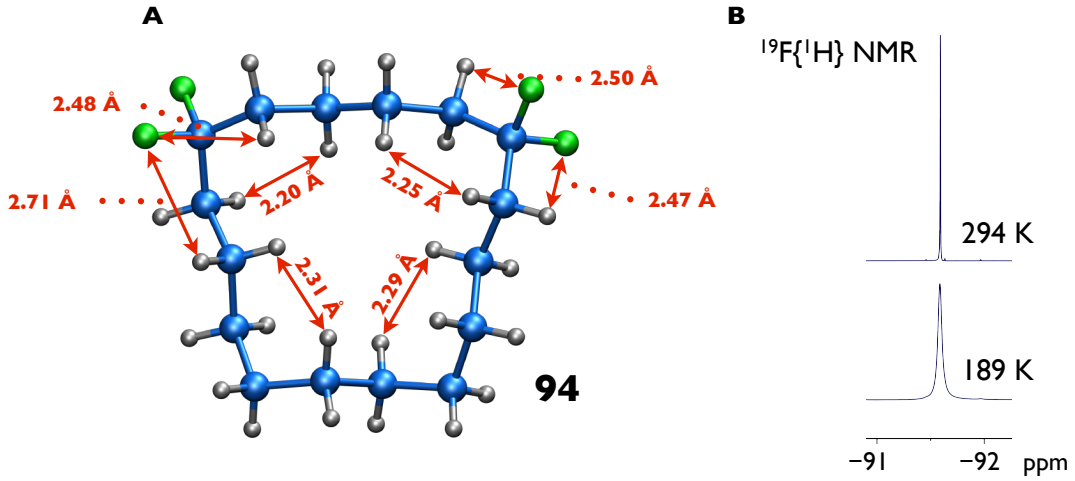

Figure 3.24 Representation of 1,2- and 1,3-H,F together with 1,4-H,H transannular contacts within the X-ray crystal structure of 1,1,6,6-tetrafluorocyclohexadecane **94** (**A**). Partial plot of proton decoupled ^{19}F spectra of 1,1,6,6-tetrafluorocyclohexadecane **94** at 294 and 189 K (**B**) (with T. Lebl).

The melting point of the conformationally distorted **94** (m.p. = 39.5 ºC) is more than 20 ºC lower than the melting point of the previously reported 1,1,5,5-tetrafluorocyclohexadecane **92** (m.p. = 62.5 ºC). This could be explained by less organised crystal packing, resulting from its lower symmetry. $^{19}F\{^{1}H\}$ NMR spectroscopic analysis of 1,1,6,6-tetrafluorocyclohexadecane **94** (CD_2Cl_2, 189 K) did not enable resolution of the spin system (Figure 3.24B). Again, a sharp signal was recorded, implying rapid ring interconversion due to the dynamic nature of the large C_{16} ring.

3.3 Conclusions

In this Chapter, the stereoelectronic influence of the CF_2 group has been studied in larger cycloalkanes using cyclotetradecane **88** and cyclohexadecane **89** as molecular frameworks. In order to access the target

CF_2-cyclotetradecanes (**91** and **93**), and cyclohexadecanes (**92** and **94**), a novel synthetic route was designed, based on Corey-Seebach dithiane chemistry and ring-closing metathesis. Cyclisation reactions and subsequent hydrogenations were successfully conducted using sulfur-compatible ruthenium catalysts (**M_{20}** and **99**). Three of the unsaturated dithiane intermediates (**104**, **108**, **116**) were obtained as crystalline solids, shown to be exclusively present as their *E*-stereoisomers when analysed by X-ray crystallography (Figure 3.25).

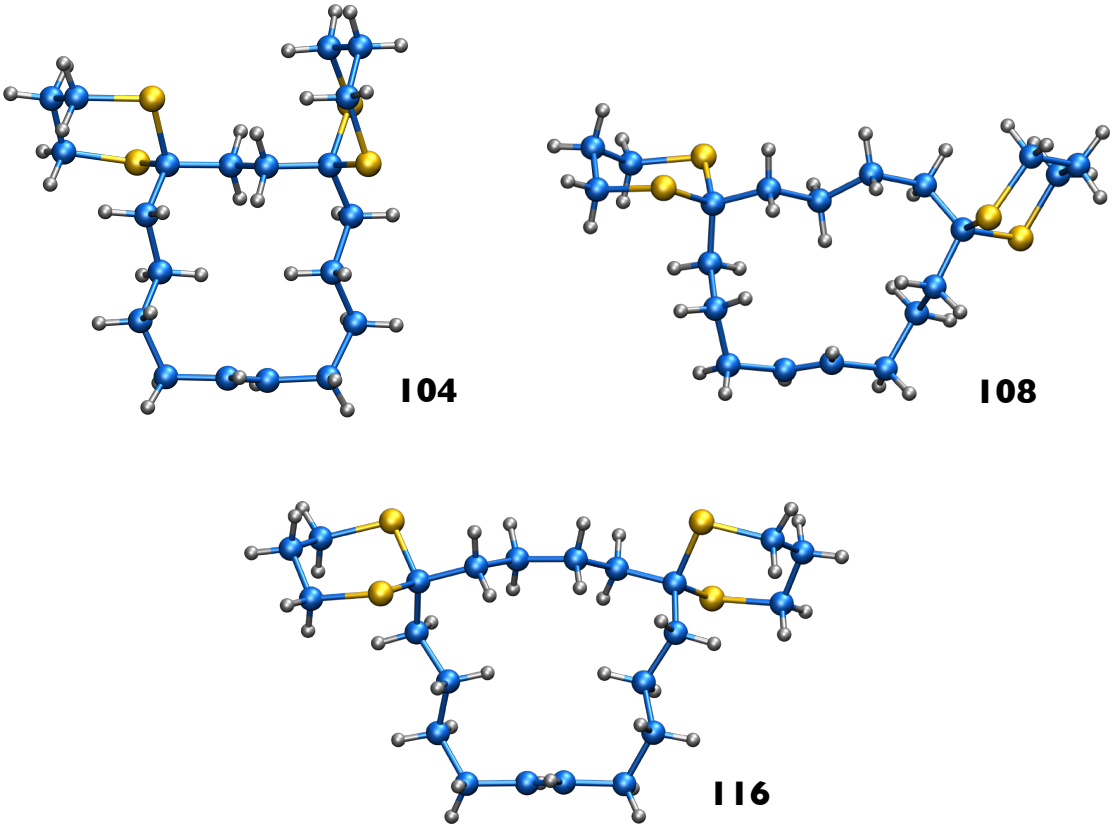

Figure 3.25 X-Ray crystal structures of unsaturated bisdithiane intermediates **104**, **108** and **116**. (with A. M. Z. Slawin)

As the stereoselectivity of the ring closing metathesis reaction depends on the ring strain, observation of *E*-stereoisomers indicates low strain in these systems.[19] All of the four saturated (**105**, **109**, **114**, **117**) dithianes were

isolated as crystalline solids allowing for X-ray crystal structure determination. Substitution with dithiane groups in the 1,4-positions in cyclotetradecane **88** and the 1,5-positions in cyclohexadecane **89** maintained the ideal conformations predicted by Dale (rectangular [3434] conformation in the C_{14} ring and square [4444] conformation in the C_{16} ring). In each case the dithiane groups were found to locate at the corner positions, despite the resulting distortion of the ring in the mismatched 1,6-substituted cycloalkanes **109** and **117** as shown in Figure 3.26.

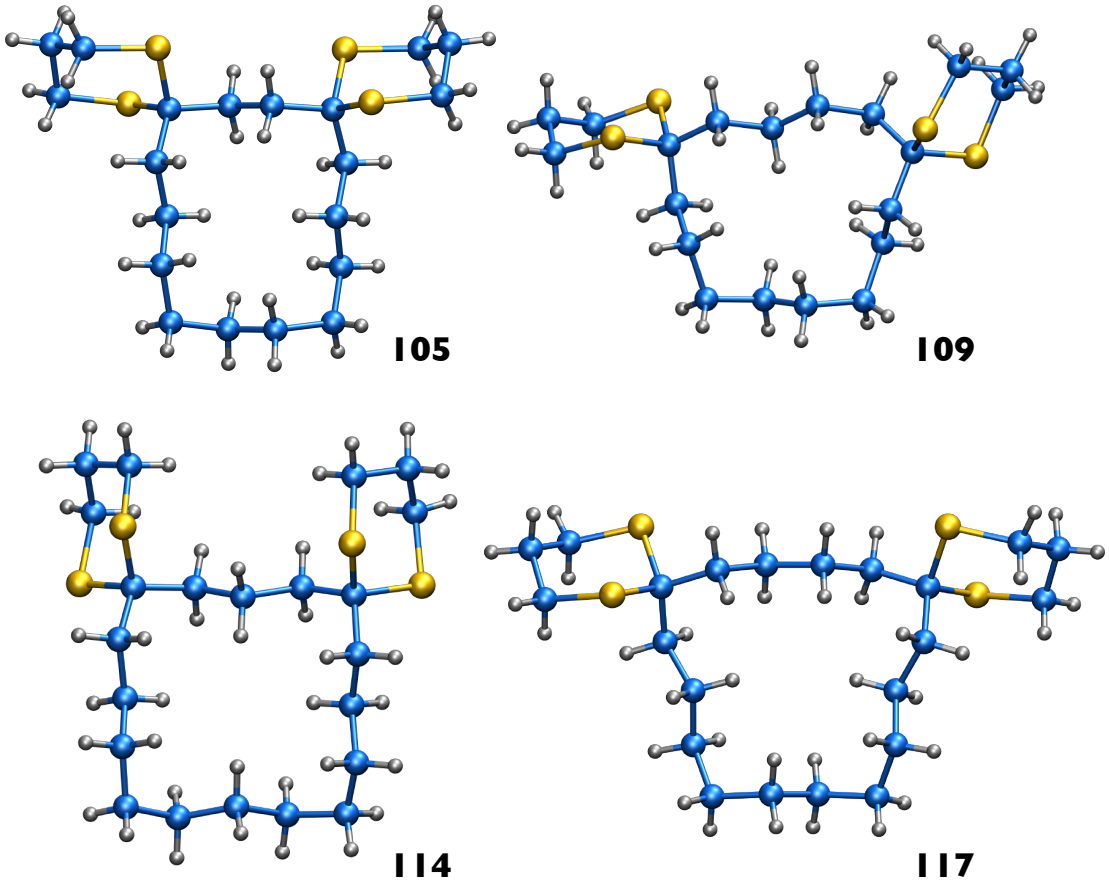

Figure 3.26 X-Ray crystal structures of bisdithiane intermediates **105**, **109, 114** and **117**. (with A. M. Z. Slawin)

Surprisingly, substitution with a small difluoromethylene group exhibited a similar conformational influence on the large C_{14} and C_{16} alicyclic systems as

that of the bulky dithiane moiety. The solid state conformations of tetrafluorocyclotetradecanes (**91**, **93**) and tetrafluorocyclohexadecanes (**92**, **94**) confirmed the strong preference for the difluoromethylene group to occupy corner positions (Figure 3.27).

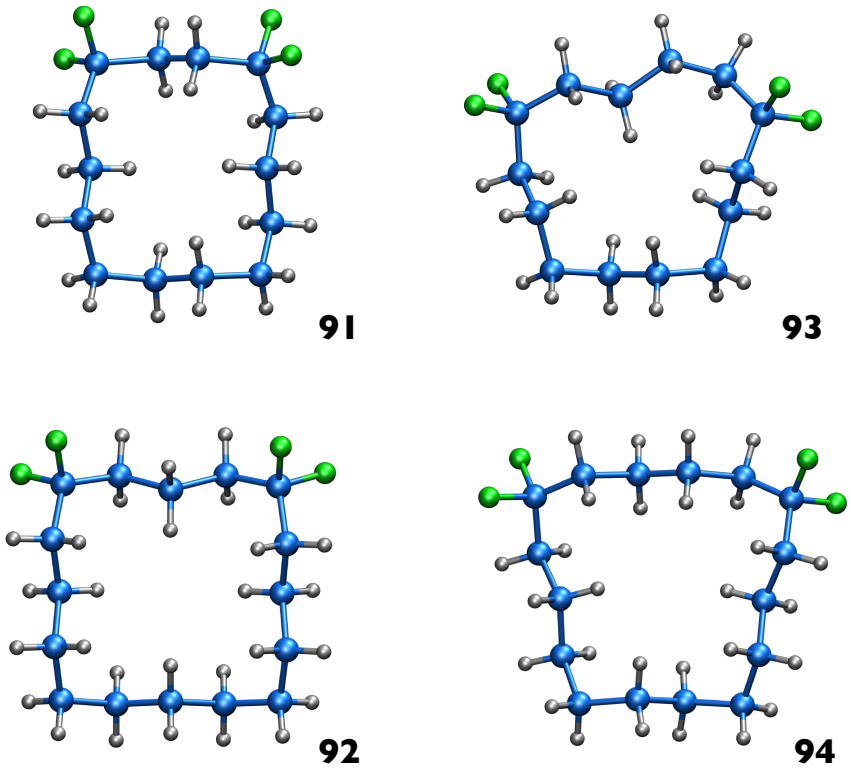

Figure 3.27 X-Ray crystal structures of CF_2-cyclotetradecanes (**91** and **93**) and CF_2-cyclohexadecanes (**92** and **94**). (with A. M. Z. Slawin)

When the relative positions of the CF_2 groups did not correspond to the predicted ideal corner positions (**93** and **94**), the ring rearranged in such a way as to allow both CF_2 substituents to hold the corner locations. This conformational change ensured that unfavourable steric tension which could arise if the C-F bond projected into the ring interior, was avoided. The same phenomenon was found for 1,1,6,6-tetrafluorocyclododecane **76** (Chapter 2).

In contrast to the dithiane group which generally compresses the CH_2-$C(S_2C_3H_6)$-CH_2 angle (on the basis of steric hindrance), substitution with the CF_2 group resulted in a significant CH_2-CF_2-CH_2 angle widening. Such widening is now generally observed for the $CH_2CF_2CH_2$ motif and originates from to the high electronegativity of the fluorine atom as described in Chapter 1.

The results presented in Chapters 1 and 2 have revealed the ability of the CF_2 group to enforce a conformational preference in alicyclic hydrocarbon systems while increasing rigidity and polarity at the same time. These properties offer the potential for design of novel performance materials, by strategic incorporation of the CF_2 group.

3.4 References

1. J. Dale, *Acta Chem. Scand.*, 1973, **27**, 1115–1129.
2. P. Groth, *Acta Chem. Scand.*, 1976, **30**, 155–156.
3. J. D. Dunitz, H. M. M. Shearer, *Helv. Chim. Acta*, 1960, **43**, 18–35.
4. J. Dale, A. J. Hubert, G. S. D. King, *J. Chem. Soc.*, 1963, 73–86.
5. P. Groth, *Acta Chem. Scand.*, 1976, **30**, 294–296.
6. J. Dale, *Acta Chem. Scand.*, 1973, **27**, 1149–1158.
7. P. Groth, *Acta Chem. Scand.*, 1974, **28**, 808–810.
8. F. Boeda, H. Clavier, S. P. Nolan, *Chem. Commun.*, 2008, 2726–2740.
9. C. Samojłowicz, M. Bieniek, K. Grela, *Chem. Rev.*, 2009, **109**, 3708–3742.
10. G. C. Vougioukalakis, R. H. Grubbs, *Chem. Rev.*, 2010, **110**, 1746–1787.
11. J. Broggi, C. A. Urbina-Blanco, H. Clavier, A. Leitgeb, C. Slugovc, A. M. Z. Slawin, S. P. Nolan, *Chem. Eur. J.*, 2010, **16**, 9215–9225.
12. C. A. Urbina-Blanco, S. Manzini, J. P. Gomes, A. Doppiu, and S. P. Nolan, *Chem. Commun.*, 2011, **47**, 5022–5024.
13. S. C. Sondej, J. A. Katzenellenbogen, *J. Org. Chem.*, 1986, **51**, 3508–3513.
14. E. J. Corey, D. Seebach, *Angew. Chem. Int. Ed.*, 1965, **4**, 1075–1077.
15. D. Seebach, E. J. Corey, *J. Org. Chem.*, 1975, **40**, 231–237.
16. S. Monfette, D. E. Fogg, *Chem. Rev.*, 2009, **109**, 3783–3816.
17. V. Cerè, F. Massaccesi, S. Pollicino, A. Ricci, *Synth. Commun.*, 1996, **26**, 899–907.
18. S. Alvarez, *Dalton Trans.*, 2013, **42**, 8617–8636.
19. C. W. Lee, R. H. Grubbs, *Org. Lett.*, 2000, **2**, 2145–2147.

4

Accelerating influence of the CF_2 group in ring-closing metathesis of nona-1,8-dienes

4.1 Introduction

Incorporation of one or more geminal substituents into cyclisation precursors is a known strategy for improving the efficiency of many ring-closing reactions.[1] In Chapter 3, results were described that showed the incorporation of two dithiane groups into long aliphatic chains bearing terminal olefin moieties. This resulted in a successful ring-closing metathesis reaction and allowed access to a family of CF_2-containing cyclotetradecanes and cyclohexadecanes.[2]

4.1.1 Thorpe-Ingold effect

The fact that *gem*-disubstitution of the methylene hydrogens (CH_2) with alkyl groups facilitates cyclisation reactions was first reported by Beesley, Thorpe and Ingold in 1915.[3] Their rationale for the observed phenomenon was the difference in the relative volumes of the geminal substituents leading to a deviation (narrowing) in the C-CX_2-C angles. Ingold proposed that *"the tetrahedron representing a carbon is approximately regular only when the carbon atom is attached to four atoms of a similar kind, for example, to four carbon atoms"*.[4] Accordingly, *gem*-dimethyl substituents C-$C(CH_3)_2$-C are sterically more demanding than methylene hydrogen atoms C-CH_2-C, and thus a relaxation of the angle ***Φ*** occurs in order to relax unfavourable steric interactions between these substituents (Figure 4.1). This relaxation results in compression of the corresponding angle ***Θ***. It follows that the narrower the angle ***Θ*** the shorter the distance between the two reactive groups (**X** and **Y**) and therefore the easier the cyclisation (Figure 4.1). Such a change in the valence angles upon such substitution is known as the Thorpe-Ingold effect.[1]

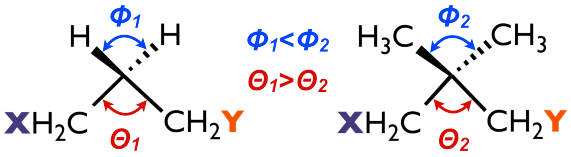

Figure 4.1 Graphical representation of angle deviation accounting for the Thorpe-Ingold effect.

The angle compression resulting from substitution is apparent by comparison of the angles in propane **6** and isobutane **118** (112.4º *versus* 111.2º respectively).[5] Replacement of the methylene hydrogen atom with the more

bulky methyl group results in a narrower angle in isobutane **118** (Figure 4.2). The angle observed in neopentane **119** was found to be tetrahedral (109.5º), as the substituents at the central quaternary carbon are sterically equivalent (Figure 4.2).[5]

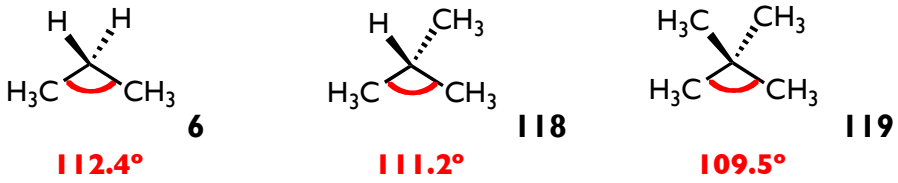

Figure 4.2 Valence angles in propane[6] **6**, isobutane[7] **118** and neopentane[8] **119** as presented by Schleyer.[5]

In 1960, Schleyer, exploring the Thorpe-Ingold effect, compared the degree of intramolecular hydrogen bonding in propane-1,3-diol **120a** and a group of 2-substituted analogues (**120b-f**) (Table 4.1).[5] In order to quantify the H…OH interactions in dilute (0.005 M) solutions of propane-1,3-diols (**120a-f**) IR spectroscopy was employed. It was previously observed by Kuhn, that the stronger the hydrogen bond the greater the difference in wave numbers (Δv) between the bands representing bonded and free OH groups.[9] Schleyer's study showed a correlation between the degree of substitution in propane-1,3-diol and an increase of the H…OH interactions, as summarised in Table 4.1.[5]

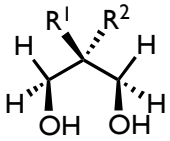

120

120	R^1	R^2	Δv [cm^{-1}]
a	H	H	77.7
b	H	CH_3	84.7
c	H	*i*Pr	84.6
d	CH_3	CH_3	88.0
e	C_2H_5	C_2H_5	90.0
f	*i*Pr	*i*Pr	84.8

Table 4.1 Hydrogen bonding in propane-1,3-diols **120a-f** as determined by Schleyer.[5]

The two 2-monosubstituted derivatives of propane-1,3-diol, **120b** and **120c,** exhibited larger Δv than the parent **120a**, indicating stronger intramolecular hydrogen bonds. Geminally disubstituted propane-1,3-diols **120d-e** displayed a further increase in the H…OH interactions as a consequence of the shorter distance between two hydroxyl groups. The closer proximity of the hydroxyl groups was enforced by C-CR_2-C angle compression. Interestingly, substitution with a sterically more demanding *gem*-diisopropyl group resulted in decreased Δv in **120f** compared to those reported for the *gem*-dimethyl **120d** and *gem*-diethyl **120e** counterparts. It was thought that the greater substitution in **120f** resulted in longer H...OH distances as a result of steric interactions between the hydroxyl and isopropyl groups.

4.1.2 Reactive rotamer effect

An alternative theory explaining the difference in the cyclisation rates of substituted and unsubstituted hydrocarbons was proposed by Bruice and Pandit in 1960.[10] In order for cyclisation reactions to occur the two reactive termini need to be in proximity. It was suggested that substitution in the alkyl

chain results in an increased population of the *gauche* relative to the *anti* rotamers as a consequence of transannular interactions between the sterically more demanding substituents and the hydrocarbon chain. Such a conformational bias, from the *anti* to the *gauche* conformation, would shorten the distance between the reactive sites **X** and **Y** and promote cyclisation (Figure 4.3).

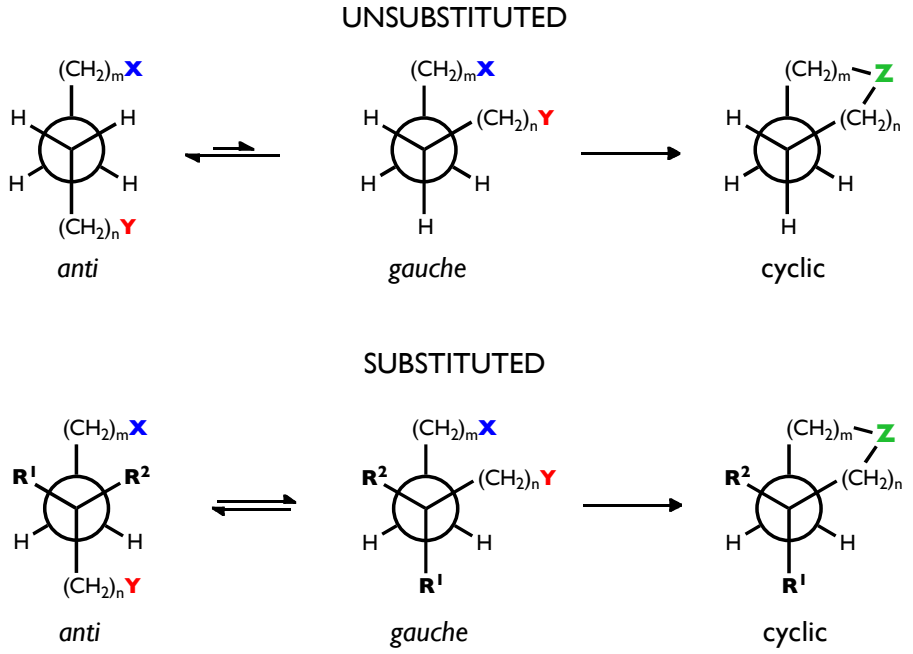

Figure 4.3 Graphical representation of the reactive rotamer effect as proposed by Jung.[11] Figure adapted from Ref. 11.

Thus, substitution of the methylene hydrogens with more bulky substituents has a tendency to increase the ground state energy, thus lowering the activation energy $\Delta H^{\ddagger}$ required for the cyclisation and therefore accelerates the reaction (Figure 4.4). This has been termed the “reactive rotamer effect”.

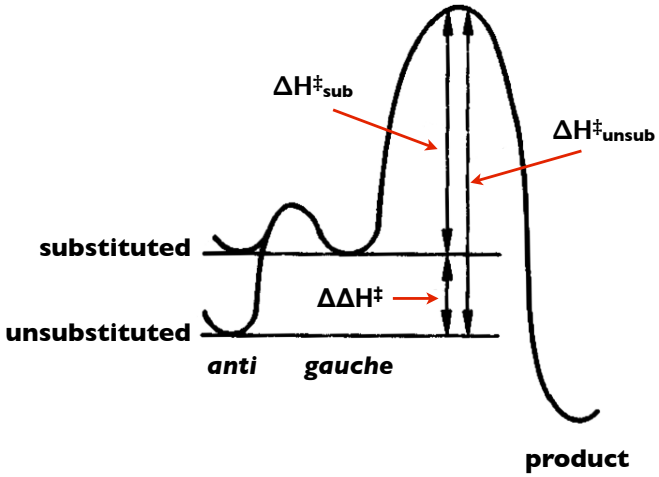

Figure 4.4 Influence of the reactive rotamer effect on the activation energy of cyclisation reaction as proposed by Jung.[11] Figure adapted from Ref 11.

In 1990, Jung presented a study on intramolecular Diels-Alder cycloaddition of 2-furfuryl fumarate **121a** and its methylene-substituted furfuryl derivatives **121b-e** (Table 4.2).[11]

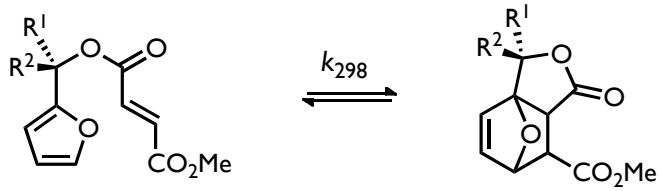

121 **122**

121	**R¹**	**R²**	k_{298} (s^{-1})	k_{rel}
a	H	H	2.0×10^{-7}	1.0
b	H	CH_3	1.1×10^{-6}	5.5
c	$-CH_2CH_2-$		1.3×10^{-6}	6.5
d	$-CH_2CH_2CH_2-$		3.6×10^{-5}	180
e	CH_3	CH_3	3.4×10^{-4}	1700

Table 4.2 Intramolecular Diels-Alder cyclisation rates for the 2-furfuryl fumarates **121a-e** as determined by Jung.[11]

Comparison of the cyclisation rates of the fumarates **121a-e** indicated a role of the reactive rotamer effect on the reaction efficiency. Cyclopropyl and

cyclobutyl fumarates (**121c** and **121d)** were expected to undergo less efficient cyclisations than the unsubstituted fumarate **121a** as their angles ***Θ*** are wider than that of **121a** as a consequence of the significantly compressed angles ***Φ*** in their strained cyclic substituents (Figure 4.5). However, both cyclic substituents provided rate enhancements relative to the unsubstituted fumarate **121a**.

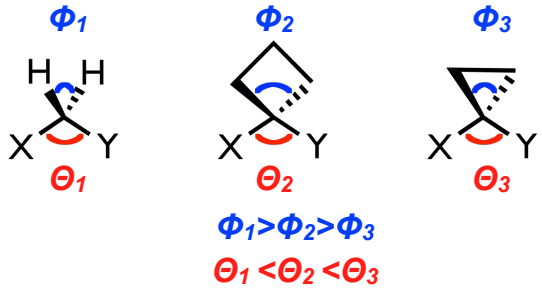

Figure 4.5 Effect of the cyclopropyl and cyclobutyl substituents on the internal angle ***Θ*** as proposed by Jung.[11]

This rate enhancement is contradictory to predictions based on the Thorpe-Ingold effect, indicating the role of the reactive rotamer effect. Remarkably, the authors did not comment on *gem*-dimethyl fumarate **121e**, which displayed the fastest cyclisation profile. Such a significant rate acceleration for **121e** could be due to a combination of the Thorpe-Ingold and reactive rotamer effects, since substitution with the *gem*-dimethyl group provides both angle compression and an increased population of the *gauche* rotamers (Figure 4.3).

4.2 Aims and design of the project

It was previously found that incorporation of the CF_2 group into a hydrocarbon system leads to significant widening of the CH_2-CF_2-CH_2 $\boldsymbol{\Theta}$ angle (Chapter 2 and 3).[2,12] Following a Thorpe-Ingold analysis, such a deviation in bond angle should result in a less efficient cyclisation reaction as a consequence of a larger distance between the two reactive centres. It was also expected that *gem*-disubstitution of the methylene hydrogens with fluorine atoms would not lead to a significant increase in the population of reactive rotamers, considering the relatively small difference in the van der Waals radii between the fluorine and hydrogen atoms (1.46 Å *versus* 1.20 Å).[13]

The high demand for fluorinated molecules,[14] combined with a drive to develop a deeper understanding of ring-closing metathesis formed the basis of this project.

In order to investigate the influence of the CF_2 group on the efficiency of ring-closing metathesis, a series of nona-1,8-dienes bearing various substituents at the C5 position (**123-128**), including the CF_2 group was designed (Figure 4.6).

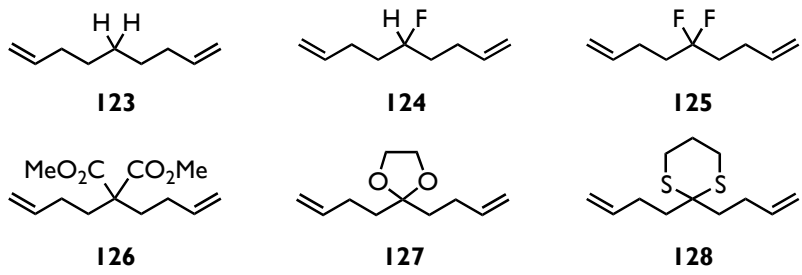

Figure 4.6 Dienes **123-128** selected for the ring-closing metathesis assays.

The other selected substituents, such as the diester **126**, dioxolane **127** and dithiane **128** had previously been shown to facilitate ring closing metathesis reactions.[15–18] Conversely, attempts to access cycloheptene **135** from nona-1,8-diene **123** through ring-closing metathesis proved difficult due to competing oligomerisation (Scheme 4.1).[19,20]

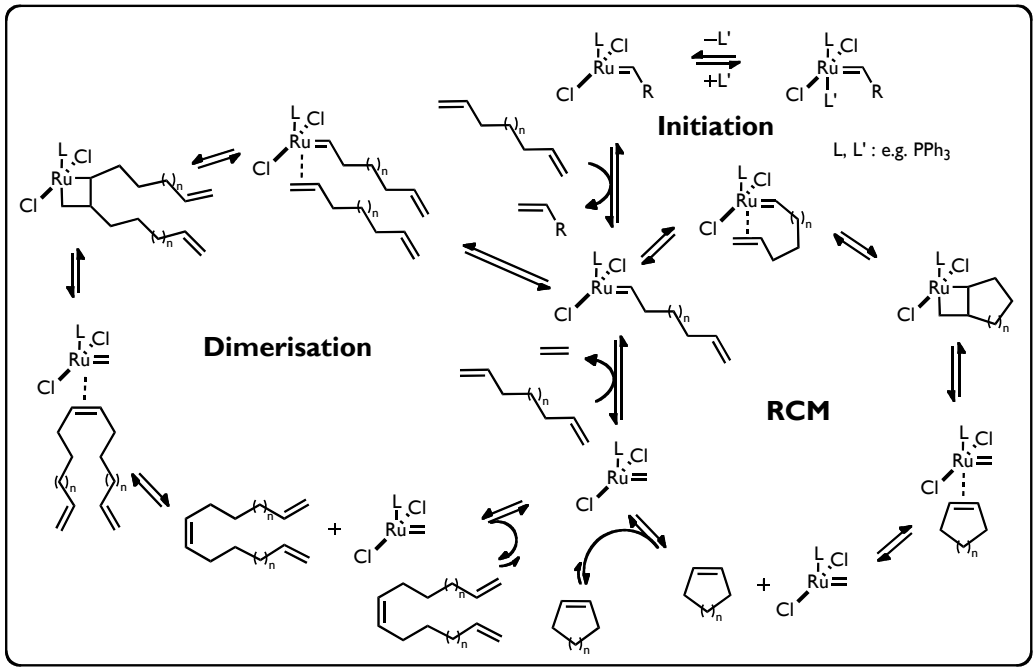

Scheme 4.1 Catalytic cycle of RCM and competing dimerisation. Scheme adapted from Ref. 20.

The general effect of these four substituents on the RCM reaction is relatively well established and offered a useful baseline for evaluating the monofluoro

and *gem*-difluoro groups that have not previously been examined in this context.

It was envisaged that the target dienes **123**-**128** will be cyclised to generate the corresponding cycloheptenes through RCM reactions (in a collaboration with Prof. Steven Nolan) (Scheme 4.2). In terms of analysis ^{1}H or ^{19}F NMR spectroscopy offered a practical tool.

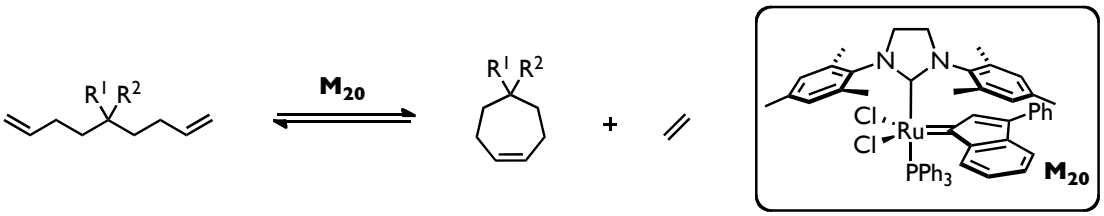

Scheme 4.2 **M_{20}** mediated ring-closing metathesis of nona-1,8-diene **123** and selected derivatives **124-128**.

Cyclisation conditions were maintained constant in order to allow a direct comparison between the substrate profiles. **M_{20}**,[21,22] an efficient RCM catalyst, which was previously employed in the synthesis of the C_{14} and C_{16} ring systems (Chapter 3) was selected as a catalyst for this project.

4.3 Results and discussion

4.3.1 Substitution dependant angle deviation – a CSD search

As a background to this study, a Cambridge Structural Database (CSD) search was conducted in order to investigate the influence of the substituents employed in this project on the deviation of the CH_2-CR_2-CH_2 ***Θ*** bond angles.

It is expected that substituents inducing the most dominant compression of the angle ***Θ*** could exhibit more efficient cyclisation reactions assuming Thorpe-Ingold effect.

The magnitude of the internal angle ***Θ*** does not simply depend on the stereo-electronic properties of the examined substituents. A preliminary search of the CSD revealed that $R^3CH_2CR_2CH_2R^4$ motifs are predominantly incorporated in cycloalkanes, fused rings or heterocycles. Therefore, in order to minimise the influence of the structural environment of the examined motifs on the ***Θ*** angles (*e.g.* ring strain) it was decided that only molecules in which the $R^3CH_2CR_2CH_2R^4$ motifs are a part of an open hydrocarbon chain will be considered. This afforded significantly more homogenous ***Θ*** angle distribution profiles.

It is difficult to assess the possible influence of the crystal packing on the observed ***Θ*** and ***Φ*** angles and how these angles would differ in solution, however, some general trends in the angle deviation can be tentatively concluded from the resultant profiles.

As previously discussed in Chapter 2, the CF_2 group consistently shows a significant CH_2-CF_2-CH_2 ***Θ*** angle widening (~117.1º) from the tetrahedral angle (T_d = 109.5º) (Figure 4.7a). Twelve motifs were found. The corresponding F-C-F ***Φ*** angles were found to be respectively narrower (~104.4º) than T_d (Figure 4.7b).

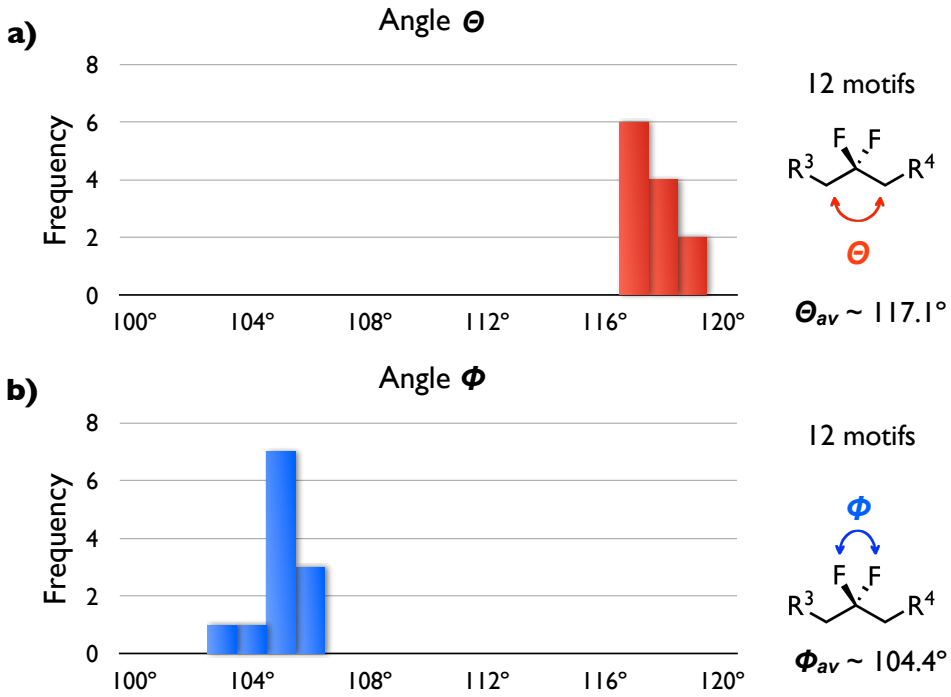

Figure 4.7 Histograms reporting the range of angles from 12 $R^3CH_2CF_2CH_2R^4$ motifs within the Cambridge Structural Database. a) CH_2-CF_2-CH_2 ***Θ*** angles; b) F-C-F ***Φ*** angles.

The **Θ** angle widening and the **Φ** angle compression were found to be less significant in hydrocarbons bearing a single fluorine atom. Nine motifs were found. The average CH_2-CHF-CH_2 **Θ** angle was found to be ~114.5º (Figure 4.8a). The corresponding F-C-H **Φ** angle was found to be on average narrower (~108.9º), than a typical tetrahedral angle (Figure 4.8b).

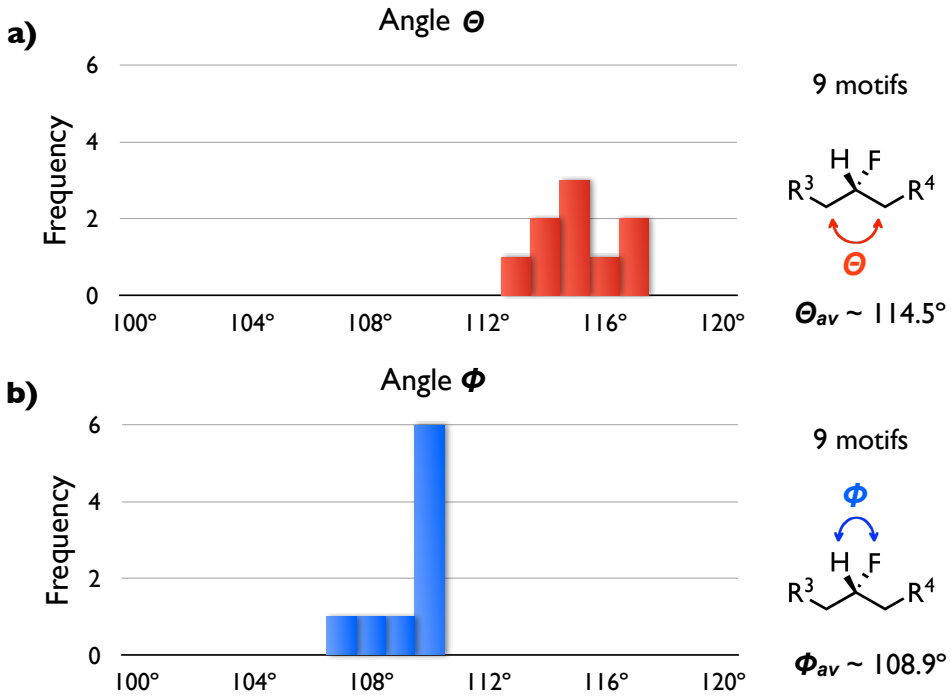

Figure 4.8 Histograms reporting the range of angles from 9 $R^3CH_2CHFCH_2R^4$ motifs within the Cambridge Structural Database. a) CH_2-CHF-CH_2 **Θ** angles; b) F-C-H **Φ** angles.

The ***Θ*** angles in 22 acyclic hydrocarbons, bearing the 1,3-dioxolane group were found to be consistently wider (~112.9º) than T_d. However, the ***Θ*** angle distribution presented in Figure 4.9a is bimodal, and therefore the average Θ_{av} does not truly represent the variety of angles observed in this search (Figure 4.9a). By contrast, the O-C-O ***Φ*** angle showed a more homogenous distribution, and the average ***Φ*** angle was found to be significantly narrower (~105.6º) than T_d (Figure 4.9b). Similar narrowing of the O-C-O ***Φ*** angle was observed for the structures of 1,3-dioxolane (105.8º) and 2,2-dimethyl-1,3-dioxolane (106.1º) derived from theory calculations.[23]

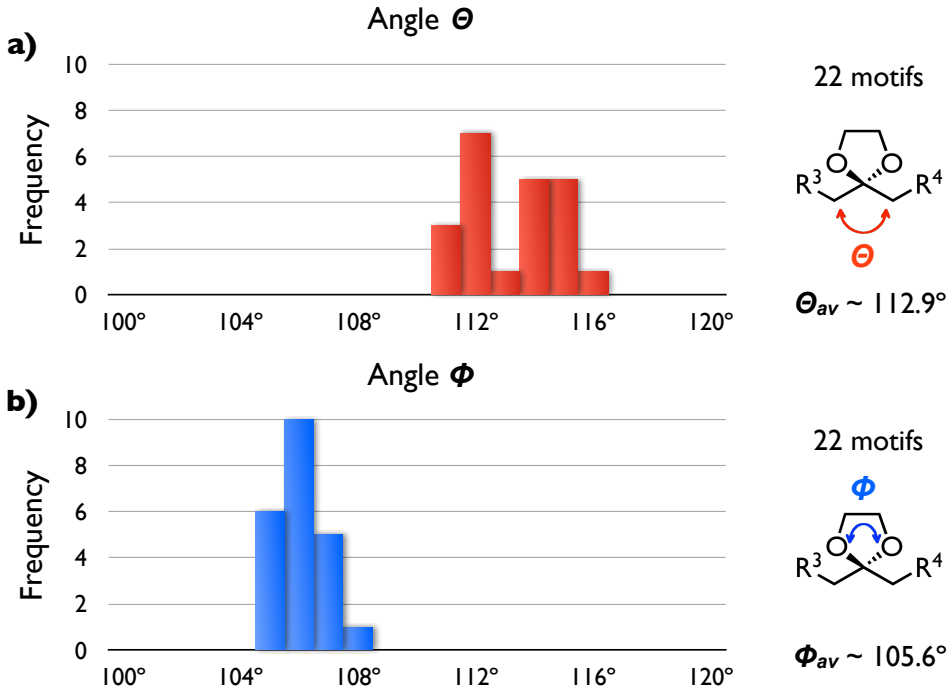

Figure 4.9 Histograms reporting the range of angles from 22 $R^3CH_2C(O_2C_2H_4)CH_2R^4$ motifs within the Cambridge Structural Database. a) CH_2-C($O_2C_2H_4$)-CH_2 ***Θ*** angles; b) O-C-O ***Φ*** angles.

The sterically bulky diester groups did not display an obvious **Θ** angle compression. As presented in Figure 4.10a, the average CH_2-$C(CO_2Me)_2$-CH_2 **Θ** angle was found to be ~112.5º and thus there is no particular support for a Thorpe-Ingold angle compression from this data. The corresponding C-C-C **Φ** angle ~107.2º (Figure 4.10b).

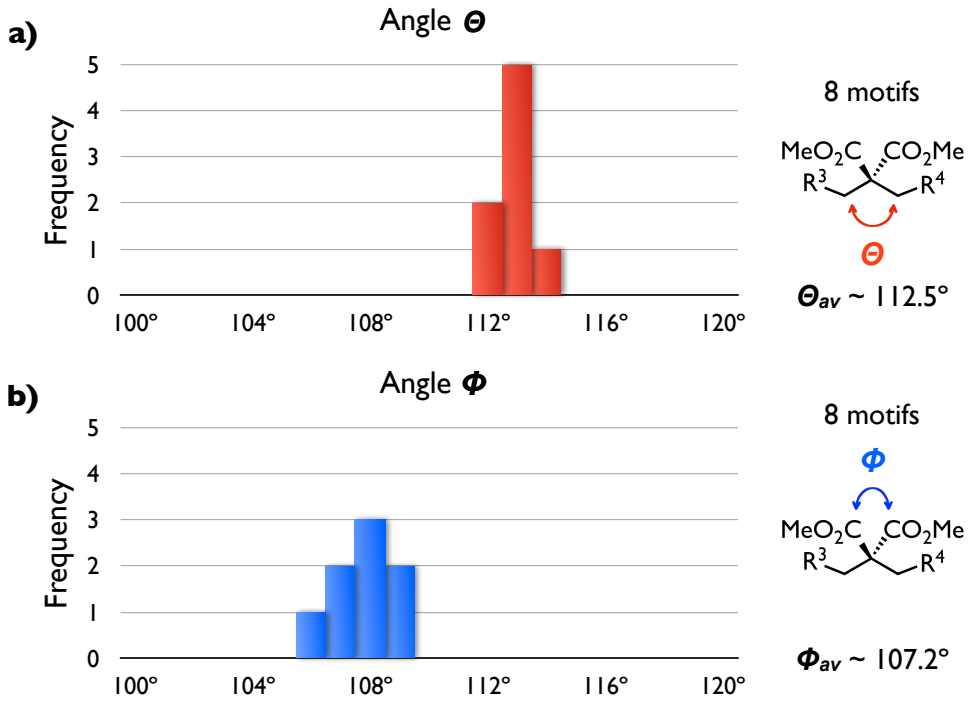

Figure 4.10 Histograms reporting the range of angles from 8 $R^3CH_2C(CO_2Me)_2CH_2R^4$ motifs within the Cambridge Structural Database (CSD). a) CH_2-$C(CO_2Me)_2$-CH_2 **Θ** angles; b) C-C-C **Φ** angles.

Only three open-chain hydrocarbon structures bearing a 1,3-dithiane group were found in the CSD. The CH_2-$C(S_2C_3H_6)$-CH_2 ***Θ*** angles were found to be narrower (~111.5º) on average than the ***Θ*** angles displayed by the previously analysed motifs (Figure 4.11a). The corresponding S-C-S ***Φ*** angles display a geometry (~110.3º) close to tetrahedral (Figure 4.11b). The sample size is however very small (3 structures).

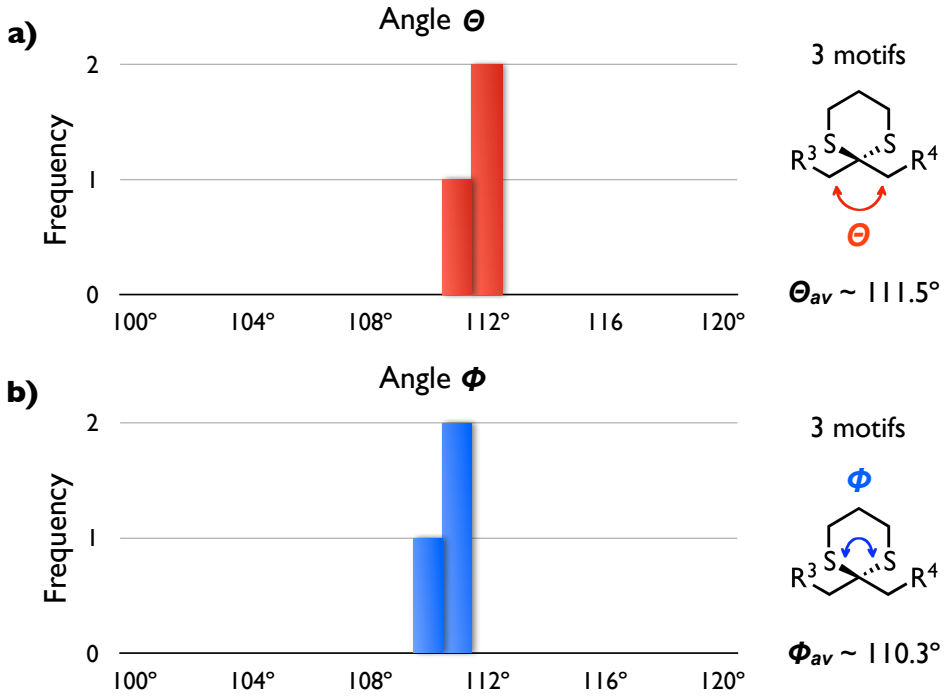

Figure 4.11 Histograms reporting the range of angles from 3 $R^3CH_2C(S_2C_2H_6)R^4$ motifs within the Cambridge Structural Database (CSD). a) CH_2-$C(S_2C_2H_6)$-CH_2 ***Θ*** angles; b) S-C-S ***Φ*** angles.

A summary of the CSD searches, showing the perturbation of ***Θ*** and ***Φ*** bond angles in substituted hydrocarbons, is presented in Figure 4.12.

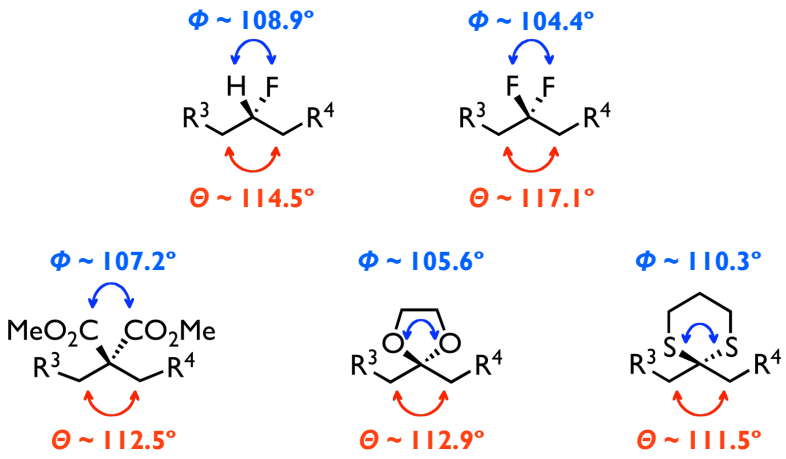

Figure 4.12 Perturbation of the ***Θ*** and ***Φ*** bond angles in substituted open-chain hydrocarbon motifs. Summary of the average angles found in Cambridge Structural Database.

The results from these CSD searches suggest at the outset that cyclisation should proceed more efficiently with nona-1,8-dienes bearing dithiane (**128**), *gem*-diester (**126**) and dioxolane (**127**) groups, because of their narrower ***Θ*** angles, rather than fluoromethylene (**124**) and *gem*-difluoromethylene (**125**) motifs, which have wider ***Θ*** angles.

4.3.2 Synthesis of RCM precursors

4.3.2.1 Nona-1,8-dien-5-ol

The synthesis of nona-1,8-dien-5-ol **131** was carried out following a protocol described in the literature (Scheme 4.3).[24] The reaction involved generation of 3-buten-1-yl-magnesium bromide **130** by treating 4-bromobut-1-ene **129** with magnesium turnings in dry THF. Once the magnesium was consumed, the resultant Grignard reagent **130** was treated with ethyl formate *in situ*, affording

the desired alcohol **131** as a colourless oil. The yield over the two steps was 94%.

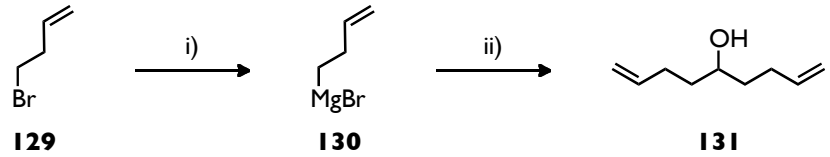

Scheme 4.3 Synthesis of nona-1,8-dien-5-ol **131**. Reagents and conditions: i) Mg, THF; ii) ethyl formate, 0 ºC to RT, 94%.

4.3.2.2 5-Fluorononа-1,8-diene

5-Fluorononа-1,8-diene **124** was generated by treatment of the previously prepared nona-1,8-dien-5-ol **131** with DAST **22** (Scheme 4.4).

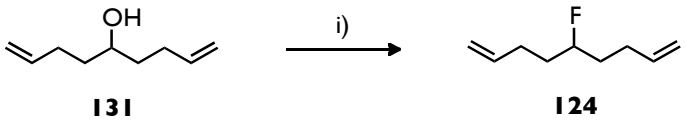

Scheme 4.4 Synthesis of 5-fluorononа-1,8-diene **124**. Reagents and conditions: i) DAST **22**, DCM, −78 ºC to RT, 36%.

The resulting product was found to be extremely volatile, making the reaction workup difficult. Distillation through a Vigreux column at atmospheric pressure was employed instead of using a rotary evaporator, in order to minimise material loss during bulk solvent removal. The residual solvent was removed by further Vigreux distillation under reduced pressure. The product **124** was isolated as a colourless oil in 36% yield. The increase in volatility of fluorinated products in comparison to their non-fluorinated hydrocarbons was previously rationalised by Uneyama.[25] He suggested that the hard fluorine atoms attract the surrounding electrons and lower the energy of the

surrounding molecular orbitals, thus limiting intermolecular van der Waals forces and resulting in a lower boiling point.

4.3.2.3 Nona-1,8-dien-5-one

A Jones oxidation of the previously prepared nona-1,8-dien-5-ol **131** was carried out to access nona-1,8-dien-5-one **132** (Scheme 4.5). The resulting ketone was isolated as a colourless oil in 91% yield and was subsequently used as the precursor for diolefins **125**, **127** and **128**.

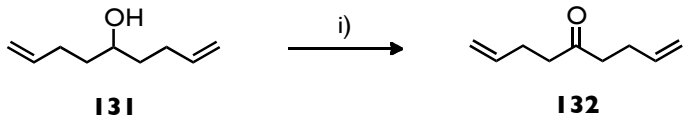

131 **132**

Scheme 4.5 Synthesis of nona-1,8-dien-5-one **132**. Reagents and conditions: i) CrO_3, H_2O, H_2SO_4, acetone, 0 ºC to RT, 91%.

4.3.2.4 5,5-Difluorononа-1,8-diene

5,5-Difluorononа-1,8-diene **125** was prepared by deoxofluorination of nona-1,8-dien-5-one **132** with DAST **22** (Scheme 4.6). As previously noted for the preparation of the monofluoro analogue **124**, introduction of the fluorine resulted in increased volatility of the product **125**. In this case, Vigreux distillation was also employed instead of using a rotary evaporator to remove the residual solvent. The diene **125** was successfully isolated in 55% yield as a colourless oil.

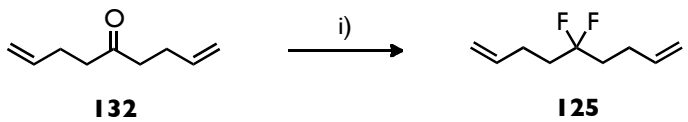

132 **125**

Scheme 4.6 Synthesis of 5,5-difluorononа-1,8-diene **125**. Reagents and conditions: i) DAST **22**, 45 ºC, 55%.

4.3.2.5 2,2-Bis(but-3-en-1-yl)-1,3-dioxolane

Nona-1,8-dien-5-one **132** was treated with ethane-1,2-diol in the presence of *p*-toluenesulfonic acid monohydrate ($TsOH \cdot H_2O$) in a Dean-Stark apparatus (Scheme 4.7). The reaction afforded 2,2-bis(but-3-en-1-yl)-1,3-dioxolane **127** as a colourless oil in moderate yield (54%).

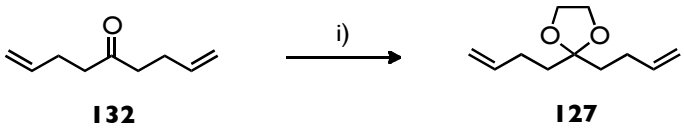

Scheme 4.7 Synthesis of 2,2-bis(but-3-en-1-yl)-1,3-dioxolane **127**. Reagents and conditions: i) ethane-1,2-diol, $TsOH \cdot H_2O$, toluene, reflux, 54%.

4.3.2.6 2,2-Bis(but-3-en-1-yl)-1,3-dithiane

Nona-1,8-dien-5-one **132** was converted to the corresponding bis-dithiolane derivative **128** through dithioacetalisation using 1,3-propanedithiol in the presence of $BF_3 \cdot Et_2O$ (Scheme 4.8). The resulting 2,2-bis(but-3-en-1-yl)-1,3-dithiane **128** was isolated as a colourless oil in 94% yield.

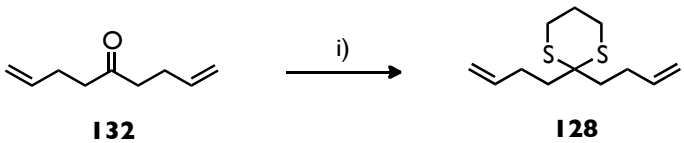

Scheme 4.8 Synthesis of 2,2-bis(but-3-en-1-yl)-1,3-dithiane **128**. Reagents and conditions: i) 1,3-propanedithiol, $BF_3 \cdot Et_2O$, DCM, RT, 94%.

4.3.2.7 Dimethyl 2,2-bis(but-3-en-1-yl)malonate

The synthesis of dimethyl 2,2-bis(but-3-en-1-yl)malonate **126** started with sodium hydride mediated deprotonation of dimethyl malonate **133**, followed by alkylation with 4-bromobut-1-ene **129** (Scheme 4.9). The deprotonation/alkylation sequence was repeated twice to improve the

conversion towards the dialkylated product. In the event, the resulting bis-olefin **126** was isolated as a colourless oil in 64% yield.

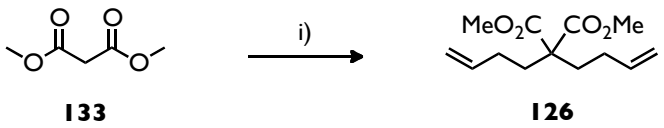

133 **126**

Scheme 4.9 Synthesis of 2,2-bis(but-3-en-1-yl)malonate **126**. Reagents and conditions: i) NaH, 4-bromobut-1-ene, DMF, 0 ºC to RT, 64%.

4.3.2.8 5,5-Difluorocyclohept-1-ene

5,5-Difluorocyclohept-1-ene **134** was synthesised by a ring-closing metathesis reaction with 5,5-difluorononа-1,8-diene **125**, and using 1 mol% of $\mathbf{M_{23}}$ as the catalyst (Scheme 4.10).[22]

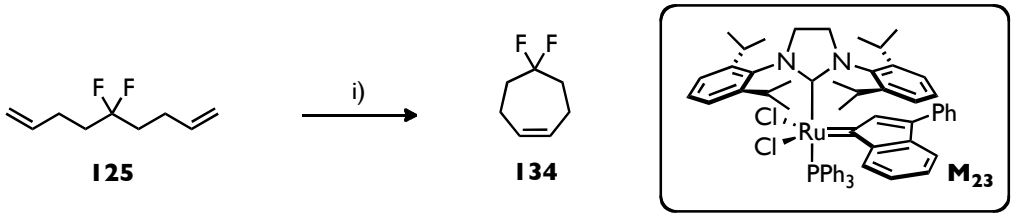

125 **134**

Scheme 4.10 Synthesis of 5,5-difluorocyclohept-1-ene **134**. Reagents and conditions: i) $\mathbf{M_{23}}$ (1.0 mol%), pentane, RT, 67%.

$\mathbf{M_{23}}$ was employed as the catalyst in preference to $\mathbf{M_{20}}$, the latter of which was used previously in the synthesis of C_{14} and C_{16} ring systems (Chapter 2). Firstly, the increased solubility of $\mathbf{M_{23}}$ over $\mathbf{M_{20}}$ in the non-polar reaction solvent (pentane) made it a better catalyst of choice. Secondly, 5,5 difluorocyclohept-1-ene **134** was expected to be volatile, which demanded the use of a low-boiling solvent, as opposed to the more commonly used DCE or toluene. This facilitated removal of the pentane at atmospheric or reduced pressure from the product by Vigreux distillation. Lastly, the low polarity of

pentane also proved beneficial during the purification stage, as the fluorinated product **134** exhibited low affinity to silica gel during chromatography. In the event 5,5-difluorocyclohept-1-ene **134** was isolated as a colourless oil in 67% yield and was used as a reference compound for the assessment of the cyclisation profile of 5,5-difluorononа-1,8-diene **125**.

4.3.3 RCM conversion profiles

With all of the RCM substrates successfully synthesised, it was possible to investigate the relative accelerating influence of the CF_2 substituent on the ring closing metathesis reaction. These RCM kinetic assays were carried out in close collaboration with César A. Urbina-Blanco in the group of Prof. Steven P. Nolan. Initially, the cyclisation profile of 5,5-difluorononа-1,8-diene **125** was compared to cyclisation profiles of a series of nona-1,8-dienes bearing various substituents at the C5 position (**123, 124, 126-128**) (Scheme 4.11). The reactions were conducted at a relatively high concentration (0.25 M) in a sealed screw-cap NMR tube, employing $\mathbf{M_{20}}$ (2 mol%) as the catalyst. The reaction progress was monitored by ^{1}H or ^{19}F NMR spectroscopy using trimethoxybenzene or trifluorotoluene as the internal standard (more details are available in the Experimental section 5.4.8).

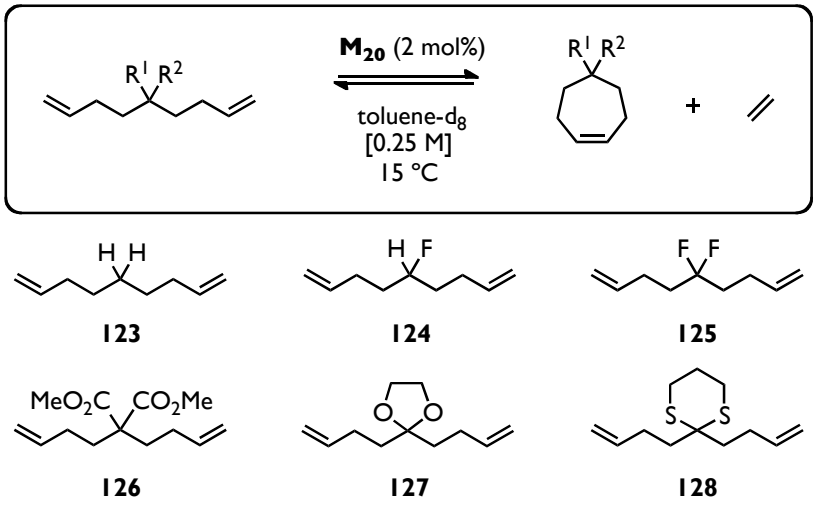

Scheme 4.11 Ruthenium mediated RCM reactions of the nonadiene substrates **123-128**. Reagents and conditions: **M_{20}** (2 mol%), toluene-d_8, 15 ºC.

The resulting reaction profiles revealed that the *gem*-disubstituted nonadienes (**125** and **126**) cyclised readily to give the corresponding cycloheptene derivatives (Figure 4.13). Similar behaviour was observed for nonadienes bearing bulky dioxolane **127** and dithiane **128** substituents. By contrast, nona-1,8-diene **123** and 5-fluorononа-1,8-diene **124** did not show good cyclisation rates, instead they underwent oligomerisation reactions resulting in a complex mixture of products. *Gem*-disubstitution with fluorine at the C5 position of nona-1,8-diene **123** dramatically promoted cyclisation over oligomerisation when compared to the profiles for 5-fluorononа-1,8-diene **124** and nona-1,8-diene **123**.

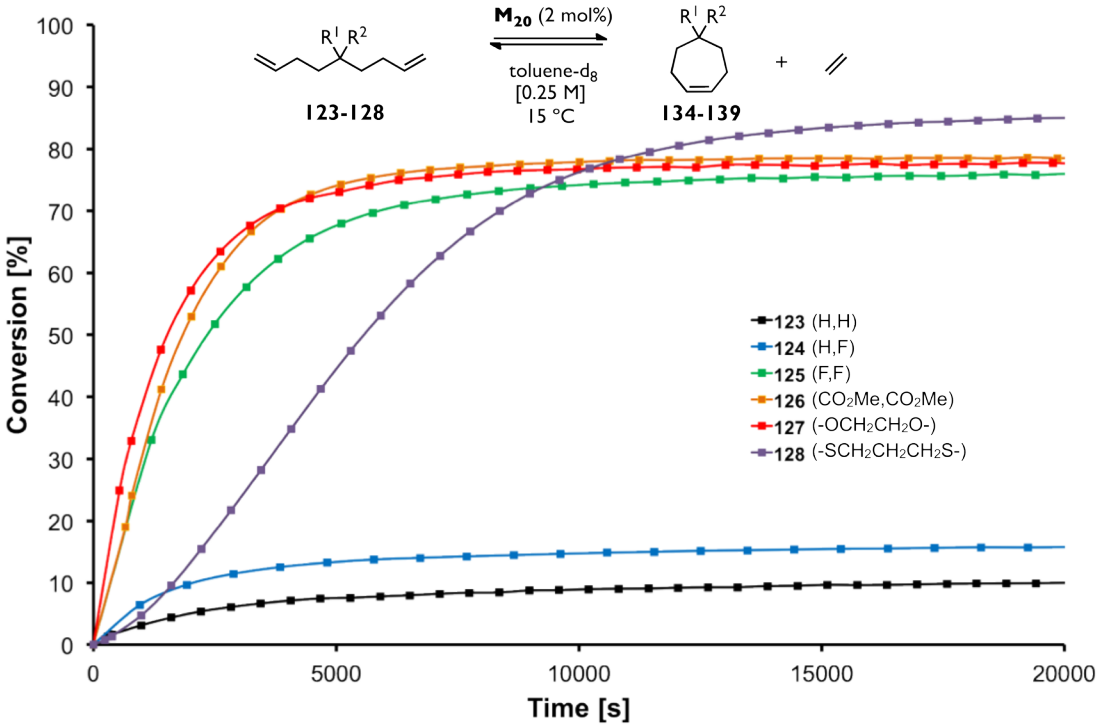

Figure 4.13 RCM conversion profiles of the nonadiene substrates **123-128** to their cycloheptene derivatives **134-139** [0.25 M] in toluene-d_8 with **M_{20}** (2 mol%) as the catalyst at 15 ºC. The conversion for non-fluorinated substrates was monitored by ^{1}H NMR spectroscopy (500 MHz) (1 scan per datapoint). Alternately, the reaction profiles of fluorinated compounds were followed by $^{19}F\{^{1}H\}$ NMR spectroscopy (470 MHz).[26] (Reaction profiles as determined by C. A. Urbina-Blanco)

The experimental data clearly shows that C5 substituents have a dramatic effect on the rate of cyclisation. The CF_2 group promoted the conversion to the cycloheptene species as efficiently as the sterically more demanding dioxolane and *gem*-diester groups. In addition 5,5-difluorononа-1,8-diene **125** was found to cyclise more readily than the dithiane analogue **128**. This enhanced cyclisation of **125** was somewhat unexpected based on a straightforward Thorpe-Ingold analysis.

4.3.4 Rotational energy profiles of the RCM substrates

In order to better understand how the conformational preorganisation (*anti/gauche*) of the nonadiene substrates **123-128** influences the RCM reaction profiles, rotational energy profiles for each substrate were obtained from DFT theory calculations at the B3LYP/6-311+G(d,p) level (Figure 4.14). This study was carried out by César A. Urbina-Blanco. The B3LYP/6-311+G(d,p) level of theory was previously employed in the conformational studies of various hydrocarbons and will not be discussed in detail here.[27]

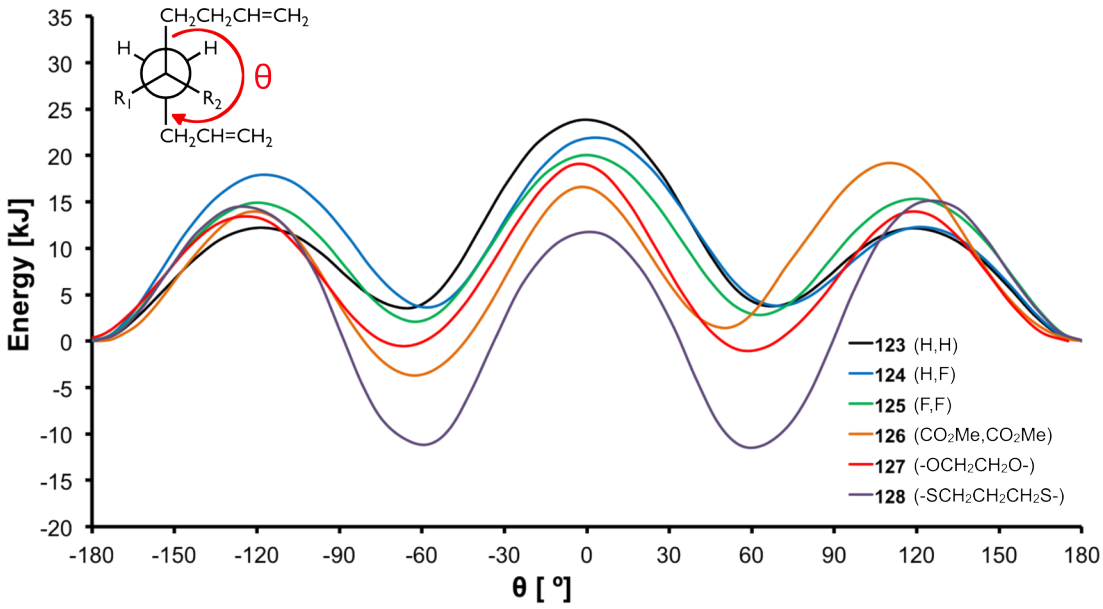

Figure 4.14 Energy [B3LYP/6-311+G(d,p)] *vs.* angle **θ** for the given nonadiene substrates **123-128**. All energies are relative to E(θ = 180°) and presented in kJ mol^{-1}.[26] (as determined by C. A. Urbina-Blanco)

Analysis of the rotational energy profiles (Figure 4.14) revealed that the *gauche* conformers were lower than the *anti* for only three substrates. These were the dithiane **128** (ΔE = −11.2 kJ mol^{-1}), diester **126** (ΔE = −3.7 kJ mol^{-1}) and dioxolane **127** (ΔE = −0.9 kJ mol^{-1}) respectively. This is entirely

consistent with expectations following the ***Θ*** angles reported in Figure 4.12 (p. 123). However, in experiment the cyclisation of dithiane substrate **128** was found to be slower than that of the dioxolane **127**, diester **126** and the CF_2 **125** nonadienes. This slow cyclisation may be the result of coordinative interactions between the sulfur atoms and the ruthenium catalyst (**M_{20}**), which are clearly not considered in the DFT calculations. The better compatibility of the diester substrate **126** with the ruthenium catalyst, together with a strong conformational preference towards the *gauche* conformer is consistent with its rapid cyclisation rate.

In contrast to the dithiane **128** and diester **126** substrates, which exhibited a strong preference towards the *gauche* conformers, only a very small energy difference, in favour of the *gauche* over *anti* conformer, was observed for dioxolane **127** ($\Delta E = -0.9$ kJ mol^{-1}). However, RCM of 1,3-dioxolane **127** displayed a similar cyclisation rate when compared to diester **126**. The *gauche* conformation of the CF_2 substrate **125** was found to be energetically less favoured than the *anti* conformation ($\Delta E = 2.1$ kJ mol^{-1}), yet this olefin cyclised almost as efficiently as the diester **126** and dioxolane **127**. The reactions of nona-1,8-diene **123** ($\Delta E = 3.6$ kJ mol^{-1}) and 5-fluorononа-1,8-diene **124** ($\Delta E = 3.8$ kJ mol^{-1}) resulted in complex mixtures of oligomers regardless of the small energy difference between their *gauche* and *anti* conformers.

4.3.5 Analysis of the thermodynamic stability of the RCM products

A comparison of the calculated rotational energy profiles with the kinetic RCM data revealed that the experimental rates of the RCM reactions cannot be readily explained in terms of the relative preference of the substrates to adopt *gauche* conformers. For this reason it was decided to explore a thermodynamic explanation. Thus the relative energies ΔH (kJ mol^{-1}) of the substrates and products were calculated from isodesmic reactions. This involved comparing the absolute energies of the acyclic substrates to their products (including ethene). Assessing the changes in entropy (ΔS) is more difficult, however, the greatest contributing factor to ΔS is expected to be the release of ethane gas, which is a constant for all of the reactions. Therefore, the resultant ΔH was considered to be a good approximation for the overall free energy change (ΔG). The DFT derived [B3LYP/6-311+G(d,p)] data for the isodesmic reactions is summarised in Table 4.3.

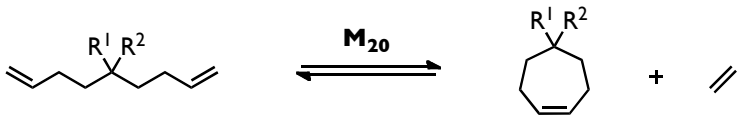

Substrate	Substituent	**ΔH** (kJ mol^{-1})	**ΔΔH** (kJ mol^{-1})
123	H,H	19.7	0.0
124	H,F	16.4	−3.3
125	F,F	12.3	−7.5
127	-OCH_2CH_2O-	10.2	−9.6
126	CO_2Me, CO_2Me	4.5	−15.2
128	-$SCH_2CH_2CH_2S$-	−1.2	−20.9

Table 4.3 DFT [B3LYP/6-311+G(d,p)] derived relative energies (ΔH) from isodesmic reactions comparing substrates **123-128** and products **134-139**.[26] (as determined by C. A. Urbina-Blanco)

Analysis of the calculated energies (ΔH) revealed a stabilising effect for all of the geminal substituents relative to **123**. The greatest stabilisation was calculated for the dithiane **128** ($\Delta\Delta H = -20.9$ kJ mol^{-1}) and diester **126** ($\Delta\Delta H = -15.2$ kJ mol^{-1}). Additionally, the substrates bearing dioxolane and difluoromethylene substituents also displayed stabilising effects relative to the hydrocarbon **123** ($\Delta\Delta H = -9.6$ and -7.5 kJ mol^{-1} respectively). In contrast, substitution with a single fluorine had a very limited stabilising effect ($\Delta\Delta H = -3.3$ kJ mol^{-1}) in **124**.

The correlation between the most efficient RCM conversions (Figure 4.13) and the differences in the relative energies (ΔH) (Table 4.3), suggests that the observed cyclisation efficiency of geminally substituted nona-1,8-dienes **125**-**128** has a largely thermodynamic origin. In other words, the product stability influences the observed rates. Nonetheless, it is likely that efficiencies of cyclisation are also affected by the energies of the transition states, which are affected by the examined substituents. However, the DFT transition state calculations for the RCM reactions, required for a more complete understanding of the origin of the observed rates, are computationally too complex, and are beyond the scope of this work.

In an attempt to explore the structure of the products in some detail a conformational analysis was carried out for each of **134-139**. This used DFT [B3LYP/6-311+G(d,p)] to derive a minimum energy structure in each case (Figure 4.15).

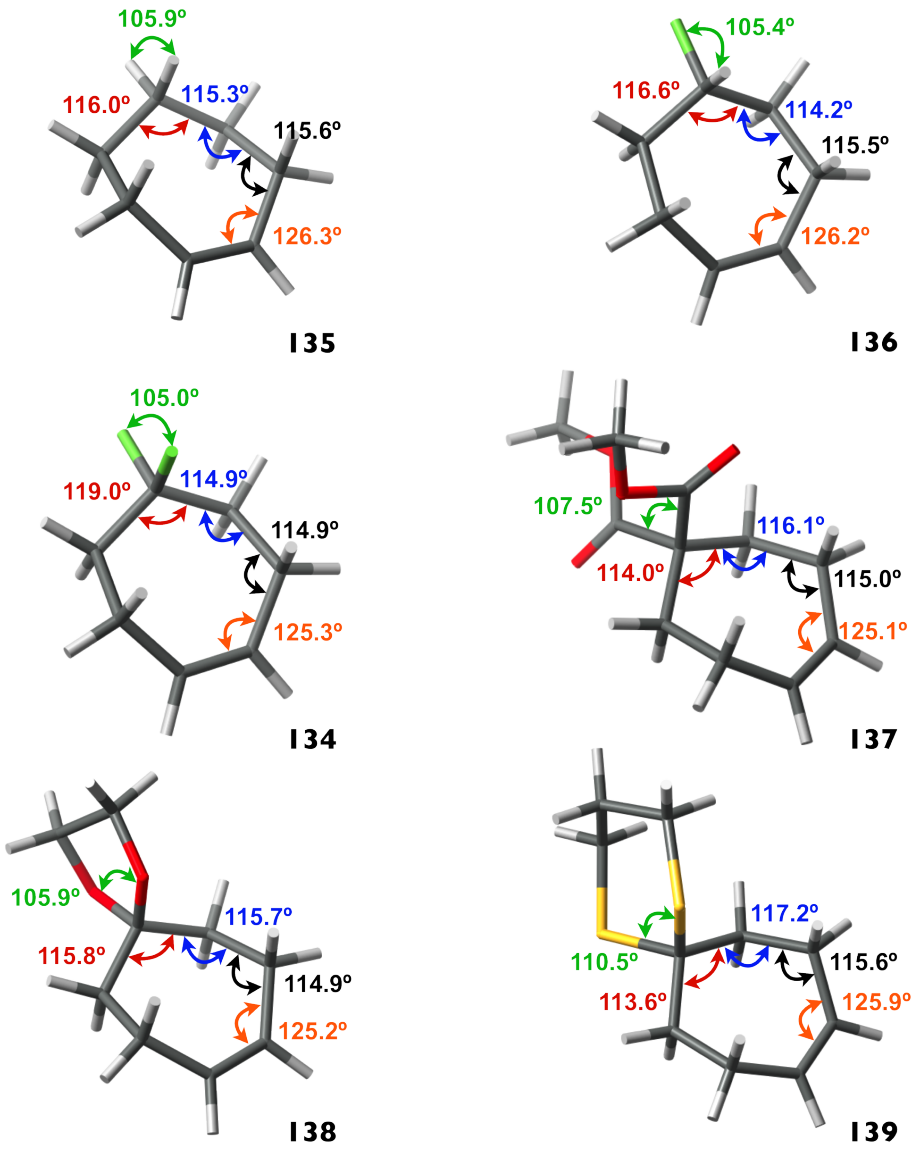

Figure 4.15 Gaussian DFT modelling (B3LYP/6-311+G(d,p)) of cycloheptenes **134-139**. Representation of the C-C-C and R-C-R angles.[26] (as determined by C. A. Urbina-Blanco)

The calculated structure of the parent ring system, cycloheptene **135** revealed that the internal CH_2-CH_2-CH_2 angles are significantly wider than T_d, indicating inherent ring strain. The widest CH_2-CH_2-CH_2 angle was centred around the C5 carbon and was calculated at 116.0º. This has also been observed previously by theory calculations at MP2/6-31G level.[28] Only a minor change in the internal angles was observed for the 5-fluorocyclohept-1-ene

136 and dioxolane **138**. However, geminal substitution with fluorine atoms at C5 in **134** resulted in a notably wider CH_2-CF_2-CH_2 angle (119.0º). The overall ring strain in 5,5-difluorocyclohept-1-ene **134** is therefore absorbed by this angle widening, which is observed for the CF_2 group (Figure 4.15) in its most relaxed state. Both diester **137** and dithiane **139** groups displayed Thorpe-Ingold compression of the CH_2-CR_2-CH_2 angle (113.5º and 113.6º respectively), consistent with the overall angle deviation trend found in the CSD (Figure 4.12, p. 122). Additionally, the observed puckering of the conformation of the diester **137** is presumably a result of ring strain compensation.

Further DFT analyses revealed that the geometries of selected axial C-R bonds, antiperiplanar to the axial C-H bonds can accommodate hyperconjugative stabilising interactions ($\sigma_{CH} \rightarrow \sigma^*_{CR}$ and $\sigma_{CR} \rightarrow \sigma^*_{CH}$) in **134**, **135**, **136**, **138** and **139** (Figure 4.16).

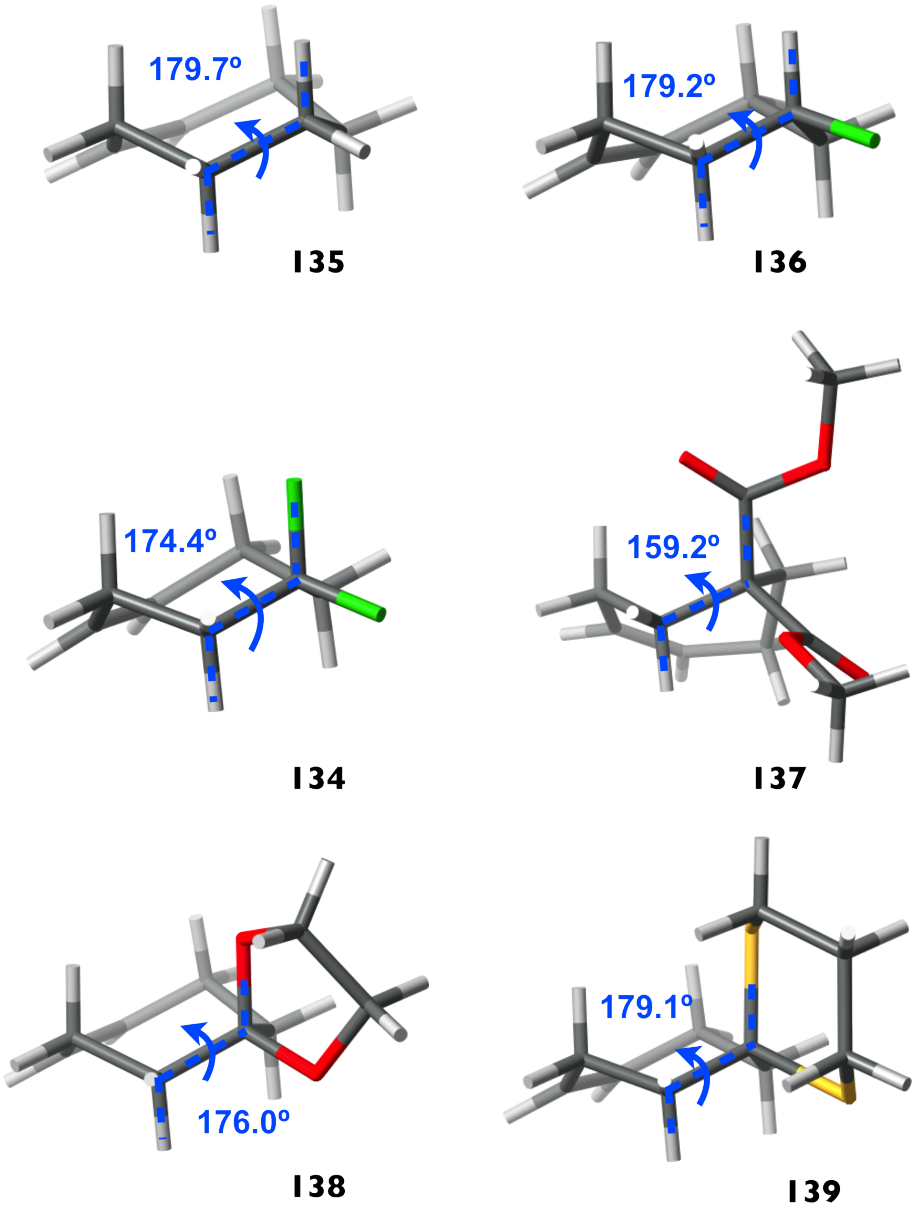

Figure 4.16 DFT derived [B3LYP/6-311+G(d,p)] models of cycloheptenes **134-139**. The geometries of H-C-C-R angles can accommodate stabilising $\sigma_{CH} \rightarrow \sigma^*_{CR}$ and $\sigma_{CR} \rightarrow \sigma^*_{CH}$ interactions in **134**, **135**, **136**, **138** and **139**. (with C. A. Urbina-Blanco)

Natural Bond Orbital (NBO) analysis[29] was carried out on the optimised geometries [B3LYP/6-311+G(d,p)] obtained for the cycloheptene **135** and the substituted derivatives **134**, **136**, **138** and **139**. The results summarising the stabilising hyperconjugative interactions between the orbitals of the substituents at C4, C5 and C6 are presented in Table 4.4.

No.	R^1	R^2	H-C-C-R^1	$\sigma_{CH}\rightarrow\sigma^*_{CR^1}$	$\sigma_{CR^1}\rightarrow\sigma^*_{CH}$	$\Sigma(\sigma_{CH}\rightarrow\sigma^*_{CR^1} + \sigma_{CR^1}\rightarrow\sigma^*_{CH})$	ΔE
135	H	H	179.7º 179.7º	2.83 2.83	2.87 2.87	11.40	0.00
136	H	F	179.2º 179.2º	2.64 2.64	2.77 2.77	10.82	−0.58
134	F	F	174.4º 174.4º	5.12 5.12	1.11 1.11	12.46	1.06
138	O	O	176.0º 176.0º	5.29 5.50	1.22 1.13	13.14	1.74
139	S	S	179.1º 175.2º	6.10 5.20	2.23 2.78	16.31	4.91

Table 4.4 NBO analysis of the DFT derived [B3LYP/6-311+G(d,p)] cycloheptenes **134-136, 138** and **139**. Calculated hyperconjugative energy (ΔE) is relative to cycloheptene **135**. The values showing the hyperconjugative interactions ($\sigma_{CH}\rightarrow\sigma^*_{CR^1}$, $\sigma_{CR^1}\rightarrow\sigma^*_{CH}$, ΔE) are provided in kcal mol^{-1}. (with R. A. Cormanich)

The most pronounced stabilising interactions are calculated for the dithiane **139** (ΔE = 4.91 kcal mol^{-1}) and are presumably a consequence of the favourable overlap between the low lying σ^*_{CS} orbitals with the neighbouring σ_{CH} and antibonding σ^*_{CH} orbitals. Similarly, substantial stabilisation of the cycloheptene ring was induced by both the dioxolane (ΔE = 1.74 kcal mol^{-1}) and difluoromethylene groups (ΔE = 1.06 kcal mol^{-1}). Conversely, the hyperconjugative interactions in 5-fluorocyclohept-1-ene **136** were found to be ~0.58 kcal mol^{-1} weaker than the corresponding interactions of the parent cycloheptene **135**. However, the fluorine orbitals of 5-fluorocyclohept-1-ene **136** (σ_{CF} and σ^*_{CF}) did not take part in the hyperconjugative stabilisation due to their unfavourable geometry (Figure 4.16). The DFT structural analysis of diester **137** indicates that the dihedral angle (H-C-C-C) is 159.2º. This is ~20º less than the ideal angle required for hyperconjugative interactions to take place and so these interactions are not present around C5 in diester **137**. At

this point the origin of the small energy difference (ΔH = 4.5 kJ mol^{-1}) between open chain **126** and its cyclic product **137** remains unclear.

The NBO analysis suggests a significant increase in hyperconjugative interactions in the geminally substituted cycloheptenes **134**, **138** and **139**. In addition, these nonbonded interactions were shown to make a significant contribution to the overall stability of the seven-membered rings. These observations contribute support to the thermodynamic origin of the observed rate enhancements.

4.4 Conclusions

The study presented in this chapter describes an accelerating role of the CF_2 group on ring-closing metathesis.

It was observed experimentally that 5,5-difluorononа-1,8-diene **125** displays a significant cyclisation rate enhancement comparable to nona-1,8-dienes bearing the sterically more demanding dithiane **128**, diester **126** and dioxolane **127** groups. In contrast, the parent nona-1,8-diene **123** and its 5-fluoro analogue **124** were found to predominantly oligomerise.

The electronegative fluorine atoms in CF_2 group consistently induce CH_2-CF_2-CH_2 angle widening rather than contraction and therefore the enhanced RCM efficiency cannot be explained in terms of the classical Thorpe-Ingold effect.

Analysis of the DFT derived rotational energy profiles of the acyclic substrates **123-128** revealed a correlation between the size of the substituent at C5 and the population of reactive *gauche* rotamers. Nona-1,8-dienes bearing large diester **126** and dioxolane **127** groups displayed the highest cyclisation rates. Interestingly, dithiane **128** cyclised slower than 5,5-difluorononа-1,8-diene **125** despite a higher calculated population of reactive *gauche* rotamers and a thermodynamically most favourable product **139**. It was envisaged that perhaps sulfur atoms interact with the ruthenium catalyst (**M_{20}**), supressing its catalytic activity. The sterically less demanding CF_2 group unexpectedly provided comparable reaction rates to the diester **126** and dioxolane analogues **127** and this is a key highlight result.

Both 5-fluorononа-1,8-diene **124** and nona-1,8-diene **123** readily oligomerised, despite having similar rotational energy profiles to 5,5-difluorononа-1,8-diene **125**, which cyclised efficiently. It is evident that examination of the rotational energy profiles alone is not sufficient to explain the observed conversion profiles (Figure. 4.13). In order to assess the magnitude of the kinetic effect, transition state calculations for each RCM reaction would need to be carried out. However, these are beyond the scope of this experimental research. Nevertheless, comparison of the DFT derived thermodynamic stabilities of cycloheptene products **134-139** relative to their acyclic precursors **123-128** (ΔH), allows the contrasting reactivity of the olefins **123-128** to be rationalised in terms of product stability. *Gem*-disubstitution at C5 of nona-1,8-diene **123** resulted in lower ΔH values, thus providing a rationale for the observed preference for cyclisation over oligomerisation. Additionally, it was concluded

that angle widening, absorbing ring strain and hyperconjugative *trans*-axial interactions ($\sigma_{CH} \rightarrow \sigma^*_{CR}$ and $\sigma_{CR} \rightarrow \sigma^*_{CH}$) provide the major contributions to the stability of the geminally-substituted cycloheptenes.

It remains to be seen whether the accelerating effect will extend to the synthesis of rings of different sizes.

4.4 References

1. M. E. Jung, G. Piizzi, *Chem. Rev.*, 2005, **105**, 1735–1766.

2. M. Skibiński, C. A. Urbina-Blanco, A. M. Z. Slawin, S. P. Nolan, D. O'Hagan, *Org. Biomol. Chem.*, 2013, **11**, 8209–8213.

3. R. M. Beesley, C. K. Ingold, J. F. Thorpe, *J. Chem. Soc., Trans.*, 1915, **107**, 1080–1106.

4. C. K. Ingold, *J. Chem. Soc., Trans.*, 1921, **119**, 305–329.

5. P. von Ragué Schleyer, *J. Am. Chem. Soc.*, 1961, **83**, 1368–1373.

6. D. R. Lide, *J. Chem. Phys.*, 1960, **33**, 1514–1518.

7. D. R. Lide, D. E. Mann, *J. Chem. Phys.*, 1958, **29**, 914–920.

8. R. L. Livingston, C. Lurie, C. N. Rao, *Nature*, 1960, **185**, 458–459.

9. L. P. Kuhn, *J. Am. Chem. Soc.*, 1952, **74**, 2492–2499.

10. T. C. Bruice, U. K. Pandit, *J. Am. Chem. Soc.*, 1960, **82**, 5858–5865.

11. M. E. Jung, *Synlett*, 1990, 186–190.

12. M. Skibiński, Y. Wang, A. M. Z. Slawin, T. Lebl, P. Kirsch, D. O'Hagan, *Angew. Chem. Int. Ed.*, 2011, **50**, 10581–10584.

13. S. Alvarez, *Dalton Trans.*, 2013, **42**, 8617–8636.

14. K. Müller, C. Faeh, F. Diederich, *Science*, 2007, **317**, 1881–1886.

15. A. Fürstner, A. F. Hill, M. Liebl, J. Wilton-Ely, *Chem. Commun.*, 1999, **7**, 601–602.

16. M. Tanaka, Y. Demizu, M. Nagano, M. Hama, Y. Yoshida, M. Kurihara, H. Suemune, *J. Org. Chem.*, 2007, **72**, 7750–7756.

17. H. Hopf, Z. Hussain, R. S. Menon, V. Raev, P. G. Jones, L. M. Pohl, *Synlett*, 2011, 1273–1276.

18. G. Spagnol, M.-P. Heck, S. P. Nolan, C. Mioskowski, *Org. Lett.*, 2002, **4**, 1767–1770.

19. D. J. Nelson, I. W. Ashworth, I. H. Hillier, S. H. Kyne, S. Pandian, J. A. Parkinson, J. M. Percy, G. Rinaudo, M. A. Vincent, *Chem. Eur. J.*, 2011, **17**, 13087–13094.

20. I. H. Hillier, S. Pandian, J. M. Percy, M. A. Vincent, *Dalton Trans.*, 2011, **40**, 1061-1072.

21. J. Broggi, C. A. Urbina-Blanco, H. Clavier, A. Leitgeb, C. Slugovc, A. M. Z. Slawin, S. P. Nolan, *Chem. Eur. J.*, 2010, **16**, 9215–9225.

22. C. A. Urbina-Blanco, S. Manzini, J. P. Gomes, A. Doppiu, S. P. Nolan, *Chem. Commun.*, 2011, **47**, 5022–5024.

23. Q. Shen, T. L. Mathers, T. Raeker, R. L. Hilderbrandt, *J. Am. Chem. Soc.*, 1986, **108**, 6888–6893.

24. G. Lemière, V. Gandon, K. Cariou, A. Hours, T. Fukuyama, A.-L. Dhimane, L. Fensterbank, M. Malacria, *J. Am. Chem. Soc.*, 2009, **131**, 2993–3006.

25. K. Uneyama, *Organofluorine Chemistry*, Blackwell Publishing Ltd., Oxford, UK, 2006, pp. 3–6.

26. C. A. Urbina-Blanco, M. Skibiński, D. O'Hagan, S. P. Nolan, *Chem. Commun.*, 2013, **49**, 7201–7203.

27. F. Groenewald, J. Dillen, *Struct. Chem.*, 2012, **23**, 723–732.

28. M. K. Leong, V. S. Mastryukov, J. E. Boggs, *J. Mol. Struct.*, 1998, **445**, 149–160.

29. NBO 5.0 Program, E. D. Glendening, J. K. Badenhoop, A. E. Reed, J. E. Carpenter, J. A. Bohmann, C. M. Morales, F. Weinhold, Theoretical Chemistry Institute; University of Wisconsin, Madison, 2001.

5

Experimental

5.1 General methods

5.1.1 Reagents, solvents and reaction conditions

All commercially available reagents were purchased and used without further purification unless otherwise stated. Complexes **M_{20}** and **M_{23}** were supplied by Umicore. Complex $[Ru_3O(OAc)_6(H_2O)_3]OAc$ **99** was purchased from Strem Chemicals. 2,2'-Ethylenebis(1,3-dithiane) **102** was purchased from Alfa Aesar. *n*-BuLi was purchased from Acros Organics as 2.5 M solution in hexanes, and was titrated against diphenylacetic acid prior to use. Hydrogen fluoride-pyridine, triethylamine trihydrofluoride, Deoxofluor **30**, MOST **31** Fluolead **32**, and XtalFluor-E **33** were purchased from Sigma Aldrich. DAST **22** was purchased from Fluorochem. All reactions were conducted under an atmosphere of argon using standard vacuum line techniques. All glassware was flamedried and allowed to cool under high vacuum. PTFE flasks were

oven dried (60 ºC) and allowed to cool under high vacuum. Dry solvents DCM, Et_2O, THF, toluene were obtained from the MBraun SPS-800 Solvent Purification System, by passing the solvent through two drying columns under an argon atmosphere. Anhydrous 1,2-dichloroethane (DCE) and DMF were available commercially. Reaction temperatures of −78 ºC to −10 ºC were obtained using isopropyl alcohol bath together with LabPlant Refrigerated Immersion Probe. Temperature of 0 ºC was obtained using an ice/water bath. Reactions requiring heating or reflux were carried out using a heating block with a contact thermometer.

5.1.2 Chromatography

Thin layer chromatography (TLC) was performed using Merck TLC silica gel 60 F_{254} aluminium-backed plates. Compounds were visualised by either UV light (254 nm) or by the use of potassium permanaganate stain or molybdenum-based stain. Column chromatography was performed using Merck silica gel 60 (40-63 μm). Gas chromatography-mass spectroscopy (GC-MS) analysis was performed on an Agilent 5890 gas chromatograph (GC) equipped with 5973N mass selective detector and 7683 injector. The GC was equipped with 30 m long Supleco MDN-35 column. The oven temperature was programmed to hold for 10 min at 50 °C, and then ramped at 10 °C/min to 280 °C, with 1 mL/min helium flow.

5.1.3 Nuclear magnetic resonance (NMR) spectroscopy

NMR spectra were acquired on either Bruker Avance 300 (^{1}H at 300 MHz, ^{13}C at 75 MHz, ^{19}F at 282 MHz), Bruker Avance II 400 spectrometer (^{1}H at 400 MHz, ^{13}C at 100 MHz, ^{19}F at 376 MHz), Bruker Avance 500 spectrometer or Bruker Avance III 500 (^{1}H at 500 MHz, ^{13}C 125 MHz ^{19}F at 470 MHz). Chemical shifts ($\boldsymbol{\delta}$) are reported in parts per million (ppm) and are quoted relative to centre of the residual non-deuterated solvent peak for $\boldsymbol{\delta_H}$ ($CDCl_3$: 7.26 ppm; CD_2Cl_2: 5.31 ppm; C_7D_8: 2.08 ppm) and $\boldsymbol{\delta_C}$ ($CDCl_3$: 77.16 ppm; CD_2Cl_2: 53.80 ppm). Chemical shifts $\boldsymbol{\delta_F}$ are quoted relative to CCl_3F ($\boldsymbol{\delta_F}$ CCl_3F: 0.00 ppm). ^{13}C NMR spectra were recorded with ^{1}H decoupling. Spectra were processed and analysed using iNMR 3.6.1 software. Coupling constants (*J*) are given in Hertz (Hz). Signal splitting patterns are described as: bs - broad singlet, s - singlet, t - triplet, tt - triplet of triplets, ddd - doublet of doublets of doublets, ddt - doublet of doublets of triplets m - multiplet. ^{1}H COSY, HSQC and HMBC experiments were carried out as required during the process of structural assignment. Carbon atoms in every structure are numbered in order to facilitate structural assignment. It should be noted that these numbers have no relation to the names of compounds.

Variable Temperature NMR experiments and further determination of the activation parameters were conducted by Dr Tomas Lebl at the University of St Andrews. The spectra were recorded using Bruker AVANCE 500 MHz spectrometer equipped with 5 mm QNP-probe, employing CD_2Cl_2 as a

solvent. The accurate temperatures for particular experiments were determined using 4% MeOH in CD_3OD sample. Complete lineshape analysis was carried out using Bruker Topspin D-NMR module.

5.1.4 Mass spectrometry

Mass spectrometric data was acquired by electron impact ionisation (EI), electrospray ionisation (ES) or chemical ionisation (CI). At the University of St Andrews LRMS and HRMS examination was carried out by Mrs. C. Horsburgh on a Waters Micromass LCT (ES) or GCT (EI/CI) spectrometers. At the EPSRC National Mass Spectrometry Service Centre, Swansea, the LRMS assessment was performed on Thermofisher DSQ-II spectrometer (EI/CI) and HRMS was performed on Finnigan MAT 95 XP (EI/CI) or Thermofisher LTQ Orbitrap XL (ES/CI). Values are reported in Daltons as a ratio of mass to charge (*m/z*).

5.1.5 Other analysis

Single crystal X-ray Diffraction analysis was carried out by Prof Alexandra M. Z. Slawin at the University of St Andrews. The Crystallographic Information Files (CIF) were analysed using Mercury software and are attached on a CD disc.

The Cambridge Structure Database (CSD) searches of organic compounds containing the specified motifs were conducted using ConQuest and Mercury software.

Melting points were determined in Pyrex capillaries using a Gallenkamp Griffin Melting Point Apparatus 350 and were uncorrected.

Differential scanning calorimetry (DSC) analysis was carried out by Mrs. S. Williamson, at the University of St Andrews, on a NETZSCH DCS 204 F1 calorimeter, providing corrected melting points.

5.2 Protocols for Chapter 2

5.2.1 1,4-Dithiaspiro[4.11]hexadecane (47)

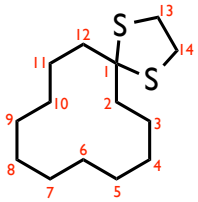

Boron trifluoride acetic acid complex (0.84 mL, 5.8 mmol, 1 eq) was added to a stirred mixture of cyclododecanone **70** (1.05 g, 5.8 mmol, 1 eq) and 1,2-ethanedithiol (1.0 mL, 11.5 mmol, 2 eq). The biphasic solution was stirred vigorously for 20 min at RT. The reaction mixture was diluted with DCM (100 mL) and subsequently washed with saturated $NaHCO_3$ solution (50 mL), NaOH solution (15% w/v, 50 mL), and brine (50 mL). The organic extracts were dried over $MgSO_4$ and concentrated. Purification over silica gel, eluting with hexane and Et_2O (99:1), yielded 1,4-dithiaspiro[4.11]hexadecane **47** (1.27 g, 92%) as a colourless crystalline solid:

R_f = 0.31 (hexane:DCM, 80:20); **m.p.** = 81-83 ºC (from DCM) [lit.[1] 85-86 ºC]; **^{1}H NMR** (400 MHz, $CDCl_3$) **δ_H** 3.28 (4H, s, *CH_2-13,14*), 2.05-1.98 (4H, m, *CH_2-2,12*), 1.52-1.43 (4H, m, *CH_2*), 1.40-1.28 (14H, m, *CH_2*); **^{13}C NMR** (100 MHz, $CDCl_3$) **δ_C** 71.3 (*C-1*), 39.0 (*CH_2*), 38.8 (*CH_2*), 26.5 (*CH_2*), 26.1 (*C-7*), 22.8 (*CH_2*), 22.7 (*CH_2*), 22.6 (*CH_2*); **HRMS** *m/z* (CI^+) Found: $[M+H]^+$ 259.1564. $C_{14}H_{27}S_2$ requires $[M+H]^+$ 259.1554.

5.2.2 1,1-Difluorocyclododecane (50)

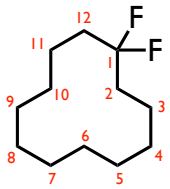

Hydrogen fluoride-pyridine (0.5 mL, 18.5 mmol, 80 eq) was added to a solution of *N*-iodosuccinimide **40** (0.16 g, 0.6 mmol, 3 eq) in DCM (2 mL) at −78 ºC. The resulting mixture was stirred for 10 min at −78 ºC. A solution of 1,4-dithiaspiro[4.11]hexadecane **47** (0.06 g, 0.2 mmol, 1 eq) in DCM (3 mL) was added dropwise to the mixture over 10 min. The reaction mixture was stirred for 2 h, warming gradually to −10 ºC. The solution was diluted with hexane (40 mL) and filtered through a column of basic alumina. Purification over silica gel, eluting with hexane, yielded 1,1-difluorocyclododecane **50** (13 mg, 0.06 mmol, 32%) as a colourless waxy solid:

R_f = 0.59 (hexane:DCM, 80:20); **m.p.** = 42-44 ºC (from DCM) [lit.[2] 42-44 ºC]; **^{1}H NMR** (400 MHz, $CDCl_3$) **δ_H** 1.95-1.81 (4H, m, *CH_2-2,12*), 1.53-1.44 (4H, m, *CH_2-3,11*), 1.43-1.30 (16H, m, *CH_2-3-10*); **^{13}C NMR** (100 MHz, CD_2Cl_2) **δ_C** 127.4 (t, *J* = 240.3 Hz, *C-1*), 31.5 (t, *J* = 25.3 Hz, *C-2,12*), 25.8 (*CH_2*), 25.7 (*CH_2*), 22.6 (*CH_2*), 22.2 (*CH_2*), 19.4 (t, *J* = 5.5 Hz, *C-3,11*); **^{19}F{^{1}H} NMR** (376 MHz, $CDCl_3$) **δ_F** −91.6 (*CF_2-1*); **LRMS** *m/z* (EI^+) 184.2 $[M-HF]^{+\cdot}$ 186.2 $[M-2HF]^{+\cdot}$.

5.2.3 Cyclododecane-1,4-dione (71)

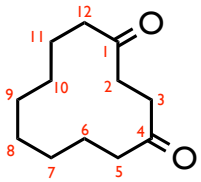

A solution of cyclododecanone **70** (3.00 g, 16.1 mmol) in cyclohexane (15 mL) was irradiated with UV light for 72 h at RT, using medium pressure mercury lamp (λ = 200-1000 nm) until no further change was observed by TLC. The solvent was removed under reduced pressure, affording a colourless oil (2.27 g), which was used in the subsequent step without further purification. Concentrated sulfuric acid (4.2 mL) was added dropwise to a solution of chromium trioxide (4.98 g, 49.8 mmol, 4 eq) in water (14.5 mL). The resulting Jones reagent was added dropwise to a solution of crude bicyclo[8.2.0]dodecanol **77** (2.27 g, 12.5 mmol, 1 eq) in acetone (50 mL) at 0 ºC. After 30 min the mixture was allowed to warm to RT and was stirred for 12 h. The solvent was removed under reduced pressure and water (75 mL) was added to the residue. The resulting mixture was extracted into Et_2O (3 × 75 mL). The organic extracts were dried over $MgSO_4$, filtered and concentrated *in vacuo*, affording a colourless white solid. Purification over silica gel, eluting with hexane and EtOAc (90:10), yielded cyclododecane-1,4-dione **71** (0.65 g, 21% over two steps) as a colourless crystalline solid:

R_f = 0.28 (hexane:EtOAc, 65:35); **m.p.** = 74-76 ºC (from DCM) [lit.[3] 74-76 ºC]; **^{1}H NMR** (400 MHz, $CDCl_3$) **δ_H** 2.72 (4H, s, *CH_2-2,3*), 2.41 (4H, t, *J* = 6.1 Hz,

CH₂-5,12), 1.68-1.59 (4H, m, *CH₂*), 1.28-1.20 (4H, m, *CH₂*), 1.15-1.08 (4H, m, *CH₂*); **^{13}C NMR** (100 MHz, $CDCl_3$) **δ_C** 211.3 (*C-1,4*), 41.7 (*C-5,12*), 37.8 (*C-2,3*), 26.0 (*CH₂*), 25.7 (*CH₂*), 21.9 (*CH₂*); **HRMS** *m/z* (ES^+) Found: $[M+Na]^+$ 219.1362. $C_{12}H_{20}O_2Na$ requires $[M+Na]^+$ 219.1361.

5.2.4 1,4,9,12-Tetrathiadispiro[4.2.4.8]icosane (78)

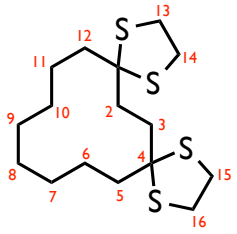

Boron trifluoride acetic acid complex (0.7 mL, 5.0 mmol, 2 eq) was added to a stirred mixture of cyclododecane-1,4-dione **71** (0.5 g, 2.5 mmol, 1 eq) and 1,2-ethanedithiol (0.86 mL, 10.2 mmol, 4.1 eq). The biphasic solution was stirred vigorously for 20 min at RT. When the starting material was consumed (TLC analysis), the reaction mixture was diluted with DCM (50 mL) and then washed with saturated aqueous $NaHCO_3$ solution (30 mL), aqueous NaOH solution (15% w/v, 30 mL), and brine (30 mL). The organic extracts were dried over $MgSO_4$ and concentrated. Purification over silica gel, eluting with hexane and DCM (80:20, 70:30), yielded 1,4,9,12-tetrathiadispiro[4.2.4.8]icosane **78** (0.81 g, 92%) as a colourless crystalline solid:

R_f = 0.32 (DCM:hexane, 50:50); **m.p.** = 157-158 ºC (from DCM); **^{1}H NMR** (400 MHz, $CDCl_3$) **δ_H** 3.28 (8H, s, *CH₂-13,14,15,16*), 2.14 (4H, s, *CH₂-2,3*),

2.04 (4H, t, *J* = 7.9 Hz, *CH*$_2$*-5,12*), 1.54-1.33 (12H, m, *CH*$_2$*-6-11*); **^{13}C NMR** (100 MHz, $CDCl_3$) **δ_C** 70.7 (*C-1,4*), 38.9 (*CH*$_2$), 38.8 (*CH*$_2$), 38.1 (*C-2,3*), 26.5 (*CH*$_2$), 23.2 (*CH*$_2$), 22.7 (*CH*$_2$); **HRMS** *m/z* (CI^+) Found: $[M+H]^+$ 349.1147. $C_{16}H_{29}S_4$ requires $[M+H]^+$ 349.1152.

5.2.5 1,1,4,4-Tetrafluorocyclododecane (74)

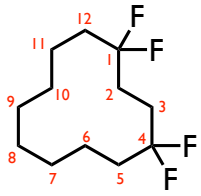

Hydrogen fluoride-pyridine (2.6 mL, 100.1 mmol, 112.4 eq) was added to a solution of *N*-iodosuccinimide **40** (1.19 g, 5.3 mmol, 5.9 eq) in DCM (7 mL) at −78 ºC. The resulting mixture was stirred for 10 min at −78 ºC. A solution of 1,4,9,12-tetrathiadispiro[4.2.4.8]icosane **78** (0.31 g, 0.89 mmol, 1 eq) in DCM (5 mL) was added dropwise over 10 min. The reaction mixture was stirred at −78 ºC for 4 h and gradually warmed to RT overnight. The crude mixture was added portionwise to a biphasic mixture of saturated aqueous $NaHCO_3$ solution (50 mL) and DCM (40 mL) at 0 ºC. The aqueous layer was separated and extracted with DCM (3 × 30 mL). The organic extracts were washed with aqueous $Na_2S_2O_3$ solution (10% w/v, 2 × 50 mL), brine (60 mL), dried over $MgSO_4$, filtered and concentrated under reduced pressure. Purification over silica gel, eluting with hexane, yielded 1,1,4,4-tetrafluorocyclododecane **74** (0.06 g, 28%) as a colourless crystalline solid:

R_f = 0.64 (DCM:hexane, 60:40); **m.p.** = 80 ºC (from DCM); **$^1H\{^{19}F\}$ NMR** (400 MHz, $CDCl_3$) **δ_H** 2.02 (4H, s, *CH_2-2,3*), 1.88 (4H, t, *J* = 7.8 Hz, *CH_2-5,12*), 1.54-1.33 (12H, m, *CH_2-6-11*); **^{13}C NMR** (100 MHz, CD_2Cl_2) **δ_C** 126.1 (t, *J* = 241.2 Hz, *C-1,4*), 30.9 (t, *J* = 25.5 Hz, *C-5,12*), 28.1 (tt, *J* = 28.2 Hz, 5.4 Hz, *C-2,3*), 25.8 (*CH_2*), 22.2 (*CH_2*), 19.5 (bs, *C-6,11*); **$^{19}F\{^1H\}$ NMR** (376 MHz, $CDCl_3$) **δ_F** −92.80 (*CF_2-1,4*) **HRMS** *m/z* (CI^+) Found: $[M-3HF+H]^+$ 181.1391. $C_{12}H_{18}F$ requires $[M-3HF+H]^+$ 181.1393; **LRMS** *m/z* (CI^+) 221.15 $[M-HF+H]^+$.

5.2.6 Cyclododecane-1,7-dione (72)

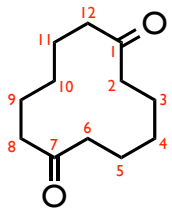

Freshly cut sodium (0.26 g, 11.4 mmol, 0.4 eq) was added portionwise to vigorously stirred, flame-dried, neutral, activity I aluminium oxide (5 g, 49 mmol, 1.6 eq) at 260 ºC. The molten metal became dispersed on the alumina surface, which assumed a dark blue colour. The sodium on alumina catalyst was then cooled down to RT and a solution of *cis,trans,trans*-cyclododeca-1,5,9-triene **79** (5.6 mL, 30 mmol, 1 eq) in dry heptane (50 mL) was added in one portion. The reaction mixture was refluxed for approximately 3 hours until the GC-MS analysis showed that all the starting material had been consumed. Hydrogen gas was then introduced, stirring and refluxing was continued overnight. The gas-chromatogram simplified to two

main peaks. The catalyst was then filtered off through a pad of celite and washed with heptane (3 × 15 mL). The resulting heptane solution was combined with a mixture of acetic acid (75 mL) and water (75 mL). Ozone was bubbled through the reaction mixture over 10 min at 0 ºC. The aqueous layer was separated and concentrated under reduced pressure. To the resulting oily residue was added saturated aqueous $NaHCO_3$ solution (100 mL) and extracted with Et_2O (3 × 75 mL). The organic extracts were dried over $MgSO_4$ and concentrated *in vacuo*, affording a colourless oil. The product was crystallised from pentane and recrystallised from boiling pentane. Further purification over silica gel, eluting with hexane and EtOAc (85:15), yielded cyclododecane-1,7-dione **72** (0.21 g, 4% over three steps) as a colourless crystalline solid:

R_f = 0.26 (hexane:EtOAc, 65:35); **m.p.** = 132-134 ºC (from DCM) [lit.[4] 133-135 ºC]; **^{1}H NMR** (300 MHz, $CDCl_3$) **δ_H** 2.44-2.40 (8H, m, *CH_2-2,6,8,12*), 1.73-1.64 (8H, m, *CH_2-3,5,9,11*), 1.14 (4H, q, *J* = 7.3 Hz, *CH_2-4,10*); **^{13}C NMR** (75 MHz, $CDCl_3$) **δ_C** 212.2 (*C-1,7*), 40.6 (*C-2,6,8,12*), 26.0 (*C-3,5,9,11*), 22.7 (*C-4,10*); **HRMS** *m/z* (CI^+) Found: $[M+H]^+$ 197.1534. $C_{12}H_{21}O_2$ requires $[M+H]^+$ 197.1542.

5.2.7 1,4,12,15-Tetrathiadispiro[4.5.4.5]icosane (82)

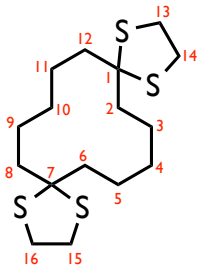

Boron trifluoride acetic acid complex (0.25 mL, 1.7 mmol, 2 eq) was added dropwise to a stirred mixture of cyclododecane-1,7-dione **72** (0.17 g, 0.85 mmol, 1 eq) and 1,2-ethanedithiol (0.30 mL, 3.5 mmol, 4.1 eq). The biphasic solution was stirred vigorously for 20 min. When the starting material was consumed (TLC), the reaction mixture was diluted with DCM (20 mL) and washed with saturated $NaHCO_3$ solution (10 mL), NaOH solution (15% w/v, 10mL), and brine (10 mL). The organic extracts were dried over $MgSO_4$ and concentrated. Purification over silica gel, eluting with hexane and EtOAc (98:2), yielded 1,4,12,15-tetrathiadispiro[4.5.4.5]icosane **82** (0.16 g, 54%) as a colourless crystalline solid:

R_f = 0.57 (hexane: EtOAc, 90:10); **m.p.** = 224-227 ºC (from DCM); **^{1}H NMR** (400 MHz, $CDCl_3$) **δ_H** 3.28 (8H, s, *CH_2-13,14,15,16*), 2.06-1.97 (8H, m, *CH_2-2,6,8,12*), 1.52-1.32 (12H, m, *CH_2-3-5,9-11*); **^{13}C NMR** (100 MHz, $CDCl_3$) **δ_C** 70.6 (*C-1,7*), 39.0 (*CH_2*), 38.8 (*CH_2*), 25.9 (*CH_2*), 23.0 (*CH_2*); **HRMS** *m/z* (EI^+) Found: $[M]^{+\cdot}$ 348.1067 $C_{16}H_{28}S_4$ requires $[M]^{+\cdot}$ 348.1068.

5.2.8 1,1,7,7-Tetrafluorocyclododecane (75)

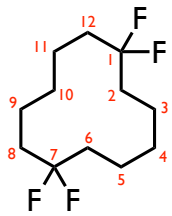

Hydrogen fluoride-pyridine (0.72 mL, 27.7 mmol, 121 eq) was added to a solution of *N*-iodosuccinimide **40** (0.38 g, 1.69 mmol, 7 eq) in DCM (10 mL) at −78 ºC. The resulting mixture was stirred for 5 min at −78 ºC. A solution of 1,4,12,15-tetrathiadispiro[4.5.4.5]icosane **82** (0.08 g, 0.23 mmol, 1 eq) in DCM (10 mL) was then added dropwise over 10 min. The reaction mixture was stirred for 5 h, maintaining the temperature below −70 ºC. The solution was diluted with DCM (50 mL) and solid $NaHCO_3$ was added. The biphasic mixture was stirred for 2 h and water (30 mL) was added portionwise. After one hour, the mixture was filtered through a pad of celite, the organic layer was collected and dried over $MgSO_4$ and concentrated. Purification over silica gel, eluting first with hexane, followed by hexane and DCM (70:30), yielded 1,1,7,7-tetrafluorocyclododecane **75** (31 mg, 0.13 mmol, 57%) as a colourless crystalline solid:

R_f = 0.58 (DCM:hexane, 50:50); **m.p.** = 137 ºC (from $CHCl_3$); **$^1H\{^{19}F\}$ NMR** (400 MHz, $CDCl_3$) **δ_H** 1.96-1.82 (8H, m, *CH_2-2,6,8,12*), 1.54-1.39 (12H, m, *CH_2-3-5,9-11*); **^{13}C NMR** (100 MHz, $CDCl_3$) **δ_C** 126.8 (t, *J* = 240.4 Hz, *C-1,7*), 31.2 (t, *J* = 25.4 Hz, *C-2,6,8,12*), 25.1 (*C-4,10*), 19.1 (t, *J* = 5.4 Hz,

C-3,5,9,11); **$^{19}F\{^{1}H\}$ NMR** (376 MHz, $CDCl_3$) δ_F −91.99 (*CF_2-1,7*). **HRMS** *m/z* (CI^+) Found: $[M-HF+H]^+$ 221.1525 $C_{12}H_{20}F_3$ requires $[M-HF+H]^+$ 221.1517; **LRMS** *m/z* (CI^-) 240.2 $[M]^-$.

5.2.9 1,1,6,6-Tetrafluorocyclododecane (76)

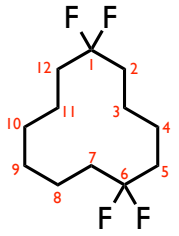

Hydrogen fluoride-pyridine (0.43 mL, 16.6 mmol, 115 eq) was added to a solution of *N*-iodosuccinimide **40** (0.26 g, 1.16 mmol, 8 eq) in DCM (10 mL) at −78 ºC. The mixture was stirred for 5 min before a solution of 1,4,11,14-tetrathiadispiro[4.4.4.6]icosane **87** (0.05 g, 0.14 mmol, 1 eq) in DCM (2 mL) was added dropwise over 10 min. The reaction mixture was stirred at −78 ºC for 4 h and gradually warmed to RT overnight. It was diluted with 50 mL of DCM and solid $NaHCO_3$ (20 g) was added. The biphasic mixture was stirred for 2 h and water (30 mL) was added protionwise. The organic layer was separated, dried over $MgSO_4$ and concentrated. Purification over silica gel, eluting with hexane yielded 1,1,6,6-tetrafluorocyclododecane **76** (0.02 g, 58%) as a colourless crystalline solid:

R_f = 0.22 (hexane:DCM, 90:10); **m.p.** = 31 °C (from $CHCl_3$); **$^{1}H\{^{19}F\}$ NMR** (400 MHz, $CDCl_3$) δ_H 2.02-1.92 (4H, m, *CH_2*), 1.91-1.84 (4H, m, *CH_2*),

1.58-1.53 (4H, m, *CH*$_2$), 1.50-1.41 (8H, m, *CH*$_2$); **^{13}C NMR** (100 MHz, $CDCl_3$) **δ_C** 126.8 (t, *J* = 240.8 Hz, *C-1,6*), 33.0 (t, *J* = 25.5 Hz, *CH*$_2$), 31.0 (t, *J* = 6.0 Hz, *CH*$_2$), 24.6 (s, *CH*$_2$*-9,10*), 20.7 (t, *J* = 5.6 Hz, *CH*$_2$), 18.6 (t, *J* = 5.3 Hz, *CH*$_2$); **^{19}F{^{1}H} NMR** (376 MHz, $CDCl_3$) **δ_F** −90.00 (*CF*$_2$*-1,6*); **HRMS** (CI^+) Found: $[M-3HF+H]^+$ 181.1401 $C_{12}H_{18}F$ requires $[M-3HF+H]^+$ 181.1393; **LRMS** *m/z* (EI^+) 220.1 $[M-HF]^{+\cdot}$, 200.2 $[M-2HF]^{+\cdot}$.

5.3 Protocols for Chapter 3

5.3.1 2,2'-Ethylenebis(2-(hex-5-enyl)-1,3-dithiane) (103)

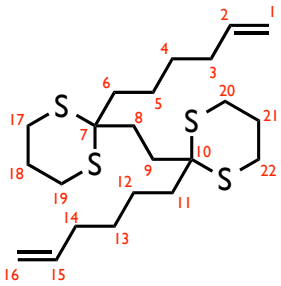

n-BuLi (31.1 mL, 2.5 M, 77.8 mmol, 2.6 eq) was added to a solution of 2,2'-ethylenebis(1,3-dithiane) **102** (7.90 g, 29.6 mmol, 1 eq) in THF (300 mL) at −20 ºC, stirred for 20 min and gradually warmed to −5 ºC over 80 min. 6-Bromohex-1-ene (9.2 mL, 68.8 mmol, 2.3 eq) was added portionwise at −25 ºC and the mixture was stirred overnight at −5 ºC. A mixture of mono- and di- alkylated products was observed (TLC/^{1}H NMR). A further aliquot of *n*-BuLi (8.35 mL, 2.5 M, 20.9 mmol, 0.7 eq) was added at −15 ºC and the mixture was stirred for 90 min at that temperature. 6-Bromohex-1-ene (2.78 mL,

20.8 mmol, 0.7 eq) was added dropwise at −15 ºC and stirred for 4 h. The deprotonation/alkylation sequence was repeated again at −15 ºC, using *n*-BuLi (3.50 mL, 2.5 M, 8.75 mmol, 0.3 eq) and 6-bromohex-1-ene (1.59 mL, 11.9 mmol, 0.4 eq). The reaction mixture was stirred for 4 h, warmed to 0 ºC, quenched with saturated aqueous NH_4Cl solution (200 mL) and extracted with Et_2O (4 × 200 mL). The organic extracts were washed with brine (150 mL), dried over $MgSO_4$, filtered and concentrated. Purification over silica gel, eluting with petroleum ether and EtOAc (99:1, 97:3), yielded 2,2'-Ethylenebis(2-(hex-5-enyl)-1,3-dithiane) **103** (9.34 g, 73%) as a colourless viscous oil:

R_f = 0.41 (petroleum ether:Et_2O, 88:12); **^{1}H NMR** (400 MHz, $CDCl_3$) **δ_H** 5.80 (2H, ddt, *J* = 17.1, 10.2, 6.7 Hz, *CH-2,15*), 5.01 (2H, ddt, *J* = 17.1, 2.1, 1.5 Hz, *CH_{trans}-1,16*), 4.95 (2H, ddt, *J* = 10.2, 2.1, 1.2 Hz, *CH_{cis}-1,16*), 2.96 (4H, ddd, *J* = 14.5, 10.2, 3.1 Hz, *CH_a-17,19,20,22*), 2.73 (4H, ddd, *J* = 14.6, 6.5, 3.2 Hz, *CH_b-17,19,20,22*), 2.12-1.97 (10H, m, *CH_a-18,21, CH_2-3,8,9,14*), 1.96-1.84 (2H, m, *CH_b-18,21*), 1.83-1.75 (4H, m, *CH_2-6,11*), 1.55-1.32 (8H, m, *CH_2-4,5,12,13*); **^{13}C NMR** (100 MHz, $CDCl_3$) **δ_C** 138.8 (*C-2,15*), 114.8 (*C-1,16*), 53.4 (*C-7,10*), 38.8 (*C-6,11*), 33.7 (*C-3,14*), 32.6 (*C-8,9*), 29.2 (*C-4,13*), 26.2 (*C-17,19,20,22*), 25.6 (*C-18,21*), 23.4 (*C-5,12*); **HRMS** *m/z* (ES^+) Found: $[M+Na]^+$ 453.1762. $C_{22}H_{38}S_4Na$ requires $[M+Na]^+$ 453.1749.

5.3.2 1,5,10,14-Tetrathiadispiro[5.2.5.10]tetracos-19-ene (104)

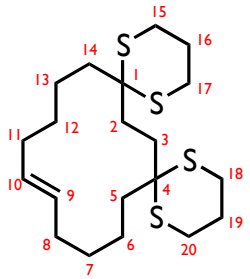

M_{20} (16 mg, 17 μmol, 1.5 mol%) was added in one portion to a 0.04 M solution of 2,2'-ethylenebis(2-(hex-5-enyl)-1,3-dithiane) **103** (0.50 g, 1.16 mmol,) in DCE (29 mL) and stirred for 20 h at 40 °C. The crude reaction was concentrated under reduced pressure affording a brown waxy solid. Purification over silica gel, eluting with pentane and Et_2O (95:5), yielded 1,5,10,14-tetrathiadispiro[5.2.5.10]tetracos-19-ene **104** (0.33 g, 71%) as a white crystalline solid:

R_f = 0.35 (pentane:Et_2O, 88:12); **m.p.** = 135-136 ºC (from hexane:DCM, 60:40); **^{1}H NMR** (500 MHz, $CDCl_3$) **δ_H** 5.25-5.16 (2H, m, *CH-9,10*), 2.93 (4H, ddd, *J* = 14.2, 10.7, 2.8 Hz, *CH_a-15,17,18,20*), 2.72 (4H, ddd, *J* = 14.2, 6.1, 3.2 Hz, *CH_b-15,17,18,20*), 2.12-1.97 (10H, m, *CH_a-16,19; CH_2-2,3,8,11*), 1.96-1.87 (2H, m, *CH_b-16,19*), 1.83-1.75 (4H, m, *CH_2-5,14*), 1.47-1.37 (4H, m, *CH_2-6,13*), 1.36-1.27 (4H, m, *CH_2-7,12*); **^{13}C NMR** (125 MHz, $CDCl_3$) **δ_C** 132.3 (*C-9,10*), 52.6 (*C-1,4*), 38.5 (*C-5,14*), 32.5 (*C-8,11*), 30.3 (*C-2,3*), 28.1 (*C-7,12*), 26.2 (*C-15,17,18,20*), 26.0 (*C-16,19*), 21.7 (*C-6,13*); **HRMS** *m/z* (ES^+) Found: $[M+Na]^+$ 425.1443. $C_{20}H_{34}S_4Na$ requires $[M+Na]^+$ 425.1436.

5.3.3 1,5,10,14-Tetrathiadispiro[5.2.5.10]tetracosane (105)

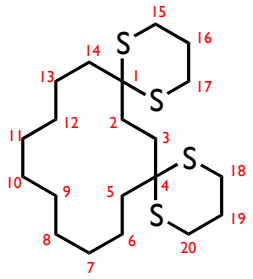

1,5,10,14-Tetrathiadispiro[5.2.5.10]tetracos-19-ene **104** (100 mg, 0.25 mmol) and the catalyst **99** (30 mg, 3.8 μmol, 15 mol%) were dissolved in DMF (2 mL) in a glass vial. The vial was introduced inside an autoclave, and the system was pressurised with hydrogen at 10 bar. The reactor was heated at 80 °C for 48 h. The product was then extracted with a mixture of Et_2O and DCM. Purification over silica gel, eluting with DCM afforded 1,5,10,14-tetrathiadispiro[5.2.5.10]tetracosane **105** (60 mg, 60% yield) as a white crystalline solid:

R_f = 0.30 (pentane:Et_2O, 88:12); **m.p.** = 149-150 ºC (from DCM); **^{1}H NMR** (500 MHz, $CDCl_3$) **δ_H** 2.90 (4H, ddd, *J* = 14.6, 9.9, 3.0 Hz, *CH_a-15,17,18,20*), 2.75 (4H, ddd, *J* = 14.6, 6.7, 3.2 Hz, *CH_b-15,17,18,20*), 2.09 (4H, s, *CH_2-2,3*), 2.08-2.00 (2H, *CH_a-16,19*), 1.97-1.88 (2H, m, *CH_b-16,19*), 1.88-1.82 (4H, m, *CH_2-5,14*), 1.47-1.24 (16H, m, *CH_2*); **^{13}C NMR** (125 MHz, $CDCl_3$) **δ_C** 52.6 (*C-1,4*), 38.0 (*C-5,14*), 30.1 (*C-2,3*), 26.5 (*CH_2*), 26.2 (*C-15,17,18,20*), 25.9 (*C-16,19*), 25.7 (*CH_2*), 21.8 (*CH_2*), 21.0 (*CH_2*); **HRMS** m/z (ES^+) Found: $[M+H]^+$ 405.1771. $C_{20}H_{37}S_4$ requires $[M+H]^+$ 405.1773.

5.3.4 1,1,4,4-Tetrafluorocyclotetradecane (91)

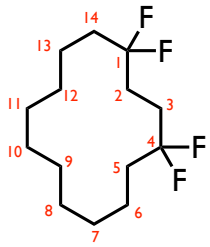

Hydrogen fluoride-pyridine (2.33 mL, 89.7 mmol, 121 eq) was added to a solution of *N*-iodosuccinimide **40** (1.40 g, 6.22 mmol, 8 eq) in DCM (12 mL) at −78 ºC. The resulting mixture was stirred for 5 min at −78 ºC. A solution of 1,5,10,14-tetrathiadispiro[5.2.5.10]tetracosane **105** (0.30 g, 0.74 mmol, 1 eq) in DCM (5 mL) was added dropwise to the mixture over 10 min. The reaction mixture was stirred at −78 ºC for 4 h and gradually warmed to RT overnight. The crude reaction was added portionwise to a biphasic mixture of saturated aqueous $NaHCO_3$ solution (80 mL) and DCM (40 mL) at 0 ºC. The aqueous layer was separated and extracted with DCM (3 × 50 mL). The organic extracts were washed with aqueous $Na_2S_2O_3$ solution (10% w/v, 2 × 80 mL), brine (100 mL), dried over $MgSO_4$, filtered and concentrated under reduced pressure. Purification over silica gel, eluting with pentane, yielded 1,1,4,4-tetrafluorocyclotetradecane **91** (0.14 g, 68%) as a white crystalline solid:

R_f = 0.34 (pentane:DCM, 90:10); **m.p.** = 74 ºC (from $CDCl_3$); **^{1}H NMR** (500 MHz, $CDCl_3$) **δ_H** 2.06-1.94 (4H, m, *CH_2-2,3*), 1.93-1.81 (4H, m, *CH_2-5,14*), 1.48-1.34 (12H, m, *CH_2*), 1.33-1.27 (4H, m, *CH_2*); **^{1}H{^{19}F} NMR** (500 MHz,

$CDCl_3$) δ_H 2.00 (4H, s, *CH_2-2,3*), 1.90-1.85 (4H, m, *CH_2-5,14*), 1.48-1.34 (12H, m, *CH_2*), 1.33-1.27 (4H, m, *CH_2*); **^{13}C NMR** (125 MHz, $CDCl_3$) δ_C 125.7 (t, *J* = 240.8 Hz, *C-1,4*), 34.4 (t, *J* = 25.3 Hz, *C-5,14*), 28.2 (tt, *J* =27.6, 5.2 Hz, *C-2,3*), 25.9 (*CH_2*), 25.2 (*CH_2*), 23.4 (*CH_2*), 20.9 (t, *J* = 5.4 Hz, *C-6,13*); **^{19}F{^{1}H} NMR** (470 MHz, $CDCl_3$) δ_F −91.59 (s, *CF_2-1,4*); **HRMS** *m/z* (EI^+) Found: $[M-HF]^{+\cdot}$ 248.1747. $C_{14}H_{23}F_3$ requires $[M-HF]^{+\cdot}$ 248.1746; **LRMS** *m/z* (EI^+) 248.18 $[M-HF]^{+\cdot}$, 228.16 $[M-2HF]^{+\cdot}$.

5.3.5 2,2'-Butylenebis(1,3-dithiane) (106)

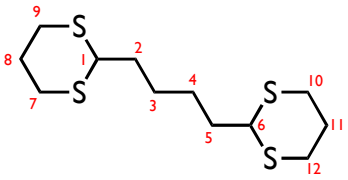

n-BuLi (46.1 mL, 2.31 M, 106.5 mmol, 1.1 eq) was added portionwise to a solution of 1,3-dithiane **62** (11.6 g, 96.5 mmol, 1 eq) in THF (250 mL) at −30 ºC and stirred for 2 h. 1,4-Dibromobutane (5.6 mL, 46.9 mmol, 0.49 eq) was added dropwise and the mixture stirred at −30 ºC for 2 h. The temperature was increased to −5 ºC and stirring continued for 24 h. The reaction was quenched with saturated aqueous NH_4Cl solution (200 mL) and extracted with Et_2O (4 × 150 mL). The organic extracts were washed with brine (150 mL), dried over $MgSO_4$, filtered and concentrated. Purification over silica gel, eluting with hexane and DCM (80:20, 40:60), yielded 2,2'-butylenebis(1,3-dithiane) **106** (8.87 g, 65%) as a white crystalline solid:

R_f = 0.20 (petroleum ether:Et_2O, 88:12); **m.p.** = 103-104 ºC (from $CDCl_3$) (lit.[5] 102.5-103.5 ºC); **^{1}H NMR** (500 MHz, $CDCl_3$) **δ_H** 4.04 (2H, t, *J* = 6.9 Hz, *CH-1,6*), 2.91-2.79 (8H, m, *CH_2-7,9,10,12*), 2.15-2.08 (2H, m, *CH_a-8,11*), 1.91-1.80 (2H, m, *CH_b-8,11*), 1.79-1.72 (4H, m, *CH_2-2,5*), 1.56-1.49 (4H, m, *CH_2-3,4*); **^{13}C NMR** (75 MHz, $CDCl_3$) **δ_C** 47.6 (*C-1,6*), 35.3 (*C-2,5*), 30.6 (*C-7,9,10,12*), 26.4 (*C-3,4*) 26.2 (*C-8,11*); **HRMS** *m/z* (ES^+) Found: $[M+Na]^+$ 317.0507. $C_{12}H_{22}S_4Na$ requires $[M+Na]^+$ 317.0502.

5.3.6 2,2'-Butylenebis(2-(pent-4-enyl)-1,3-dithiane) (107)

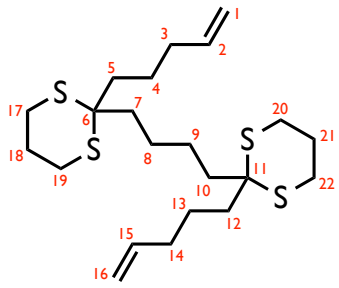

n-BuLi (17.4 mL, 2.42 M, 42.1 mmol, 3 eq) was added to a solution of 2,2'-butylenebis(1,3-dithiane) **106** (4.14 g, 14.1 mmol, 1 eq) in THF (150 mL) at −30 ºC, stirred for 30 min, and gradually warmed to −10 ºC over 60 min. 5-Bromopent-1-ene (5.0 mL, 42.2 mmol, 3 eq) was added in small portions at −30 ºC and the mixture was stirred overnight at −30 ºC. A mixture of mono- and di- alkylated products was observed (TLC/^{1}H NMR). A further aliquot of *n*-BuLi (5.81 mL, 2.42 M, 14.1 mmol, 1 eq) was added at −20 ºC and stirred for 90 min at that temperature. 5-Bromopent-1-ene (1.67 mL, 14.1 mmol, 1 eq) was added dropwise −20 ºC and stirred for 2 h. The deprotonation/alkylation sequence was repeated again at −15 ºC, using

n-BuLi (5.81 mL, 2.42 M, 14.1 mmol, 1 eq) and 5-bromopent-1-ene (0.83 mL, 7.0 mmol, 0.5 eq). The reaction mixture was stirred for 2 h, warmed to 0 ºC, quenched with saturated aqueous NH_4Cl solution (100 mL) and extracted with Et_2O (4 × 100 mL). The organic extracts were washed with brine (150 mL), dried over $MgSO_4$, filtered and concentrated. Purification over silica gel, eluting with petroleum ether and Et_2O (99:1, 98:2), yielded 2,2'-butylenebis(2-(pent-4-enyl)-1,3-dithiane) **107** (4.54 g, 75%) as a colourless viscous oil:

R_f = 0.33 (petroleum ether:Et_2O, 88:12); **^{1}H NMR** (300 MHz, $CDCl_3$) **δ_H** 5.81 (2H, ddt, *J* = 17.1, 10.2, 6.7 Hz, *CH-2,15*), 5.04 (2H, ddt, *J* = 17.1, 1.9, 1.4 Hz, *CH_{trans}-1,16*), 4.98 (2H, ddt, *J* = 10.1, 1.9, 1.2 Hz, *CH_{cis}-1,16*), 2.85-2.75 (8H, m, *CH_2-17,19,20,22*), 2.13-2.03 (4H, m, *CH_2-3,14*), 2.00-1.91 (4H, m, *CH_2-18,21*), 1.91-1.82 (8H, m, *CH_2-5,7,10,12*), 1.59-1.49 (4H, m, *CH_2-4,13*), 1.49-1.41 (4H, m, *CH_2-8,9*); **^{13}C NMR** (125 MHz, $CDCl_3$) **δ_C** 138.4 (*C-2,15*), 115.2 (*C-1,16*), 53.3 (*C-6,11*), 38.3 (*C-7,10*), 37.8 (*C-5,12*), 33.9 (*C-3,14*), 26.2 (*C-17,19,20,22*), 25.6 (*C-18,21*), 24.5 (*C-8,9*), 23.5 (*C-4,13*); **HRMS** *m/z* (ES^+) Found: $[M+Na]^+$ 453.1743. $C_{22}H_{38}S_4Na$ requires $[M+Na]^+$ 453.1749.

5.3.7 1,5,12,16-Tetrathiadispiro[5.4.5.8]tetracos-20-ene (108)

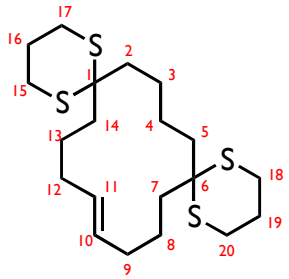

M_{20} (12 mg, 17 µmol, 0.01 eq) was added in one portion to a 0.02 M solution of 2,2'-butylenebis(2-(pent-4-enyl)-1,3-dithiane) **107** (0.50 g, 1.16 mmol) in DCE (58 mL) and stirred for 20 h at RT. The crude reaction was concentrated under reduced pressure affording a brown waxy solid. Purification over silica gel, eluting with pentane and Et_2O (95:5), afforded 1,5,12,16-tetrathiadispiro[5.4.5.8]tetracos-20-ene **108** (0.12 g, 31%) as a white crystalline solid:

R_f = 0.22 (petroleum ether:Et_2O, 88:12); **m.p.** = 139-140 ºC (from $CHCl_3$); **^{1}H NMR** (500 MHz, $CDCl_3$) **δ_H** 5.65-5.55 (2H, m, *CH-10,11*), 2.86-2.71 (8H, m, *CH_2-15,17,18,20*), 2.08-1.99 (4H, m, *CH_2-9,12*), 1.99-1.90 (8H, m, *CH_2-2,5,16,19*), 1.90-1.82 (4H, m, *CH_2-7,14*), 1.59-1.49 (4H, m, *CH_2-8,13*), 1.47-1.38 (4H, m, *CH_2-3,4*); **^{13}C NMR** (125 MHz, $CDCl_3$) **δ_C** 131.7 (*C-10,11*), 53.6 (*C-1,6*), 37.2 (*C-2,5*), 35.7 (*C-7,14*), 30.6 (*C-9,12*), 26.1 (*C-15,17,18,20)*, 25.8 (*C-16,19*), 25.2 (*C-3,4)*, 25.0 (*C-8,13*); **HRMS** *m/z* (ES^+) Found: $[M+Na]^+$ 425.1435. $C_{20}H_{34}S_4Na$ requires $[M+Na]^+$ 425.1436.

5.3.8 1,5,12,16-Tetrathiadispiro[5.4.5.8]tetracosane (109)

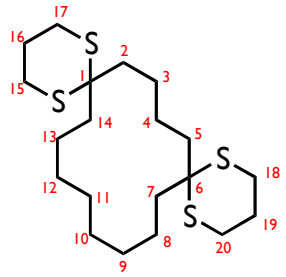

1,5,12,16-Tetrathiadispiro[5.4.5.8]tetracos-20-ene **108** (124 mg, 0.31 mmol) and the catalyst **99** (73 mg, 9.2 μmol, 30 mol%) were dissolved in DMF (3 mL) in a glass vial, and introduced inside an autoclave. The system was pressurised with hydrogen at 10 bar. The reactor was heated at 80 °C for 48 h. The product was then extracted with a mixture of Et_2O and DCM. Purification over silica gel, eluting with DCM afforded 1,5,10,14-tetrathiadispiro[5.2.5.10]tetracosane **109** (87 mg, 70% yield) as a white solid:

R_f = 0.27 (petroleum ether:Et_2O, 88:12); **m.p.** = 152-153 ºC (from $CHCl_3$); **^{1}H NMR** (400 MHz, $CDCl_3$) **δ_H** 2.83-2.72 (8H, m, *CH_2-15,17,18,20*), 2.00-1.91 (8H, m, *CH_2-7,14,16,19*), 1.90-1.81 (4H, m, *CH_2-2,5*), 1.46-1.35 (12H, m, *CH_2-3,4,8,13* and *9,12* or *10,11*), 1.34-1.28 (4H, m, *CH_2-9,12 or 10,11*); **^{13}C NMR** (100 MHz, $CDCl_3$) **δ_C** 53.1 (*C-1,6*), 36.7 (*C-7,14*), 36.0 (*C-2,5*), 27.6 (*C-8,13*), 26.1 (*C-15,17,18,20)*, 25.9 (*C-16,19*), 25.7 (*CH_2)*, 24.9 (*CH_2*), 20.8 (*C-3,4*); **HRMS** *m/z* (ES^+) Found: $[M+Na]^+$ 427.1593. $C_{20}H_{36}S_4Na$ requires $[M+Na]^+$ 427.1592.

5.3.9 1,1,6,6-Tetrafluorocyclotetradecane (93)

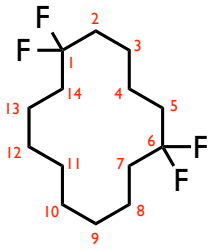

Hydrogen fluoride-pyridine (1.05 mL, 40.4 mmol, 117 eq) was added to a solution of *N*-iodosuccinimide **40** (0.62 g, 2.76 mmol, 8 eq) in DCM (6 mL) at −78 ºC. The resulting mixture was stirred for 5 min at −78 ºC. A solution of 1,5,10,14-tetrathiadispiro[5.2.5.10]tetracosane **109** (0.14 g, 0.35 mmol, 1 eq) in DCM (3 mL) was added dropwise to the mixture over 10 min. The reaction mixture was stirred at −78 ºC for 4 h and gradually warmed to RT overnight. Crude reaction was added portionwise to a biphasic mixture of saturated aqueous $NaHCO_3$ solution (40 mL) and DCM (30 mL) at 0 ºC. The aqueous layer was separated and extracted with DCM (3 × 30 mL). The organic extracts were washed with aqueous $Na_2S_2O_3$ solution (10% w/v, 2 × 50 mL), brine (80 mL), dried over $MgSO_4$, filtered and concentrated under reduced pressure. Purification over silica gel, eluting with petroleum ether and DCM (95:5), yielded 1,1,6,6-tetrafluorocyclotetradecane **93** (0.05 g, 53%) as a white crystalline solid:

R_f = 0.38 (petroleum ether:DCM, 80:20); **m.p.** = 50 ºC (from $CDCl_3$); **^{1}H NMR** (400 MHz, $CDCl_3$) **δ_H** 1.96-1.76 (8H, m, *CH_2*), 1.53-1.39 (12H, m, *CH_2*), 1.38-1.29 (4H, m, *CH_2*); **^{1}H{^{19}F} NMR** (400 MHz, $CDCl_3$) **δ_H** 1.92-1.86 (4H, m,

CH$_2$), 1.86-1.80 (4H, m, *CH*$_2$), 1.53-1.39 (12H, m, *CH*$_2$), 1.38-1.29 (4H, m, *CH*$_2$); **^{13}C NMR** (125 MHz, $CDCl_3$) **δ_C** 126.5 (t, *J* = 240.2 Hz, *C*-1,6), 34.5 (t, *J* = 25.8 Hz, *CH*$_2$), 33.3 (t, *J* = 25.4 Hz, *CH*$_2$), 26.5 (*CH*$_2$), 24.5 (*CH*$_2$), 23.0 (t, *J* = 5.4 Hz, *CH*$_2$), 20.0 (t, *J* = 5.0 Hz, *CH*$_2$); **^{19}F{^{1}H} NMR** (376 MHz, $CDCl_3$) **δ_F** −91.36 (s, *CF*$_2$-1,6); **HRMS** *m/z* (CI^+) Found: $[M-2HF+H]^+$ 229.1773. $C_{14}H_{23}F_2$ requires $[M-2HF+H]^+$ 229.1768; **LRMS** *m/z* (EI^+) 248.18 $[M-HF]^{+\cdot}$, 228.1 $[M-2HF]^{+\cdot}$.

5.3.10 2,2'-Propylenebis(1,3-dithiane) (110)

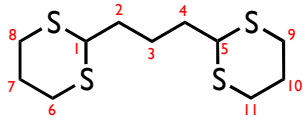

n-BuLi (49.4 mL, 2.35 M, 116.1 mmol, 1.1 eq) was added portionwise to a solution of 1,3-dithiane **62** (12.7 g, 105.6 mmol, 1 eq) in THF (250 mL) at −30 ºC and stirred for 2.5 h. 1,3-Dibromopropane (4.93 mL, 48.6 mmol, 0.46 eq) was added dropwise and the mixture stirred for 2 h at −30 ºC. Temperature was increased to −5 ºC and stirring was continued for 48 h. Reaction was quenched with saturated aqueous NH_4Cl solution (200 mL) and extracted with Et_2O (4 × 150 mL). The organic extracts were washed with brine (150 mL), dried over $MgSO_4$, filtered and concentrated. The product was recrystallised from boiling MeOH, affording 2,2'-propylenebis(1,3-dithiane) **110** (8.37 g, 62%) as a white crystalline solid:

R_f = 0.19 (petroleum ether:Et_2O, 88:12); **m.p.** = 100-101 ºC (from MeOH) (lit.[5] 101.5-102 ºC); **^{1}H NMR** (500 MHz, $CDCl_3$) **δ_H** 4.06-4.01 (2H, m, *CH-1,5*), 2.91-2.79 (8H, m, *CH_2-6,8,9,11*), 2.15-2.08 (2H, m, *CH_a-7,10*), 1.91-1.81 (2H, m, *CH_b-7,10*), 1.81-1.70 (6H, m, *CH_2-2,3,4*); **^{13}C NMR** (125 MHz, $CDCl_3$) **δ_C** 47.3 (*C-1,5*), 34.9 (*C-2,4*), 30.6 (*C-6,8,9,11*), 26.2 (*C-3*), 23.9 (*C-7,10*); **HRMS** *m/z* (ES^+) Found: $[M+H]^+$ 281.0518. $C_{11}H_{21}S_4$ requires $[M+H]^+$ 281.0521.

5.3.11 1-(2-(hex-5-enyl)-1,3-dithian-2-yl)-3-(1,3-dithian-2-yl)propane (111)

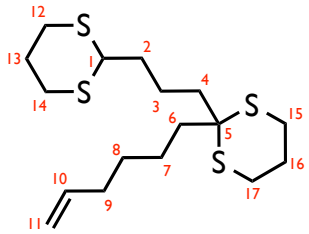

n-BuLi (4.81 mL, 2.23 M, 10.7 mmol, 1 eq) was added to a solution of 2,2'-propylenebis(1,3-dithiane) **110** (3.01 g, 10.7 mmol, 1 eq) in THF (150 mL) at −35 ºC and gradually warmed to −15 ºC over 2 h. 6-Bromohex-1-ene (1.43 mL, 10.7 mmol, 1 eq) was added dropwise at −30 ºC and the mixture stirred for 4 h. The reaction was quenched with saturated aqueous NH_4Cl solution (150 mL), extracted with Et_2O (4 × 150 mL). The organic extracts were washed with brine (150 mL), dried over $MgSO_4$, filtered and concentrated. Purification over silica gel, eluting with petroleum ether and Et_2O (97:3), yielded 1-(2-(hex-5-enyl)-1,3-dithian-2-yl)-3-(1,3-dithian-2-yl)propane **111** (3.19 g, 82%) as a colourless viscous oil:

R_f = 0.25 (petroleum ether:Et_2O, 88:12); **^{1}H NMR** (500 MHz, $CDCl_3$) **δ_H** 5.81 (1H, ddt, *J* = 17.1, 10.2, 6.7 Hz, *CH-10*), 5.01 (1H, ddt, *J* = 17.1, 2.1, 1.6 Hz, *CH_{trans}-11*), 4.95 (1H, ddt, *J* = 10.2, 2.1, 1.2 Hz, *CH_{cis}-11*), 4.06 (1H, t, *J* = 7.0 Hz, *CH-1*), 2.92-2.74 (8H, m, *CH_2-12,14,15,17*), 2.16-2.04 (3H, m, *CH_2-9, CH_a-13*), 2.01-1.91 (2H, m, *CH_2-16*), 1.91-1.81 (5H, m, *CH_2-4,6, CH_b-13*), 1.81-1.74 (2H, m, *CH_2-2*), 1.69-1.61 (2H, m, *CH_2-3*), 1.49-1.36 (4H, m, *CH_2-7,8*); **^{13}C NMR** (125 MHz, $CDCl_3$) **δ_C** 138.9 (*C-10*), 114.7 (*C-11*), 53.2 (*C-5*), 47.4 (*C-1*), 38.3 (*C-6*), 37.6 (*C-4*), 35.6 (*C-2*), 33.7 (*C-9*), 30.6 (*C-12,14*), 29.2 (*C-8*), 26.19 (*C-15,17*), 26.17 (*C-13*), 25.6 (*C-16*), 23.6 (*C-7*), 21.6 (*C-3*); **HRMS** *m/z* (ES^+) Found: $[M+H]^+$ 363.1299. $C_{17}H_{31}S_4$ requires $[M+H]^+$ 363.1303.

5.3.12 1-(2-(Hept-6-enyl)-1,3-dithian-2-yl)-3-(2-(hex-5-enyl)-1,3-dithian-2-yl)propane (112)

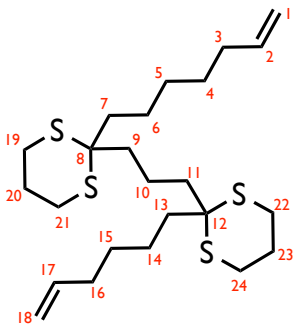

n-BuLi (4.0 mL, 2.23 M, 8.92 mmol, 1.2 eq) was added to a solution of 1-(2-(hex-5-enyl)-1,3-dithian-2-yl)-3-(1,3-dithian-2-yl)propane **111** (2.69 g, 7.42 mmol, 1 eq) in THF (70 mL) at −10 ºC. The mixture was gradually warmed to 0 ºC and stirred for 45 min. 7-Bromohept-1-ene (1.36 mL,

8.92 mmol, 1.2 eq) was added dropwise at −10 ºC. The reaction mixture was stirred for 90 min, warmed to 0 ºC, quenched with saturated aqueous NH_4Cl solution (50 mL) and extracted with Et_2O (4 × 50 mL). The organic extracts were washed with brine (50 mL), dried over $MgSO_4$, filtered and concentrated. Purification over silica gel, eluting with petroleum ether and Et_2O (94:6), yielded 1-(2-(hept-6-enyl)-1,3-dithian-2-yl)-3-(2-(hex-5-enyl)-1,3-dithian-2-yl)propane **112** (2.66 g, 78%) as a colourless viscous oil:

R_f = 0.27 (petroleum ether:Et_2O, 88:12); **^{1}H NMR** (500 MHz, $CDCl_3$) **δ_H** 5.85-5.75 (2H, m, *CH-2,17*), 5.04-4.91 (4H, m, *CH_2-1,18*), 2.85-2.75 (8H, m, *CH_2 19,21,22,24*), 2.11-2.02 (4H, m, *CH_2-3,16*), 1.99-1.91 (4H, m, *CH_2-20,23*), 1.91-1.83 (8H, m, *CH_2-7,9,11,13*), 1.61-1.51 (2H, m, *CH_2-10*), 1.49-1.37 (8H, m, *CH_2*), 1.37-1.28 (2H, m, *CH_2-11*); **^{13}C NMR** (125 MHz, $CDCl_3$) **δ_C** 139.1 (*C-2 or 17*), 138.8 (*C-2 or 17*), 114.7 (*C-1 or 18*), 114.5 (*C-1 or 18*), 53.3 (*C-8,12*), 38.4 (*CH_2*), 38.3 (*CH_2*), 38.2 (*CH_2*), 33.8 (*C-3 or 16*), 33.7 (*C-3 or 16*), 29.4 (*CH_2*), 29.2 (*CH_2*), 28.9 (*CH_2*), 26.2 (*C-19,21,22,24*), 25.6 (*C-20,23*), 24.0 (*CH_2*), 23.7, (*CH_2*), 19.2 (*C-10*); **HRMS** *m/z* (ES^+) Found: $[M+Na]^+$ 481.2054. $C_{24}H_{42}S_4Na$ requires $[M+Na]^+$ 481.2062.

5.3.13 1,5,11,15-Tetrathiadispiro[5.3.5.11]hexacos-21-ene (113)

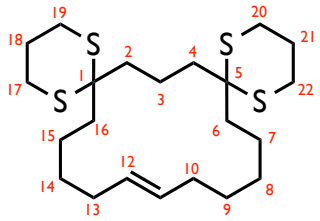

M_{20} (37 mg, 0.04 mmol, 1 mol%) was added in one portion to a 0.02 M solution of 1-(2-(hept-6-enyl)-1,3-dithian-2-yl)-3-(2-(hex-5-enyl)-1,3-dithian-2-yl)propane **112** (1.80 g, 3.92 mmol) in DCE (196 mL) and stirred for 16 h at RT. A further aliquot of **M_{20}** was added (37 mg, 0.04 mmol, 1 mol%) and stirring was continued for 8 h. The crude reaction was concentrated under reduced pressure affording a brown waxy solid. Purification over silica gel, eluting with petroleum ether and Et_2O (97:3, 96:4), yielded 1,5,11,15-tetrathiadispiro[5.3.5.11]hexacos-21-ene **113** (1.17 g, 69%) as a colourless viscous oil:

R_f = 0.49 (DCM); **^{1}H NMR** (500 MHz, $CDCl_3$) **δ_H** 5.48-5.40 (1H, m, *CH-11 or 12*), 5.33-5.25 (1H, m, *CH-11 or 12*), 2.83-2.77 (8H, m, *CH_2-17,19,20,22*), 2.08-2.00 (4H, m, *CH_2-10,12*), 2.00-1.94 (4H, m, *CH_2-18,21*), 1.94-1.82 (8H, m, *CH_2*), 1.49-1.41 (4H, m, *CH_2*), 1.40-1.34 (4H, m, *CH_2*), 1.31-1.24 (4H, m, *CH_2*); **^{13}C NMR** (125 MHz, $CDCl_3$) **δ_C** 130.7 (*C-11 or 12*), 130.4 (*C-11 or 12*), 52.6 (*C-1 or 5*), 52.4 (*C-1 or 5*), 38.0 (*CH_2*), 37.6 (*CH_2*), 37.4 (*CH_2*), 37.1 (*CH_2*), 31.6 (*C-10 or 13*) 30.42 (*C-10 or 13*), 30.37 (*CH_2*), 27.5 (*CH_2*), 27.3 (*CH_2*), 26.1 (*CH_2-17,19,20,22*), 26.0 (*C-18,21*), 22.8 (*CH_2*), 22.0 (*CH_2*), 18.5 (*CH_2*); **HRMS** m/z (ES^+) Found: $[M+H]^+$ 431.1923. $C_{22}H_{39}S_4$ requires $[M+H]^+$ 431.1929.

5.3.14 1,5,11,15-Tetrathiadispiro[5.3.5.11]hexacosane (114)

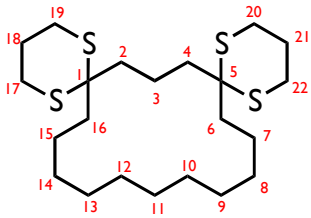

1,5,11,15-Tetrathiadispiro[5.3.5.11]hexacos-21-ene **113** (1.0 g, 2.4 mmol) and the catalyst **99** (146 mg, 18.5 μmmol, 7.6 mol%) were dissolved in DMF (10 mL) in a glass vial, and placed in the autoclave. The system was pressurised with hydrogen at 10 bar. The reactor was heated at 80 °C for 48 h. The product was then extracted with a mixture of Et_2O and DCM. Purification over silica gel, eluting with DCM afforded 1,5,11,15-tetrathiadispiro[5.3.5.11]hexacosane **114** (0.59 g, 56% yield) as a white crystalline solid:

R_f = 0.23 (petroleum ether:Et_2O, 88:12); **m.p.** = 126-128 ºC (from DCM); **^{1}H NMR** (500 MHz, $CDCl_3$) **δ_H** 2.83-2.77 (8H, m, *CH_2-17,19,20,22*), 2.00-1.94 (4H, m, *CH_2-18,21*), 1.94-1.84 (8H, m, *CH_2-2,4,6,16*), 1.51-1.44 (2H, m, *CH_2-3*), 1.44-1.38 (4H, m, *CH_2-8,14*), 1.38-1.24 (12H, m, *CH_2-7,9,10,12,13,15*), 1.21-1.13 (2H, m, *CH_2-11*); **^{13}C NMR** (125 MHz, $CDCl_3$) **δ_C** 52.4 (*C-1,5*), 37.8 (*C-6,16*), 37.5 (*C-2,4*), 27.0 (*C-8,14*), 26.6 (*CH_2*), 26.4 (*CH_2*), 26.1 (*C-17,19,20,22*), 26.0 (*C-18,21*), 24.3 (*C-11*), 22.0 (*CH_2*), 18.5 (*C-3*); **HRMS** m/z (ES^+) Found: $[M+H]^+$ 433.2087. $C_{22}H_{41}S_4$ requires $[M+H]^+$ 433.2086;

5.3.15 1,1,5,5-Tetrafluorocyclohexadecane (92)

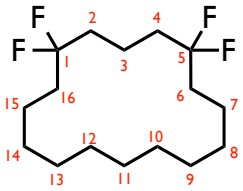

Hydrogen fluoride-pyridine (2.28 mL, 87.8 mmol, 119 eq) was added to a solution of *N*-iodosuccinimide **40** (1.33 g, 5.96 mmol, 8 eq) in DCM (12 mL) at −78 ºC. The resulting mixture was stirred for 5 min at −78 ºC. A solution of 1,5,11,15-tetrathiadispiro[5.3.5.11]hexacosane **114** (0.32 g, 0.74 mmol, 1 eq) in DCM (5 mL) was added dropwise to the mixture over 10 min. The reaction mixture was stirred at −78 ºC for 4 h and gradually warmed to RT overnight. The crude reaction was added portionwise to a biphasic mixture of saturated aqueous $NaHCO_3$ solution (80 mL) and DCM (40 mL) at 0 ºC. The aqueous layer was separated and extracted with DCM (3 × 50 mL). The organic extracts were washed with aqueous $Na_2S_2O_3$ solution (10% w/v, 2 × 80 mL), brine (100 mL), dried over $MgSO_4$, filtered and concentrated under reduced pressure. Purification over silica gel, eluting with petroleum ether and DCM (95:5), yielded 1,1,5,5-tetrafluorocyclohexadecane **92** (0.09 g, 43%) as a white crystalline solid:

R_f = 0.83 (DCM); **m.p.** = 62.5 ºC (from $CDCl_3$); **^{1}H NMR** (500 MHz, $CDCl_3$) **δ_H** 1.97-1.77 (8H, m, *CH_2-2,4,6,16*), 1.53-1.44 (2H, m, *CH_2-3*), 1.43-1.29 (16H, m, *CH_2*), 1.28-1.21 (2H, m, *CH_2-11*) ; **^{1}H{^{19}F} NMR** (400 MHz, $CDCl_3$) **δ_H** 1.93-1.88 (4H, m, *CH_2-2,4*), 1.86-1.81 (4H, m, *CH_2-6,16*), 1.53-1.44 (2H, m,

CH$_2$*-3*), 1.43-1.29 (16H, m, *CH*$_2$), 1.28-1.21 (2H, m, *CH*$_2$*-11*); **^{13}C NMR** (125 MHz, $CDCl_3$) **δ_C** 125.8 (t, *J* = 240.1 Hz, *C-1,5*), 34.8 (t, *J* = 26.4 Hz, *C-2,4*), 34.7 (t, *J* = 25.4 Hz, *C-6,16*), 26.7 (*CH*$_2$), 26.6 (*CH*$_2$), 26.4 (*CH*$_2$), 25.4 (*C-11*), 21.4 (t, *J* = 5.3 Hz, *C-7,15*), 17.9 (q, *J* = 5.9 Hz, *C-3*); **^{19}F{^{1}H} NMR** (470 MHz, $CDCl_3$) **δ_F** −91.92 (s, *CF*$_2$-1, 5); **HRMS** *m/z* (CI^+) Found: $[M-2HF+H]^+$ 257.2088. $C_{16}H_{27}F_2$ requires $[M-2HF+H]^+$ 257.2081; **LRMS** *m/z* (EI^+) 276.21 $[M-HF]^{+\cdot}$, 256.19 $[M-2HF]^{+\cdot}$.

5.3.16 2,2'-Butylenebis(2-(hex-5-enyl)-1,3-dithiane) (115)

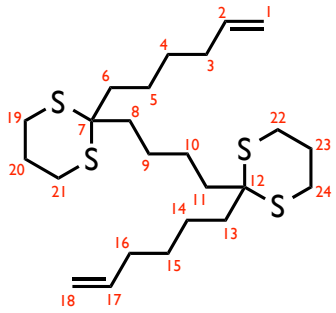

n-BuLi (15.4 mL, 2.42 M, 37.2 mmol, 3 eq) was added to a solution of 2,2'-butylenebis(1,3-dithiane) **106** (3.65 g, 12.4 mmol, 1 eq) in THF (140 mL) at −30 ºC. The mixture was stirred for 30 min, and gradually warmed to −10 ºC over 60 min. 6-Bromohex-1-ene (4.97 mL, 37.2 mmol, 3 eq) was added portionwise at −30 ºC and the mixture stirred overnight at −30 ºC. A mixture of mono- and di- alkylated products was observed (TLC/^{1}H NMR). A further aliquot of *n*-BuLi (5.12 mL, 2.42 M, 12.4 mmol, 1 eq) was added at −20 ºC and stirred for 90 min at that temperature. 6-Bromohex-1-ene

(1.66 mL, 12.4 mmol, 1 eq) was added dropwise −20 ºC and stirred for 2 h. The deprotonation/alkylation sequence was repeated again at −15 ºC using *n*-BuLi (5.12 mL, 2.42 M, 12.4 mmol, 1 eq) and 6-bromohex-1-ene (0.83 mL, 6.20 mmol, 0.5 eq). The reaction mixture was stirred for 2 h, warmed to 0 ºC, quenched with saturated aqueous NH_4Cl solution (100 mL) and extracted with Et_2O (4 × 100 mL). The organic extracts were washed with brine (150 mL), dried over $MgSO_4$, filtered and concentrated. Purification over silica gel, eluting with petroleum ether and DCM (80:20, 60:40), yielded 2,2'-Butylenebis(2-(hex-5-enyl)-1,3-dithiane) **115** (3.51 g, 62%) as a colourless viscous oil:

R_f = 0.36 (petroleum ether:Et_2O, 88:12); **^{1}H NMR** (300 MHz, $CDCl_3$) **δ_H** 5.81 (2H, ddt, *J* = 17.1, 10.2, 6.7 Hz, *CH-2,17*), 5.01 (2H, ddt, *J* = 17.1, 2.1, 1.6 Hz, *CH_{trans}-1,18*), 4.95 (2H, ddt, *J* = 10.2, 2.1, 1.2 Hz, *CH_{cis}-1,18*), 2.84-2.76 (8H, m, *CH_2-19,21,22,24*), 2.14-2.02 (4H, m, *CH_2-3,16*), 2.00-1.91 (4H, m, *CH_2-20,23*), 1.91-1.79 (8H, m, *CH_2-6,8,11,13*), 1.51-1.33 (12H, m, *CH_2-4,5,9,10,14,15*); **^{13}C NMR** (100 MHz, $CDCl_3$) **δ_C** 138.8 (*C-2,17*), 114.7 (*C-1,18*), 53.4 (*C-7,12*), 38.27 (*C-6,13 or 8,11*), 38.25 (*C-6,13 or 8,11*), 33.7 (*C-3,16*), 29.2 (*C-4,15*), 26.2 (*C-19,21,22,24*), 25.6 (*C-20,23*), 24.5 (*C-9,10*), 23.5 (*C-5,14*); **HRMS** *m/z* (CI^+) Found: $[M+H]^+$ 459.2234. $C_{24}H_{43}S_4$ requires $[M+H]^+$ 459.2242.

5.3.17 1,5,12,16-Tetrathiadispiro[5.4.5.10]hexacos-21-ene (116)

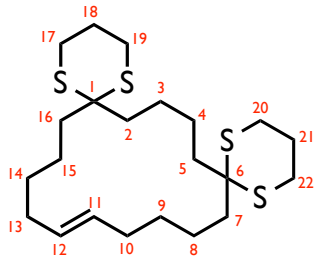

M_{20} (17 mg, 18 µmol, 1 mol%) was added in one portion to a solution of 2,2'-Butylenebis(2-(hex-5-enyl)-1,3-dithiane) **115** (0.85 g, 1.85 mmol) in DCE (92 mL, 0.02 M) and stirred for 20 h at RT. A further aliquot of **M_{20}** was added (17 mg, 18 µmol, 1 mol%) and stirring continued for 8 h. The crude reaction was concentrated under reduced pressure affording a brown waxy solid. Purification over silica gel, eluting with petroleum ether and Et_2O (97:3), yielded 1,5,12,16-tetrathiadispiro[5.4.5.10]hexacos-21-ene **116** (0.54 g, 68%) as a white crystalline solid:

R_f = 0.27 (petroleum ether:Et_2O, 88:12); **m.p.** = 154-156 ºC (from EtOAc); **^{1}H NMR** (500 MHz, $CDCl_3$) **δ_H** 5.35-5.25 (2H, m, *CH-11,12*), 2.86-2.74 (8H, m, *CH_2-17,19,20,22*), 2.10-2.00 (4H, m, *CH_2-10,13*), 2.00-1.93 (4H, m, *CH_2-18,21*), 1.93-1.82 (8H, m, *CH_2-2,5,7,16*), 1.41-1.29 (12H, m, *CH_2-3,4,8,9,14,15*); **^{13}C NMR** (125 MHz, $CDCl_3$) **δ_C** 131.1 (*C-11,12*), 52.5 (*C-1,6*), 38.2 (*C-2,5 or 7,16*), 37.4 (*C-2,5 or 7,16*), 32.1 (*C-10,13*), 28.8 (*C-9,14*), 26.2 (*C-17,19,20,22)*, 25.9 (*C-18,21*), 24.4 (*C-3,4)*, 22.3 (*C-8,15*); **HRMS** *m/z* (ES^+) Found: $[M+H]^+$ 431.1919. $C_{22}H_{39}S_4$ requires $[M+H]^+$ 431.1929.

5.3.18 1,5,12,16-Tetrathiadispiro[5.4.5.10]hexacosane (117)

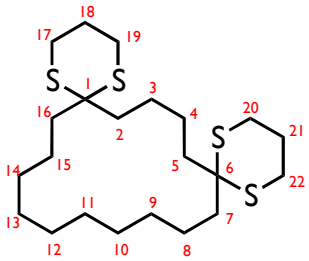

1,5,12,16-Tetrathiadispiro[5.4.5.10]hexacos-21-ene **116** (270 mg, 0.63 mmol) and the catalyst **99** (37 mg, 4.8 µmol, 7.6 mol%) were dissolved in DMF (4 mL).The vial was introduced inside an autoclave, and the system was pressurised with hydrogen at 10 bar. The reactor was heated at 80 °C for 48 h. The product was then extracted with a mixture of Et_2O and DCM. Purification over silica gel, eluting with DCM afforded 1,5,12,16-tetrathiadispiro[5.4.5.10]hexacosane **117** (208 mg, 77% yield) as a white crystalline solid:

R_f = 0.17 (DCM); **m.p.** = 136-137 ºC (from $CHCl_3$); **^{1}H NMR** (500 MHz, $CDCl_3$) **δ_H** 2.85-2.74 (8H, m, *CH_2-17,19,20,22*), 2.00-1.92 (8H, m, *CH_2-18,21 and 2,5 or 7,16*), 1.91-1.84 (4H, m, *CH_2-2,5 or 7,16*), 1.43-1.31 (16H, m, 4 × *CH_2*), 1.34-1.28 (4H, m, *CH_2-11,12*); **^{13}C NMR** (125 MHz, $CDCl_3$) **δ_C** 52.5 (*C-1,6*), 37.3 (*C-2,5 or 7,16*), 37.1 (*C-2,5 or 7,16*), 27.8 (*C-10,13*), 27.1 (*CH_2*), 26.2 (*C-17,19,20,22)*, 26.1 (*CH_2*), 25.9 (*C-18,21)*, 24.7 (*CH_2*), 21.4 (*CH_2*); **HRMS** *m/z* (ES^+) Found: $[M+H]^+$ 433.2081. $C_{22}H_{41}S_4$ requires $[M+H]^+$ 433.2086.

5.3.19 1,1,6,6-Tetrafluorocyclohexadecane (94)

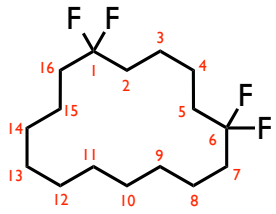

Hydrogen fluoride-pyridine (1.50 mL, 57.8 mmol, 119 eq) was added to a solution of *N*-iodosuccinimide **40** (0.87 g, 3.87 mmol, 8 eq) in DCM (8 mL) at −78 ºC. The resulting mixture was stirred for 5 min at −78 ºC. A solution of 1,5,12,16-tetrathiadispiro[5.4.5.10]hexacosane **117** (0.21 g, 0.49 mmol, 1 eq) in DCM (3 mL) was added dropwise to the mixture over 10 min. The reaction mixture was stirred at −78 ºC for 4 h and gradually warmed to RT overnight. Crude reaction was added portionwise to a biphasic mixture of saturated aqueous $NaHCO_3$ solution (50 mL) and DCM (25 mL) at 0 ºC. The aqueous layer was separated and extracted with DCM (3 × 30 mL). The organic extracts were washed with aqueous $Na_2S_2O_3$ solution (10% w/v, 2 × 50 mL), brine (80 mL), dried over $MgSO_4$, filtered and concentrated under reduced pressure. Purification over silica gel, eluting with petroleum ether, yielded 1,1,6,6-tetrafluorocyclohexadecane (0.09 g, 65%) **94** as a white crystalline solid:

R_f = 0.82 (DCM); **m.p**. = 39.5 ºC (from $CDCl_3$); **^{1}H NMR** (500 MHz, $CDCl_3$) **δ_H** 1.95-1.77 (8H, m, *CH_2-2,5,7,16*), 1.52-1.45 (4H, m, *CH_2-3,4*), 1.45-1.34 (12H, m, *CH_2*), 1.33-1.25 (4H, m, *CH_2*); **^{1}H{^{19}F} NMR** (500 MHz, $CDCl_3$) **δ_H** 1.92-1.86 (4H, m, *CH_2-2,5*), 1.86-1.80 (4H, m, *CH_2-7,16*), 1.52-1.45 (4H, m,

CH_2-3,4), 1.45-1.34 (12H, m, *CH_2*), 1.33-1.25 (4H, m, *CH_2*); **^{13}C NMR** (125 MHz, $CDCl_3$) **δ_C** 126.2 (t, *J* = 240.2 Hz, *C-1,6*), 34.9 (t, *J* = 25.8 Hz, *C-2,5*), 34.3 (t, *J* = 25.3 Hz, *C-7,16*), 27.0 (*CH_2*), 26.8 (*CH_2*), 26.2 (*CH_2*), 23.2 (t, *J* = 5.4 Hz, *C-3,4*), 21.0 (t, *J* = 5.0 Hz, *C-8,15*); **^{19}F{^{1}H} NMR** (470 MHz, $CDCl_3$) **δ_F** −92.18 (s, *CF_2-1,6*); **HRMS** m/z (CI^+) Found: $[M-2HF+H]^+$ 257.2084. $C_{16}H_{27}F_2$ requires $[M-2HF+H]^+$ 257.2081; **LRMS** m/z (EI^+) 276.21 $[M-HF]^{+\cdot}$, 256.20 $[M-2HF]^{+\cdot}$.

5.4 Protocols for Chapter 4

5.4.1 Nona-1,8-dien-5-ol (131)

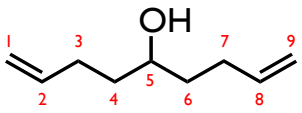

A solution of 4-bromobut-1-ene **129** (31.6 mL, 302 mmol, 2.45 eq) in THF (180 mL) was added dropwise to a flask containing flamedried magnesium (7.31 g, 301 mmol, 2.44 equiv.) over 90 min. The resulting mixture was stirred at room temperature for 2 h. A solution of ethyl formate (10.2 mL, 123 mmol, 1 eq) in THF (40 mL) was then added dropwise at 0 ºC. The biphasic mixture was left to stir overnight at RT and quenched with saturated aqueous NH_4Cl solution (150 mL). It was extracted with Et_2O (4 × 150 mL), washed with brine (200 mL), dried over $MgSO_4$ and concentrated under reduced pressure. Purification by distillation under reduced pressure yielded nona-1,8-dien-5-ol **131** (16.3 g, 94%) as a colourless oil:

R_f = 0.21 (DCM); **^{1}H NMR** (400 MHz, $CDCl_3$) **δ_H** 5.83 (2H, ddt, *J* = 17.1, 10.2, 6.7 Hz, *CH-2,8*), 5.04 (2H, ddt, *J* = 17.1, 2.0, 1.6 Hz, *CH_{trans}-1,9*), 4.96 (2H, ddt, *J* = 10.2, 2.0, 1.2 Hz, *CH_{cis}-1,9*), 3.64 (1H, tt, *J* = 7.7, 4.6 Hz *CH-5*), 2.27-2.06 (4H, m, *CH_2-3,7*), 1.63-1.46 (4H, m, *CH_2-4,6*), 1.42 (1H, bs, *OH*); **^{13}C NMR** (100 MHz, $CDCl_3$) **δ_C** 138.7 (*C-2,8*), 115.0 (*C-1,9*), 71.2 (*C-5*), 36.6 (*C-3,7*), 30.2 (*C-4,6*); **LRMS** *m/z* (ES^+) 163.011 $[M+Na]^+$.

5.4.2 5-Fluorononona-1,8-diene (124)

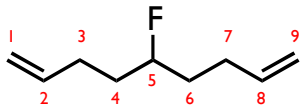

DAST **22** (3.59 mL, 36.8 mmol, 2 eq) was added dropwise to a solution of nona-1,8-dien-5-ol **131** (2.58 g, 18.4 mmol, 1 eq) in DCM (40 mL) at −78 ºC. The resulting mixture was stirred for 5 h and gradually warmed to RT. Stirring was continued for 2 h. The reaction mixture was quenched with saturated aqueous $NaHCO_3$ solution (80 mL) and extracted with DCM (3 × 40 mL). The combined organic extracts were dried over $MgSO_4$ and concentrated by Vigreux distillation. The concentrate was purified over silica gel, eluting with pentane. Bulk solvent was removed by Vigreux distillation (atmospheric pressure, 55 ºC). Traces of solvent were removed by Vigreux distillation at reduced pressure (conditions: 500 mbar, 40-50 ºC) yielding 5-fluorononona-1,8-diene **124** (0.95 g, 36%) as a colourless oil:

R_f = 0.25 (pentane); **^{1}H NMR** (400 MHz, CD_2Cl_2) **δ_H** 5.83 (2H, ddt, *J* = 17.1, 10.2, 6.7 Hz, *CH-2,8*), 5.04 (2H, ddt, *J* = 17.1, 2.0, 1.6 Hz, *CH_{trans}-1,9*), 4.97 (2H, ddt, *J* = 10.2, 2.0, 1.3 Hz, *CH_{cis}-1,9*), 4.49 (1H, dtt, *J* = 49.4, 8.2, 4.1 Hz, *CH-5*), 2.27-2.06 (4H, m, *CH_2-3,7*), and 1.79-1.53 (4H, m, *CH_2-4,6*); **^{1}H{^{19}F} NMR** (400 MHz, CD_2Cl_2) **δ_H** 5.83 (2H, ddt, *J* = 17.1, 10.2, 6.7 Hz, *CH-2,8*), 5.04 (2H, ddt, *J* = 17.1, 2.0, 1.6 Hz, *CH_{trans}-1,9*), 4.97 (2H, ddt, *J* = 10.2, 2.0, 1.3 Hz, *CH_{cis}-1,9*), 4.49 (1H, tt, *J* = 8.2, 4.1 Hz, *CH-5*), 2.27-2.06 (4H, m, *CH_2-3,7*), and 1.77-1.57 (4H, m, *CH_2-4,6*); **^{13}C NMR** (100 MHz, CD_2Cl_2) **δ_C** 138.3 (*C-2,8*), 115.1 (*C-1,9*), 93.5 (d, *J* = 167.3 Hz, *C-5*), 34.7 (d, *J* = 21.1 Hz, *C-4,6*), and 29.7 (d, *J* = 4.5 Hz, *C-3,7*); **^{19}F{^{1}H} NMR** (376 MHz, CD_2Cl_2) **δ_F** −182.97; **^{19}F NMR** (376 MHz, CD_2Cl_2) **δ_F** −182.97 (dtt, *J* = 49.4, 30.8, 16.9 Hz, *CF-5*). **HRMS** *m/z* (EI^+) Found: $[M]^{+\cdot}$ 142.1151. $C_9H_{15}F$ requires $[M]^{+\cdot}$ 142.1152; **LRMS** *m/z* (EI^+) 142.1 $[M]^{+\cdot}$.

5.4.3 Nona-1,8-dien-5-one (132)

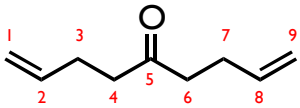

Concentrated sulfuric acid (16.3 mL) was added dropwise to a solution of chromium trioxide (19.4 g, 193.5, 2.5 eq) in distilled water (56.4 mL). The resulting Jones reagent was added dropwise to a solution of nona-1,8-dien-5-ol **131** (10.8 g, 76.6 mmol, 1 eq) in acetone (200 mL) at 0 ºC. Reaction mixture was left to stir overnight at RT and was quenched with isopropanol (10 mL). Acetone was removed under reduced pressure and the residue

extracted with Et_2O (4 × 150 mL). The combined organic extracts were washed with water (150 mL), saturated aqueous $NaHCO_3$ solution (150 mL), brine (150 mL), dried over $MgSO_4$ and concentrated. Purification by distillation under reduced pressure yielded nona-1,8-dien-5-one **132** (9.64 g, 91%) as a colourless oil:

R_f = 0.61 (DCM); **^{1}H NMR** (300 MHz, $CDCl_3$) **δ_H** 5.76 (2H, ddt, *J* = 17.0, 10.3, 6.6 Hz, *CH-2,8*), 4.98 (2H, ddt, *J* = 17.0, 1.8, 1.6 Hz, *CH_{trans}-1,9*), 4.93 (2H, ddt, *J* = 10.3, 1.8, 1.3 Hz *CH_{cis}-1,9*), 2.51-2.43 (4H, m, *CH_2-4,6*), 2.34-2.23 (4H, m, *CH_2-3,7*); **^{13}C NMR** (125 MHz, $CDCl_3$) **δ_C** 209.5 (*C-5*), 137.2 (*C-2,8*), 115.4 (*C-1,9*), 42.0 (*C-4,6*), 27.8 (*C-3,7*). **LRMS** *m/z* (ES^+) 161.09 $[M+Na]^+$.

5.4.4 5,5-Difluorononona-1,8-diene (125)

A mixture of nona-1,8-dien-5-one **132** (3.86 g, 27.9 mmol, 1 eq) and neat DAST **22** (10.9 mL, 111.7 mmol, 4 eq) was stirred for 6 days at 45 ºC. Crude reaction was added portionwise to a biphasic mixture of saturated aqueous $NaHCO_3$ solution (300 mL) and pentane (150 mL) at 0 ºC. The aqueous layer was separated and extracted with pentane (3 × 100 mL). The combined organic extracts were dried over $MgSO_4$ and concentrated by Vigreux distillation. The concentrate was purified over silica gel, eluting with pentane. Bulk solvent was removed by Vigreux distillation (conditions: atmospheric

pressure, 55 ºC). Traces of solvent were removed by Vigreux distillation at reduced pressure (conditions: 700 mbar, 45-60 ºC) yielding 5,5-difluorononona-1,8-diene **125** (2.47 g, 55%) as a colourless oil:

R_f = 0.44 (pentane); **^{1}H NMR** (300 MHz, $CDCl_3$) **δ_H** 5.83 (2H, ddt, *J* = 17.1, 10.2, 6.6 Hz, *CH-2,8*), 5.07 (2H, ddt, *J* = 17.1, 1.7, 1.7 Hz, *CH_{trans}-1,9*), 5.01 (2H, ddt, *J* = 10.2, 1.7, 1.3 Hz *CH_{cis}-1,9*), 2.30-2.19 (4H, m, *CH_2-3,7*), and 2.03-1.83 (4H, m, *CH_2-4,6*); **^{1}H{^{19}F} NMR** (300 MHz, $CDCl_3$) **δ_H** 5.83 (2H, ddt, *J* = 17.1, 10.2, 6.6 Hz, *CH-2,8*), 5.07 (2H, ddt, *J* = 17.1, 1.7, 1.6 Hz, *CH_{trans}-1,9*), 5.01 (2H, ddt, *J* = 10.2, 1.7, 1.3 Hz, *CH_{cis}-1,9*), 2.30-2.19 (4H, m, *CH_2-3,7*), and 1.97-1.88 (4H, m, *CH_2-4,6*); **^{13}C NMR** (75 MHz, $CDCl_3$) **δ_C** 137.1 (*C-2,8*), 124.7 (t, *J* = 241.0 Hz, *C-5*), 115.4 (*C-1,9*), 35.9 (t, *J* = 25.4 Hz, *C-4,6*), 26.6 (t, *J* =5.2 Hz, *C-3,7*); **^{19}F{^{1}H} NMR** (282 MHz, $CDCl_3$) **δ_F** −99.06; **^{19}F NMR** (282 MHz, $CDCl_3$) **δ_F** −99.06 (quintet, *J* = 16.51 Hz, *CF_2-5*). **HRMS** *m/z* (EI^+) Found: $[M]^{+\cdot}$ 160.1056. $C_9H_{14}F_2$ requires $[M]^{+\cdot}$ 160.1058; **LRMS** *m/z* (EI^+) 160.0 $[M]^{+\cdot}$.

5.4.5 2,2-Bis(but-3-en-1-yl)-1,3-dioxolane (127)

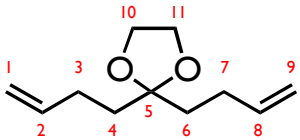

p-Toluenesulfonic acid monohydrate (0.04 g, 0.2 mmol) was added to a mixture of nona-1,8-dien-5-one **132** (3.05 g, 22.1 mmol, 1 eq) and ethane-1,2-diol (1.60 mL, 28.7 mmol, 1.3 eq) in toluene (60 mL). The resulting mixture

was refluxed for 2.5 h, until 0.4 mL of water had been collected in a Dean-Stark trap. The remaining solution was washed with aqueous NaOH solution (10% w/v, 15 mL), water (5 × 10 mL), and brine (20 mL). The organic extracts were dried over $MgSO_4$ and concentrated. Purification by Vigreux distillation under reduced pressure yielded 2,2-bis(but-3-en-1-yl)-1,3-dioxolane **127** (2.17 g, 54%) as a colourless oil:

R_f = 0.5 (pentane:Et_2O, 92:8); **^{1}H NMR** (500 MHz, $CDCl_3$) **δ_H** 5.83 (2H, ddt, *J* = 17.0, 10.2, 6.5 Hz, *CH-2,8*), 5.02 (2H, ddt, *J* = 17.0, 1.7, 1.6 Hz, *CH_{trans}-1,9*), 4.97-4.91 (2H, m, *CH_{cis}-1,9*), 3.95 (4H, s, *CH_2-10,11*), 2.16-2.10 (4H, m, *CH_2-3,7*), 1.74-1.68 (4H, m, *CH_2-4,6*); **^{13}C NMR** (125 MHz, $CDCl_3$) **δ_C** 138.6 (*C-2,8*), 114.4 (*C-1,9*), 111.3 (*C-5*), 65.2 (*C-10,11*), 36.6 (*C-4,6*), 28.2 (*C-3,7*). **HRMS** *m/z* (ES^+) Found: $[M+H]^+$ 183.1387. $C_{11}H_{19}O_2$ requires $[M+H]^+$ 183.1385; **LRMS** *m/z* (ES^+) 183.12 $[M+H]^+$.

5.4.6 2,2-Bis(but-3-en-1-yl)-1,3-dithiane (128)

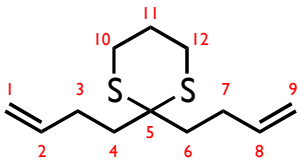

Boron trifluoride diethyl etherate complex (1.0 mL, 7.7 mmol, 0.3 eq) was added to a stirred mixture of nona-1,8-dien-5-one **132** (3.5 g, 25.6 mmol, 1 eq) and 1,3-propanedithiol (3.9 mL, 38.4 mmol, 1.5 eq) in DCM (50 mL). Reaction mixture was stirred for 6 h at RT and then washed with saturated

$NaHCO_3$ solution (40 mL), NaOH solution (15% w/v, 60 mL), water (3 × 100 mL), and brine (40 mL). The organic extracts were dried over $MgSO_4$ and concentrated. Purification over silica gel, eluting with pentane and Et_2O (99:1), yielded 2,2-bis(but-3-en-1-yl)-1,3-dithiane **128** (5.48 g, 24.0 mmol, 94%) as a colourless oil:

R_f = 0.64 (pentane:Et_2O, 92:8); **^{1}H NMR** (300 MHz, $CDCl_3$) **δ_H** 5.82 (2H, ddt, *J* = 17.0, 10.2, 6.6 Hz, *CH-2,8*), 5.05 (2H, ddt, *J* = 17.0, 1.9, 1.6 Hz, *CH_{trans}-1,9*), 4.97 (2H, ddt, *J* = 10.2, 1.9, 1.2 Hz *CH_{cis}-1,9*), 2.84-2.77 (4H, m, *CH_2-10,12*), 2.25-2.14 (4H, m, *CH_2-3,7*), 2.00-1.89 (6H, m, *CH_2-4,6,11*); **^{13}C NMR** (100 MHz, $CDCl_3$) **δ_C** 138.1 (*C-2,8*), 115.2 (*C-1,9*), 53.0 (*C-5*), 37.6 (*C-4,6*), 28.8 (*C-3,7*), 26.2 (*C-10,12*), 25.6 (*C-11*). **HRMS** *m/z* (ES^+) Found: $[M+H]^+$ 229.1086. $C_{12}H_{21}S_2$ requires $[M+H]^+$ 229.1085; **LRMS** *m/z* (ES^+) 229.07 $[M+H]^+$.

5.4.7 Dimethyl 2,2-bis(but-3-en-1-yl)malonate (126)

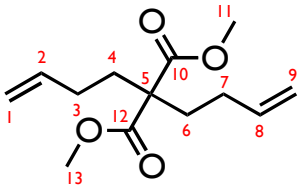

Dimethyl malonate **133** (4 mL, 34.4 mmol) was added dropwise to a suspension of NaH (1.30 g, 51.5 mmol) in DMF (80 mL) at 0 ºC. After 20 min, 4-bromobut-1-ene (4.68 mL, 44.7 mmol) was added dropwise, the mixture was stirred for 2 h at RT. A further aliquot of NaH (1.30 g, 51.5 mmol) and

4-bromobut-1-ene (4.68 mL, 44.7 mmol) were added at 0 ºC and solution stirred for 12 h at RT. A third aliquot of NaH (0.87 g, 34.4 mmol) followed by 4-bromobut-1-ene (3.60 mL, 34.4 mmol) was added at 0 ºC and stirring wascontinued for 4 h. The reaction was quenched with saturated aqueous NH_4Cl solution (50 mL), diluted with DCM (150 mL) and washed with brine (5 × 100 mL). Organic extracts were dried over $MgSO_4$, filtered and concentrated under reduced pressure. Purification over silica gel, eluting with pentane and DCM (30:70), followed by Vigreux distillation at reduced pressure yielded 5,5-bis(dimethylcarboxyl)-nona-1,8-diene **126** (5.33 g, 64%) as a colourless oil:

R_f = 0.41 (DCM); **^{1}H NMR** (500 MHz, $CDCl_3$) **δ_H** 5.76 (2H, ddt, *J* = 17.0, 10.3, 6.4 Hz, *CH-2,8*), 5.02 (2H, ddt, *J* = 17.0, 1.8, 1.4 Hz, *CH_{trans}-1,9*), 4.96 (2H, ddt, *J* = 10.3, 1.8, 1.2 Hz, *CH_{cis}-1,9*), 3.71 (6H, s, *CH_3-11,13*), 2.02-1.90 (8H, m, *CH_2-3,4,6,7*); **^{13}C NMR** (100 MHz, $CDCl_3$) **δ_C** 172.0 (*C-10,12*), 137.5 (*C-2,8*), 115.2 (*C-1,9*), 57.2 (*C-5*), 52.5 (*C-11,13*), 31.9 (CH_2), 28.5 (CH_2). **HRMS** *m/z* (ES^+) Found: $[M+Na]^+$ 263.1254. $C_{13}H_{20}NaO_4$ requires $[M+Na]^+$ 263.1259.

5.4.7 5,5-Dufluorocyclohept-1-ene (134)

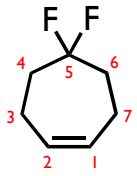

M_{23} (0.10 g, 0.10 mmol) was added to a solution of 5,5-difluorononа-1,8-diene **125** (1.67 g, 10.4 mmol) in pentane (520 mL). The reaction was stirred for 3 h at RT. The bulk solvent was removed by Vigreux distillation. The concentrate was purified over silica gel, eluting with pentane. Bulk solvent was removed by Vigreux distillation (conditions: atmospheric pressure, 45-55 ºC). Traces of pentane were removed by Vigreux distillation at reduced pressure (conditions: 700 mbar, 45-60 ºC) yielding 5,5-difluorocyclohept-1-ene **134** (0.92 g, 67%) as a colourless oil:

R_f = 0.44 (pentane); **^{1}H NMR** (500 MHz, $CDCl_3$) **δ_H** 5.90-5.81 (2H, m, *CH-1,2*), 2.22-2.08 (4H, m, *CH_2-3,7*), 2.04-1.89 (4H, m, *CH_2-4,6*); **^{1}H NMR** (500 MHz, C_7D_8) δ_H 5.60-5.51 (2H, m, *CH-1,2*), 1.85-1.76 (4H, m, *CH_2-3,7*), 1.75-1.65 (4H, m, *CH_2-4,6*); **^{1}H{^{19}F} NMR** (500 MHz, $CDCl_3$) **δ_H** 5.90-5.81 (2H, m, *CH-1,2*), 2.20-2.10 (4H, m, *CH_2-3,7*), 2.01-1.92 (4H, m, *CH_2-4,6*); **^{13}C NMR** (125 MHz, $CDCl_3$) **δ_C** 131.7 (*C*-1,2), 126.1 (t, *J* = 239.4 Hz, *C-5*), 35.6 (t, *J* = 25.4 Hz, *C-4,6*), 21.1 (t, *J* = 6.8 Hz, *C-3,7*); **^{19}F{^{1}H} NMR** (470 MHz, $CDCl_3$) **δ_F** −89.98; **^{19}F{^{1}H} NMR** (470 MHz, C_7D_8) **δ_F** −89.85; **^{19}F NMR** (470 MHz, $CDCl_3$) **δ_F** −89.98 (quintet, *J* = 15.0 Hz, *CF_2-5*). **HRMS** *m/z* (EI^+)

Found: $[M]^{+\cdot}$ 132.0755. $C_7H_{10}F_2$ requires $[M]^{+\cdot}$ 132.0751; **LRMS** *m/z* (EI^+) 132.08 $[M]^{+\cdot}$.

5.4.8 Procedure for the RCM reaction kinetics

Studies on RCM reaction kinetics of the nonadiene substrates **123-128** were conducted by Dr C. A. Urbina-Blanco from Prof. Stephen Nolan's Group.

Inside a glovebox, 800 µL of a stock solution of the substrate in toluene-d_8 (0.25 mmol/800 µL; 0.3125 mmol/5 mL) and the internal standard (1,3,5-trimethoxybenzene or α,α,α-trifluorotolune, 0.125 mmol/800 µL; 0.1562 mmol/5 mL) were introduced in a Wilmad® screw-cap NMR tube. The NMR tube was left to equilibrate at 15 °C inside the Bruker Avance 500 spectrometer. 200 µL of a stock solution of the $\mathbf{M_{20}}$ catalysts (0.05mmol/200µL; 0.125mmol/5mL) were injected into the NMR tube. The progress of the reaction was followed by ^1H NMR and $^{19}F\{^1H\}$ NMR (1 scan per datapoint). Spectra were processed and analysed using MestReNova 7.1.1 software. The resulting RCM conversion profiles are presented in Table 5.1 and on Figure 4.13 (Chapter 4). For further details see Ref. 6.[6]

5.4.9 Density Functional Theory calculations

All the Generalized Gradient Approximation DFT calculations were carried out by C. A. Urbina-Blanco in collaboration with Dr Albert Poater, using the

Gaussian09 set of programs,[7] with B3LYP functional,[8,9] and a 6-311+G(d,p) basis set.

Natural Bond Orbital (NBO) analysis of the DFT derived [B3LYP/6-311+G(d,p)] cycloheptenes **134-139** was carried out by R. A. Cormanich employing Gaussian09.

5.5 References

1. S. C. Sondej, J. A. Katzenellenbogen, *J. Org. Chem.*, 1986, **51**, 3508-3513.

2. D. R. Strobach, G. A. Boswell, *J. Org. Chem.*, 1971, **36**, 818–820.

3. R. Helder, H. Wynberg, *Tetrahedron*, 1975, **31**, 2551–2557.

4. T. Alvik, J. Dale, *Acta Chem. Scand.*, 1971, **25**, 1153–1154.

5. D. Seebach, E. J. Corey, *J. Org. Chem.*, 1975, **40**, 231–237.

6. C. A. Urbina-Blanco, M. Skibiński, D. O'Hagan, S. P. Nolan, *Chem. Commun.*, 2013, **49**, 7201–7203.

7. M. J. Frisch, G. W. Trucks, H. B. Schlegel, G. E. Scuseria, M. A. Robb, J. R. Cheeseman, G. Scalmani, V. Barone, B. Mennucci, G. A. Petersson, H. Nakatsuji, M. Caricato, X. Li, H. P. Hratchian, A. F. Izmaylov, J. Bloino, G. Zheng, J. L. Sonnenberg, M. Hada, M. Ehara, K. Toyota, R. Fukuda, J. Hasegawa, M. Ishida, T. Nakajima, Y. Honda, O. Kitao, H. Nakai, T. Vreven, J. A. Montgomery Jr., J. E. Peralta, F. Ogliaro, M. Bearpark, J. J. Heyd, E. Brothers, K. N. Kudin, V. N. Staroverov, R. Kobayashi, J. Normand, K. Raghavachari, A. Rendell, J. C. Burant, S. S. Iyengar, J. Tomasi, M. Cossi, N. Rega, J. M. Millam, M. Klene, J. E. Knox, J. B. Cross, V. Bakken, C. Adamo, J. Jaramillo, R. Gomperts, R. E. Stratmann, O. Yazyev, A. J. Austin, R. Cammi, C. Pomelli, J. W. Ochterski, R. L. Martin, K. Morokuma, V. G. Zakrzewski, G. A. Voth, P. Salvador, J. J. Dannenberg, S. Dapprich, A. D. Daniels, Ö. Farkas, J. B. Foresman, J. V Ortiz, J. Cioslowski, D. J. Fox, *Gaussian Inc Wallingford CT*, 2009, 34, Wallingford CT.

8. A. D. Becke, *Phys. Rev. A*, 1988, **38**, 3098–3100.

9. P. J. Stephens, F. J. Devlin, C. F. Chabalowski, M. J. Frisch, *J. Phys. Chem.*, 1994, **98**, 11623–11627.

APPENDIX

Publications

"Synthesis and structure of large difluoromethylene containing alicycles by ring-closing metathesis"
M. Skibiński, C. A. Urbina-Blanco, A. M. Z. Slawin, S. P. Nolan, D. O'Hagan, *Org. Biomol. Chem.*, 2013, **11**, 8209-8213.

"Accelerating influence of the *gem*-difluoromethylene group in a ring-closing olefin metathesis reaction"
C. A. Urbina-Blanco, M. Skibiński, D. O'Hagan, S. P. Nolan, *Chem. Commun.*, 2013, **49**, 7201-7203.

"Influence of the difluoromethylene group (CF_2) on the conformation and properties of selected organic compounds"
Y. Wang, M. Skibiński, A. M. Z. Slawin, D. O'Hagan, *Pure Appl. Chem.*, 2012, **84**, 1587-1595.

"Alicyclic Ring Structure: Conformational Influence of the CF_2 Group in Cyclododecanes"
M. Skibiński, Y. Wang, A. M. Z. Slawin, T. Lebl, P. Kirsch, D. O'Hagan, *Angew. Chem. Int. Ed.*, 2011, **50**, 10581-10584.

Conferences and presentations

10th Organic Chemistry Postgraduate Symposium, University of St Andrews, 2013. Oral presentation.

12th RSC Annual Fluorine Group Meeting, University of St Andrews, 2012. Poster presentation.

42nd RSC Scottish Organic Division Meeting, University of St Andrews, 2012.

20th International Symposium on Fluorine Chemistry, Kyoto, Japan. Poster presentation (Best Poster prize winner).

11th RSC Annual Fluorine Group Meeting, University of Aberdeen, 2011. Poster presentation.

Syngenta Post Graduate Workshop, University of Strathclyde, Glasgow, 2011.

10th RSC Annual Fluorine Group Meeting, Durham University, 2010.